



**HAL**  
open science

# Regulatory mechanisms of mexEF-oprN efflux operon in *Pseudomonas aeruginosa*: from mutations in clinical isolates to its induction as response to electrophilic stress

Paulo Juarez

## ► To cite this version:

Paulo Juarez. Regulatory mechanisms of mexEF-oprN efflux operon in *Pseudomonas aeruginosa*: from mutations in clinical isolates to its induction as response to electrophilic stress. Bacteriology. Université Bourgogne Franche-Comté, 2017. English. NNT : 2017UBFCE015 . tel-01842272

**HAL Id: tel-01842272**

**<https://theses.hal.science/tel-01842272>**

Submitted on 18 Jul 2018

**HAL** is a multi-disciplinary open access archive for the deposit and dissemination of scientific research documents, whether they are published or not. The documents may come from teaching and research institutions in France or abroad, or from public or private research centers.

L'archive ouverte pluridisciplinaire **HAL**, est destinée au dépôt et à la diffusion de documents scientifiques de niveau recherche, publiés ou non, émanant des établissements d'enseignement et de recherche français ou étrangers, des laboratoires publics ou privés.

**THESIS OF DOCTORATE FROM BOURGOGNE FRANCHE-COMTE UNIVERSITY  
PREPARED AT THE FACULTY OF MEDICAL AND PHARMACEUTICAL SCIENCES**

Ecole Doctorale No. 554  
Environnements-Santé

Doctorate in Biochemistry and Molecular Biology

By

**Paulo JUAREZ**

**Regulatory mechanisms of *mexEF-oprN* efflux operon of  
*Pseudomonas aeruginosa*: from mutations in clinical  
isolates to its induction as response to electrophilic stress**

Thesis presented and defended at Besançon, France on December 15th 2017

Jury:

Pr. Emile VAN SCHAFTINGEN (President)

Pr. Antonio OLIVER

Dr. Christophe BORDI

Dr. Thilo KÖHLER

Dr. Catherine LLANES

Pr. Patrick PLESIAT

Reviewer

Reviewer

Moderator

Moderator

Thesis director

Thesis director





## Acknowledgments

This manuscript is the result of the collaboration and support of several people that I would like to acknowledge.

I would like to start by thanking the two reviewers of my work, Pr. Emile Van Schaftingen and Pr. Antonio Oliver. Thank you for accepting to read and to review my work. Your comments and suggestions will be very valuable for me and for our team.

To Dr. Thilo Köhler, “father” of MexEF-OprN, for accepting to participate to the jury and for all the recommendations and suggestions that you gave to me during the annual thesis committee.

A special greeting to Dr. Christophe Bordi. More than thanking you for your participation to the jury and to my thesis committee, I would especially like to thank you for always being available when I needed some advice or an external opinion about unusual regulation mechanisms. I really appreciated all your good will and your enthusiasm when talking about science.

During this work I could collaborate with Pr. Isabelle Broutin (Université Paris Descartes), Pr. Mustapha Si-Tahar and Dr. Eric Morello (Université de Tours). I would like to thank them for all the suggestions and ideas that they gave to the “CmrA project”; working with you was very pleasant. Thanks to Sylvie Elsen (CEA, Grenoble) for all the discussions that we had concerning the AraC-like regulators. Your passion for science and your charism were always inspiring.

To my PhD advisors, Pr. Patrick Plésiat and Dr. Catherine Llanes; words would not be enough to thank all that you have done for me. Thank you for all the advices, the time that you spent discussing with me and your good will.

To my team co-workers; Isabelle Patry, Anaïs Potron, Katy Jeannot, Damien Fournier, Arnaud Bolard, Hélène Puja, Eleni Liapis, Loïs Andrey. To the mycology team members; Steffi, Audrey, Adéline, Coralie, Alice, Jenny. To the hygiene team members; Didier, Benoît, Marie. Thank you for helping me and giving me advice when I needed; for all the sharing and for keeping the good mood at the lab. I told you that I would be brief, but I hope you know how much I appreciated to work with you.

To the former and temp members of the team; Charlotte Richardot, Aurélie Noguès, Mélanie Grosjean, Corentin Daguinot, Luana Silva, Camille Robin, Xiyu Tian, Camil Hadjar, Alexandre

Tetard. Thank you all for all your laughter, your advice, your technical support and so other things. For those who are starting this adventure I wish you all the best.

A very special thanks to my co-workers at Smaltis SAS from whom I got a lot of support during the last phases of this work. Cédric and Sophie, I would like to thank you for trusting me and for giving me the opportunity to work with you, I have no doubt that I will learn a lot from both of you; your work and your innovation are very inspiring. I would also like to thank Marjorie and Elise for giving me the support and the words that I needed when finishing this work. I am quite sure that working with you will be awesome.

\*\*\*

Quisiera hacer un agradecimiento especial a mi familia y amigos. Frieda y Roberto. Ustedes me abrieron las puertas de su casa cuando esta aventura comenzaba solamente y durante los días que pasé con ustedes aprendí muchísimas cosas que de no haber estado con ustedes puede ser que no hubiera logrado quedarme. Les estaré siempre agradecido. A mis padres, Sandra y Héctor y mis hermanos; José y Paula. Siempre les estaré agradecidos por todo el esfuerzo que han hecho durante toda la vida. Ustedes cuatro son un ejemplo de trabajo, prosperidad, honestidad, humildad y responsabilidad. Cualidades y valores morales que todo científico necesita.

A mis amigos, Car, Seba, Ate, Lili, Juanpa, Gil, Alex, Aleja, Eli. Gracias por ser parte de esta aventura y por ser tan comprensivos cuando moría de estrés.

## Abbreviations

<b>A<sub>420</sub></b> : absorbance at 420 nm	<b>EBP</b> : enhancing binding protein
<b>A<sub>600</sub></b> : absorbance at 600nm	<b>gDNA</b> : genomic DNA
<b>AAP</b> : abridged adapter primer	<b>Glo1</b> : glyoxalase I
<b>ABS</b> : activation binding site	<b>Glo2</b> : glyoxalase II
<b>AC</b> : adenylate cyclase	<b>Glo3</b> : glyoxalase III
<b>AGEs</b> : advanced glycation-end products	<b>GO</b> : glyoxal
<b>ATP</b> : adenosine triphosphate	<b>GSH</b> : reduced glutathione
<b>BACTH</b> : bacterial adenylate cyclase two-hybrid	<b>GSNO</b> : S-nitrosoglutathione
<b>CA-SFM</b> : comité de l'antibiogramme de la société française de microbiologie	<b>GSP</b> : gene specific primer
<b>cAMP</b> : cyclic adenosine monophosphate	<b>GSSG</b> : oxidized glutathione
<b>CAP</b> : catabolite activator protein	<b>H-NS</b> : histone-like nucleoid structuring
<b>cDNA</b> : complementary DNA	<b>HPTLC</b> : high performance thin layer chromatography
<b>CDS</b> : coding sequence	<b>HTH</b> : helix-turn-helix motif
<b>CF</b> : cystic fibrosis	<b>HQNO</b> : 2-n-heptyl-4-hydroxyquinoline-N-oxide
<b>CFU</b> : colony forming unit	<b>LBD</b> : ligand binding domain
<b>CHL</b> : chloramphenicol	<b>LTTR</b> : LysR-type transcriptional regulator
<b>ChIP</b> : chromatin immunoprecipitation	<b>MCTH</b> : MacConkey two-hybrid plate
<b>CIP</b> : ciprofloxacin	<b>MBP</b> : mannose binding protein
<b>CLSI</b> : clinical and laboratory standards institute	<b>MCDR</b> : medium chain dehydrogenases/reductases
<b>cMHA</b> : calibrated Mueller Hinton agar	<b>MDR</b> : multidrug resistance
<b>cMHB</b> : calibrated Mueller Hinton broth	<b>MFP</b> : periplasmic membrane fusion protein
<b>CNA</b> : cinnamaldehyde	<b>MG</b> : methylglyoxal
<b>CT</b> : cycle threshold	<b>MHTH</b> : Mueller Hinton two-hybrid plate
<b>DBD</b> : DNA binding domain	<b>MIC</b> : minimal inhibitory concentration
<b>DA</b> : diamide	<b>mRNA</b> : messenger RNA
<b>DETA</b> : diethylenetriamine NONate	<b>ncRNA</b> : non-coding RNA
<b>DMSO</b> : dimethyl sulfoxide	<b>OMP</b> : outer membrane protein
<b>DTT</b> : dithiothreitol	<b>oPCR</b> : overlapping PCR
<b>E</b> : efficacy	

**ORF:** open reading frame  
**PBS:** phosphate buffered saline  
**PCP:** pentachlorophenol  
**PCR:** polymerase chain reaction  
**PIA:** *Pseudomonas* isolation agar  
**PQ:** paraquat  
**RACE:** rapid amplification of cDNA ends  
**RBS:** ribosomal binding site  
**RBS:** regulatory binding site  
**RES:** reactive electrophilic species  
**RLU:** relative light unit  
**RNAseq:** high-throughput RNA sequencing  
**RND:** resistance nodulation cell division  
**RNS:** reactive nitrogen species  
**ROS:** reactive oxygen species  
**rpm:** rotations per minute  
**rRNA:** ribosomal RNA  
**RT:** retro-transcription  
**sBAP:** sheep blood-agar plate  
**SBS:** sequencing by synthesis  
**SDS-PAGE:** sodium dodecyl sulfate polyacrylamide gel electrophoresis  
**SHG:** S-2-hydroxyethylglutathione  
**SLG:** S-D-lactoylglutathione  
**SNP:** single nucleotide polymorphism  
**SOD:** superoxide dismutase  
**TCS:** two-component system  
**TSS:** transcription start site  
**TdT:** terminal deoxynucleotidyl transferase  
**TMP:** trimethoprim  
**U:** enzymatic unit  
**UTR:** untranslated region

# Summary

<b>I.</b>	<b>INTRODUCTION .....</b>	<b>1</b>
<b>II.</b>	<b>REGULATION OF OPERON <i>MEXEF-OPRN</i> IN CLINICAL <i>NFXC</i> MUTANTS .....</b>	<b>7</b>
1	BACKGROUND: RND EFFLUX SYSTEMS IN <i>PSEUDOMONAS AERUGINOSA</i> .....	9
1.1	Overview.....	9
1.2	Efflux Systems of Clinical Importance .....	11
1.2.1	MexAB-OprM.....	11
1.2.2	MexXY/OprM.....	12
1.2.3	MexCD-OprJ.....	14
1.2.4	MexEF-OprN .....	15
2	RESULTS.....	22
2.1	Amino Acid Substitutions Account for Most MexS Alterations in Clinical <i>nfxC</i> Mutants of <i>Pseudomonas aeruginosa</i> .....	22
2.2	Constitutive Activation of MexT by Amino Acid Substitutions found in Clinical Isolates of <i>Pseudomonas aeruginosa</i> .....	41
<b>III.</b>	<b>INDUCTION OF <i>MEXEF-OPRN</i> BY ELECTROPHILIC STRESS.....</b>	<b>45</b>
1	BACKGROUND: ACTIVATION OF RND EFFLUX SYSTEMS IN RESPONSE TO OXIDATIVE STRESS.....	47
1.1	Overview.....	47
1.2	Efflux operons induced by classical oxidative stress .....	49
1.2.1	Operon <i>mexAB-oprM</i> .....	49
1.2.2	Operon <i>mexXY</i> .....	50
1.3	Induction of <i>mexEF-oprN</i> by non-classical oxidative stress .....	51
1.3.1	Nitrosative stress .....	51
1.3.2	Disulfide stress.....	52
1.4	Bacterial response to electrophilic stress .....	54
1.4.1	Electrophile sensing.....	55
1.4.2	Detoxification of electrophiles.....	58
1.4.3	Protective mechanisms against electrophiles.....	59
2	RESULTS.....	61
2.1	Toxic Electrophiles Induce Expression of the Multi-Drug Efflux Pump MexEF-OprN in <i>Pseudomonas aeruginosa</i> Through a Novel Transcriptional Regulator, CmrA .....	61
2.2	Electrophilic Stress Induce Expression of RND Efflux Pumps in <i>Pseudomonas aeruginosa</i> .....	95
<b>IV.</b>	<b>CONCLUSION AND PERSPECTIVES.....</b>	<b>99</b>
<b>V.</b>	<b>MATERIALS AND METHODS .....</b>	<b>109</b>
1	MICROBIOLOGICAL TECHNIQUES .....	111
1.1	Bacterial Strains and Plasmids .....	111
1.1	Culture Media .....	115
1.2	<i>In Vitro</i> Selection of Chloramphenicol Resistant Mutants .....	115
1.3	Determination of Antibiotic Sensitivity .....	116
1.3.1	Antibiograms .....	116
1.3.2	Minimum Inhibitory Concentration (MIC) .....	116
1.4	Virulence Factors Determination .....	116
1.4.1	Swarming Mobility.....	116
1.4.2	Detection of Biofilm Formation by Adherence Test .....	116
1.4.3	Pyocyanin Production .....	117
1.4.4	Elastase Activity .....	117
1.4.5	Rhamnolipid Production .....	117



1.5	Bacterial Growth.....	118
1.6	Killing Experiments .....	118
2	MOLECULAR BIOLOGY TECHNIQUES .....	118
2.1	Nucleic Acid Extraction.....	118
2.1.1	Genomic DNA Extraction .....	118
2.1.2	Plasmid Extraction .....	118
2.2	DNA Amplification by PCR (Polymerase Chain Reaction) .....	118
2.3	Cloning Techniques .....	124
2.3.1	DNA Digestion using Restriction Enzymes .....	124
2.3.2	Agarose Gel Electrophoresis .....	124
2.3.3	Purification of DNA Fragments .....	124
2.3.4	DNA Ligation .....	124
2.4	Bacterial Transformation .....	125
2.4.1	Heat-shock Transformation .....	125
2.4.2	Electroporation.....	125
2.4.3	Bacterial Conjugation .....	125
2.5	Gene Inactivation using Overlapping PCR and Homologous Recombination.....	125
2.1	Chromosomal Complementation .....	126
2.2	Gene Overexpression using the araBAD Promoter.....	127
2.3	Luminescent Reporter of the CmrA-pathway .....	127
2.4	Bioluminescence Induction Assays.....	128
2.5	mRNAs Quantitation using RT-qPCR .....	128
2.5.1	RNA Extraction.....	128
2.5.2	cDNA Synthesis by RT-PCR.....	128
2.5.3	cDNA Amplification by qPCR.....	129
2.5.4	Relative Quantitation of Gene Expression .....	129
3	DNA SEQUENCING .....	129
3.1	Sanger Sequencing.....	129
3.2	Ion-Torrent® Amplicon Sequencing .....	130
3.2.1	Overview.....	130
3.2.2	Extraction of Genomic DNA .....	131
3.2.3	Preparation of a Genomic DNA Library.....	131
3.2.4	Template Preparation.....	131
3.2.5	Sequencing .....	132
3.2.6	Data Analysis .....	132
4	IDENTIFICATION OF THE TRANSCRIPTION START SITE USING 5'-RACE.....	133
4.1	Overview.....	133
4.2	RNA extraction .....	133
4.3	cDNA synthesis using GSP1 primer .....	133
4.4	S.N.A.P. Column Purification of cDNA .....	134
4.5	TdT Tailing of cDNA .....	134
4.6	Nested PCR, cloning and sequencing of RACE product .....	135
5	TRANSCRIPTOMIC ANALYSIS USING RNA SEQUENCING .....	135
5.1	Overview.....	135
5.2	Preparation of the cDNA library and sequencing .....	135
5.3	Cluster Generation .....	136
5.4	Sequencing.....	136
5.5	Data Analysis .....	137
6	PROTEIN-PROTEIN INTERACTION USING BACTERIAL TWO-HYBRID SYSTEM .....	137
6.1	Overview.....	137
6.1	Cloning of gene <i>mexT</i> .....	138

6.1	Cloning of gene <i>cmrA</i> .....	138
6.2	Hybrid Expression and Interaction Assay .....	139
6.3	$\beta$ -Galactosidase Assay in 96-well Arrays .....	139
7	ANALYSIS OF METABOLITES BY HPTLC .....	140
8	MBP PROTEIN FUSION AND PURIFICATION .....	140
8.1	Overview.....	140
8.2	Cloning and Production of MBP-tagged proteins .....	141
<b>VI.</b>	<b>APPENDIX .....</b>	<b>143</b>
<b>VII.</b>	<b>REFERENCES.....</b>	<b>155</b>



## List of Figures

Figure 1: General structure and function of a RND efflux system and its coding genes.....	9
Figure 2: Regulation of <i>mexAB-oprM</i> operon.....	12
Figure 3: Regulation of <i>mexXY</i> operon.....	13
Figure 4: Regulation of <i>mexCD-oprJ</i> operon.....	14
Figure 5: Regulation of <i>mexEF-oprN</i> operon.....	16
Figure 6: Subunit structure of LysR-type transcriptional regulator CbnR.....	17
Figure 7: Schematic representation of LTTR mode of action.....	18
Figure 8: Crystal structure of the DntR dimer.....	44
Figure 9: Subcategories of oxidative stress.....	48
Figure 10: Efflux pump encoding operons induced by classical oxidative stress.....	49
Figure 11: Crystal structure of non-oxidized and oxidized MexR protein.....	50
Figure 12: Induction of operon <i>mexEF-oprN</i> by non-classical oxidative stresses.....	52
Figure 13: Effect of redox environment on MexT.....	53
Figure 14: Chemical structure of common Reactive Electrophilic Species (RES).....	54
Figure 15: Formation of RES and cellular damage.....	55
Figure 16: Catabolic pathways of electrophiles.....	57
Figure 17: Biochemical reactions catalyzed by the glyoxalase system.....	59
Figure 18: Activation of KefB/C potassium channels by glutathione-adducts.....	60
Figure 19: Antimicrobial activity of cinnamaldehyde on <i>P. aeruginosa</i> .....	97
Figure 20: Relative expression of gene <i>mexE</i> from clinical and complemented strains according to the type of mutations found in <i>mexS</i> .....	102
Figure 21: Survival of BALB/cJRj mice infected with different strains of <i>P. aeruginosa</i> ....	105
Figure 22: Gene inactivation by overlapping PCR and homologous recombination.....	126
Figure 23: Representation of the luminescent reporter used to evaluate the activation of the CmrA pathway. ....	128

Figure 24: Schematic representation of a single well of an Ion Torrent sequencing chip .....	130
Figure 25: Preparation of gDNA library .....	131
Figure 26: Template preparation .....	132
Figure 27: Ion Torrent® Sequencing .....	132
Figure 28: Overview of the 5' RACE procedure .....	134
Figure 29: Overview of Illumina sequencing for RNAseq experiments.....	136
Figure 30: Rational of the BACTH technique based on T25 and T18 domains and the reconstitution of adenylate cyclase activity .....	138
Figure 31: Workflow of MBP-protein production and purification.....	140

## List of Tables

Table 1: Substrate specificities and regulatory genes of characterized RND efflux pumps of <i>Pseudomonas aeruginosa</i> .....	10
Table 2: Characteristics of a conventional <i>nfxC</i> mutant selected <i>in vitro</i> .....	15
Table 3 : Non-exhaustive list of <i>mexS</i> mutations in clinical strains of <i>P. aeruginosa</i> .....	20
Table 4: Characterization of clinical <i>nfxC</i> mutants harboring single-amino acid substitutions in MexT.....	41
Table 5: Effect of mutated alleles of <i>mexT</i> from clinical isolates on gene expression and drug susceptibility.....	42
Table 6: Bacterial two-hybrid experiments for modified MexT .....	43
Table 7: Mechanisms of antibiotic resistance induced by stress in <i>P. aeruginosa</i> .....	47
Table 8: Electrophilic stress response in <i>E. coli</i> and homologous genes in <i>P. aeruginosa</i> .....	56
Table 9: Effect of electrophiles on drug susceptibility and gene expression in strain PA14...	95
Table 10: Genotypic and phenotypic features of MexEF-OprN overproducers .....	104
Table 11: Bacterial strains.....	111
Table 12: Plasmids .....	114
Table 13: Culture Media .....	115
Table 14: Primers used in this work.....	119



# **I. Introduction**

---





*Pseudomonas aeruginosa*, a Gram-negative non-fermentative bacillus, has an extraordinary capacity to survive in different stressful environments, probably due to its relatively large genome (~ 5–7 Mbp) allowing the recruitment of an arsenal of responsive mechanisms (Burrows, 2012; Kazmierczak et al., 2015; King et al., 2009).

Thus, in addition to its ubiquitous presence in aquatic environments, this bacterium has become one of the most important opportunistic pathogens of our time. Its implication in acute and chronic infections has been mainly reported in immunocompromised patients and those suffering from cystic fibrosis (CF), as a cause of morbidity and mortality (McCarthy, 2015). To fight *P. aeruginosa* infections, clinicians can rely on a restricted number of antimicrobials because of the relative high resistance of this bacterium to a wide range of antibiotics (McCarthy, 2015). In fact, *P. aeruginosa* has been recently classified by the World Health Organization as a critical priority urgently needing new antibiotics, as the emergence of multi-resistant strains in the clinical setting is constantly increasing (Tacconelly and Magrini, 2017). Such resistance is due to intrinsic mechanisms including the low permeability of the outer membrane, production of enzymes capable to degrade or modify antibiotics (AmpC, OXA-50 and APH(3')-IIb) and the action of two efflux systems (MexAB-OprM and MexXY/OprM) able to export multiple molecules outside the cell (Poole, 2004). Nevertheless, the spectrum of this resistance can be expanded or intensified by acquired mechanisms, usually selected in presence of antibiotics, resulting from the transfer of mobile genetic elements or from genetic mutations altering expression of resistance-associated genes.

Consequently, multi-drug resistance (MDR) phenotypes are the result of accumulation of individual drug-specific mechanisms and the contribution of multi-drug efflux systems, principally those belonging to the resistance-nodulation-cell division (RND) family (Li and Nikaido, 2009; Li et al., 2015; Nikaido, 2003). These systems are multi-component transmembrane nano-machineries capable to extrude antibiotics out of the cell, reducing the impact of these molecules on their targets. Even though these systems are highly regulated (Li and Plésiat, 2016), antibiotics do not usually behave as inducers of their expression, suggesting that the primary role of RND pumps may not be the efflux of such molecules. In contrast, evidence emerges that RND pumps are components of adaptive stress responses (Poole, 2014).

Genomic analysis had shown that most of *P. aeruginosa* strains harbor operons coding for 12 RND-type transporters. The substrate profiles of these transporters have been partially

established while the contribution of four pumps to antibiotic resistance has been confirmed (namely, MexAB-OprM, MexXY/OprM, MexCD-OprJ and MexEF-OprN) (Li et al., 2015).

The MexEF-OprN efflux pump encoded by operon *mexEF-oprN*, is produced at very-low levels in wild-type strains grown under standard laboratory conditions; therefore it does not significantly contribute to the natural resistance of the species to antimicrobials (Köhler et al., 1997; Li et al., 2000). When upregulated in *nfxC* mutants, MexEF-OprN tends to decrease intracellular accumulation of a rather limited spectrum of antibiotics (fluoroquinolones, chloramphenicol, trimethoprim and tetracycline) (Köhler et al., 1997), of biocides (Chuanchuen et al., 2001) and of quorum sensing precursors (Lamarche and Déziel, 2011). Of note, *nfxC* mutants are resistant to carbapenems and more susceptible to  $\beta$ -lactams and aminoglycosides when compared to wild-type strains, due to concomitant repression of antibiotic-resistance genes such as *oprD*, *mexAB-oprM* and *mexXY*, respectively (Köhler et al., 1997).

The mode of regulation of operon *mexEF-oprN* is quite different from that of other efflux operons. Indeed, while these latter are regulated by local repressors, *mexEF-oprN* is positively controlled by a local activator, MexT. In addition, other several genes such as *mexS* (Sobel et al., 2005a), *mvaT* (Westfall et al., 2006), *ampR* (Balasubramanian et al., 2012), *mxtR* (Zaoui et al., 2012), *brlR* (Liao et al., 2013), *parR* (Wang et al., 2013), *nmoR* (Vercammen et al., 2015) and PA2449 (Lundgren et al., 2013) are also known to influence, either positively or negatively, expression of the efflux operon. *NfxC* mutants have been identified among isolates from cystic fibrosis (CF) and non-CF patients (Terzi et al., 2014; Wolter et al., 2009). However, the regulatory pathways by which *mexEF-oprN* is activated in some clinical resistant mutants remain to be clarified. The observation that nitrosative (Fetar et al., 2011) or disulfide (Fargier et al., 2012) stresses induce operon expression provides some clues on its physiological role. Lines of evidence suggest that MexEF-OprN is one of the mechanisms that *P. aeruginosa* sets up in response to redox stressors (Fargier et al., 2012).

This manuscript is divided in two main chapters dealing with: (i) the regulation of operon *mexEF-oprN* in clinical *nfxC* mutants and (ii) induction of *mexEF-oprN* by electrophilic stress. Each chapter begins with a literature review and presents the results obtained on the topic during the doctoral training. The first chapter provides a general description of regulation of the four major RND efflux operons of clinical importance in *P. aeruginosa*. A special focus is made on contribution of MexEF-OprN to multidrug resistance phenotype in

clinical isolates and on the role of mutations in operon dysregulation. The second chapter presents data of literature on induction of some of the RND efflux systems of *P. aeruginosa* by oxidative stress. We then describe how MexEF-OprN can be induced by toxic electrophiles through the action of a novel regulator named CmrA.

The manuscript ends with a general conclusion and give research perspectives and finally the last section describes all materials and methods used all along this work.



## **II. Regulation of operon *mexEF-oprN* in clinical *nfxC* mutants**

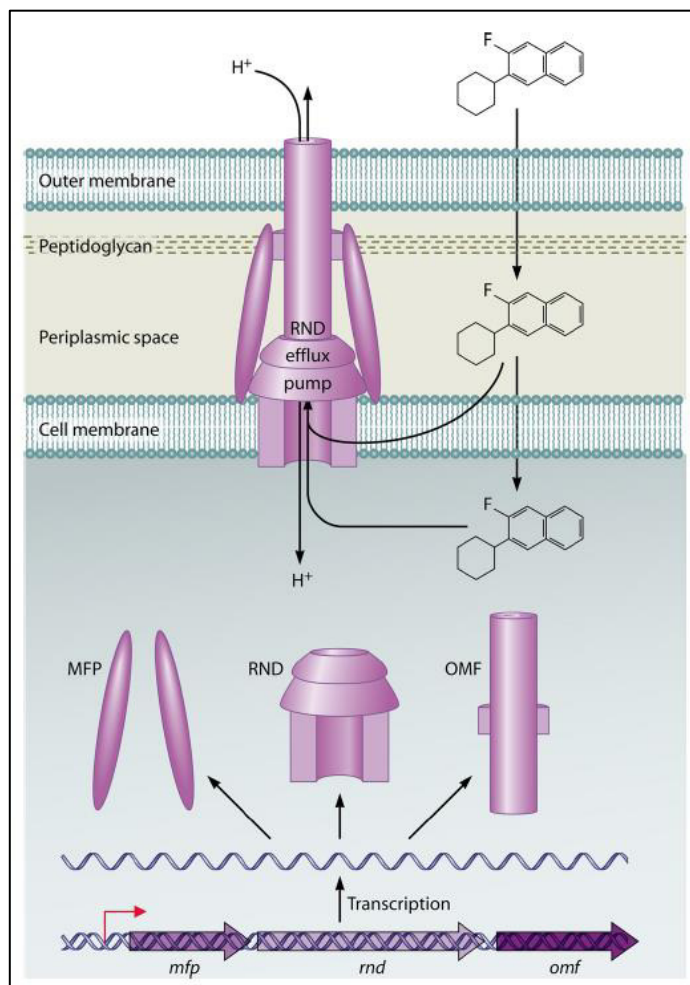
---



## 1 Background: RND Efflux systems in *Pseudomonas aeruginosa*

### 1.1 Overview

Efflux systems belonging to the Resistance Nodulation cell Division (RND) family are encoded in Gram negative species by chromosomal genes organized in operons (Li and



**Figure 1: General structure and function of a RND efflux system and its coding genes.** MFP: membrane fusion protein, RND: resistance nodulation cell division, OMF: outer membrane factor. Lister et al., 2009

rather poly-specific, most RND pumps are able to extrude a wide variety of substrates such as antibiotics, biocides, dyes, detergents, organic solvents, aromatic hydrocarbons and homoserine lactones (Poole and Srikumar, 2001; Schweizer, 2003).

RND pumps play an important role in natural and acquired resistance to antibiotics of *Pseudomonas aeruginosa* (Nikaido, 2011). So far, 12 operons coding for RND-type efflux systems have been detected in the genome of this species (Lee et al., 2006; Stover et al., 2000) (Table 1). While all these pumps have been experimentally proved to accommodate antibiotic molecules and to confer some degree of resistance when overexpressed, only a minority of them appears to have a real impact in the clinical context.



**Table 1: Substrate specificities and regulatory genes of characterized RND efflux pumps of *Pseudomonas aeruginosa***

Efflux pump	Regulatory gene	Substrates
<b>Clinically important</b>		
MexAB-OprM	<i>mexR, nalC, nalD, armR, rocS1/2-A2, brlR, mexT, cpxR, PA3225</i>	BL, CHIR, CHL, COL, CP, CRL, CV, EB, FQ, ID, QL, ML, NOV, OS, PDM, QS, SDS, SUL, TC, TLM, TMP, TRI
MexXY/OprM or MexXY-OprA	<i>mexZ, armZ, amgRS, parRS, suhB, rplU, rpmA, PA2572, PA2573</i>	ACR, AG, BPR, EB, FEP, FQ, LBM, ML, TC, TGC
MexCD-OprJ	<i>nfxB, esrC, algU, vqsM, PA2572</i>	AZI, BPR, CHIR, CHL, COL, CHX, FEP, FQ, NBTI, NCD, OS, PDM, QAC, QL, TC, TGC, TRI
MexEF-OprN	<i>mexT, mexS, mvaT, ampR, brlR, parRS, mxtR, nmoR, PA2449</i>	CHIR, CHL, DA, FQ, QL, HHQ, TC, TMP, TRI
<b>Other systems</b>		
MexGHI-OpmD	<i>soxR</i>	ACR, EB, FQ, TET, TPP, QS, $Va^{2+}$ , 5-Me-PCA
MexJK/OprM	<i>mexL</i>	ERY, TET
MexJK/OpmH	<i>mexL</i>	TRI
MexMN/OprM	unknown	CHL, TLM
MexPQ-OpmE	unknown	ML, QL, TPP
MexVW/OprM	unknown	ACR, CHL, EB, ERY, FQ, QL, TC
MuxABC-OpmB	unknown	ATM, COL, ML, NOV, TET
TriABC-OpmH	unknown	TRI
CzcCBA	<i>czcRS, copRS</i>	$Cd^{2+}$ , $Zn^{2+}$

5-Me-PCA, 5-methylphenazine-1-carboxylate; ACR, acriflavine; AG, aminoglycosides; ATM, aztreonam; AZI, azithromycin; BL,  $\beta$ -lactams (except carbapenems); BPR, ceftobiprole; CHIR, LpxC inhibitor CHIR-090; CHL, chloramphenicol; CHX, chlorhexidine; COL, colistin (in biofilm); CP, carbapenems (except imipenem); CRL, cerulenin; CV, crystal violet; DA, diamide; EB, ethidium bromide; ERY, erythromycin; FEP, cefepime; FQ, fluoroquinolones; HHQ, 4-hydroxy-2-heptylquinoline; ID, indoles; LBM, peptide deformylase inhibitor LBM415; ML, macrolides; NBTI, bacterial type II topoisomerase inhibitor NBTI5463; NCD, N-chloramine derivative; NOV, novobiocin; OS, organic solvents; PDM, pacidamycin; QAC, quaternary ammonium compounds; QL, quinolones; QS, quorum-sensing molecules/inhibitors; SDS, sodium dodecyl sulfate; SUL, sulfonamides; TC, tetracyclines; TGC, tigecycline; TLM, thiolactomycin; TMP, trimethoprim; TPP, tetraphenylphosphonium; TRI, triclosan

Adapted from Li and Plésiat, 2016.

## 1.2 Efflux Systems of Clinical Importance

As stated before, RND efflux systems can be involved in natural (baseline) susceptibility to antibiotics and/or can contribute to acquisition of higher resistance levels when overexpressed upon mutations (Nikaido, 2011). Of the 12 RND-type transporters encoded by *P. aeruginosa*, only four have been shown to be associated with multidrug resistance phenotypes in clinical isolates, namely MexAB-OprM, MexXY/OprM, MexCD-OprJ and MexEF-OprN (Li et al., 2015; Lister et al., 2009).

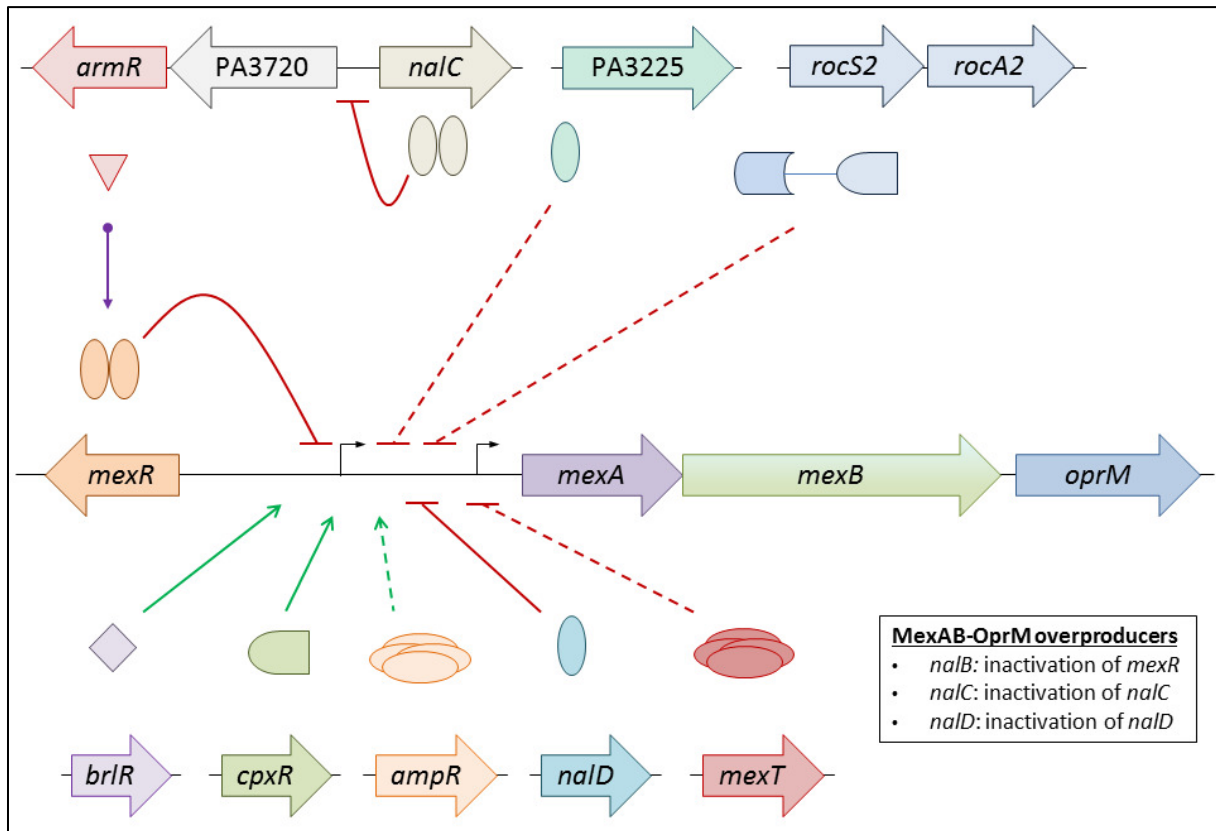
### 1.2.1 MexAB-OprM

The efflux system MexAB-OprM is a major contributor to natural resistance of *P. aeruginosa* because of its constitutive, though growth-phase dependent expression, and its poly-specificity (Evans and Poole, 1999; Li et al., 1995; Yang et al., 2011). Inactivation of any of its three components (MexA, MexB or OprM) results in a strong decrease in the minimal inhibitory concentrations (MICs) of antibiotics exported by the pump (i.e.  $\beta$ -lactams or fluoroquinolones) (Li et al., 1995). The very broad substrate specificity of transporter MexA includes several antibiotic classes (Köhler et al., 1996; Li et al., 1994a, 1994b, 1995; Mistry et al., 2013; Schweizer, 1998), dyes (Li et al., 2003), antiseptic molecules such as triclosan (Schweizer, 1998), organic solvents (Li and Poole, 1999; Li et al., 1998), and quorum sensing molecules or inhibitors (Minagawa et al., 2012; Moore et al., 2014; Pearson et al., 1999) (**Table 1**).

The *mexAB-oprM* operon expression is tightly controlled by several regulators. MarR-like repressor MexR, whose gene is located upstream and is divergently transcribed from *mexAB-oprM*, ensures a local regulation of the operon (Poole et al., 1996a). However, other regulatory proteins such as ArmR (depending on NalC) (Cao et al., 2004), NalD (Morita et al., 2006a; Sobel et al., 2005b), MexT (Maseda et al., 2004), the two-component system RocS1/2-A2 (Sivaneson et al., 2011), AmpR (Balasubramanian et al., 2012), BrlR (Liao et al., 2013), CpxR (Tian et al., 2016), and PA3225 (Hall et al., 2017) are also involved in the complex regulation of the pump (**Figure 2**).

Several types of mutants (*nalB*, *nalC* and *nalD*) respectively harboring inactivating mutations in genes *mexR*, *nalC* and *nalD* have been characterized (Cao et al., 2004; Poole et al., 1996a; Sobel et al., 2005b). They can be found in the clinical setting and exhibit significant resistance to most MexAB-OprM substrates (e.g. carbenicillin MIC from 4- to 8-fold higher than a WT strain) (Campo Esquisabel et al., 2011; Llanes et al., 2004; Quale et al., 2006). However, the

role of the other genes listed above in MexAB-OprM derepression remains unclear in strains recovered from infections or colonizations.

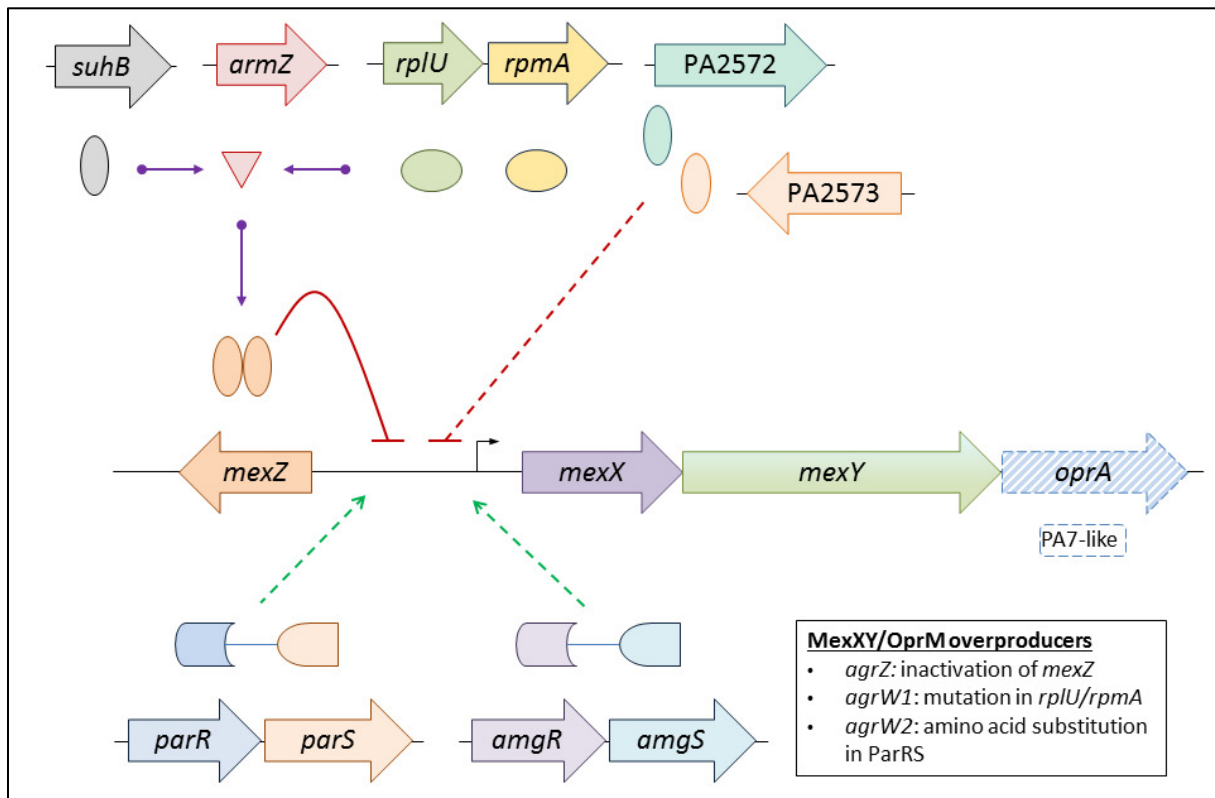


**Figure 2: Regulation of *mexAB-oprM* operon.** Self-regulated local repressor MexR ensures basal expression of operon *mexAB-oprM* in wild-type strains by binding as a homodimer to the distal promoter. A second repressor, NalD, directly binds as a monomer to the proximal promoter of the *mexAB-oprM* operon. The third repressor, NalC, has an indirect effect on *mexAB-oprM* expression as it represses the expression of gene *armR*, the product of which acts as an anti-repressor of MexR. Mutations in these three repressors have been reported in *nalB*, *nalD*, and *nalC* mutants, respectively. Two direct activators of *mexAB-oprM* have been described, namely CpxR and BrIR (this latter being active exclusively in biofilms). Finally, the products of four other genes would have an indirect negative (*mexT*, *rocS1/2-A2*, *PA3225*) or positive (*ampR*) impact on *mexAB-oprM* expression.

### 1.2.2 MexXY/OprM

Like MexAB-OprM, the efflux pump MexXY/OprM plays a significant role in wild-type resistance phenotype of *P. aeruginosa* to antibiotics. Most of strains harbor a chromosomally-located operon composed of only two genes, *mexX* and *mexY* (Mine et al., 1999). The outer membrane component OprM required to form a functional efflux pump is provided by the *mexAB-oprM* locus (Aires et al., 1999). Remarkably and for unclear reasons, strains belonging to PA7 lineage possess a three-gene operon, *mexXY-oprA*, encoding an OMP named OprA sharing 47% of sequence identity with OprM (Morita et al., 2012). The MexXY/OprM and MexXY/OprA pumps exhibit very close substrates profiles that include aminoglycosides, macrolides and tetracyclines (Aires et al., 1999; Masuda et al., 2000a) (Table 1).

Expression of *mexXY/oprA* is maintained at low-basal levels in wild-type strains by a TetR-like regulator, MexZ, whose gene resides upstream the operon (Aires et al., 1999). In addition to MexZ, transcription of the efflux operon can be influenced by several genes such as *armZ* (Yamamoto et al., 2009), *rplU-rpmA* (Lau et al., 2012), *subB* (Shi et al., 2015), and PA2572-PA2573 (McLaughlin et al., 2012) as well as by activity of two-component systems ParRS (Muller et al., 2011) and AmgRS (Lau et al., 2013) (**Figure 3**).

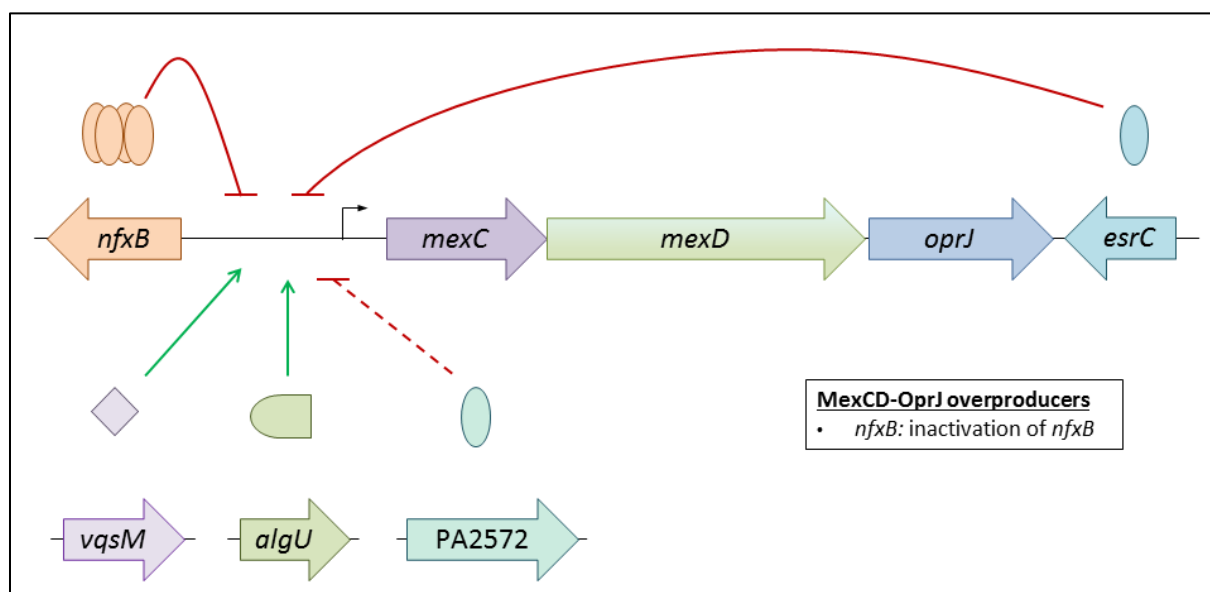


**Figure 3: Regulation of *mexXY* operon.** Acting as a local repressor, MexZ binds as a homodimer to the promoter region upstream of *mexXY*. Gene *armZ* encodes an anti-repressor that interacts with and inhibits MexZ. The product of gene *subB* or defects in ribosomal proteins encoded by genes *rplU* and *rpmA*, result in overproduction of ArmZ and subsequent overexpression of *mexXY*. The operon can also be indirectly activated by mutations occurring in operons *parRS* and *amgRS* that code for two-component regulatory systems ParRS and AmgRS, respectively. Finally, the products of genes PA2572-PA2573 have been reported to indirectly repress *mexXY* by still unknown mechanisms. To date, three types of MexXY-overproducing mutants have been characterized among clinical isolates, namely *agrZ* mutants (harboring mutations in *mexZ*), *agrW1* mutants (exhibiting alterations in various ribosomal proteins or 23S rRNA) and *agrW2* mutants (with mutations activating ParRS).

The three types of MexXY-overproducing mutants identified so far (*agrZ*, *agrW1* and *agrW2*) show a 2- to 8-fold increased resistance to the pump substrates as compared with wild-type strains (Li and Plésiat, 2016). All of them can be isolated from CF and non-CF patients (El’Garch et al., 2007; Hocquet et al., 2008; Muller et al., 2011; Vogne et al., 2004) though *agrZ* mutants are predominant in the CF lung (Feliziani et al., 2010; Smith et al., 2006). The role of PA2572-PA2573 and AmgRS as cause of MexXY-dependent drug resistance remains uncertain in clinical isolates.

### 1.2.3 MexCD-OprJ

The MexCD-OprJ efflux system is thought to be quiescent in wild-type strains, as inactivation of its encoding operon, *mexCD-oprJ*, does not affect the susceptibility of *P. aeruginosa* to antibiotics (Poole et al., 1996b; Srikumar et al., 1997). On the other hand, overproduction of the pump in so-called *nfxB* mutants is responsible for a significant increase in MICs of antibiotics such as chloramphenicol (4-fold), quinolones/fluoroquinolones (8-fold), and fourth-generation cephalosporins (8-fold) (Masuda et al., 2000b; Poole et al., 1996b). Other cytotoxic molecules listed in **Table 1** can also be actively exported by MexCD-OprJ (Li and Plésiat, 2016). The paradoxical hypersusceptibility of *nfxB* mutants to aminoglycosides and  $\beta$ -lactams (except those cited above) would result from operons *mexXY* and *mexAB-oprM* being downregulated to counterbalance *mexCD-oprJ* overexpression (Gotoh et al., 1998; Jeannot et al., 2008; Li et al., 2000). In addition, MexCD-OprJ overproducers exhibit impaired fitness and virulence (Linares et al., 2005; Martínez-Ramos et al., 2014; Stickland et al., 2010), reinforcing the notion of the strong impact that this pump may have on *P. aeruginosa* physiology.



**Figure 4: Regulation of *mexCD-oprJ* operon.** Acting as a local repressor, NfxB binds as a tetramer to the DNA region ahead of *mexCD-oprJ*. The product of *esrC* gene also acts as a local repressor of the operon. Other proteins such as VqsM and AlgU would positively affect the expression of *mexCD-oprJ*, while the product of gene PA2572 seems to have an indirect impact. Only *nfxB* mutants harboring a disrupted *nfxB* gene have been recognized in the clinical setting so far.

Operon *mexCD-oprJ* is regulated by two so-called “local repressors”, NfxB and EsrC, whose genes are located upstream and downstream from the operon, respectively (**Figure 4**). Additionally, *mexCD-oprJ* transcription can be influenced by VqsM, an AraC-type transcriptional regulator involved in regulation of virulence factors and quorum sensing molecules (Liang et al., 2014), by AlgU, a sigma factor mediating the bacterial response to

envelope stress (Fraud et al., 2008), and by the product of gene PA2572 (McLaughlin et al., 2012).

MexCD-OprJ upregulating mutants isolated in the clinical context, for instance from urinary tract infections, harbor disrupted *nfxB* genes (Shigemura et al., 2015). Interestingly, the pump has been found to be co-produced along with MexAB-OprM or MexXY in fluoroquinolone- and/or carbapenem-resistant clinical isolates, suggesting additional effects on resistance to shared substrates such as fluoroquinolones (Li and Plésiat, 2016).

#### 1.2.4 MexEF-OprN

This efflux system is expressed at very low levels in wild-type strains grown under standard laboratory conditions and thus does not significantly contribute to intrinsic resistance to antibiotics or biocides (Köhler et al., 1997). In *nfxC*-type mutants, the pump is overproduced and provides *P. aeruginosa* with a higher resistance to a rather limited number of substrates including chloramphenicol, fluoroquinolones/quinolones, trimethoprim and tetracycline (Li and Plésiat, 2016) (**Table 1**). The *nfxC* mutants exhibit some additional phenotypic traits listed in **Table 2**, such as a tolerance to carbapenems (i.e. imipenem), an increased susceptibility to various  $\beta$ -lactams (i.e. ticarcillin) and to aminoglycosides (i.e. gentamicin), which are not related to MexEF-OprN activity but to downregulation of gene *oprD* and of operons *mexAB-oprM* and *mexXY*, respectively (Fukuda et al., 1995; Köhler et al., 1997). These mutants are also strongly defective in production of some extracellular virulence factors (Köhler et al., 2001). This lower pathogenicity would result from lower, efflux-mediated intracellular concentrations of quorum sensing molecules in the mutants (Lamarche and Déziel, 2011; Olivares et al., 2012) and/or repression of quorum-sensing-related genes (Tian et al., 2009a).

**Table 2: Characteristics of a conventional *nfxC* mutant selected *in vitro***

Strain	Relative gene expression <sup>a</sup>				Resistance (fold change in MICs) <sup>b</sup>						Virulence score <sup>c</sup>
	<i>mexE</i>	<i>oprD</i>	<i>mexB</i>	<i>mexY</i>	CIP	CHL	TMP	IMP	TIC	GEN	
WT	1x	1x	1x	1x	1x	1x	1x	1x	1x	1x	5/5
<i>nfxC</i>	≥100x	-10x	-10x	-5x	32x	32x	16x	4x	0.5x	0.25x	1/5

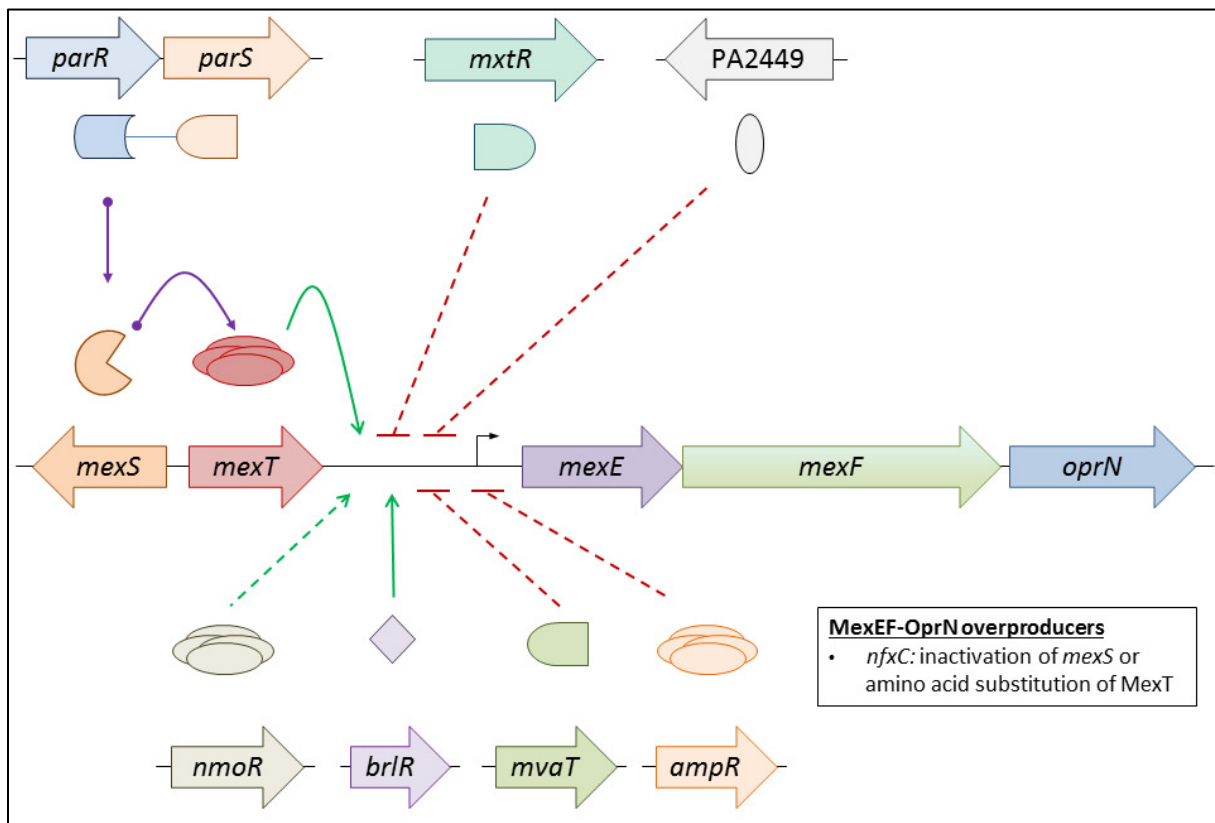
<sup>a</sup>Expressed as a ratio to wild-type strain PA14

<sup>b</sup>CIP, ciprofloxacin; CHL, chloramphenicol; IMP, imipenem; TIC, ticarcillin; GEN, gentamicin

<sup>c</sup>Based on the capacity of the strain to express virulence traits: (1) pyocyanin, (2) elastase, (3) biofilm, (4) rhamnolipids and (5) swarming motility.

Based on laboratory data

The pump MexEF-OprN is encoded by a three-gene operon, the regulation of which is quite different from those of the other RND efflux systems present in *P. aeruginosa*, in that it involves a LysR-type “local” activator, named MexT (Köhler et al., 1999). The expression of *mexEF-oprN* can be modulated by several other genes including *mexS* (Sobel et al., 2005a), *mvaT* (Westfall et al., 2006), *ampR* (Balasubramanian et al., 2012), *mxtR* (Zaoui et al., 2012), *brlR* (Liao et al., 2013), *parR* (Wang et al., 2013), *nmoR* (Vercammen et al., 2015) and PA2449 (Lundgren et al., 2013) (Figure 5).



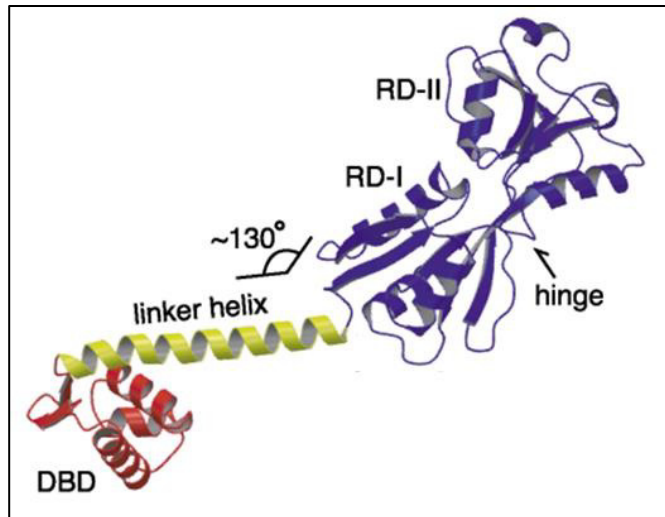
**Figure 5: Regulation of *mexEF-oprN* operon.** Operon *mexEF-oprN* is the sole RND-type operon of *P. aeruginosa* known to be controlled by an activator, named MexT. The MexT-dependent expression of *mexEF-oprN* can be triggered by mutational inactivation or impairment of a putative oxido-reductase, MexS, whose gene resides upstream *mexT*. The two-component system ParRS would interact with MexS and indirectly activate *mexEF-oprN*. The products of genes *nmoR* and *brlR* (only active in biofilm) are also thought to have a positive impact on *mexEF-oprN* expression, while genes *mvaT*, *ampR*, *mxtR*, and PA2449 would have negative effects.

It is generally considered that *nfxC* mutants are rather uncommon among CF and non-CF clinical isolates (Henrichfreise et al., 2007; Klockgether et al., 2013; Llanes et al., 2011, 2013; Smith et al., 2006; Xavier et al., 2010), though recent studies suggest they might be more prevalent than previously thought (Bubonja-Sonje et al., 2015; Marvig et al., 2015; Terzi et al., 2014). At the beginning of my research work, overexpression of *mexEF-oprN* had only been associated with mutational events affecting gene *mexT* (missense mutations) or gene

*mexS* (missense and disruptive mutations) (Henrichfreise et al., 2007; Klockgether et al., 2013; Llanes et al., 2011; Marvig et al., 2015; Richardot et al., 2016; Smith et al., 2006).

#### 1.2.4.1 The LysR-type Activator *MexT*

*MexT*, a LysR-type transcriptional regulator (LTTR) of 305 residues, is essential to operon *mexEF-oprN* expression (Köhler et al., 1999) (Figure 5). However, in addition to its role in the control of efflux activity in *P. aeruginosa*, *MexT* is involved in direct or indirect, positive or negative regulation of about 143 genes. For instance, this protein acts as a repressor of porin *OprD* encoding gene and PQS (*Pseudomonas* Quinolone Signal) biosynthesis operon *pqsABCDE* (Tian et al., 2009b). Of note, a sequence

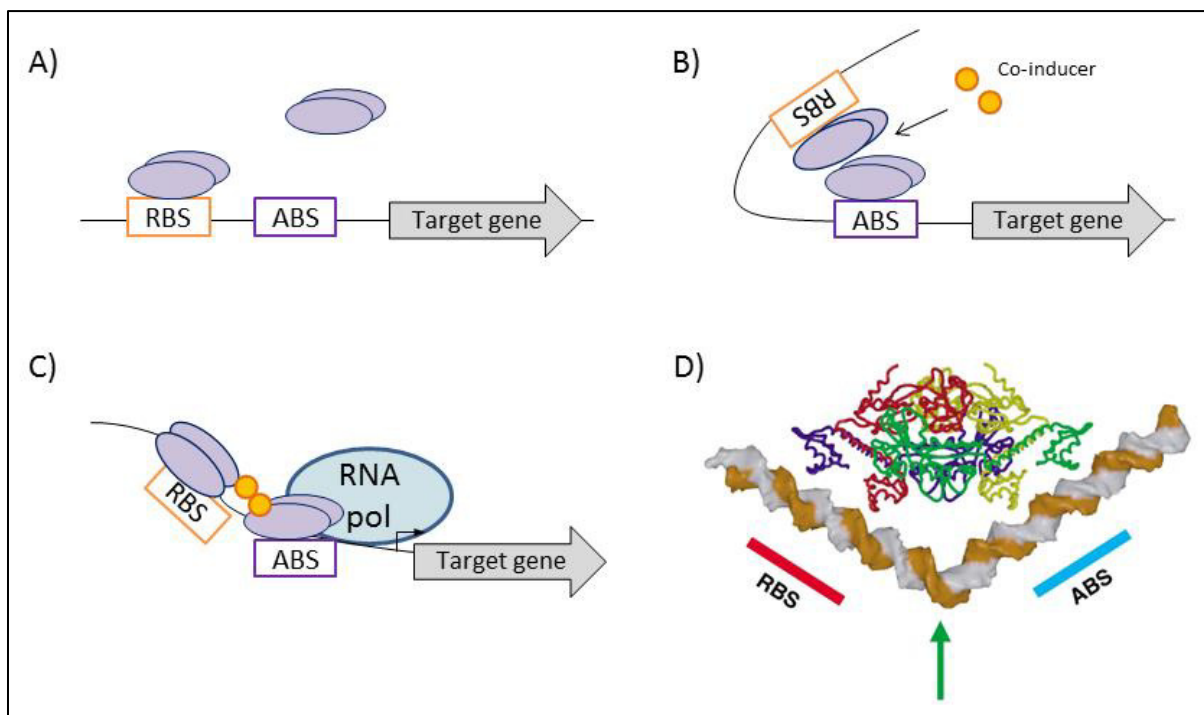


**Figure 6: Subunit structure of LysR-type transcriptional regulator CbnR.** In *Ralstonia eutropha*, CbnR initiates chlorocatechol degradation. In red, the N-terminus contains the DNA binding domain (DBD). In blue, the C-terminus harbors the co-factor binding domain composed of two subdomains RD-I and RD-II connected by a hinge. The linker between the two domains is represented in yellow (Muraoka et al., 2003).

polymorphism or mutations in gene *mexT* have been reported to cause inactivation of the regulator in some PAO1-like strains sub-cultured in research labs (Henrichfreise et al., 2007; Köhler et al., 1999; Luong et al., 2014; Maseda et al., 2000; Olivas et al., 2012; Tian et al., 2009b; Vercammen et al., 2015). Usually composed of 330 residues, LTTRs are global regulators that positively or negatively regulate expression of target genes (Maddocks and Oyston, 2008). The family is highly conserved and ubiquitous among bacteria, with orthologous members identified in *Archaea* and eukaryotic organisms (Pérez-Rueda and Collado-Vides, 2001). Most of these regulators are activated upon binding of specific ligands some of which can be intermediates of biosynthetic or catabolic pathways (Maddocks and Oyston, 2008). The canonical structure of a LTTR (Figure 6) contains an N-terminal helix-turn-helix (HTH) motif for DNA binding, and a C-terminal co-factor binding domain composed of two distinct  $\alpha/\beta$  subdomains (RD-I and RD-II). These subdomains are connected by a hinge which is thought to accommodate co-inducer molecules (Maddocks and Oyston, 2008; Muraoka et al., 2003; Stec et al., 2006).



LTTRs are functionally active as tetramers. They regulate expression of target genes through a particular mechanism. DNA-footprinting experiments using several of these regulators have revealed the existence of two binding sites upstream from target promoters, namely a regulatory binding site (RBS) and an activation-binding site (ABS). These two DNA regions, formerly named “Nod-box”, are not occupied at the same time in absence of co-inducer. Indeed, the apo-form has less affinity to bind DNA than the co-inducer-bound form (Maddocks and Oyston, 2008). When a co-inducer is present, the affinity of the LTTR for DNA is increased and thus both sites are occupied. The formation of the functional tetramer and its binding to the regulatory sequences provoke a bending of DNA allowing the stabilization of RNA polymerase and thereby triggering gene expression (**Figure 7**) (Maddocks and Oyston, 2008).



**Figure 7: Schematic representation of LTTR mode of action.** The dimeric conformation of the apo-form of the LTTR usually binds the regulatory binding site (RBS) with high affinity, and the activation binding site (ABS) with low affinity (A); once the co-inducer is produced at relevant levels, the affinity of the co-inducer-bound LTTR is increased; binding of two dimers to regulatory sequences creates a bending of the DNA (B); the functional tetramer stabilizes RNA polymerase and triggers the expression of the target gene (C); based on Maddocks and Oyston, 2008. A three-dimensional structure of the functional tetramer of a LTTR is represented (D) (Muraoka et al., 2003).

Following the general mode of action of LTTRs, MexT binds a consensus sequence (ATC-N<sub>9</sub>-GAT-N<sub>7</sub>-ATC-N<sub>9</sub>-GAT) upstream from operon *mexEF-oprN*, consistent with the presence of two “Nod-boxes” in the intergenic region between *mexT* and *mexE* (Köhler et al., 1999; Maseda et al., 2010; Tian et al., 2009a). Specific amino acid substitutions in LTTRs have been reported to constitutively activate some of these regulators without the need of co-

inducer, as exemplified by BenM from *Acinetobacter baylyi* and CysB from *Salmonella enterica* serovar Typhimurium (Colyer and Kredich, 1996; Craven et al., 2009). Single point mutations have also been identified in MexT from *nfxC* mutants of *P. aeruginosa*, but their impact on protein functionality has remained undetermined so far (Llanes et al., 2011).

#### **1.2.4.2 Oxidoreductase MexS**

Most of *nfxC* mutants selected *in vitro* harbor disruptive mutations in another gene, named *mexS*, located close to, and transcribed divergently from *mexT* (**Figure 5**) (Köhler et al., 1999; Sobel et al., 2005a). Inactivation of *mexS* triggers the MexT-dependent overexpression of *mexEF-oprN* which in turn results in a typical NfxC resistance phenotype (**Table 2**) (Sobel et al., 2005a).

Gene *mexS* (1020 bp) is predicted to encode a putative quinone oxidoreductase belonging to the Medium Chain Dehydrogenases-Reductases superfamily (MCDR) (Winsor et al., 2016). Most of bacterial MCDR enzymes are active as tetramers and composed of two domains, namely an N-terminal catalytic domain and a C-terminal co-factor binding domain, which likely utilizes NAD(P)H as co-factor (Nordling et al., 2002; Persson et al., 2008). According to several investigators, MexS could be involved in detoxification of toxic secondary metabolites, that would behave as MexT co-inducers when accumulating in the cell (Fargier et al., 2012; Köhler et al., 1999; Sobel et al., 2005a).

In clinical strains of *P. aeruginosa*, gene *mexS* is subject to sequence variations most of which have an unknown impact on *mexEF-oprN* expression (Henrichfreise et al., 2007; Klockgether et al., 2013; Marvig et al., 2015; Smith et al., 2006) (Llanes et al., 2011; Richardot et al., 2016). Compared to missense mutations (9.4% of strains in average), indels and nonsense mutations appear to be rather infrequent (1.7%) among the *mexS* mutants (**Table 3**).

Table 3 : Non-exhaustive list of *mexS* mutations in clinical strains of *P. aeruginosa*

Patients	Strain screening	Sequencing method	<i>n</i> <sup>a</sup>	Frameshift mutations		Missense mutations		Gene <i>mexE</i> expression	References
				Prevalence	Nature	Prevalence	Amino acid substitutions		
CF	Sequentially collected isolates	WGS/Sanger	91	1.1%	Δ6bp	7.6%	R <sub>47</sub> C, A <sub>52</sub> D, P <sub>93</sub> S, D <sub>102</sub> Y, T <sub>177</sub> A, G <sub>244</sub> S, F <sub>312</sub> C	ND	(Smith et al., 2006)
CF and non-CF	Multi-resistant isolates	Sanger	22	ND	ND	9.1%	G <sub>68</sub> S, F <sub>273</sub> I	ND	(Henrichfreise et al., 2007)
Non-CF	Fluoroquinolone resistant isolates	Sanger	85	1.2%	+3bp	10.6%	K <sub>17</sub> T, E <sub>54</sub> G, A <sub>75</sub> V, G <sub>78</sub> S, T <sub>152</sub> A, A <sub>175</sub> V, E <sub>181</sub> D, C <sub>269</sub> Y, S <sub>289</sub> T, V <sub>308</sub> I, V <sub>318</sub> I, R <sub>332</sub> W	From 128- to 2,281-fold†	(Llanes et al., 2011)
CF	Sequentially collected isolates	WGS	474	3.1%	ND	10.9%	G <sub>39</sub> S, P <sub>59</sub> L, P <sub>94</sub> S, T <sub>119</sub> A, G <sub>224</sub> D, G <sub>238</sub> S, G <sub>275</sub> A, A <sub>291</sub> V, H <sub>321</sub> Y	ND	(Marvig et al., 2015)
Non-CF	Ciprofloxacin and imipenem resistant isolates	Sanger	221	1.4%	Δ8bp, ΔC <sub>293</sub> , Δ30bp	8.6%	D <sub>44</sub> E, S <sub>60</sub> F, S <sub>60</sub> P, V <sub>73</sub> A, V <sub>104</sub> A, A <sub>166</sub> P, F <sub>185</sub> L, C <sub>245</sub> G, N <sub>249</sub> D, F <sub>253</sub> L, L <sub>263</sub> Q,	From 29- to 825-fold‡	(Richardot et al., 2016)*

<sup>a</sup> number of strains used in the study

WGS: whole genome sequencing

ND: not determined

† compared to PAO1 reference strain, threshold equal to 100-fold minimum

‡ compared to PA14 reference strain, threshold equal to 20-fold minimum

\*Single-amino acid substitutions proven to be cause of *mexEF-oprN* overexpression, by chromosomal complementation in PA14Δ*mexS*: this work.

### 1.2.4.3 Other regulators of *mexEF-oprN*

So far, upregulation of operon *mexEF-oprN* in clinical strains has only been associated with mutations occurring in genes *mexT* and *mexS* (Llanes et al., 2011). However, according to the results of experiments performed on *in vitro* mutants, at least four repressors (MvaT, AmpR, MxtR and PA2449) and three activators (BrlR, ParRS and NmoR) can also influence operon expression (Li and Plésiat, 2016) (**Figure 5**).

MvaT is a member of Histone-like Nucleoid Structuring proteins (H-NS) family, that negatively controls about 150 virulence-related genes in *P. aeruginosa* (Castang and Dove, 2010). A deletion mutant, PAO1 $\Delta$ *mvaT*, was found to exhibit a modest 5- to 7-fold increase in *mexEF-oprN* transcription relative to wild-type strain PAO1, suggesting an indirect effect of this global regulator on pump activity (Westfall et al., 2006).

AmpR, a LTTR regulator, is known to differentially modulate the expression of target genes depending on which ligand is bound to it (Balcewich et al., 2010). AmpR regulates the expression of gene *bla<sub>ampC</sub>* encoding for the intrinsic  $\beta$ -lactamase AmpC (Kong et al., 2005). The repression this regulator exerts on *mexEF-oprN* is likely indirect (Balasubramanian et al., 2012).

Homologue of ArcB from *Escherichia coli*, MxtR is an orphan sensor kinase encoded by gene PA3271 in *P. aeruginosa*. Via its action on MexT, this sensor represses biosynthesis of PQS and the pump MexEF-OprN (Zaoui et al., 2012).

Finally, gene PA2449 encodes a TyrR-like member of the Enhancer Binding Proteins (EBP) family known to stabilize the interaction of sigma factor RpoN with DNA, thereby enhancing expression of target genes. Interestingly, a deletion mutant, PAO1 $\Delta$ PA2449, appeared to strongly overexpress the efflux operon (139-fold), but its antibiotic susceptibility was not investigated further; thus limiting conclusions on the role PA2449 could play in resistance (Lundgren et al., 2013).

BrlR belongs to the MerR-like family of regulators and is exclusively active in the biofilm mode of life (Liao et al., 2013). Supporting a role for BrlR as activator of *mexEF-oprN*, a 200-fold decrease in gene *mexE* transcripts was scored in biofilms of deletion mutant PAO1 $\Delta$ *brlR* compared to biofilms of wild-type strain. Confirming these data, direct binding of BrlR to the upstream region of *mexEF-oprN* could be established by several approaches including

chromatin immunoprecipitation (ChIP), streptavidin bead-pulldown and electrophoretic mobility shift assays (EMSA) (Liao et al., 2013).

The two-component regulatory system (TCS) ParRS has been reported by our laboratory to positively control the expression of another pump-encoding operon, namely *mexXY* (Muller et al., 2011). Activation of *mexEF-oprN* by ParRS is expected to be indirect through a negative impact on *mexS* expression (Wang et al., 2013).

The last activator of pump MexEF-OprN described so far, NmoR, is a LTTR having a role in the defense against nitro molecules. A PAO1 $\Delta$ *nmoR* mutant showed a decreased expression (20-fold) of operon *mexEF-oprN* and other MexT-dependent genes, but whether NmoR directly binds to the promoter region of the operon remains to be determined (Vercammen et al., 2015).

## **2 Results**

### **2.1 Amino Acid Substitutions Account for Most MexS Alterations in Clinical *nfxC* Mutants of *Pseudomonas aeruginosa***

Charlotte Richardot, **Paulo Juarez**, Katy Jeannot, Isabelle Patry, Patrick Plésiat and Catherine Llanes  
Antimicrobial Agents and Chemotherapy. 2016 Mars. 25;60(4): 2302 – 10. Doi: 10.1128/AAC.02622-15

# Amino Acid Substitutions Account for Most MexS Alterations in Clinical *nfxC* Mutants of *Pseudomonas aeruginosa*

Charlotte Richardot,<sup>a</sup> Paulo Juarez,<sup>a</sup> Katy Jeannot,<sup>a,b</sup> Isabelle Patry,<sup>b</sup> Patrick Plésiat,<sup>a,b</sup> Catherine Llanes<sup>a</sup>

Laboratoire de Bactériologie EA4266, Faculté de Médecine-Pharmacie, Université de Franche-Comté, Besançon, France<sup>a</sup>; Laboratoire de Bactériologie, Centre Hospitalier Universitaire de Besançon, Besançon, France<sup>b</sup>

**Multidrug-resistant mutants of *Pseudomonas aeruginosa* that overproduce the active efflux system MexEF-OprN (called *nfxC* mutants) have rarely been characterized in the hospital setting. Screening of 221 clinical strains exhibiting a reduced susceptibility to ciprofloxacin (a substrate of MexEF-OprN) and imipenem (a substrate of the negatively coregulated porin OprD) led to the identification of 43 (19.5%) *nfxC* mutants. Subsequent analysis of 22 nonredundant mutants showed that, in contrast to their *in vitro*-selected counterparts, only 3 of them (13.6%) harbored a disrupted *mexS* gene, which codes for the oxidoreductase MexS, whose inactivation is known to activate the *mexEF-oprN* operon through a LysR-type regulator, MexT. Nine (40.9%) of the clinical *nfxC* mutants contained single amino acid mutations in MexS, and these were associated with moderate effects on resistance and virulence factor production in 8/9 strains. Finally, the remaining 10 (45.5%) *nfxC* mutants did not display mutations in any of the regulators known to control *mexEF-oprN* expression (the *mexS*, *mexT*, *mvaT*, and *ampR* genes), confirming that other loci are responsible for pump upregulation in patients. Collectively, these data demonstrate that *nfxC* mutants are probably more frequent in the hospital than previously thought and have genetic and phenotypic features somewhat different from those of *in vitro*-selected mutants.**

*Pseudomonas aeruginosa* is a notorious cause of acute and chronic infections in vulnerable patients. The ability of this environmental Gram-negative bacterium to produce a broad range of virulence factors (1) and to become resistant to multiple antimicrobial agents is considered a key to its success in the hospital setting. When overexpressed upon mutation, several efflux systems belonging to the resistance-nodulation-cell division (RND) family of drug transporters are able to decrease the susceptibility of the pathogen to structurally unrelated antibiotics (2). One of these systems, named MexEF-OprN, is quiescent in wild-type strains grown under standard laboratory conditions. Its contribution to the intrinsic resistance of *P. aeruginosa* is therefore minimal. In contrast, in so-called *nfxC* mutants, stable overproduction of the pump results in a significant increase in the MICs (4- to 16-fold) of chloramphenicol, trimethoprim, and fluoroquinolones (3). Compared with the susceptibility of wild-type strains, typical *nfxC* mutants exhibit a hypersusceptibility to some antipseudomonal  $\beta$ -lactams (penicillins, cephalosporins) and aminoglycosides, a phenotype possibly due to the impaired activity of two other RND pumps, namely, MexAB-OprM and MexXY/OprM (4). Furthermore, this typical *NfxC* phenotype includes a decreased susceptibility to carbapenems, linked to the downregulation of the *oprD* gene, which codes for the specific porin OprD, allowing the facilitated diffusion of these antibiotics into the cell (3).

In *P. aeruginosa*, while most RND pumps have their expression modulated by repressors (5), transcription of the *mexEF-oprN* operon is controlled by a LysR-type activator, MexT, encoded by an adjacent gene (6). In some drug-susceptible laboratory strains of the PAO1 lineage, *mexT* is inactivated by an 8-bp insert (7). Spontaneous excision of this intragenic fragment restores the open reading frame of *mexT* with the concomitant overexpression of *mexEF-oprN* and the development of the typical *NfxC* phenotype (6). In other strains, *mexEF-oprN* transcription is triggered by mutations in another gene, *mexS*, which is divergently transcribed

from *mexT* and encodes an oxidoreductase (8). In any case, a functional MexT is mandatory for the *in vitro* selection of MexEF-OprN-overproducing mutants. This regulator has been reported to increase *mexS* expression (6), even if the consensus *nod*-box DNA sequence, considered the binding site of MexT, remains to be identified in the promoter region of *mexS* (9). To explain the MexS/MexT-dependent regulation of *mexEF-oprN*, it has been postulated that MexS is involved in the detoxification of some endogenously produced MexT-activating molecule(s) (10, 11). In this scenario, if it is not processed by MexS, the toxic metabolite(s) would be exported out of the cell by MexEF-OprN as a rescue mechanism.

In clinical strains, *nfxC* mutations are difficult to characterize because of polymorphic variations in the MexS and MexT protein sequences (<http://pseudomonas.com>). Moreover, data suggest that still uncharacterized pathways might influence *mexEF-oprN* expression (12). Supporting this notion, *in vitro* mutants with alterations in the *mvaT*, *ampR*, or *mxtR* gene have been reported to overexpress *mexEF-oprN* and to exhibit a multidrug resistance phenotype (13–15). However, the relevance of such mutations in clinical strains awaits confirmation.

*In vitro*-selected *nfxC* mutants were found to be deficient in the

Received 29 October 2015 Returned for modification 13 November 2015

Accepted 25 January 2016

Accepted manuscript posted online 1 February 2016

Citation Richardot C, Juarez P, Jeannot K, Patry I, Plésiat P, Llanes C. 2016. Amino acid substitutions account for most MexS alterations in clinical *nfxC* mutants of *Pseudomonas aeruginosa*. *Antimicrob Agents Chemother* 60:2302–2310. doi:10.1128/AAC.02622-15.

Address correspondence to Catherine Llanes, [cllanesb@univ-fcomte.fr](mailto:cllanesb@univ-fcomte.fr).

Supplemental material for this article may be found at <http://dx.doi.org/10.1128/AAC.02622-15>.

Copyright © 2016, American Society for Microbiology. All Rights Reserved.

TABLE 1 Bacterial strains and plasmids used in this study

Strain or plasmid	Relevant characteristics	Source or reference
<b>Strains</b>		
<i>Pseudomonas aeruginosa</i>		
PAO1	Wild-type reference strain PAO1-UW (University of Washington)	B. Holloway
PAO7H	<i>nfxC</i> mutant derived from wild-type strain PAO1-UW	3
PA14	Wild-type reference strain PA14	B. Ausubel
PA14ΔS	PA14 with a <i>mexS</i> ( <i>nfxC</i> -type) deletion	This study
PA14ΔT	PA14 with a <i>mexT</i> deletion	This study
PA14ΔS <sub>PA14</sub>	PA14 Δ <i>mexS</i> <i>trans</i> -complemented with <i>mexS</i> from reference strain PA14	This study
PA14ΔS <sub>PAO1</sub>	PA14 Δ <i>mexS</i> <i>trans</i> -complemented with <i>mexS</i> from reference strain PAO1	This study
PA14ΔS <sub>1307</sub>	PA14 Δ <i>mexS</i> <i>trans</i> -complemented with <i>mexS</i> from clinical strain 1307	This study
PA14ΔS <sub>2310</sub>	PA14 Δ <i>mexS</i> <i>trans</i> -complemented with <i>mexS</i> from clinical strain 2310	This study
PA14ΔS <sub>2505</sub>	PA14 Δ <i>mexS</i> <i>trans</i> -complemented with <i>mexS</i> from clinical strain 2505	This study
PA14ΔS <sub>3005</sub>	PA14 Δ <i>mexS</i> <i>trans</i> -complemented with <i>mexS</i> from clinical strain 3005	This study
PA14ΔS <sub>0911</sub>	PA14 Δ <i>mexS</i> <i>trans</i> -complemented with <i>mexS</i> from clinical strain 0911	This study
PA14ΔS <sub>1009</sub>	PA14 Δ <i>mexS</i> <i>trans</i> -complemented with <i>mexS</i> from clinical strain 1009	This study
PA14ΔS <sub>0801</sub>	PA14 Δ <i>mexS</i> <i>trans</i> -complemented with <i>mexS</i> from clinical strain 0801	This study
PA14ΔS <sub>1409</sub>	PA14 Δ <i>mexS</i> <i>trans</i> -complemented with <i>mexS</i> from clinical strain 1409	This study
PA14ΔS <sub>2311</sub>	PA14 Δ <i>mexS</i> <i>trans</i> -complemented with <i>mexS</i> from clinical strain 2311	This study
PA14ΔS <sub>2609</sub>	PA14 Δ <i>mexS</i> <i>trans</i> -complemented with <i>mexS</i> from clinical strain 2609	This study
PA14ΔS <sub>1709</sub>	PA14 Δ <i>mexS</i> <i>trans</i> -complemented with <i>mexS</i> from clinical strain 1709	This study
PA14ΔS <sub>1711</sub>	PA14 Δ <i>mexS</i> <i>trans</i> -complemented with <i>mexS</i> from clinical strain 1711	This study
PA14ΔS <sub>0607</sub>	PA14 Δ <i>mexS</i> <i>trans</i> -complemented with <i>mexS</i> from clinical strain 0607	This study
PA14ΔT <sub>0810</sub>	PA14 Δ <i>mexT</i> <i>trans</i> -complemented with <i>mexT</i> from clinical strain 0810	This study
PA14ΔT <sub>1510</sub>	PA14 Δ <i>mexT</i> <i>trans</i> -complemented with <i>mexT</i> from clinical strain 1510	This study
<i>Escherichia coli</i>		
CC118	Δ( <i>ara-leu</i> ) <i>araD</i> Δ <i>lacX74</i> <i>galE</i> <i>galk</i> <i>phoA20</i> <i>thi-1</i> <i>rpsE</i> <i>rpoB</i> <i>argE</i> (Am) <i>recA1</i>	43
CC118λpir	CC118 lysogenized with λpir phage	44
DH5α	F <sup>-</sup> <i>supE44</i> <i>endA1</i> <i>hsdR17</i> (r <sub>K</sub> <sup>-</sup> m <sub>K</sub> <sup>-</sup> ) <i>thi-1</i> <i>recA1</i> Δ( <i>argF-lacZYA</i> )U169 φ80 <i>dlacZ</i> ΔM15 <i>phoA</i> <i>gyrA96</i> <i>relA1</i> <i>deoR</i> λ <sup>-</sup>	Invitrogen
HB101	<i>supE44</i> <i>hsd</i> (r <sub>B</sub> <sup>-</sup> m <sub>B</sub> <sup>-</sup> ) <i>recA13</i> <i>ara-14</i> <i>proA2</i> <i>lacY1</i> <i>galk2</i> <i>rpsL20</i> <i>xyl-5</i> <i>mtl-1</i> <i>leuB6</i> <i>thi-1</i>	45
<b>Plasmids</b>		
pCR-Blunt	Cloning vector for blunt-end PCR products, <i>lacZ</i> ΔColE1 f1 <i>ori</i> Ap <sup>r</sup> Km <sup>r</sup>	Invitrogen
pRK2013	Helper plasmid, ColE1 <i>ori</i> Tra <sup>+</sup> Mob <sup>+</sup> Km <sup>r</sup>	25
mini-CTX1	Self-proficient integration vector, <i>tet</i> Ω-FRT- <i>attP</i> -MCS <i>ori</i> <i>int</i> <i>oriT</i> Tc <sup>r</sup> <sup>a</sup>	33
pKNG101	Suicide vector in <i>P. aeruginosa</i> , <i>sacB</i> Sm <sup>r</sup>	32

<sup>a</sup> FRT, FLP recombination target; MCS, multiple-cloning site.

production of several quorum-sensing-dependent virulence factors (16) without an apparent loss of fitness (17). The mutants derived from reference strain PAO1 typically produce less pyocyanin, rhamnolipids, and elastase than the wild-type parents (3, 16) and less type III secretion system (T3SS) effector toxin ExoS (18). This phenotype was attributed to (i) reduced intracellular levels of the *Pseudomonas* quinolone signal (PQS), caused by a shortage of a metabolic precursor (kynurenine or 4-hydroxy-2-heptylquinoline [HHQ]) exported by the pump (17, 19), and (ii) MexT acting as a global regulator and indirectly impairing the T3SS in an MexEF-OprN-independent way (18).

Information about the rates and traits of *nfxC* mutants in cystic fibrosis (CF) patients (20, 21) and non-CF patients (12, 22–24) remains scarce. As a plausible explanation, the low virulence of these mutants would be detrimental to their survival in the host or in the hospital setting and would account for their infrequent isolation from clinical samples. Alternatively, these mutants would be phenotypically and genetically distinct from their *in vitro* counterparts (i.e., they would keep some degree of pathogenicity or persistence) and thus would be underrecognized. In this study, we show that most clinical *nfxC* mutants have mild de-

fects in MexS and are still able to produce substantial amounts of virulence factors.

## MATERIALS AND METHODS

**Bacterial strains, plasmids, and growth conditions.** The reference strains and cloning plasmids used in this study are listed in Table 1. Twenty-two clinical *nfxC* mutants collected between May 2012 and May 2013 at the University Hospital of Besançon, Besançon, France (see Table S1 in the supplemental material), and 7 drug-susceptible strains of *P. aeruginosa* collected from surface waters (PE1, PE1346, PE1361, PE1393, PE1423, PE1446, and PE1450) were also investigated. All the bacterial cultures were grown in Mueller-Hinton broth (MHB) with adjusted concentrations of Ca<sup>2+</sup> (range, 20 to 25 mg liter<sup>-1</sup>) and Mg<sup>2+</sup> (range, 10 to 12.5 mg liter<sup>-1</sup>) (Becton Dickinson and Company, Cockeysville, MD) or on Mueller-Hinton agar (MHA; Bio-Rad, Marnes-la-Coquette, France). *Escherichia coli* transformants were selected on MHA containing 50 μg ml<sup>-1</sup> kanamycin (a marker of the vector pCR-Blunt), 15 μg ml<sup>-1</sup> tetracycline (a marker of the vector mini-CTX1), or 50 μg ml<sup>-1</sup> streptomycin (a marker of the vector pKNG101). Recombinant plasmids were introduced into *P. aeruginosa* strains by triparental matings and mobilization with broad-host-range vector pRK2013 in *E. coli* HB101 as a helper strain (25). Transconjugants were selected on *Pseudomonas* isolation agar (PIA;

Becton, Dickinson and Company) supplemented with 200  $\mu\text{g ml}^{-1}$  tetracycline or 2,000  $\mu\text{g ml}^{-1}$  streptomycin, as required. Excision of pKNG101 was obtained by selection on M9 minimal medium (8.54 mM NaCl, 25.18 mM  $\text{NaH}_2\text{PO}_4$ , 18.68 mM  $\text{NH}_4\text{Cl}$ , 22 mM  $\text{KH}_2\text{PO}_4$ , 2 mM  $\text{MgSO}_4$ , pH 7.4) supplemented with 5% sucrose and 0.8% agar.

**Antibiotic susceptibility testing.** The MICs of selected antibiotics were determined by the standard serial 2-fold dilution method in MHA with an inoculum of  $10^4$  CFU per spot, according to CLSI recommendations (26). Growth was assessed visually after 18 h of incubation at 37°C.

**RT-qPCR experiments.** Specific gene expression levels were measured by real-time quantitative PCR (RT-qPCR) after reverse transcription, as described previously (27). Briefly, 2  $\mu\text{g}$  of total RNA was reverse transcribed with ImProm-II reverse transcriptase as specified by the manufacturer (Promega, Madison, WI). The amounts of specific cDNA were assessed in a Rotor Gene RG6000 instrument (Qiagen, Courtaboeuf, France) by using a QuantiFast SYBR PCR green kit (Qiagen). When primers were not already published, the primers used for amplification were designed from the gene sequences available in the *Pseudomonas* Genome Database, version 2, by using primer3 software (<http://bioinfo.ut.ee/primer3-0.4.0/>) (see Table S2 in the supplemental material). For each strain, the mRNA levels of the target genes were normalized to those of the *rpsL* housekeeping gene and expressed as a ratio to the level in wild-type reference strain PA14. Mean gene expression values were calculated from two independent bacterial cultures, each of which was assayed in duplicate. Strain PA14 $\Delta$ S was used as a positive control for *mexE* gene overexpression. As shown in preliminary experiments, all *mexE* transcript levels  $\geq 20$ -fold above the *mexE* transcript level of PA14 were associated with a decreased susceptibility ( $\geq 2$ -fold) of the strains to MexEF-OprN substrate antibiotics and considered significant.

**Virulence factor analysis.** Biofilm production was assessed by measuring bacterial adhesion to 96-well polystyrene plates (28). Cultures were incubated in triplicate in MHB medium overnight at 30°C and washed twice with 200  $\mu\text{l}$  of distilled water to eliminate planktonic bacteria. Attached bacteria were colored by 1% (wt/vol) crystal violet and solubilized by 99% (vol/vol) ethanol. Attachment was evaluated at 600 nm and considered negative when the optical density (OD) was  $< 1$ , as previously reported (19).

Swarming motility was tested on freshly prepared M8 medium (42.2 mM  $\text{Na}_2\text{HPO}_4$ , 22 mM  $\text{KH}_2\text{PO}_4$ , 7.8 mM NaCl, pH 7.4) supplemented with 2 mM  $\text{MgSO}_4$ , 0.5% casein, 0.5% agar, and 1% glucose (29). After 15 min of incubation of the plates at 37°C, 5  $\mu\text{l}$  of culture ( $7.5 \times 10^5$  CFU) was spotted onto the medium surface, with strain PA14 being used as a positive control. The formation of dendrites after 24 h of culture at 37°C was considered a positive result, while a steady spot was considered negative.

Elastase activity was assessed by using MHA plates supplemented with 4 mg  $\text{ml}^{-1}$  elastin-Congo red (Sigma-Aldrich, St. Louis, MO) and inoculated with 5- $\mu\text{l}$  volumes of bacterial suspension ( $7.5 \times 10^5$  CFU). Enzymatic degradation of the substrate formed clear halos around the culture spots after 48 h of incubation at 37°C (30). The absence of a visible halo was considered a negative result.

Rhamnolipid production was appreciated using a hemolysis assay. Briefly, after 18 h of growth at 37°C in agitated MHB ( $A_{600} = 6.7 \pm 0.4$ ), bacterial supernatants containing rhamnolipids were collected and mixed with defibrinated horse blood diluted 1/100 (vol/vol) in phosphate-buffered saline. After 30 min of incubation at room temperature, the mixture was centrifuged for 10 min at  $950 \times g$ . The concentration of hemoglobin in the supernatants was determined spectrophotometrically at 405 nm. OD values were expressed as the percent hemolysis relative to the complete hemolysis achieved with Triton X-100 (by definition, 100%). The results presented are mean values from two independent experiments. Hemolytic activity was considered to be significantly reduced when it was less than 50% of that for the control.

Finally, pyocyanin assays were carried out on culture supernatants after 18 h of growth at 37°C in a specific broth [120 mM Tris HCl, pH 7.2,

0.1% tryptone, 20 mM  $(\text{NH}_4)_2\text{SO}_4$ , 1.6 mM  $\text{CaCl}_2$ , 10 mM KCl, 24 mM sodium citrate, 50 mM glucose] ( $A_{600} = 1.6 \pm 0.2$ ). The pigment was extracted from the cultures with chloroform (1 volume) and mixed with 0.1 M HCl (0.06 volume) before spectrophotometric measurement at 520 nm (31). Results are mean values from two independent experiments. Pyocyanin production was considered to be significantly reduced when it was less than 50% of that of reference strain PA14 grown under the same conditions.

The virulence factor production of individual clinical strains was rated by a global score ranging from 0 to 5, which corresponds to the number of positive or significant results obtained by each of the 5 assays mentioned above, the result of each of which was given a value of 1 if it was positive or significant.

**Construction of deletion mutants from strain PA14.** Single *mexS* and *mexT* deletion mutants were constructed by using overlapping PCRs and recombination events, as described by Kaniga et al. (32). First, the 5' and 3' regions flanking *mexS* (417 and 433 bp, respectively) and *mexT* (408 and 453 bp, respectively) were individually amplified by PCR with specific primers (see Table S2 in the supplemental material) under the following conditions: 3 min of denaturation at 98°C followed by 30 cycles of amplification, each of which was composed of 10 s at 98°C, 30 s at 60°C, and 30 s at 72°C, and a final extension step of 7 min at 72°C. The resultant amplicons were used as the templates for overlapping PCRs with external pairs of primers to generate the mutagenic DNA fragments. The reaction mixtures contained  $1 \times$  iProof HF master mix, 3% dimethyl sulfoxide, and 0.5  $\mu\text{M}$  each primer (Bio-Rad). The amplified products were cloned into plasmid pCR-Blunt according to the manufacturer's instructions (Invitrogen, Carlsbad, CA) and next subcloned as BamHI/ApaI fragments into the suicide vector pKNG101 in *E. coli* CC118 $\lambda$ pir (32). The recombinant plasmids were transferred into *P. aeruginosa* by conjugation and selected on PIA containing 2,000  $\mu\text{g ml}^{-1}$  streptomycin. The excision of the undesired pKNG101 sequence was performed by plating transformants on M9 minimal medium plates containing 5% (wt/vol) sucrose and 1% (wt/vol) glucose. Negative selection on streptomycin was carried out to confirm the loss of the plasmid. The allelic exchanges were confirmed by PCR. Nucleotide sequencing experiments confirmed deletion of 826 bp in *mexS* and 929 bp in *mexT*, yielding strains PA14 $\Delta$ S and PA14 $\Delta$ T, respectively.

**Chromosomal complementation with full-length *mexS* and *mexT*.** A search for mutations in the *mexS* and *mexT* genes, as well as in the *mexS-mexT* and *mexT-mexE* intergenic regions, was performed with 43 clinical strains by using the primers listed in Table S2 in the supplemental material. The mutated *mexS* and *mexT* genes along with their respective promoter regions were amplified from purified genomic DNA by PCR. The resulting DNA fragments were cloned into plasmid pCR-Blunt and next ligated to BamHI/HindIII-linearized plasmid mini-CTX1 (33). The recombinant plasmids were then transferred from *E. coli* CC118 to *P. aeruginosa* strains PA14 $\Delta$ *mexS* or PA14 $\Delta$ *mexT* by conjugation with subsequent selection on PIA plates containing 200  $\mu\text{g ml}^{-1}$  tetracycline, to allow their chromosomal insertion into the *attB* site. Chromosomal integration was confirmed by PCR and sequencing.

## RESULTS AND DISCUSSION

**Wild-type genes *mexS* and *mexT*.** Strains PAO1 (3, 8, 34), PA14 (10), and PAK (35) have alternatively been used as wild-type reference strains in studies on the MexEF-OprN efflux pump. However, the *mexS* and *mexT* genes in these strains show a nonsilent sequence polymorphism whose impact on the functionality of the encoded proteins, MexS and MexT, respectively, remained to be clarified. For instance, in addition to carrying an 8-bp intragenic fragment inactivating *mexT* (7), most of the laboratory strains of the PAO1 lineage differ from PA14 (or PAK) by an aspartic acid residue (D) instead of an asparagine (N) at position 249 ( $D_{249}$ ) in MexS (<http://pseudomonas.com>).



TABLE 2 Genotypes and resistance profiles of *nfxC* mutants

Strain	Sequence		<i>mexE</i> transcript level <sup>c</sup>	MIC ( $\mu\text{g ml}^{-1}$ ) <sup>d</sup>				
	MexS or <i>mexS</i> <sup>a</sup>	MexT or <i>mexT</i> <sup>b</sup>		CHL	CIP	IMP	TIC	AMK
Reference strains								
PA14	WT	WT	1	64	0.12	1	16	2
PA14 $\Delta$ S	$\Delta$ 809 bp (bp 1–809)	WT	<b>427</b>	2,048	2	2	8	0.5
PA14 $\Delta$ S <sub>PA14</sub>	WT	WT	1.9	64	0.12	1	16	2
PA14 $\Delta$ S <sub>PAO1</sub>	N <sub>249</sub> D	WT	<b>87</b>	2,048	2	2	8	1
PA14 $\Delta$ T	WT	$\Delta$ 883 bp (bp 32–915)	<b>0.4</b>	64	0.12	1	16	2
PA14 $\Delta$ T <sub>PA14</sub>	WT	WT	6.2	64	0.12	1	16	2
PAO1	N <sub>249</sub> D	+8 bp (at bp 118)	0.2	16	0.12	1	16	8
PAO7H	N <sub>249</sub> D	WT	<b>265</b>	2,048	2	4	8	4
Clinical strains with no mutation in <i>mexS</i> and <i>mexT</i>								
2502	WT	WT	<b>35</b>	256	0.25	8	64	2
1206	WT	WT	<b>41</b>	512	0.5	2	64	4
0708	WT	WT	<b>53</b>	256	0.25	1	64	4
0309	WT	WT	<b>28</b>	128	1	1	64	2
2607	WT	WT	<b>39</b>	256	0.5	2	64	4
0712	WT	WT	<b>325</b>	2,048	2	4	16	16
0608	WT	WT	<b>25</b>	256	0.25	2	64	8
Clinical strains with mutations in <i>mexS</i>								
1307	V <sub>104</sub> A	WT	<b>29</b>	256	16	2	64	8
2310	F <sub>253</sub> L	WT	<b>183</b>	1,024	0.5	4	32	8
2505	D <sub>44</sub> E	WT	<b>212</b>	512	64	16	32	4
3005	S <sub>60</sub> F	WT	<b>259</b>	2,048	1	4	8	4
0911	F <sub>185</sub> L	WT	<b>133</b>	1,024	0.5	4	8	2
1009	V <sub>73</sub> A + L <sub>270</sub> Q	WT	<b>312</b>	1,024	32	8	128	8
0801	C <sub>245</sub> G	WT	<b>81</b>	256	0.5	4	128	64
1409	A <sub>166</sub> P	WT	<b>179</b>	1,024	2	4	8	2
2311	S <sub>60</sub> P	WT	<b>455</b>	1,024	1	4	4	2
2609	L <sub>263</sub> Q	WT	<b>534</b>	2,048	1	4	8	2
1709	$\Delta$ 8 bp (bp 710–718)	WT	<b>552</b>	2,048	2	4	8	2
1711	$\Delta$ C <sub>293</sub>	WT	<b>825</b>	32	1	2	32	8
0607	$\Delta$ 30 bp (bp 927–956)	WT	<b>556</b>	512	1	8	4	2
Clinical strains with mutations in <i>mexT</i>								
0810	WT	G <sub>258</sub> D	<b>254</b>	512	8	4	128	2
1510	WT	Y <sub>138</sub> D + G <sub>258</sub> D	<b>20</b>	256	0.25	16	128	1

<sup>a</sup> MexS (339 aa) of PA14 is functional (N<sub>249</sub>) and is considered the wild type (WT), contrary to PAO1-UW (D<sub>249</sub>) ([www.pseudomonas.com](http://www.pseudomonas.com)). aa, amino acid.

<sup>b</sup> MexT (304 aa) of PA14 is functional and is considered the wild type, contrary to PAO1-UW (+8 bp [starting at bp 118]) ([www.pseudomonas.com](http://www.pseudomonas.com)).

<sup>c</sup> Expressed as a ratio to that of wild-type reference strain PA14. *nfxC* mutants (the values for which are in bold) have a transcript level of  $\geq 20$ .

<sup>d</sup> CHL, chloramphenicol; CIP, ciprofloxacin; IMP, imipenem; TIC, ticarcillin; AMK, amikacin.

Because the MexS-D<sub>249</sub> protein was considered either functional (7) or nonfunctional (35), we deleted *mexS* in both PA14 and PAO1 and compared the effects of this deletion on *mexEF-oprN* expression and antibiotic resistance. In PA14, suppression of *mexS* (strain PA14 $\Delta$ S) resulted in a strong increase in *mexE* transcription (427-fold) and in a 16- to 32-fold higher resistance to MexEF-OprN substrates, as in typical *nfxC* mutants (Table 2). As expected, complementation of PA14 $\Delta$ S with the PA14 *mexS* allele (PA14 $\Delta$ S<sub>PA14</sub>) restored the drug-susceptible phenotype. In contrast, the PAO1 *mexS* allele had virtually no impact on the resistance levels of strain PA14 $\Delta$ S (strain PA14 $\Delta$ S<sub>PAO1</sub>) and failed to reverse the overexpression of *mexE*, whose transcripts remained 45-fold more abundant in PA14 $\Delta$ S in comparison with PA14 *mexS* allele. Consistent with PAO1 producing inactive MexS-D<sub>249</sub>

and MexT peptides, spontaneous excision of the extra 8-bp sequence inserted in *mexT* is known to trigger MexEF-OprN production in this strain, with MexT recovering its functionality in a nonfunctional MexS background (36). Confirming that MexS-N<sub>249</sub> (and not MexS-D<sub>249</sub>) is functional, analysis of 7 drug-susceptible strains of *P. aeruginosa* collected from surface waters (PE1, PE1346, PE1361, PE1393, PE1423, PE1446, and PE1450) showed that the genomes of all of them encoded MexS-N<sub>249</sub> together with an active MexT (without any insertion in the *mexT* gene) (data not shown). Based on these results, we therefore used strain PA14 instead of PAO1 in further experiments to investigate the functionality of MexS and MexT from clinical *nfxC* mutants.

**Selection of clinical *nfxC* mutants.** We screened a collection of 221 clinical isolates of *P. aeruginosa* exhibiting a reduced suscep-

tibility to ciprofloxacin, a substrate of MexEF-OprN, and imipenem, a substrate of porin OprD, whose expression is inversely coregulated with that of MexEF-OprN (6). The ciprofloxacin and imipenem concentrations used in the screening were equal to the MIC values for reference strain PA14 (0.12  $\mu\text{g ml}^{-1}$  and 1  $\mu\text{g ml}^{-1}$ , respectively; Table 2). As resistance to these antibiotics may also be due to other efflux pumps (e.g., MexXY/OprM, MexCD-OprJ, MexAB-OprM) as well as other mechanisms (e.g., fluoroquinolone target alterations, mutational loss of porin OprD), the levels of the *mexE* transcripts were determined in all the strains by RT-qPCR. Forty-three (19.5%) of the 221 selected isolates were found to significantly overexpress *mexE* ( $\geq 20$ -fold) compared with the level of *mexE* expression by PA14 (data not shown). According to available clinical data, these 43 *nfxC* mutants were involved in the colonization or infection of 17 patients (from 1 to 12 isolates per patient) admitted to various medical and surgical units of University Hospital of Besançon, Besançon, France (see Table S1 in the supplemental material). Most of these patients (12/17) were treated with antibiotics prior to the isolation of the *nfxC* mutant strains, including 7/12 treated with fluoroquinolones known to easily select *nfxC* mutants (22, 37). Sequencing of the *mexS* and *mexT* genes (data not shown) allowed us to identify the redundant mutants in individual patients and to eventually retain 22 strains (1, 2, or 3 different strains per patient) for further investigations (see Table S1 in the supplemental material).

**Drug susceptibility of clinical *nfxC* mutant isolates.** The level of overexpression of the *mexE* gene was found to vary greatly among the 22 clinical mutants (from 20- to 825-fold the level of expression by PA14; Table 2). These elevated values were associated with an increased resistance of the strains (except strain 1711) to the MexEF-OprN substrates chloramphenicol (MIC range, 2- to 32-fold the MIC for PA14) and ciprofloxacin (MIC range, 2- to 512-fold the MIC for PA14), though the possibility that additional mechanisms may have influenced the drug MICs cannot be excluded. For unclear reasons, one strain, 1711, turned out to be more susceptible (2-fold) to chloramphenicol than PA14, despite the strong upregulation of its *mexE* gene (825-fold). As indicated in Table 2, 20/22 strains exhibited a 2- to 16-fold decrease in susceptibility to imipenem compared with that of PA14, possibly due to the MexT-dependent downregulation of specific porin OprD (6), a mutational loss of OprD, and/or carbapenemase production (38). Finally, the reported hypersusceptibility of typical *in vitro nfxC* mutants to the MexAB-OprM substrate ticarcillin and to the MexXY(OprM) substrate amikacin (4) was observed in only 7 strains and 1 strain, respectively, suggesting that this hypersusceptible phenotype either arises in specific genetic backgrounds, such as the PAO1 and PA14 backgrounds, or is masked in most clinical *nfxC* strains by additional mechanisms. It should be noted that because of this phenotypic variability, MexEF-OprN-overproducing mutants may be difficult to recognize in the medical laboratory unless molecular biology techniques are used.

**Amino acid variations in the MexT regulator.** MexT needs to be functional to activate *mexEF-oprN* operon expression in *nfxC* mutants (6). Concordant with this, DNA sequencing revealed that 20/22 strains (91%) produced a MexT protein identical to that of PA14 (Table 3). Interestingly, 2/22 strains (9%) harbored *mexT* genes with point mutations resulting in one ( $G_{258}D$ ; strain 0810) or two ( $Y_{138}D$  and  $G_{258}D$ ; strain 1510) amino acid substitutions in the effector-binding domain of MexT. In these isolates, the sequence of *mexS*, as well as the sequences of the *mexS-mexT* and

*mexT-mexE* intergenic regions, was identical to that of PA14 (Table 2). To investigate the impact of the  $G_{258}D$  substitution and the  $Y_{138}D$  plus  $G_{258}D$  substitutions on MexT activity, we complemented PA14 $\Delta T$  with the *mexT* alleles from strains 0810 and 1510. The expression of the *mexE* gene, the drug resistance, and the virulence factor score of PA14 $\Delta T$  were unaffected by the complementation (data not shown), indicating that neither  $Y_{138}D$  nor  $G_{258}D$  influences MexT activity, as the mutational activation of MexT would have induced *mexEF-oprN* expression in a functional MexS background. Also, these results indirectly imply that still unknown mutations are involved in the NfxC phenotype of isolates 0810 and 1510.

**Impact of alterations in *mexS* on resistance and virulence.** Experimental results from our university laboratory (unpublished data) and of other research groups (8) indicate that most (77% and 66%, respectively) *nfxC* mutants selected *in vitro* on MexEF-OprN substrates, such as ciprofloxacin and chloramphenicol, harbor nucleotide deletions or insertions in the *mexS* gene that are predicted to result in inactive MexS peptides. In the present study, intriguingly, only 13.6% ( $n = 3/22$ ) of the strains turned out to carry such indels in *mexS*, whereas 45.5% ( $n = 10/22$ ) exhibited point mutations resulting in one ( $n = 9$  strains) or two ( $n = 1$  strain) amino acid substitutions in the MexS oxidoreductase. The remaining 41% ( $n = 9/22$ ) harbored a PA14-like, wild-type MexS (Table 2). The latter 9 strains were found to produce a MexT identical to that of PA14 ( $n = 7$ ) or harbor the nonsignificant amino acid variations  $Y_{138}D$  and  $G_{258}D$  ( $n = 2$ ; see above). As the *mexS-mexT* and *mexT-mexE* intergenic regions were 100% identical between the 9 strains and PA14, these results unambiguously demonstrate that mutations in still unknown loci (other than *mexS* and *mexT*) are able to upregulate *mexEF-oprN* expression in clinical strains.

Because amino acid substitutions may have less dramatic effects on MexS activity than disruption of the *mexS* gene, we cloned the 13 mutated *mexS* alleles in plasmid mini-CTX and complemented mutant PA14 $\Delta S$  by chromosomal insertion of the cloned genes into the *attB* site. RT-qPCR experiments showed that all the transconjugants except one (complemented with MexS- $V_{104}A$  from strain 1307) significantly overexpressed the efflux operon (Table 3). The *mexE* mRNA levels were significantly correlated (Spearman's  $\rho = 0.96$ ,  $P < 0.01$ ) with the ciprofloxacin MICs (Fig. 1A). As expected, complementation with indel-carrying *mexS* alleles (from strains 1709, 1711, and 0607) failed to decrease the expression levels of *mexE* or the MICs of chloramphenicol (2,048  $\mu\text{g ml}^{-1}$ ) and ciprofloxacin (4  $\mu\text{g ml}^{-1}$ ) (compared with those for PA14 $\Delta S$ ; Table 3). Wild-type levels of resistance to imipenem, ticarcillin, and amikacin were also not restored in the null mutant upon complementation. Similar results were obtained with MexS- $L_{263}Q$  (from strain 2609), supporting the notion that this mutation is strongly detrimental to MexS activity. As an indication that the remaining mutations (except the well-tolerated variation  $V_{104}A$  from strain 1307) partially compromise but do not abolish MexS activity, complementation of PA14 $\Delta S$  with other MexS variants reduced the level of *mexE* expression from 1.9- to 20.3-fold and its level of resistance to both chloramphenicol and ciprofloxacin from 2- to 8-fold (Table 3). This was accompanied by the restoration of wild-type susceptibility to imipenem, ticarcillin, and amikacin in 1 (strain 2310 with MexS- $F_{253}L$ ), 8, and 0 complemented mutants, respectively. Upon complementation with MexS- $F_{253}L$ , gene *oprD* expression was increased to

TABLE 3 Genotypes and phenotypes of PA14ΔS complemented with mutated *mexS* alleles from clinical isolates

Strain	MexS sequence (339 aa <sup>f</sup> )	Transcript level <sup>g</sup>										MIC (mg ml <sup>-1</sup> ) <sup>h</sup>						Virulence factor activity <sup>e</sup>				Virulence score <sup>c</sup>
		<i>mexE</i>	<i>mexS</i>	<i>mexT</i>	<i>oprD</i>	<i>mexB</i>	<i>mexY</i>	CHL	CIP	IMP	MEM	TIC	AMK	Biofilm formation (OD <sub>600</sub> )	Swarming motility	Elastase production (mm)	Hemolytic activity <sup>d</sup> (%)	Pyocyanin production <sup>d</sup> (%)				
PA14	WT <sup>g</sup>	1	1	1	1	1	1	64	0.12	1	0.5	16	2	2.6	+	18	72	100	5			
PA14ΔS	Δ809 bp (aa 1–809)	427	ND <sup>h</sup>	0.9	0.3	0.4	0.4	2,048	4	2	1	8	0.5	0.4	–	12	22	13	1			
PA14ΔS <sub>P<sub>14</sub></sub>	WT	1.9	1.3	1.5	1	1	1	64	0.12	1	0.5	16	2	2.7	+	18	79	92	5			
PA14ΔS <sub>I307</sub>	V <sub>104</sub> A	0.8	1.2	1.4	1.8	1.1	1.2	64	0.12	1	0.5	16	2	4.4	+	16	70	114	5			
Strains with mild substitutions in MexS																						
PA14ΔS <sub>233L</sub>	F <sub>233</sub> L	21	4	1	0.9	1	0.8	256	0.5	1	0.5	16	1	2.8	+	16	70	84	5			
PA14ΔS <sub>2310</sub>	D <sub>244</sub> E	35	5.2	1.2	0.4	0.7	0.7	512	1	2	1	16	1	1.7	+	17	70	18	4			
PA14ΔS <sub>2505</sub>	S <sub>60</sub> F	71	4.8	1.2	0.4	1	0.7	512	1	2	1	16	1	1.7	+	16	68	18	4			
PA14ΔS <sub>3005</sub>	F <sub>185</sub> L	59	3.7	1.5	0.6	1.4	0.8	512	1	2	1	16	1	2.2	+	17	58	40	4			
PA14ΔS <sub>3091</sub>	V <sub>73</sub> A + I <sub>270</sub> Q	43	5.8	1.4	0.5	1.2	0.8	512	1	2	1	16	1	1.8	+	16	53	21	4			
PA14ΔS <sub>1009</sub>	C <sub>245</sub> G	83	4	1.7	0.5	1.1	0.8	512	1	2	1	16	1	2.3	+	16	71	70	5			
PA14ΔS <sub>0880</sub>	A <sub>166</sub> P	83	5.1	1.9	0.4	1.2	0.8	1,024	2	2	1	16	1	1.6	+	16	67	22	4			
PA14ΔS <sub>1409</sub>	S <sub>60</sub> P	230	9.1	1.7	0.4	1	0.8	1,024	2	2	1	16	1	1.2	+	16	59	33	4			
Strains in which MexS is inactivated																						
PA14ΔS <sub>2609</sub>	L <sub>263</sub> Q	320	6.9	1.1	0.2	0.8	0.5	2,048	4	2	1	8	0.5	0.2	+/-	16	21	14	1			
PA14ΔS <sub>1709</sub>	Δ8 bp (aa 710–718)	334	5.1	1.7	0.5	0.6	0.4	2,048	4	2	1	8	0.5	0.6	–	13	32	17	1			
PA14ΔS <sub>1711</sub>	ΔC <sub>293</sub>	404	2.6	1.7	0.7	0.6	0.6	2,048	4	2	1	8	0.5	0.7	–	11	37	13	1			
PA14ΔS <sub>8607</sub>	Δ30 bp (aa 927–956)	492	8	1.9	0.5	0.8	0.6	2,048	4	2	1	8	0.5	0.6	–	13	20	21	1			

<sup>a</sup> Expressed as a ratio relative to that of wild-type reference strain PA14. *nfxC* mutants (the values for which are in bold) have a *mexE* transcript level of  $\geq 20$ .

<sup>b</sup> CHL, chloramphenicol; CIP, ciprofloxacin; IMP, imipenem; MEM, meropenem; TIC, ticarcillin; AMK, amikacin.

<sup>c</sup> The results for virulence factors are in bold when they are positive or considered significant. OD<sub>600</sub>, OD at 600 nm.

<sup>d</sup> Hemolytic activity and pyocyanin production were measured on stationary-phase cultures after 18 h of growth (see Materials and Methods for details).

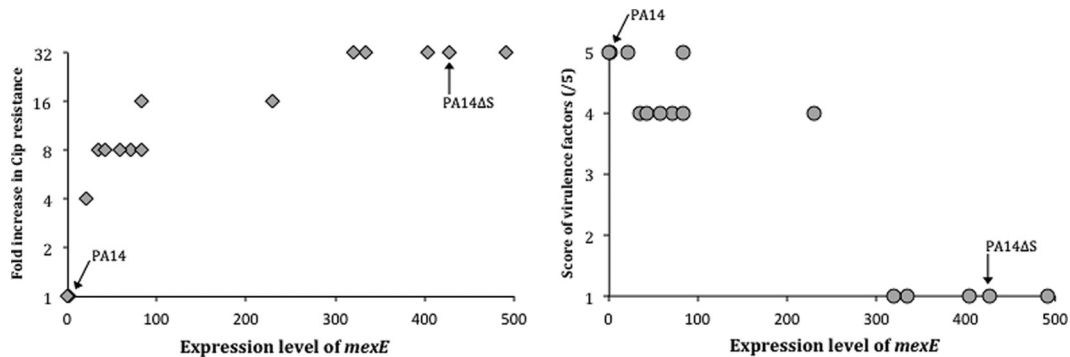
<sup>e</sup> The score was determined from the results of each test (biofilm formation, swarming motility, elastase production, hemolytic activity, pyocyanin production), positivity by each of which was given a value of 1. Of note, swarming motility and biofilm formation are correlated with rhamnolipid production.

<sup>f</sup> aa, amino acid.

<sup>g</sup> WT, wild type.

<sup>h</sup> ND, not detected.

<sup>i</sup> The strain tolerated substitutions in MexS.



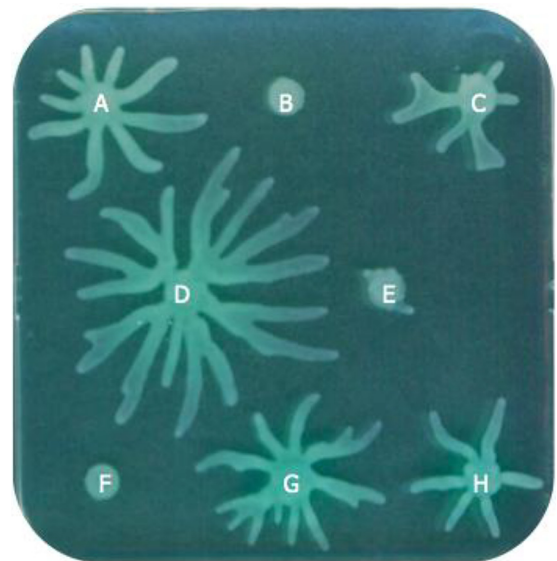
**FIG 1** Correlation between levels of *mexE* expression, resistance, and virulence factor production in strain PA14ΔS complemented with *mexS* alleles from 13 clinical isolates. The expression levels of the *mexEF-oprN* operon, as assessed by RT-qPCR of the *mexE* gene, are expressed as the ratios to the level of *mexEF-oprN* expression by wild-type strain PA14 (set at a value of 1, by definition). Ciprofloxacin (Cip) MICs (diamonds) are expressed as ratios relative to the ciprofloxacin MIC for PA14. The virulence factor scores (circles) were determined by the number of positive results by 5 different tests (biofilm formation, swarming motility, elastase production, hemolytic activity, and pyocyanin production), as indicated in Table 3. The negative and positive controls, strains PA14 and PA14ΔS, respectively, are indicated. The relationships between the variables *mexE* expression and ciprofloxacin MIC (Spearman's rho = 0.96,  $P < 0.01$ ) and the variables *mexE* expression and virulence factor scores (Spearman's rho = -0.87,  $P < 0.01$ ) were found to be significant.

wild-type levels (0.9-fold that of PA14), while *mexE* expression was strongly repressed (20.3-fold that of PA14), providing further evidence that F<sub>253</sub>L only weakly affects MexS activity. The mRNA levels of the *oprD* gene in PA14ΔS were not impacted or were only marginally impacted by expression of disrupted *mexS* genes or alleles encoding amino acid variations other than V<sub>104</sub>A and F<sub>253</sub>L, consistent with the unchanged resistance of PA14ΔS to imipenem upon complementation. The hypersusceptibility of *in vitro* *nfxC* mutants to some β-lactam antibiotics, such as ticarcillin, has been proposed to result from *nfxC*-dependent repression of the *mexAB-oprM* operon (39). As shown in Table 3, inactivation of MexS by indels or L<sub>263</sub>Q failed to restore wild-type ticarcillin susceptibility in transcomplemented strain PA14ΔS (for which the ticarcillin MIC was 2-fold lower than that for PA14), while less severe alterations did. Nevertheless, *mexB* expression was not significantly different among the transcomplemented mutants, with the level of expression by the mutants ranging from 0.6- to 1.4-fold that by PA14, which suggests the existence of more complex interplays between MexAB-OprM and MexEF-OprN in *nfxC* mutants, as already evoked (4). None of the *mexS* alleles except those encoding the V<sub>104</sub>A substitution was able to increase the levels of *mexY* expression and amikacin MICs up to wild-type levels in PA14ΔS (Table 3). However, the slight effect (a 2-fold increase in the MIC) was visible for strains with alleles with mutations resulting in mild defects but was absent for strains with alleles with mutations resulting in severe defects.

The virulence traits of the transcomplemented PA14ΔS mutants varied greatly according to the different *mexS* alleles. As for PA14ΔS, mutations leading to the complete inactivation of MexS and strong *mexE* upregulation (in alleles from strains 2609, 1709, 1711, and 0607) were associated with a low virulence score of 1 (Fig. 1B). Biofilm formation, swarming motility (Fig. 2), hemolytic activity, as well as pyocyanin production remained strongly impaired in the transcomplemented mutants (Table 3). Complementation with the other alleles (from strains 2310, 2505, 3005, 0911, 1009, 0801, 1409, and 2311) partially restored the wild-type virulence traits in PA14ΔS, yielding scores of 4 and 5. However, the level of pyocyanin

production remained low in most of these complemented mutants (from 0.2- to 0.8-fold that of PA14ΔS<sub>PA14</sub>) and showed no evident correlation with *mexE* expression levels, as was observed in mutants PA14ΔS<sub>0801</sub> and PA14ΔS<sub>1409</sub> in Table 3.

Consistent with our previous conclusions, the *mexS* allele encoding the well-tolerated substitution V<sub>104</sub>A provided PA14ΔS with a wild-type phenotype of resistance and virulence (Fig. 2), indicating that *mexEF-oprN* overexpression in strain 1307 is due to *mexS*-independent (and also *mexT*-independent) genetic events.



**FIG 2** Swarming motility of PA14ΔS complemented with different mutated *mexS* alleles from clinical isolates. Swarming motility was evaluated as the capacity to give rise to dendrite-like patterns. The patterns for strain PA14 and PA14ΔS<sub>PA14</sub> (positive controls) (A and C, respectively) and PA14ΔS (negative control) (B) are indicated. (F) Inactivation leading to an aberrant MexS protein (in PA14ΔS<sub>1711</sub>, for example) abolished the swarming. In most cases, substitutions in MexS, for example, V<sub>104</sub>A (D), F<sub>185</sub>L (G), and D<sub>44</sub>E (H), did not affect the ability of the bacteria to swarm; however, the L<sub>263</sub>Q substitution led to an almost complete loss of motility (E).

**Other regulatory genes in *nfxC* mutants.** As reported above, 10/22 clinical strains (strains 2502, 1206, 0708, 0309, 2607, 0712, 0608, 1307, 0810, and 1510) appeared to produce functional MexS and MexT proteins. Since mutations in genes coding for the global regulators MvaT and AmpR have been reported to activate the *mexEF-oprN* operon in *in vitro*-selected *nfxC* mutants (13, 14), we carried out sequencing experiments, which eventually failed to reveal alterations in these genes. Again, these results clearly indicate that other loci are implicated in pump MexEF-OprN overproduction in the clinical setting.

**Conclusion.** This study provides an insight into the genetic events leading to MexEF-OprN overproduction in clinical *nfxC* isolates. The hypothesis of preferential selection of partially derepressed MexEF-OprN mutants rather than fully derepressed ones *in vivo* is reinforced by our observation that *mexE* expression was lower in most clinical *nfxC* mutants (mean, 205-fold  $\pm$  187-fold that of wild-type strain PA14; median, 179-fold that of wild-type strain PA14) than in comparator strain PA14 $\Delta$ S (427-fold that of wild-type strain PA14) (Table 2). None of the amino acid variations found in the *mexT* product (2/22 isolates, 9%) proved to be significant, a result consistent with the observation that LysR regulators are rarely constitutively activated by mutations (e.g., BenM in *Acinetobacter baylyi* and CysB in *Salmonella enterica* serovar Typhimurium) (40, 41). In contrast, single point mutations in the MexS oxidoreductase (9/22, 40.9%) represent a significant cause of MexEF-OprN upregulation in clinical *P. aeruginosa* strains. Consistent with these findings, a decrease in ciprofloxacin MICs from 2- to 4-fold was observed in 7 clinical *nfxC* mutants upon complementation with a plasmid-borne copy of *mexS* from strain PA14 (see Table S3 in the supplemental material). Of note, another mutation in MexS (A<sub>155</sub>V) leading to multidrug resistance has recently been reported in a clinical isolate (42). Our results demonstrate that most MexEF-OprN-overproducing clinical strains either have a wild-type, PA14-like MexS (10/22, 45.5%) or are only partially deficient in MexS activity (8/22, 36.3%). Mutants harboring these mutations resulting in presumed mild defects display resistance and virulence traits intermediate between those of wild-type strains and strongly defective MexS mutants (4/22, 18.2%), which could account for their emergence *in vivo*. However, analysis of our clinical strains gave contrasting results (see Table S4 in the supplemental material), reinforcing the idea that the virulence of *P. aeruginosa* is multifactorial and factors other than those tested in this study may well contribute to the pathogenicity of strongly deficient *mexS* mutants, some of which were still able to cause infections. The MexEF-OprN overproducers studied here had similar growth rates (data not shown). Finally, this work indirectly demonstrates that still unknown regulators are involved in the activation of *mexEF-oprM* in 10/22 (45.5%) clinical *nfxC* mutants. We are currently trying to determine such regulatory pathways.

#### ACKNOWLEDGMENTS

We thank Fabrice Poncet and Amandine Mariot (SFR FED 4234, Besançon, France) for DNA sequencing data and Lois Andrey for technical assistance. We also thank the Centre National de Référence (CNR) de la Résistance aux Antibiotiques for the provision of clinical *NfxC* isolates. Steffi Rocchi contributed to statistical analyses.

This work was supported by a grant from the French Ministère de l'Enseignement Supérieur et de la Recherche.

We have no competing interests to declare.

#### FUNDING INFORMATION

French Ministère de l'Enseignement Supérieur et de la Recherche provided funding to Charlotte Richardot.

#### REFERENCES

- Gellatly SL, Hancock RE. 2013. *Pseudomonas aeruginosa*: new insights into pathogenesis and host defenses. *Pathog Dis* 67:159–173. <http://dx.doi.org/10.1111/2049-632X.12033>.
- Poole K, Srikumar R. 2001. Multidrug efflux in *Pseudomonas aeruginosa*: components, mechanisms and clinical significance. *Curr Top Med Chem* 1:59–71. <http://dx.doi.org/10.2174/1568026013395605>.
- Köhler T, Michea-Hamzehpour M, Henze U, Gotoh N, Curty LK, Pechère JC. 1997. Characterization of MexE-MexF-OprN, a positively regulated multidrug efflux system of *Pseudomonas aeruginosa*. *Mol Microbiol* 23:345–354. <http://dx.doi.org/10.1046/j.1365-2958.1997.2281594.x>.
- Li XZ, Barre N, Poole K. 2000. Influence of the MexA-MexB-OprM multidrug efflux system on expression of the MexC-MexD-OprJ and MexE-MexF-OprN multidrug efflux systems in *Pseudomonas aeruginosa*. *J Antimicrob Chemother* 46:885–893. <http://dx.doi.org/10.1093/jac/46.6.885>.
- Schweizer HP. 2003. Efflux as a mechanism of resistance to antimicrobials in *Pseudomonas aeruginosa* and related bacteria: unanswered questions. *Genet Mol Res* 2:48–62.
- Köhler T, Epp SF, Curty LK, Pechère JC. 1999. Characterization of MexT, the regulator of the MexE-MexF-OprN multidrug efflux system of *Pseudomonas aeruginosa*. *J Bacteriol* 181:6300–6305.
- Maseda H, Saito K, Nakajima A, Nakae T. 2000. Variation of the mexT gene, a regulator of the MexEF-OprN efflux pump expression in wild-type strains of *Pseudomonas aeruginosa*. *FEMS Microbiol Lett* 192:107–112. <http://dx.doi.org/10.1111/j.1574-6968.2000.tb09367.x>.
- Sobel ML, Hocquet D, Cao L, Plesiat P, Poole K. 2005. Mutations in PA3574 (nalD) lead to increased MexAB-OprM expression and multidrug resistance in laboratory and clinical isolates of *Pseudomonas aeruginosa*. *Antimicrob Agents Chemother* 49:1782–1786. <http://dx.doi.org/10.1128/AAC.49.5.1782-1786.2005>.
- Tian ZX, Fargier E, Mac Aogain M, Adams C, Wang YP, O'Gara F. 2009. Transcriptome profiling defines a novel regulon modulated by the LysR-type transcriptional regulator MexT in *Pseudomonas aeruginosa*. *Nucleic Acids Res* 37:7546–7559. <http://dx.doi.org/10.1093/nar/gkp828>.
- Fargier E, Mac Aogain M, Mooij MJ, Woods DF, Morrissey JP, Dobson AD, Adams C, O'Gara F. 2012. MexT functions as a redox-responsive regulator modulating disulfide stress resistance in *Pseudomonas aeruginosa*. *J Bacteriol* 194:3502–3511. <http://dx.doi.org/10.1128/JB.06632-11>.
- Frisk A, Schurr JR, Wang G, Bertucci DC, Marrero L, Hwang SH, Hassett DJ, Schurr MJ. 2004. Transcriptome analysis of *Pseudomonas aeruginosa* after interaction with human airway epithelial cells. *Infect Immun* 72:5433–5438. <http://dx.doi.org/10.1128/IAI.72.9.5433-5438.2004>.
- Llanes C, Köhler T, Patry I, Dehecq B, van Delden C, Plésiat P. 2011. Role of the MexEF-OprN efflux system in low-level resistance of *Pseudomonas aeruginosa* to ciprofloxacin. *Antimicrob Agents Chemother* 55:5676–5684. <http://dx.doi.org/10.1128/AAC.00101-11>.
- Westfall LW, Carty NL, Layland N, Kuan P, Colmer-Hamood JA, Hamood AN. 2006. *mvaT* mutation modifies the expression of the *Pseudomonas aeruginosa* multidrug efflux operon *mexEF-oprN*. *FEMS Microbiol Lett* 255:247–254. <http://dx.doi.org/10.1111/j.1574-6968.2005.00075.x>.
- Balasubramanian D, Schnepfer L, Merighi M, Smith R, Narasimhan G, Lory S, Mathee K. 2012. The regulatory repertoire of *Pseudomonas aeruginosa* AmpC  $\beta$ -lactamase regulator AmpR includes virulence genes. *PLoS One* 7:e34067. <http://dx.doi.org/10.1371/journal.pone.0034067>.
- Zaoui C, Overhage J, Lons D, Zimmermann A, Musken M, Bielecki P, Pustelny C, Becker T, Nimitz M, Haussler S. 2012. An orphan sensor kinase controls quinolone signal production via MexT in *Pseudomonas aeruginosa*. *Mol Microbiol* 83:536–547. <http://dx.doi.org/10.1111/j.1365-2958.2011.07947.x>.
- Köhler T, van Delden C, Curty LK, Hamzehpour MM, Pechère JC. 2001. Overexpression of the MexEF-OprN multidrug efflux system affects cell-to-cell signaling in *Pseudomonas aeruginosa*. *J Bacteriol* 183:5213–5222. <http://dx.doi.org/10.1128/JB.183.18.5213-5222.2001>.
- Olivares J, Alvarez-Ortega C, Linares JF, Rojo F, Köhler T, Martinez JL. 2012. Overproduction of the multidrug efflux pump MexEF-OprN does not impair *Pseudomonas aeruginosa* fitness in competition tests, but pro-

- duces specific changes in bacterial regulatory networks. *Environ Microbiol* 14:1968–1981. <http://dx.doi.org/10.1111/j.1462-2920.2012.02727.x>.
18. Linares JF, Lopez JA, Camafeita E, Albar JP, Rojo F, Martinez JL. 2005. Overexpression of the multidrug efflux pumps MexCD-OprJ and MexEF-OprN is associated with a reduction of type III secretion in *Pseudomonas aeruginosa*. *J Bacteriol* 187:1384–1391. <http://dx.doi.org/10.1128/JB.187.4.1384-1391.2005>.
  19. Lamarche MG, Deziel E. 2011. MexEF-OprN efflux pump exports the *Pseudomonas* quinolone signal (PQS) precursor HHQ (4-hydroxy-2-heptylquinoline). *PLoS One* 6:e24310. <http://dx.doi.org/10.1371/journal.pone.0024310>.
  20. Jalal S, Ciofu O, Hoiby N, Gotoh N, Wretling B. 2000. Molecular mechanisms of fluoroquinolone resistance in *Pseudomonas aeruginosa* isolates from cystic fibrosis patients. *Antimicrob Agents Chemother* 44:710–712. <http://dx.doi.org/10.1128/AAC.44.3.710-712.2000>.
  21. Llanes C, POURCEL C, Richardot C, Plésiat P, Fichant G, Cavallo JD, Merens A, GERPA Study Group. 2013. Diversity of  $\beta$ -lactam resistance mechanisms in cystic fibrosis isolates of *Pseudomonas aeruginosa*: a French multicentre study. *J Antimicrob Chemother* 68:1763–1771. <http://dx.doi.org/10.1093/jac/dkt115>.
  22. Fukuda H, Hosaka M, Hirai K, Iyobe S. 1990. New norfloxacin resistance gene in *Pseudomonas aeruginosa* PAO. *Antimicrob Agents Chemother* 34:1757–1761. <http://dx.doi.org/10.1128/AAC.34.9.1757>.
  23. Pumbwe L, Piddock LJ. 2000. Two efflux systems expressed simultaneously in multidrug-resistant *Pseudomonas aeruginosa*. *Antimicrob Agents Chemother* 44:2861–2864. <http://dx.doi.org/10.1128/AAC.44.10.2861-2864.2000>.
  24. Oh H, Stenhoff J, Jalal S, Wretling B. 2003. Role of efflux pumps and mutations in genes for topoisomerases II and IV in fluoroquinolone-resistant *Pseudomonas aeruginosa* strains. *Microb Drug Resist* 9:323–328. <http://dx.doi.org/10.1089/107662903322762743>.
  25. Ditta G, Stanfield S, Corbin D, Helinski DR. 1980. Broad host range DNA cloning system for gram-negative bacteria: construction of a gene bank of *Rhizobium meliloti*. *Proc Natl Acad Sci U S A* 77:7347–7351. <http://dx.doi.org/10.1073/pnas.77.12.7347>.
  26. Clinical and Laboratory Standards Institute. 2009. Methods for dilution antimicrobial susceptibility tests for bacteria that grow aerobically; approved standard, 8th ed. M07-A8, vol 29. Clinical and Laboratory Standards Institute, Wayne, PA.
  27. Dumas JL, van Delden C, Perron K, Köhler T. 2006. Analysis of antibiotic resistance gene expression in *Pseudomonas aeruginosa* by quantitative real-time-PCR. *FEMS Microbiol Lett* 254:217–225. <http://dx.doi.org/10.1111/j.1574-6968.2005.00008.x>.
  28. Vasseur P, Soscia C, Voulhoux R, Filloux A. 2007. PelC is a *Pseudomonas aeruginosa* outer membrane lipoprotein of the OMA family of proteins involved in exopolysaccharide transport. *Biochimie* 89:903–915. <http://dx.doi.org/10.1016/j.biochi.2007.04.002>.
  29. Köhler T, Curty LK, Barja F, van Delden C, Pechère JC. 2000. Swarming of *Pseudomonas aeruginosa* is dependent on cell-to-cell signaling and requires flagella and pili. *J Bacteriol* 182:5990–5996. <http://dx.doi.org/10.1128/JB.182.21.5990-5996.2000>.
  30. Ohman DE, Cryz SJ, Iglewski BH. 1980. Isolation and characterization of *Pseudomonas aeruginosa* PAO mutant that produces altered elastase. *J Bacteriol* 142:836–842.
  31. Essar DW, Eberly L, Hadero A, Crawford IP. 1990. Identification and characterization of genes for a second anthranilate synthase in *Pseudomonas aeruginosa*: interchangeability of the two anthranilate synthases and evolutionary implications. *J Bacteriol* 172:884–900.
  32. Kaniga K, Delor I, Cornelis GR. 1991. A wide-host-range suicide vector for improving reverse genetics in gram-negative bacteria: inactivation of the *blaA* gene of *Yersinia enterocolitica*. *Gene* 109:137–141. [http://dx.doi.org/10.1016/0378-1119\(91\)90599-7](http://dx.doi.org/10.1016/0378-1119(91)90599-7).
  33. Hoang TT, Kutchma AJ, Becher A, Schweizer HP. 2000. Integration-proficient plasmids for *Pseudomonas aeruginosa*: site-specific integration and use for engineering of reporter and expression strains. *Plasmid* 43:59–72. <http://dx.doi.org/10.1006/plas.1999.1441>.
  34. Tian ZX, Mac Aogain M, O'Connor HF, Fargier E, Mooij MJ, Adams C, Wang YP, O'Gara F. 2009. MexT modulates virulence determinants in *Pseudomonas aeruginosa* independent of the MexEF-OprN efflux pump. *Microb Pathog* 47:237–241. <http://dx.doi.org/10.1016/j.micpath.2009.08.003>.
  35. Jin Y, Yang H, Qiao M, Jin S. 2011. MexT regulates the type III secretion system through MexS and PtrC in *Pseudomonas aeruginosa*. *J Bacteriol* 193:399–410. <http://dx.doi.org/10.1128/JB.01079-10>.
  36. Kumar A, Schweizer HP. 2011. Evidence of MexT-independent overexpression of MexEF-OprN multidrug efflux pump of *Pseudomonas aeruginosa* in presence of metabolic stress. *PLoS One* 6:e26520. <http://dx.doi.org/10.1371/journal.pone.0026520>.
  37. Köhler T, Míchea-Hamzèhpour M, Plesiat P, Kahr AL, Pechère JC. 1997. Differential selection of multidrug efflux systems by quinolones in *Pseudomonas aeruginosa*. *Antimicrob Agents Chemother* 41:2540–2543.
  38. Fournier D, Richardot C, Muller E, Robert-Nicoud M, Llanes C, Plesiat P, Jeannot K. 2013. Complexity of resistance mechanisms to imipenem in intensive care unit strains of *Pseudomonas aeruginosa*. *J Antimicrob Chemother* 68:1772–1780. <http://dx.doi.org/10.1093/jac/dkt098>.
  39. Maseda H, Sawada I, Saito K, Uchiyama H, Nakae T, Nomura N. 2004. Enhancement of the *mexAB-oprM* efflux pump expression by a quorum-sensing autoinducer and its cancellation by a regulator, MexT, of the *mexEF-oprN* efflux pump operon in *Pseudomonas aeruginosa*. *Antimicrob Agents Chemother* 48:1320–1328. <http://dx.doi.org/10.1128/AAC.48.4.1320-1328.2004>.
  40. Craven SH, Ezezi OC, Haddad S, Hall RA, Momany C, Neidle EL. 2009. Inducer responses of BenM, a LysR-type transcriptional regulator from *Acinetobacter baylyi* ADP1. *Mol Microbiol* 72:881–894. <http://dx.doi.org/10.1111/j.1365-2958.2009.06686.x>.
  41. Colyer TE, Kredich NM. 1996. In vitro characterization of constitutive CysB proteins from *Salmonella typhimurium*. *Mol Microbiol* 21:247–256. <http://dx.doi.org/10.1046/j.1365-2958.1996.6301347.x>.
  42. Morita Y, Tomida J, Kawamura Y. 2015. Efflux-mediated fluoroquinolone resistance in the multidrug-resistant *Pseudomonas aeruginosa* clinical isolate PA7: identification of a novel MexS variant involved in upregulation of the *mexEF-oprN* multidrug efflux operon. *Front Microbiol* 6:8. <http://dx.doi.org/10.3389/fmicb.2015.00008>.
  43. Manoel C, Beckwith J. 1985. TnpA: a transposon probe for protein export signals. *Proc Natl Acad Sci U S A* 82:8129–8133. <http://dx.doi.org/10.1073/pnas.82.23.8129>.
  44. Herrero M, de Lorenzo V, Timmis KN. 1990. Transposon vectors containing non-antibiotic resistance selection markers for cloning and stable chromosomal insertion of foreign genes in gram-negative bacteria. *J Bacteriol* 172:6557–6567.
  45. Lacks S, Greenberg B. 1977. Complementary specificity of restriction endonucleases of *Diplococcus pneumoniae* with respect to DNA methylation. *J Mol Biol* 114:153–168. [http://dx.doi.org/10.1016/0022-2836\(77\)90289-3](http://dx.doi.org/10.1016/0022-2836(77)90289-3).



# Supplemental data





**Table S1: Origin of the 22 *nfxC* clinical strains of *Pseudomonas aeruginosa*.**

Strains	Patient numbers <sup>a</sup>	Dates of isolation	Hospital Units	Samples	Infection / Colonization	Antibiotic courses <sup>c</sup>
<b><i>Isolates with no mutation in mexS and mexT</i></b>						
2502	17	02/25/13	Hepatology	Urine	Infection	β-Lact, MCL, <b>FQ</b>
1206	2	06/12/12	Neurosurgery	Tracheal aspirate	ND <sup>b</sup>	β-Lact, OXZ, <b>FQ</b>
0708	2	08/07/12	Neurosurgery	Urine	ND <sup>b</sup>	β-Lact, OXZ, <b>FQ</b>
0309	8	09/03/12	Haematology	Bronchial aspirate	Infection	β-Lact, MCL
2607	6	07/26/12	Intensive Care	Peritoneal fluid	Infection	β-Lact, CBP, <b>FQ</b> , AG
0712	4	07/13/12	Vascular Surgery	Fascia of scarpa	Colonization	No antibiotic
0608	7	08/06/12	Haematology	Mouth	Colonization	β-Lact, <b>FQ</b>
<b><i>Isolates with mutations in mexS</i></b>						
1307	5	07/13/12	Pneumology	Sputum	ND <sup>b</sup>	PMX
2310	13	10/23/12	Intensive Care	Urine	Infection	β-Lact
2505	1	05/25/12	Thoracic Surgery	Mediastinal fluid	Infection	β-Lact
3005	2	05/30/12	Neurosurgery	Tracheal aspirate	ND <sup>b</sup>	β-Lact, OXZ, <b>FQ</b>
0911	14	11/09/12	Gynecology	Breast scare	Colonization	No antibiotic
1009	9	09/10/12	Intensive Care	Tracheal aspirate	Infection	SUL
0801	16	01/08/13	Pneumology	Sputum (CF)	Colonization	PMX, <b>FQ</b>
1409	10	09/14/12	Nephrology	Bone biopsy	Infection	β-Lact, AG
2311	14	11/23/12	Oncology	Breast scare	Colonization	No antibiotic
2609	11	09/26/12	Otolaryngology	Cervical wound	Colonization	No antibiotic
1709	11	09/17/12	Otolaryngology	Cervical wound	Colonization	No antibiotic
1711	15	11/17/12	Neurosurgery	Urine	Colonization	No antibiotic
0607	3	07/06/12	Urologic Surgery	Wound	Colonization	No antibiotic
<b><i>Isolates with mutations in mexT</i></b>						
0810	12	10/08/12	Intensive Care	Tracheal aspirate	Infection	CBP, GLP
1510	12	10/15/12	Intensive Care	Tracheal aspirate	Infection	CBP, GLP

<sup>a</sup> patients 2, 11, 12 and 14 harbored more than one isolate, but with a same sequence of *mexS* or *mexT*

<sup>b</sup> ND : not determined.

<sup>c</sup> before the isolation of *P. aeruginosa*. β-Lact: non-carbapenem β-lactams, CBP: carbapenems, AG: aminoglycosides, **FQ: fluoroquinolones**, MCL: macrolides, OXZ: oxazolidinones, PMX: polymyxins, SUL: sulfamides, GLP: glycopeptides.

Strains 1206 and 0708 were included in the study because they exhibited different serotypes.

**Table S2: Primers used for DNA sequencing, gene cloning, and RT-qPCR.**

<b>Primer</b>	<b>Sequence (5' --&gt; 3')</b>	<b>Source</b>
<b>Sequencing</b>		
Seq-mexS-Ch1	GAACAGGATCAGCAGGTTCA	this study
Seq-mexS-Ch2	CCACCGGGGTGAGTACCT	this study
Seq-mexS-Ch3	GTCTCGGCTTCGAACTGG	this study
Seq-mexS-Ch4	GGTGAAATCCATCAGGCAGT	this study
Seq-mexS-Ch5	GCAAGCTGGTGCTGTATGG	this study
Seq-mexS-Ch6	GAAGGCGACTTCGTCTGG	this study
Seq-mexS-Ch8	TCGAACTGTCCCTTTGCTCT	this study
seqmexT-1	CTATTGATGCCGAACCTGCT	(Llanes <i>et al.</i> 2011)
seqmexT-2	AATAGTCGTCGAGGGTCAAG	(Llanes <i>et al.</i> 2011)
seqmexT-3	TGATGAAAACGGATCACTCG	(Llanes <i>et al.</i> 2011)
seqmexT-4	GGGAACTAATCGAACGACGA	(Llanes <i>et al.</i> 2011)
Seq-mexT-mexE-Ch1	AAGCGCAAGGTGGTCTCG	this study
MvaT-1	CGCGGTTTACTTACAGTTTCG	(Llanes <i>et al.</i> 2011)
MvaT-2	AACGCTATTCGCTGGAGACT	(Llanes <i>et al.</i> 2011)
<b>Inactivation of mexS and mexT</b>		
Inac-MexS-Ch1	GACAGGTGGGCGAAGATTT	this study
Inac-MexS-Ch2	ATCCATCCATCACGGGTGAATAACCT	this study
Inac-MexS-Ch3	CGTGATGGATGGATTTACCGGTCATC	this study
Inac-MexS-Ch4	CGGCGAGATGTATGTGGTG	this study
Inac-MexT-Ch1	AGCACATCCTTCCAGCTCAC	this study
Inac-MexT-Ch2	ATAAGCCGAACACGATCAGCAGGTTCA	this study
Inac-MexT-Ch3	CGTGTTCCGGCTTATCCATCGAAAGCA	this study
Inact-MexT-Ch4	GTCGATCTGGAACAGCAGGT	this study
<b>Complementation of mexS and mexT</b>		
Int-mexS-P1	CGGGGATCCGGGGCATAGGATCACTGACA	this study
Int-mexS-P2	GCCAAGCTTGGTCAACGATCTGTGGATCTG	this study
Int-mexS-Ch2	GCCAAGCTTCGAACTGTCCCTTTGCTCTC	this study
Int-mexT-P1	CGGGGATCCCATCACGGGTGAATAACCT	this study
Int-mexT-P2	GCCAAGCTTCGATCGATTTTCCCGTTG	this study
<b>RT-qPCR</b>		
rpsL3	CAACTATCAACCAGCTGGTG	(Dumas <i>et al.</i> 2006)
rpsL5	CTGTGCTTTGCAGGTTGTG	(Dumas <i>et al.</i> 2006)
mexE4	CCAGGACCAGCACGAACTTCTTGC	(Dumas <i>et al.</i> 2006)
mexE5	CGACAACGCCAAGGGCGAGTTCACC	(Dumas <i>et al.</i> 2006)
MexSP1	CAAGGGCGTCAATGTCATCC	this study
MexSP2	GACCGGTGAAATCCATCAGG	this study
MexT1	ATCTGAACCTGCTGATCGTG	this study
MexT2	GTCCGGTACGGACGAACA	this study

**Table S3: Complementation of *mexS*-mutated clinical strains with the wild-type allele.**

Clinical strains	Sequence	CIP MICs ( $\mu\text{g ml}^{-1}$ ) after complementation by <sup>a</sup>		
	MexS (339 aa) <sup>a</sup>	None	pME6001 <sup>b</sup>	pMEQR1 <sup>c</sup>
1307	V <sub>104</sub> A	16	16	8
2310	F <sub>253</sub> L	1	1	0.25
2505	D <sub>44</sub> E	64	-	-
3005	S <sub>60</sub> F	1	1	0.5
0911	F <sub>185</sub> L	1	1	0.25
1009	V <sub>73</sub> A+ L <sub>270</sub> Q	32	-	-
0801	C <sub>245</sub> G	0.5	-	-
1409	A <sub>166</sub> P	1	1	0.5
2311	S <sub>60</sub> P	1	1	0.5
2609	L <sub>263</sub> Q	2	2	0.5

<sup>a</sup>: (-) clinical strains for which transformation with plasmid pMEQR1 failed or was not possible because of high gentamicin resistance (selection marker of pMEQR1).

<sup>b</sup>: Broad-host range vector pME6001 conferring gentamicin resistance (Blumer *et al.* 1999).

<sup>c</sup>: Plasmid pME6001 carrying the wild-type *mexS* gene (Llanes *et al.* 2011).

**Table S4: Genotype and virulence factors of clinical *nfxC* mutants.**

Strains	Sequence		Virulence factors <sup>c</sup>					
	MexS (339 aa) <sup>a</sup>	MexT (304 aa) <sup>b</sup>	Biofilm production (OD <sub>600</sub> )	Swarming motility (+/-)	Elastase activity (mm)	Haemolytic activity (%)	Pyocyanin production (%)	Virulence score (/5) <sup>d</sup>
<b>Reference strains</b>								
PA14	WT	WT	<b>2.6</b>	+	<b>18</b>	<b>72</b>	<b>100</b>	5
PA14ΔS	Δ809bp <sub>1-809</sub>	WT	0.4	-	<b>12</b>	22	13	1
PA14ΔS <sub>PA14</sub>	WT	WT	<b>2.7</b>	+	<b>18</b>	<b>79</b>	<b>92</b>	5
PA14ΔS <sub>PAO1</sub>	N <sub>249</sub> D	WT	0.9	-	<b>13</b>	<b>55</b>	13	2
PA14ΔT	WT	Δ883bp <sub>32-915</sub>	<b>1.9</b>	+	<b>16</b>	<b>78</b>	<b>86</b>	5
PA14ΔT <sub>PA14</sub>	WT	WT	<b>2</b>	+	<b>18</b>	<b>76</b>	<b>87</b>	5
PAO1	N <sub>249</sub> D	+ 8bp <sub>118</sub>	0.5	+	<b>16</b>	<b>77</b>	<b>168</b>	5
PAO7H	N <sub>249</sub> D	WT	0.6	-	0	50	17	0
<b>Clinical strains with no mutation in mexS and mexT</b>								
2502	WT	WT	0.5	+	<b>15</b>	<b>62</b>	<b>54</b>	4
1206	WT	WT	0.5	+	<b>15</b>	<b>69</b>	<b>87</b>	4
0708	WT	WT	0.5	-	0	29	24	0
0309	WT	WT	0.4	+	<b>16</b>	<b>63</b>	<b>90</b>	4
2607	WT	WT	0.5	-	<b>15</b>	<b>54</b>	15	2
0712	WT	WT	0.3	+	<b>15</b>	42	13	2
0608	WT	WT	<b>1.3</b>	+	<b>17</b>	<b>74</b>	<b>168</b>	5
<b>Clinical strains with mutations in mexS</b>								
1307	V <sub>104</sub> A	WT	<b>2.2</b>	-	0	20	13	1
2310	F <sub>253</sub> L	WT	<b>1.2</b>	-	<b>11</b>	<b>69</b>	<b>172</b>	4
2505	D <sub>44</sub> E	WT	<b>1.3</b>	-	0	<b>60</b>	12	2
3005	S <sub>60</sub> F	WT	0.5	+	<b>16</b>	<b>68</b>	13	3
0911	F <sub>185</sub> L	WT	0.3	+	<b>16</b>	<b>57</b>	<b>100</b>	4
1009	V <sub>73</sub> A+ L <sub>270</sub> Q	WT	<b>1.7</b>	-	0	29	11	1
0801	C <sub>245</sub> G	WT	0.1	-	0	15	12	0
1409	A <sub>166</sub> P	WT	0.3	+	<b>16</b>	<b>66</b>	<b>149</b>	4
2311	S <sub>60</sub> P	WT	0.5	+	<b>16</b>	<b>64</b>	11	3
2609	L <sub>263</sub> Q	WT	<b>1.8</b>	-	<b>11</b>	<b>58</b>	12	3
1709	Δ8bp <sub>710-718</sub>	WT	0.4	-	<b>13</b>	47	12	1
1711	ΔC <sub>293</sub>	WT	0.3	+	<b>11</b>	41	<b>245</b>	3
0607	Δ30bp <sub>927-956</sub>	WT	0.5	-	0	47	11	0
<b>Clinical strains with mutations in mexT</b>								
0810	WT	G <sub>258</sub> D	<b>1.4</b>	-	0	28	16	1
1510	WT	Y <sub>138</sub> D+ G <sub>258</sub> D	<b>1.4</b>	-	0	37	11	1

<sup>a</sup> MexS of PA14 is functional (N<sub>249</sub>) and considered as WT contrary to that of PAO1-UW (D<sub>249</sub>)

([www.pseudomonas.com](http://www.pseudomonas.com)).

<sup>b</sup> MexT of PA14 is functional and considered as WT, contrary to that of PAO1-UW (+8bp <sub>118</sub>)

([www.pseudomonas.com](http://www.pseudomonas.com)).

<sup>c</sup> Virulence factors are in bold when positive or considered significant.

<sup>d</sup> Results from each test (biofilm/1, swarming/1, elastase/1, haemolysis/1, pyocyanin/1). Swarming motility and biofilm production are correlated with rhamnolipid production.

## References

1. **Blumer, C., S. Heeb, G. Pessi, and D. Haas.** 1999. Global GacA-steered control of cyanide and exoprotease production in *Pseudomonas fluorescens* involves specific ribosome binding sites. *Proc Natl Acad Sci U S A* **96**:14073-8.
2. **Dumas, J. L., C. van Delden, K. Perron, and T. Köhler.** 2006. Analysis of antibiotic resistance gene expression in *Pseudomonas aeruginosa* by quantitative real-time-PCR. *FEMS Microbiol Lett* **254**:217-25.
3. **Llanes, C., T. Köhler, I. Patry, B. Dehecq, C. van Delden, and P. Plésiat.** 2011. Role of the Efflux System MexEF-OprN in Low Level Resistance of *Pseudomonas aeruginosa* to Ciprofloxacin. *Antimicrob Agents Chemother* **55**:5676-84.



## 2.2 Constitutive Activation of MexT by Amino Acid Substitutions found in Clinical Isolates of *Pseudomonas aeruginosa*

In a previous study on the role of MexEF-OprN in low-level resistance to ciprofloxacin, two non-CF clinical isolates of *P. aeruginosa* (strains 4177 and 4088) had been found to overexpress *mexEF-oprN* while having intact *mexS* genes (Llanes et al., 2011). Both strains harbored amino acid substitutions in MexT. A retrospective analysis of MexEF-OprN-overproducing CF isolates also revealed that one of them (strain 10-12) displayed a G<sub>257</sub>A change in MexT (Llanes et al., 2013). Finally, screening of our lab collection (Richardot et al., 2016) led to the identification of two other isolates, 0810 and 1510, harboring one and two amino-acid substitutions in MexT, respectively (**Table 4**). To determine whether these sequence variations could have an impact on *mexEF-oprN* expression, by constitutively activating MexT, we first reassessed the expression of *mexE* in all the selected bacteria. Confirming that all of them were *nfxC* mutants, their transcripts levels were from 20- to 112-fold higher than that of wild-type strain PA14. These results were consistent with the higher resistance of these clinical strains to MexEF-OprN substrates (**Table 4**).

**Table 4: Characterization of clinical *nfxC* mutants harboring single-amino acid substitutions in MexT**

Strains	MexT substitutions (304 aa)	Transcripts levels of <i>mexE</i> <sup>a</sup>	MICs ( $\mu\text{g mL}^{-1}$ ) <sup>b</sup>			References
			CIP	CHL	TMP	
PA14	WT	1	0.12	64	64	F. Ausubel
4177	R <sub>166</sub> H	20	0.25	1024	1024	(Llanes et al., 2011)
4088	G <sub>257</sub> S	112	1	2048	>2048	(Llanes et al., 2011)
10-12	G <sub>257</sub> A	56	2	64	>2048	(Llanes et al., 2013)
0810	G <sub>258</sub> D	32	8	1024	1024	(Richardot et al., 2016)
1510	Y <sub>138</sub> H + G <sub>258</sub> D	21	2	256	512	(Richardot et al., 2016)

<sup>a</sup>: Expressed as the ratio to the value for wild-type strain PA14. Mean values were calculated from two independent bacterial cultures each assayed in duplicate.

<sup>b</sup>: CIP, ciprofloxacin; CHL, chloramphenicol; TMP, trimethoprim.

To get an insight into the impact of the aforementioned variations on MexT activity, we next deleted *mexT* gene in strain PA14 and re-complemented this strain with individual mutated alleles. For each complemented strain, we measured the expression of *mexE* and determine the susceptibility to MexEF-OprN substrates. Gene replacement with *mexT* alleles from strains 4177, 0810, and 1510 had virtually no impact on *mexE* expression and MIC values (**Table 5**). In contrast, alleles from strains 4088 and 10-12 were associated with a strong



overexpression of *mexE* (189- and 110-fold, respectively), and increased resistance to ciprofloxacin (16x, 8x), chloramphenicol (32x, 16x), and trimethoprim ( $\geq 32x$ , 16x) (Table 5).

Table 5: Effect of mutated alleles of *mexT* from clinical isolates on gene expression and drug susceptibility.

Strain	MexT substitution (304 aa)	Transcript levels of <i>mexE</i> <sup>a</sup>	MICs ( $\mu\text{g mL}^{-1}$ ) <sup>b</sup>		
			CIP	CHL	TMP
PA14	WT	1	0.12	64	64
PA14 $\Delta$ <i>mexT</i>	-	0.4	0.12	32	32
PA14 $\Delta$ <i>mexT</i> <sub>PA14</sub>	WT	2.2	0.12	64	64
PA14 $\Delta$ <i>mexT</i> <sub>4177</sub>	R <sub>166</sub> H	3.2	0.12	64	64
PA14 $\Delta$ <i>mexT</i> <sub>4088</sub>	G <sub>257</sub> S	<b>189</b>	<b>2</b>	<b>2,048</b>	<b>&gt;2,048</b>
PA14 $\Delta$ <i>mexT</i> <sub>10-12</sub>	G <sub>257</sub> A	<b>110</b>	<b>1</b>	<b>1,024</b>	<b>1,024</b>
PA14 $\Delta$ <i>mexT</i> <sub>0810</sub>	G <sub>258</sub> D	1.9	0.12	64	64
PA14 $\Delta$ <i>mexT</i> <sub>1510</sub>	Y <sub>138</sub> H + G <sub>258</sub> D	6.3	0.25	64	64

<sup>a</sup> : Expressed as the ratio to the value for wild-type strain PA14. Mean values were calculated from two independent bacterial cultures each assayed in duplicate.

<sup>b</sup> : CIP, ciprofloxacin; CHL, chloramphenicol; TMP, trimethoprim.





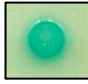

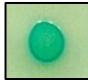

In **bold**: significant overexpression of gene *mexE* and increased resistance to MexEF-OprN substrates

If MexT conforms to the usual mode of action of LysR transcriptional regulators (LTTRs) (Maddocks and Oyston, 2008), it should be inactive in its monomeric conformation and should be active when forming oligomers upon binding of its cognate co-inducer(s). Consistent with this, it was shown that under reducing conditions, MexT forms an inactive monomer while oxidative conditions lead to an active tetrameric regulator (Fargier et al., 2012). Given that strains 4088 and 10-12 both harbor a substitution of Glycine residue-257, we thought that this position might be necessary for MexT oligomerization and thus, that changing this residue into a Serine or Alanine would generate a constitutively active form of MexT. To ascertain this hypothesis, we performed a bacterial two-hybrid experiment based on activity reconstitution of enzyme adenylate cyclase (AC) from *Bordetella pertussis* (Battesti and Bouveret, 2012). This enzyme is composed of two subunits T18 and T25 which, when physically separated, do not present any enzymatic activity. Reconstitution of AC activity can be achieved if two proteins, in our case two monomers of MexT, interact with each other and bring closer the two subunits. Production of a functional AC activates transcription factor CRP, and subsequently cAMP/CRP-upregulated genes such as those of operons maltose and lactose. The activity of these operons can be visualized by growth on reporter plates (MC

Maltose and MH X-Gal) and can be quantified by measuring  $\beta$ -galactosidase activity (Battesti and Bouveret, 2012).

In accordance with a previous work (Fargier et al., 2012), our results showed that the wild-type MexT from strain PA14 is under a monomeric form as neither the reporter plates nor the  $\beta$ -galactosidase activity turned out to be positive ( $17 \pm 1.66$  Miller units) (Table 6). In contrast, the mutated MexT variants from strains 4088 and 10-12 gave positive results with both tests (Table 6), suggesting that they are capable to form active oligomers. Of note, our results suggest that MexT<sub>4088</sub> generates a stronger interaction between its subunits ( $296 \pm 14.31$  Miller units) than MexT<sub>10-12</sub> ( $119 \pm 5.36$  Miller units), in agreement with *mexE* expression (189-fold and 110-fold for MexT<sub>4088</sub>, MexT<sub>10-12</sub>, respectively) and resistance levels to MexEF-OprN substrates (MICs increased from 16- to >32-fold for MexT<sub>4088</sub> and from 8- to 16-fold for MexT<sub>10-12</sub>) (Table 5).

**Table 6: Bacterial two-hybrid experiments for modified MexT**

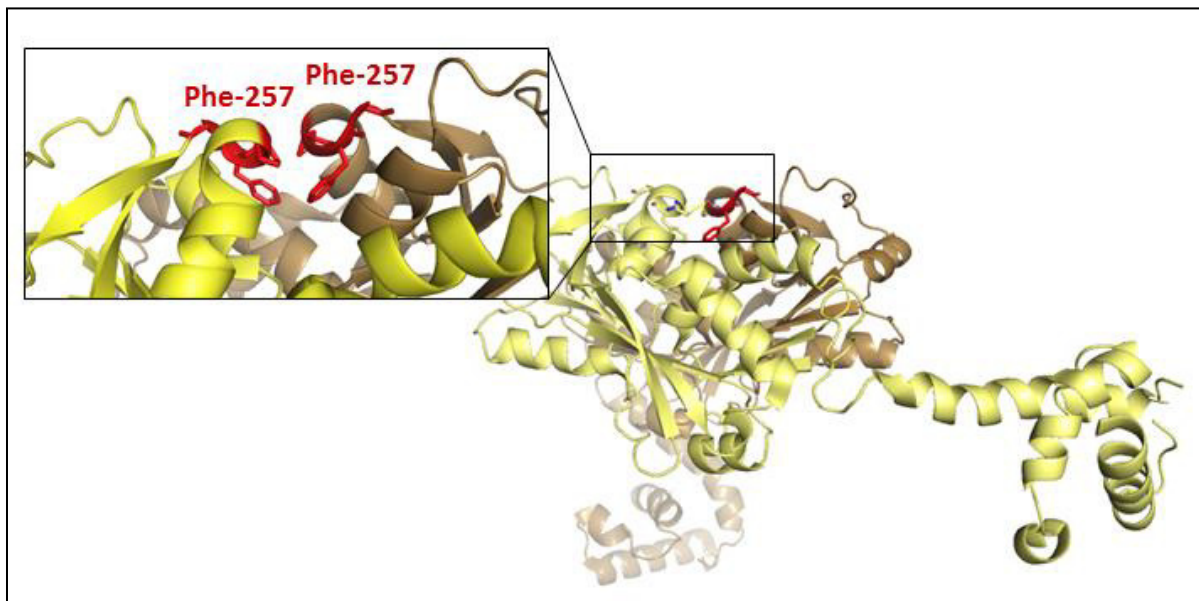
DHM1 strain containing BACTH plasmids <sup>a</sup>	Amino acid substitution	$\beta$ -Gal Activity <sup>b</sup> (Miller Units)	MH X-Gal	MC Maltose
None	-	15 ( $\pm 1.91$ )		
MexT <sub>PA14</sub>	WT	19 ( $\pm 1.66$ )		
MexT <sub>4088</sub>	G <sub>257</sub> S	296 ( $\pm 14.31$ )		
MexT <sub>10-12</sub>	G <sub>257</sub> A	119 ( $\pm 5.36$ )		

<sup>a</sup>: plasmids pUT18 and pKNT25 for which the tag is at the C-terminus of the recombinant protein were used in this experiment.

<sup>b</sup>: Mean values were calculated from five independent bacterial cultures each assayed in triplicate.

As no crystal structure is available for MexT, we used Raptor X server (Källberg et al., 2012) to obtain a prediction based on DntR (35% sequence identity with MexT), a LTTR sensor of nitrotoluene isomers in *Burkholderia* spp. (Smirnova et al., 2004). The prediction showed that MexT has the classical conformation of LTTRs with its co-inducer binding domain at the N-terminus and its DNA-binding domain at the C-terminus of the protein. According to this prediction, Gly-257 is positioned in the external phase of the co-inducer binding domain, at the end of an  $\alpha$ -helix. The location of this residue suggests its involvement in dimer/oligomer formation and regulator activation. As a dimer structure has experimentally been determined for DntR (Devesse et al., 2011), we examined the location of Phe-257 (Gly-257 in MexT) to

check out whether this position could participate in intermolecular interactions between the two monomers. As represented in **Figure 8**, Phe-257 residues of DntR monomers face each other in the dimeric model. Based on these data, one can assume that change of Gly-257 into Ser or Ala allows MexT to adopt an active conformation more easily. However, this will be confirmed once the crystal structure of MexT (either in a monomeric or dimeric form) is available. An ongoing collaboration with Pr. Isabelle Broutin at university Paris Descartes (UMR 8015, Laboratoire de Cristallographie et RMN Biologiques) is expected to provide such structural details.



**Figure 8: Crystal structure of the DntR dimer.** Crystal structure of DntR dimer from *Burkholderia* spp (PDB 2Y7K) was experimentally determined previously (Devesse et al., 2011). The two monomers are indicated in yellow and brown and Phenylalanine-257 is highlighted in red.

A short article is currently being prepared to publish these results (draft in appendix).

### **III. Induction of *mexEF-oprN* by Electrophilic Stress**

---



## 1 Background: activation of RND efflux systems in response to oxidative stress

### 1.1 Overview

Some RND efflux systems provide *P. aeruginosa* with a significant resistance to antibiotics when overproduced upon mutations affecting regulatory genes (Li and Plésiat, 2016). Nevertheless, under physiological conditions the primary role of RND systems may not be to export antimicrobials, as these molecules are often present at very low or undetectable concentrations in most of natural environments (Fruci and Poole, 2016). Indeed, evidence that at least some of these pumps are induced by environmental signals suggest that they are part of specific responses enabling bacteria to adapt to various stresses (Poole, 2014) (**Table 7**).

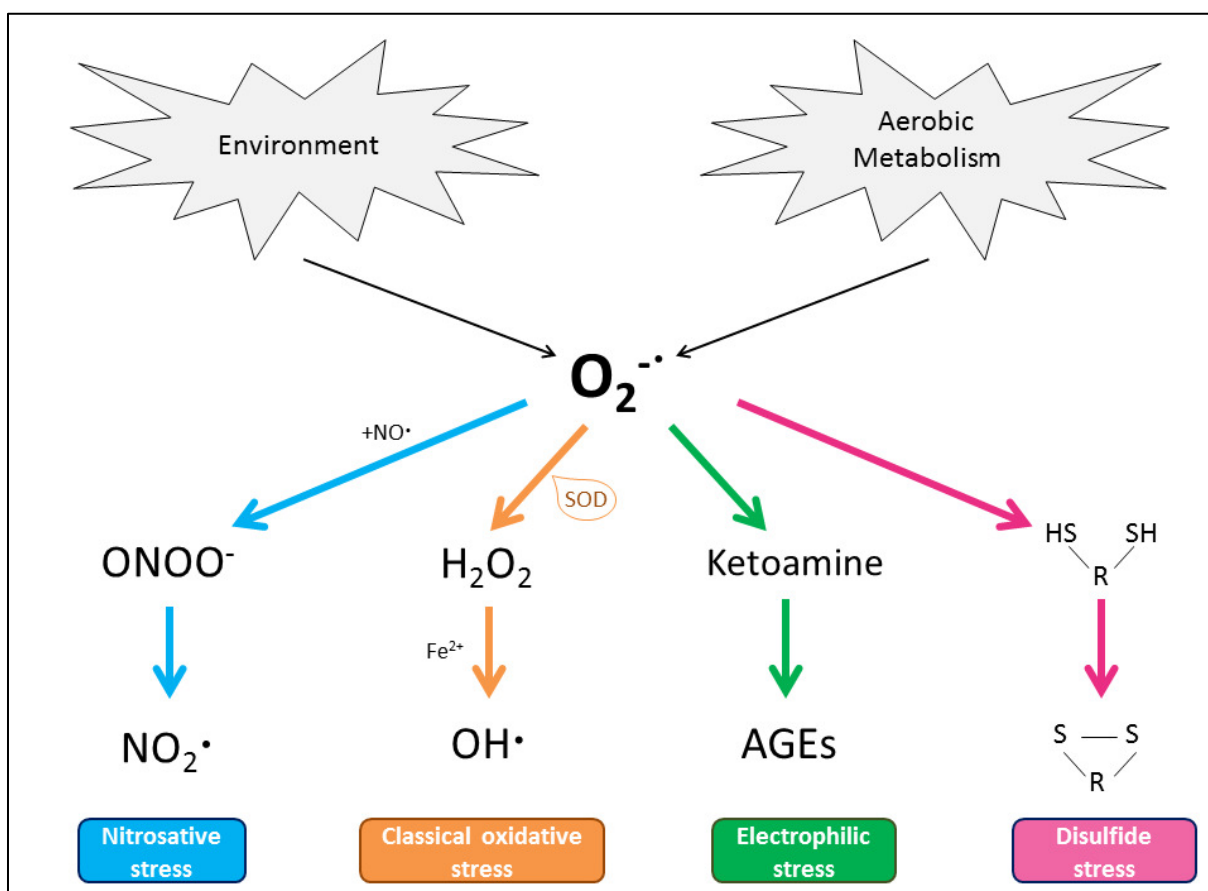
**Table 7: Mechanisms of antibiotic resistance induced by stress in *P. aeruginosa***

Stress category	Sub-category	Resistance mechanism	Stress-responsive regulator
Oxidative	Classical	-MexAB-OprM	MexR, NalC
		-MexXY/OprM	ArmZ
	Nitrosative	-MexEF-OprN	MexT
	Disulfide	-MexEF-OprN	MexT
Envelope		-LPS modification, MexXY/OprM, porin (OprD) downregulation	ParRS
		-LPS modification	CprRS
		-Protection from misfolded proteins	AmgRS
		-MexCD-OprJ	AlgU
Nutrient	Stringent response	-Antioxidant processes mediated by ppGpp production	Unknown
	Mg <sup>2+</sup> /Ca <sup>2+</sup> limitation	-LPS modification	PhoPQ, PmrAB
Ribosomal		-MexXY/OprM	ArmZ
Heat-shock		-Protection from misfolded proteins	RpoH, AsrA

Adapted from Fruci and Poole, 2016 and Poole, 2014

Because of its oxidative metabolism, *P. aeruginosa* is constantly exposed to endogenously-produced, harmful molecular species able to provoke intracellular damage. Bacterial exposure to environmental signals can be stressful for the microorganism as well. One of the most important stresses bacteria have to cope with is caused by reactive oxygen species (ROS) (Betteridge, 2000). Indeed, during cellular respiration, electrons resulting from oxidation of low-redox-potential electron donors (i.e. NADH), are sequentially transferred through the electron transport chains, up to finally reduce the high-redox-potential electron acceptor O<sub>2</sub>.

These redox reactions inevitably generate ROS (Bueno et al., 2012). Of note, environmental factors such as ultraviolet light, air pollutants, heavy metals, and host-responses can modulate ROS formation (Fang et al., 2016; Scandalios, 2005). Oxidative stress is thus defined as an unbalance between production and removal of oxygen-derived free radicals (Betteridge, 2000). This type of stress has long been considered as exclusively linked to ROS formation. However, other subcategories (nitrosative, electrophilic and disulfide) were identified further (**Figure 9**) (Bild et al., 2013; Green and Paget, 2004; Vázquez-Torres, 2012). In any case, intracellular accumulation of reactive species is deleterious to proteins, DNA, and lipids.

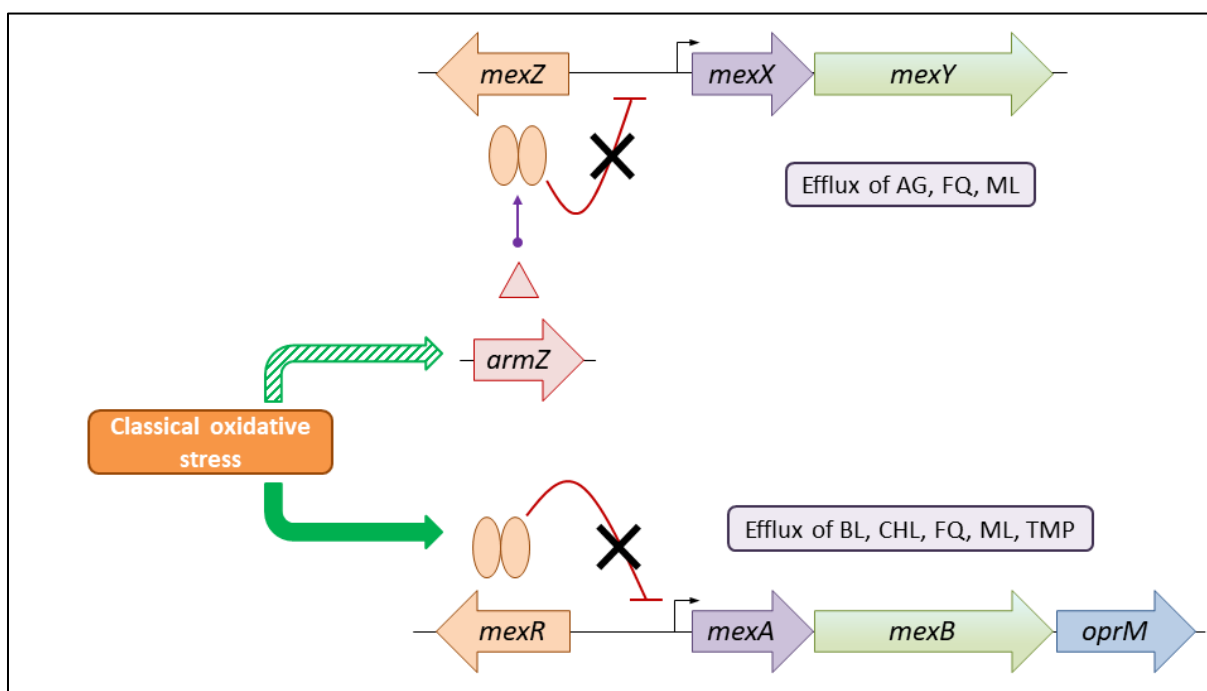


**Figure 9: Subcategories of oxidative stress.** Formation of superoxide anion ( $O_2^{\cdot-}$ ) can be achieved by environmental signals or by aerobic metabolism. Superoxide can react with different species inside the cell creating several subcategories of oxidative stress. AGEs, advanced glycation end-products;  $H_2O_2$ , hydrogen peroxide;  $NO^{\cdot}$ , nitric oxide;  $NO_2^{\cdot}$ , nitrogen dioxide;  $OH^{\cdot}$ , hydroxyl radical;  $ONOO^-$ , peroxynitrite; SOD, superoxide dismutase.

Expression of several RND-type efflux systems involved in antibiotic resistance can be affected by one or more of the oxidative stress subcategories (**Table 7**) (Fruci and Poole, 2016; Poole, 2012b, 2012a, 2014). MexAB-OprM (Chen et al., 2008; Ghosh et al., 2011; Muller et al., 2007, 2015; Starr et al., 2012), and MexXY/OprM (Fraud and Poole, 2011) are upregulated by classical oxidative stress, while MexEF-OprN production is increased upon nitrosative (Fetar et al., 2011) and disulfide (Fargier et al., 2012) stresses.

## 1.2 Efflux operons induced by classical oxidative stress

This stress results from production of ROS such as superoxide ( $O_2^{\cdot-}$ ), hydrogen peroxide ( $H_2O_2$ ), and hydroxyl radical ( $OH^{\cdot}$ ). To neutralize these harmful reactive species, *P. aeruginosa* and other bacteria produce basal levels of ROS-scavenger enzymes, such as superoxide dismutase (SOD) and catalase (Imlay, 2008). However, when ROS levels are increased under stressful conditions, other detoxification mechanisms are set up to protect the cell, including production of additional detoxifying enzymes and antioxidant molecules (e.g., ascorbate) (Ezraty et al., 2017; Fruci and Poole, 2016; Imlay, 2003).



**Figure 10: Efflux pump encoding operons induced by classical oxidative stress.** Two efflux operons are known to respond to peroxides (classical oxidative stress), namely *mexAB-oprM* and *mexXY*. Redox activation of operon *mexAB-oprM* is dependent on redox-sensing repressor MexR. The second operon, *mexXY*, is indirectly activated by peroxides *via* anti-repressor ArmZ.

AG, aminoglycosides; BL,  $\beta$ -lactams; CHL, chloramphenicol; FQ, fluoroquinolones; ML, macrolides; TMP, trimethoprim.

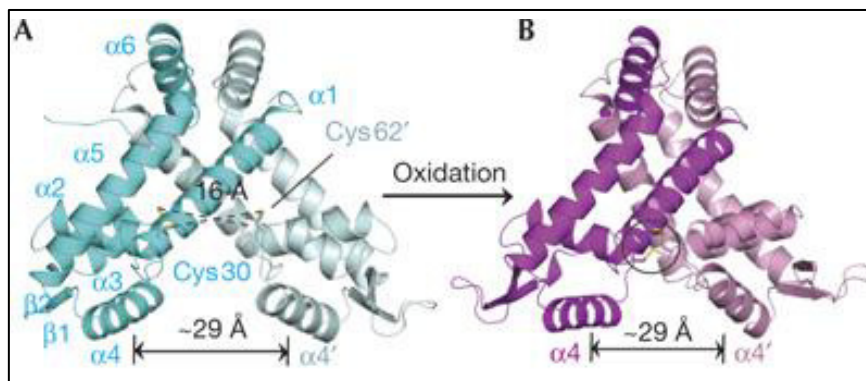
Derepression of efflux pumps is coordinated with regulation of other genes *via* regulators able to sense, directly or indirectly, the presence of ROS or to monitor the redox state of cell (Ezraty et al., 2017; Green and Paget, 2004). Since *P. aeruginosa* is constantly exposed to ROS in both natural- and host- environments, RND systems play an important role in the response to oxidative stress (Poole, 2014) (Figure 10).

### 1.2.1 Operon *mexAB-oprM*

Exposure of *P. aeruginosa* PAO1 to  $H_2O_2$  or cumene peroxide results in overexpression of operon *mexAB-oprM*, suggesting that at least one of the regulatory genes of this operon senses these reactive species. Peroxide activation of *mexAB-oprM* is in part dependent on local



repressor MexR (Chen et al., 2008). Indeed, *in vitro* experiments showed that the purified MexR protein is unable to repress operon expression when an inter-monomer disulfide bond is formed between cystein residues -30 and -62, upon peroxide treatment (Chen et al., 2008, 2010) (**Figure 11**). Redox-dependent inactivation of MexR is a good example of thiol-based oxidation sensing by which a bacterium protects itself against oxidative stressors including some antibiotics.



**Figure 11: Crystal structure of non-oxidized and oxidized MexR protein.** MexR is a local repressor of *mexAB-oprM* operon. (A) The reduced monomer (blue) is capable to bind the upstream region of *mexAB-oprM* operon and thus to repress operon expression. Upon peroxide exposure (pink), the formation of a disulfide bond between cystein residues -30 and -62 causes severe steric clashes with the DNA backbone, thereby preventing MexR binding to the *mexAB-oprM* promoter. Adapted from Chen et al., 2010.

Moreover, a transcriptomic analysis of strain PAO1 treated with environmental pollutant pentachlorophenol (PCP) revealed that *mexAB-oprM* was overexpressed under these stressing conditions (4.3-fold after 13h of treatment) (Muller et al., 2007). Later on, bacterial exposure to other chlorinated phenols was found to have similar effects (Muller et al., 2015). While regulator NalC, which controls the expression of anti-repressor ArmR, was first hold responsible for this induction of *mexAB-oprM* expression (Ghosh et al., 2011), another study demonstrated that the operon was still upregulated upon PCP exposure in absence of ArmR (Starr et al., 2012). It was thus proposed that chlorinated phenols generate an oxidative stress in *P. aeruginosa*, with subsequent inactivation of redox-sensor MexR leading to *mexAB-oprM* derepression (Chen et al., 2008; Starr et al., 2012). Whether peroxide and chlorinated phenols can promote MexAB-OprM-dependent antibiotic resistance has not been established.

### 1.2.2 Operon *mexXY*

Production of MexXY proteins is also induced by oxidative stress (Masuda et al., 2000b). Indeed, exposure of strain PAO1 to H<sub>2</sub>O<sub>2</sub> is associated with increased transcript levels of *mexXY* and stronger resistance to MexXY/OprM substrates such as amikacin (4-fold), tobramycin (4-fold), gentamicin (2-fold), and paromomycin (2-fold) (Fraud and Poole, 2011). This induction depends on ArmZ, a repressor that binds and sequester the negative regulator

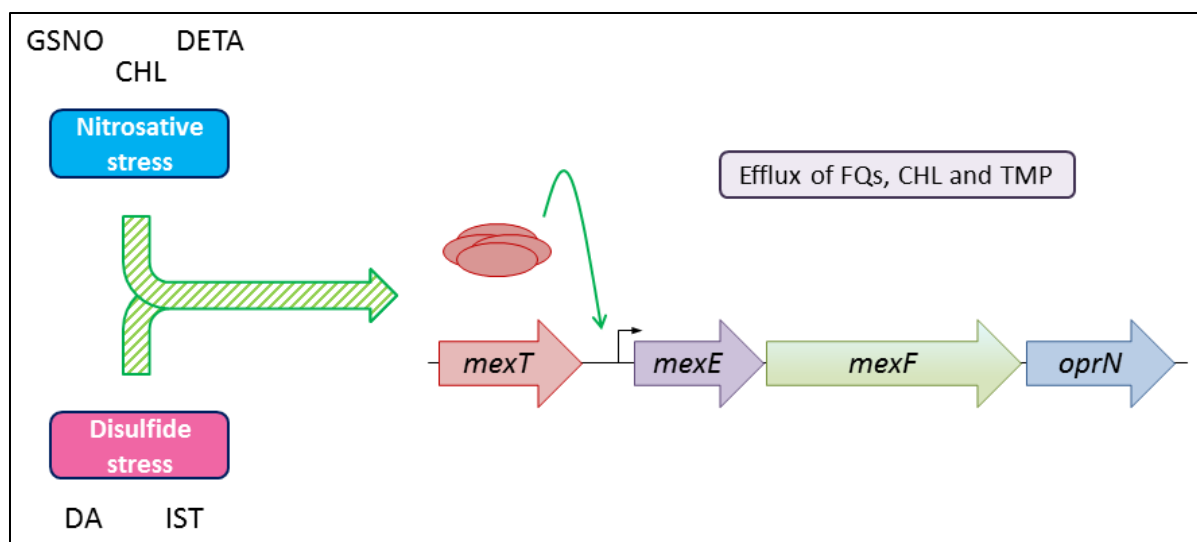
(MexZ) of operon *mexXY* (Yamamoto et al., 2009). However, the molecular mechanism by which peroxide induces gene *armZ* expression is still unresolved (Fraud and Poole, 2011). Since the pump MexXY/OprM is activated by ArmZ when *P. aeruginosa* is exposed to ribosome-targeting antibiotics (Morita et al., 2006b), one could assume that the inducing effects of ROS on ArmZ also result from their deleterious action on the ribosomal machinery (Fraud and Poole, 2011; Fruci and Poole, 2016; Jeannot et al., 2005).

### **1.3 Induction of *mexEF-oprN* by non-classical oxidative stress**

Operon *mexEF-oprN* expression remains at basal levels in cells exposed to ROS (Fetar et al., 2011), but is increased upon nitrosative and disulfide stresses (Fargier et al., 2012; Fetar et al., 2011). Several lines of evidence suggest that some stress elicitors are able to activate MexT, through a still unknown mechanism (**Figure 12**). In line with this, it was reported that *mexEF-oprN* is upregulated (12.9-fold) when bacteria are in contact with airways epithelial cells, which is believed to cause a kind of oxidative stress to *P. aeruginosa* (Frisk et al., 2004).

#### **1.3.1 Nitrosative stress**

During host colonization and/or infection, *P. aeruginosa* is exposed to nitric oxide (NO $\cdot$ ), a reactive nitrogen species (RNS) that is mostly produced by macrophages and that causes a nitrosative stress in bacterial cells (Poole, 2014). Other RNS include peroxynitrite (ONOO $\cdot$ ) and nitrogen dioxide (NO $_2\cdot$ ), two species known to be highly reactive and able to alter lipids, thiols, amino acids and DNA, though these reactions occur at relatively slow rates in comparison with ROS reactions (Fang, 2004; O'Donnell et al., 1999). Operon *mexEF-oprN* transcription is inducible by nitrosating agent S-nitrosoglutathione (GSNO) (not quantified), by (NO $\cdot$ )-generating agent diethylenetriamine NONOate (DETA) (not quantified) and by nitro-containing antibiotic chloramphenicol (3-fold increase, measured by  $\beta$ -galactosidase activity), with no evidence that these inductions do impact MICs of antibiotic substrates of MexEF-OprN (Fetar et al., 2011).

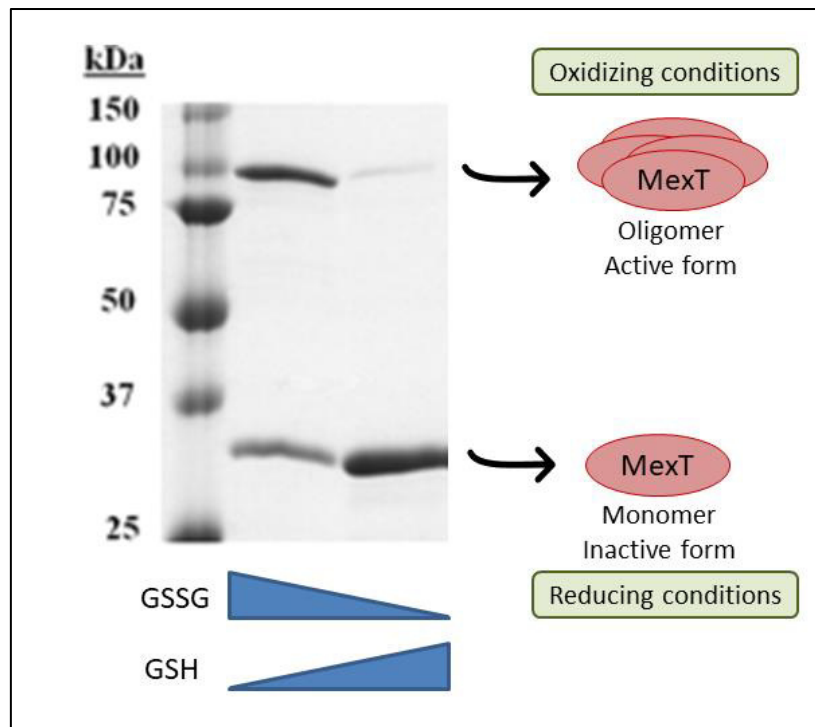


**Figure 12: Induction of operon *mexEF-oprN* by non-classical oxidative stresses.** The efflux pump MexEF-OprN is quite unique in *P. aeruginosa* as it is the only RND system known to be induced by non-classical oxidative stresses. Nitrosative or disulfide stress elicitors activate the global regulator MexT and thus operon *mexEF-oprN*. However, the exact mechanism by which MexT gets activated remains unknown. CHL, chloramphenicol; DA, diamide; DETA, diethylenetriamine NONOate; GSNO, s-nitrosoglutathione; IST, isothiocyanate.

Nitrosative upregulation of operon *mexEF-oprN* is dependent on MexT (Köhler et al., 1999). Among the many MexT-regulated genes identified by transcriptomic analysis (Tian et al., 2009b), *xenB* is of particular interest because of its role in the removal of nitro groups from xenobiotics such as nitroglycerine and trinitrotoluene, in *Pseudomonas* spp. (Blehert et al., 1999; Fuller et al., 2009; Pak et al., 2000). This link between MexT, MexEF-OprN and *xenB* has led to the hypothesis that the pump contributes to the detoxification of nitrated products formed upon nitrosative stress (Fetar et al., 2011; Poole, 2012b).

### 1.3.2 Disulfide stress

The perturbation of thiol/disulfide (-SH/S-S) balance inside the cell is referred to disulfide stress (Masip et al., 2006; Smirnova and Oktyabrsky, 2005). Such a stress occurs when thiol-reactive molecules, such as quinones, accumulate intracellularly (Liebeke et al., 2008). It has pleiotropic effects on bacterial physiology as it can modify the ratio of reduced to oxidized glutathione (GSH/GSSG). Reduced glutathione (GSH) is a protein-reducing molecule that prevents formation of aberrant disulfide bonds in cytoplasmic proteins; as such it plays an important role in bacterial protection against osmotic, acid, electrophilic, chlorinated and oxidative stresses (Masip et al., 2006).

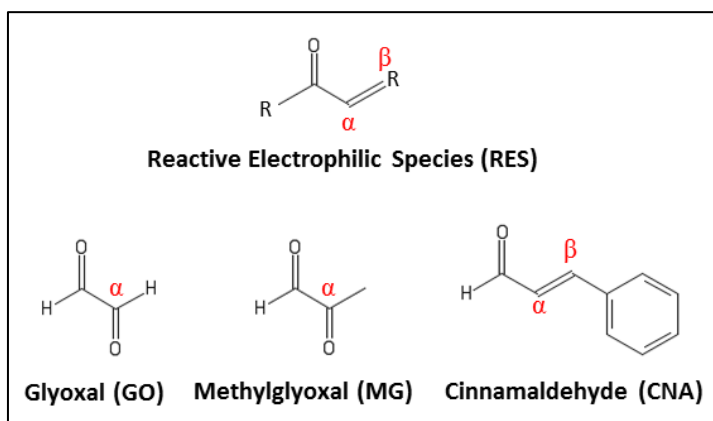


**Figure 13: Effect of redox environment on MexT.** In accordance with LTRs mode of action, MexT is under an inactive monomeric form when reduced glutathione (GSH) is predominant in the medium. In contrast, when the concentration of oxidized glutathione (GSSG) increases, MexT forms oligomers and becomes active.

Exposure of *P. aeruginosa* strain PA14 to disulfide stress elicitors diamide (Fargier et al., 2012) and isothiocyanate compound iberin (Tan et al., 2014) is associated with an increased expression of MexT-dependent genes including operon *mexEF-oprN* (180- and 129-fold, respectively). Supporting the notion that diamide is a substrate of the pump, disruption of gene *mexT*, *mexE*, or *mexF* was found to increase the susceptibility of *P. aeruginosa* to the elicitor. However, disruption of *oprN* that codes for the outer membrane component of the efflux system turned out to have minimal effects on diamide MICs, suggesting that proteins MexEF preferentially use another exit channel to extrude the inhibitor (Fargier et al., 2012). The same study showed that the purified MexT protein was capable to form an oligomer *in vitro* when treated with oxidized glutathione (GSSG), and that increasing concentrations of GSH increased formation of the monomeric form at the expense of oligomers (**Figure 13**). Of note, it was reported that under oxidizing conditions, MexT binds to the promoter region of PA4881, a MexT-regulated gene of unknown function (Fargier et al., 2012; Tian et al., 2009b).

#### 1.4 Bacterial response to electrophilic stress

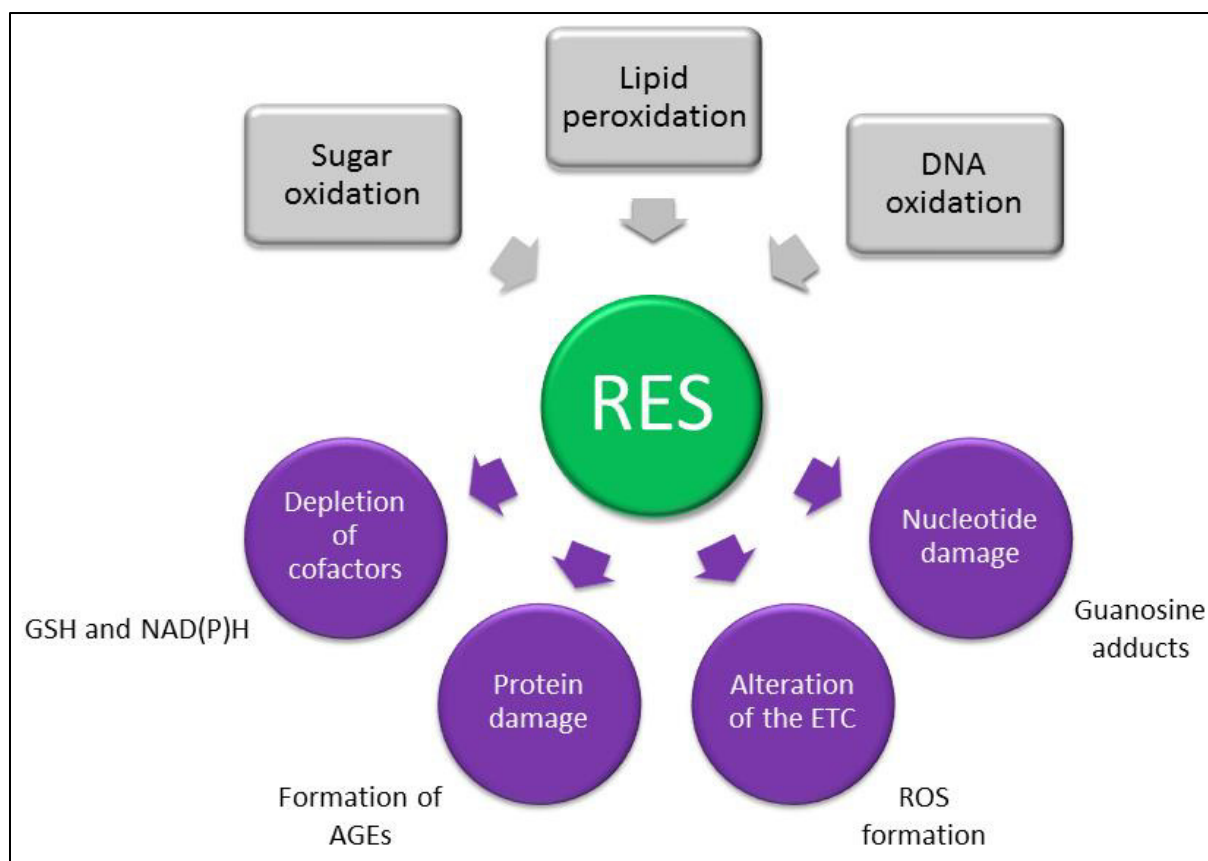
Although the bacterial stress response to classical oxidative or nitrosative stress has been extensively studied, research on electrophilic stress is somewhat scarce (Lee and Park, 2017). Electrophilic stress is defined as an unbalance between the formation and degradation of reactive electrophilic species (RES), which



**Figure 14:** Chemical structure of common Reactive Electrophilic Species (RES). RES are chemical compounds containing  $\alpha$ -unsaturated carbonyl (GO or MG) or  $\alpha,\beta$ -electrophilic groups (double bond in the case of CNA).

are compounds containing  $\alpha,\beta$ -unsaturated carbonyl or other electrophilic groups (Lee and Park, 2017). This subcategory of oxidative stress is also known as carbonyl stress as the most studied reactive species are compounds containing two carbonyl groups, the  $\alpha$ -oxoaldehydes such as glyoxal (GO) and methylglyoxal (MG) (Booth et al., 2003; Kosmachevskaya et al., 2015) (**Figure 14**). Induction of RND pumps by electrophilic stressors has not been reported thus far. Moreover, in one study exposure of strain PAO1 to MG was found to have no impact on multi-drug resistance of *P. aeruginosa* (Hayashi et al., 2014).

Like oxidative stress, electrophilic stress can be generated by endogenous sources such as the oxidative degradation of glucose, lipid peroxidation, and DNA oxidation (Kosmachevskaya et al., 2015) (**Figure 15**). Interestingly, *Escherichia coli* and several *Pseudomonas* spp. (not *P. aeruginosa*) harbor a chromosomal gene (*mgsA*) encoding a methylglyoxal synthase, suggesting an important role for MG in intracellular signaling at low concentrations (Booth et al., 2003; Töttemeyer et al., 1998; Winsor et al., 2016). Under stress conditions, RES can affect the cell redox potential at two levels: (i) by directly perturbing the electron transport chains and promoting ROS formation or (ii) by depleting redox cofactors like glutathione (GSH) and NAD(P)H (Ferguson et al., 1998a; Kosmachevskaya et al., 2015; Lee et al., 2013a). Additionally, RES react with amino groups of lysine, cysteine, arginine, and histidine residues to form Advanced Glycated-End products (AGEs) which compromise protein activities (Jacobs and Marnett, 2010) (Ferguson et al., 1998a), as well as with the guanosine residues present in DNA or other nucleotide-containing molecules to form adducts such as carboxymethyl- and carboxyethyl-guanosine that affect gene expression and cellular homeostasis (Marnett et al., 2003) (**Figure 15**).



**Figure 15: Formation of RES and cellular damage.** Formation of Reactive Electrophilic Species (RES) results from different cellular processes such as oxidation of sugars and DNA, and from lipid peroxidation. Accumulation of RES has pleiotropic effects (depletion of cofactors, alteration of electron transport chains (ETC), macromolecular damage of proteins and nucleotides) that impact cellular homeostasis.

Though RES are ubiquitous, highly reactive molecules acting on a broad spectrum of biological targets, description of bacterial responses to these stressors is scarce. *Escherichia coli* remains the model organism to understand cellular adaptation to electrophilic stress, as several studies have analyzed the mechanisms by which this bacterium senses, detoxifies, and protects itself against RES (Ferguson et al., 1998a; Kosmachevskaya et al., 2015; Lee and Park, 2017). Such mechanisms have never been studied in *P. aeruginosa*. However, several genes carried by the genome of this microorganism are homologous to genes involved in RES response in *E. coli* (Table 8).

#### 1.4.1 Electrophile sensing

In order to implement an adapted response to specific stress situations, bacteria need to detect the presence or accumulation of stressing molecules. Stress sensing usually involves one or several transcriptional regulators that are *de facto* the initial elements of the bacterial response. Such regulators directly interact with stressors or are activated by cognate membrane sensors (Table 8) (Lee and Park, 2017).

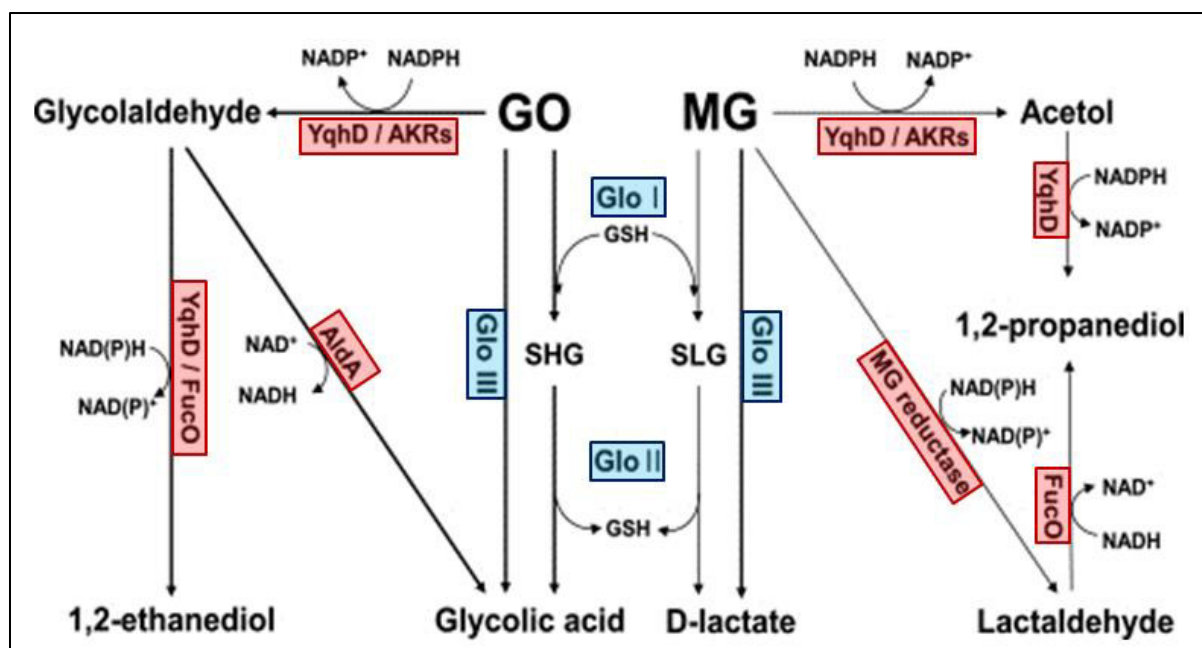
**Table 8: Electrophilic stress response in *E. coli* and homologous genes in *P. aeruginosa***

Response Mechanism	Genes in <i>E. coli</i>	Genes in <i>P. aeruginosa</i> *
<b>Electrophile sensing</b>		
	<i>yqhC</i>	PA2047, PA2276
	<i>nemR</i>	PA2196
	<i>Crp</i>	<i>dnr</i>
	<i>Fnr</i>	<i>anr</i>
	<i>nsrR</i>	-
<b>Detoxification of electrophiles</b>		
GSH-dependent glyoxalase system	<i>gloA</i> <i>gloB</i>	<i>gloA1</i> , <i>gloA2</i> , <i>gloA3</i> <i>gloB</i>
GSH-independent glyoxalase III	<i>hchA</i>	PA1135
NAD(P)H-dependent enzymes	<i>yqhD</i> <i>yqhE</i> <i>ygiN</i> <i>yafB</i> <i>yghZ</i> , <i>yajO</i> <i>yeaE</i> <i>nemA</i> <i>yhbO</i> <i>yajL</i> <i>elbB</i> <i>gldA</i>	PA2275 PA4167 PA2048 - PA1739 PA0804 <i>xenB</i> , PA2932, PA1334, PA0840 <i>pfpI</i> , PA4171 - PA5245 -
<b>Protective mechanisms</b>		
Cytoplasm acidification	<i>kefB</i> <i>kefC</i>	<i>kefB</i> -
DNA protection	<i>rpoS</i>	<i>rpoS</i>

\*Amino acid sequence homology was considered significant when identity was  $\geq 30\%$

**Adapted from Lee and Park., 2017 and Ferguson et al., 1998**

Gene *yqhC* was discovered in GO-resistant mutants of *E. coli* that overproduced aldehyde reductase YqhD, an enzyme which catalyzes transformation of GO into the less toxic molecule 1,2-ethanediol (**Figure 16**) (Lee et al., 2010). YqhC directly binds to the promoter region of operon *yqhDE*, the products of which are required for detoxification of GO, furfural, methylglyoxal and cinnamaldehyde (CNA) (Lee et al., 2010; Turner et al., 2011). However, it is still unclear whether these electrophiles directly bind to YqhC as ligands or whether the regulator is capable to indirectly detect the presence of these reactive species through a redox-sensing mechanism (Lee and Park, 2017).



**Figure 16: Catabolic pathways of electrophiles.** Glyoxal (GO) and methylglyoxal (MG) are two major Reactive Electrophilic Species (RES) that can be metabolized by two mechanisms: the glyoxalase system (in blue) and the NAD(P)H-dependent enzymes system (in red). AldA, aldehyde dehydrogenase; AKRs, aldo-keto reductases; GloI, GloII and GloIII, glyoxalases I, II and III; GSH, glutathione; SHG, S-2-hydroxyethylglutathione; SLG, S-D-lactoylglutathione.

The product of gene *nemR* is a TetR-like transcriptional regulator that represses operon *nemRA-gloA* expression in *E. coli* (Lee et al., 2013b). Loss-of-function mutations in *nemR* or bacterial exposure to inhibitory concentrations of GO, MG or quinones leads to constitutive upregulation of N-ethylmaleimide reductase gene *nemA* and glyoxalase I gene *gloA*, as well as a GO resistant phenotype (Lee et al., 2013b; Ozyamak et al., 2013). The thiol-based sensing mechanism of NemR relies on two cysteine residues (C<sub>21</sub>- and C<sub>116</sub>-) able to establish intermolecular disulfide bonds between two NemR monomers, which results in an inactive dimeric conformation (Lee et al., 2013b). Exposure of *E. coli* or the purified NemR protein to H<sub>2</sub>O<sub>2</sub> does not affect *nemRA-gloA* expression, suggesting that this regulator is sensitive to RES only (Lee et al., 2013b).

The global transcriptional regulator CRP, which is activated by cAMP, modulates expression of more than 180 genes in *E. coli* (Zheng et al., 2004). Screening of GO-resistant insertional mutants revealed that the CRP gene (named *crp*) was disrupted in some of them (Lee et al., 2016). Consistent with this, inactivation of adenylate cyclase gene *cya* also turned out to confer resistance to GO and MG (Lee et al., 2016). Actually, a number of genes involved in RES detoxification such as *yqhC*, *yqhD*, *yafB*, and *gloA* are dependent on cAMP/CRP (Lee et al., 2016).



Genes *fnr* and *nsrR* that encode repressors of aldo-keto reductase YafB gene are other players in electrophile sensing (Lee and Park, 2017). YafB catalyzes reduction of GO and MG into the less toxic metabolites glycoaldehyde and acetol, respectively (Kwon et al., 2012). Fnr and NsrR are global regulators involved in redox- and nitrite-responses, respectively. Deletion of the Fnr and NsrR binding sites upstream from *yafB* as well as exposure of *E. coli* to GO were reported to increase *yafB* expression, suggesting that this induction could be linked to the presence of electrophiles themselves or to their effects on the redox state of cell.

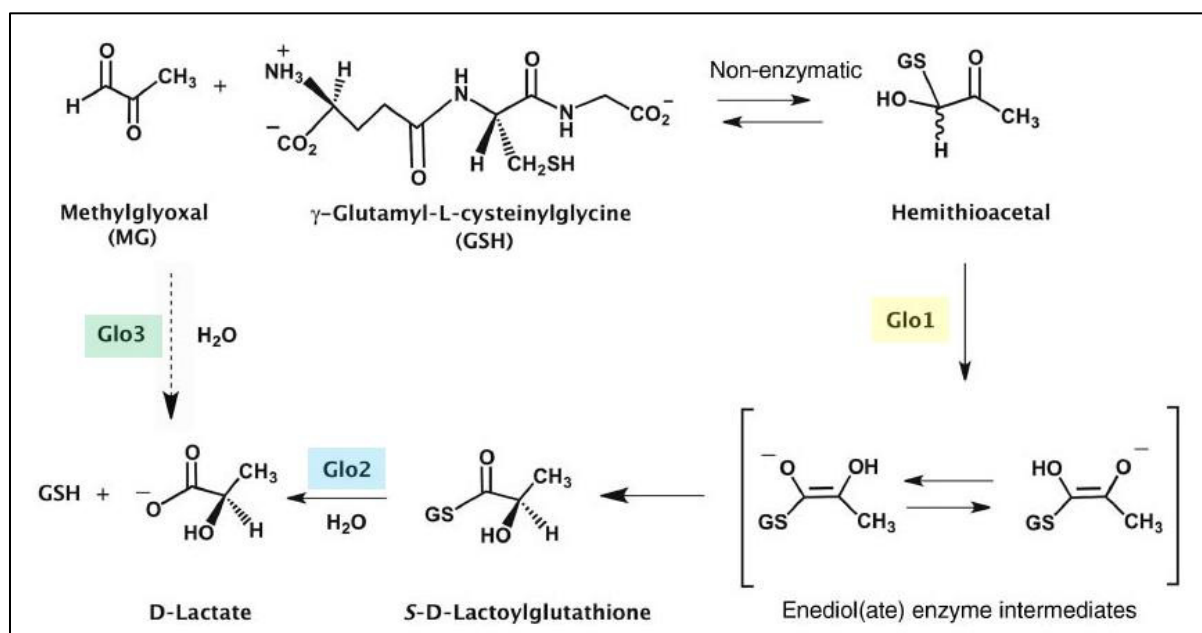
#### **1.4.2 Detoxification of electrophiles**

Bacterial detoxification of electrophiles (GO and MG) has extensively been studied. It involves both the glyoxalase system and NAD(P)H-dependent enzymes (Abdallah et al., 2016; Adams and Jia, 2005; Booth et al., 2003; Ferguson et al., 1998a; Kwon et al., 2012; Lee et al., 2010, 2013b, 2016; Ozyamak et al., 2013; Sukdeo and Honek, 2007) (**Figure 16**).

In *E. coli*, the glyoxalase system is the most efficient mechanism for detoxification of GO and MG. It consists of two glutathione (GSH)-dependent enzymes, namely glyoxalases I and II, and one GSH-independent enzyme, glyoxalase III (Kosmachevskaya et al., 2015; Lee and Park, 2017) (**Figure 17**). Glyoxalase I (Glo1) is encoded by gene *gloA*. Thanks to its S-D-lactoylglutathione lyase activity, the enzyme catalyzes formation of GSH adducts, S-2-hydroxyethylglutathion (SHG) and S-D-lactoylglutathion (SLG) with GO and MG, respectively (Thornalley, 1990). These adducts can modulate the activity of two potassium efflux pumps KefB and KefC which will be described below (Ferguson et al., 2000; MacLean et al., 1998). *P. aeruginosa* differs from *E. coli* as it harbors three glyoxalase I genes in its chromosome (*gloA1*, *gloA2*, and *gloA3*), but the differential activities of their products remain unknown (Sukdeo and Honek, 2007). Glyoxalase II (Glo2) is a hydroxyacylglutathione hydrolase that converts SHG and SLG into glycolic acid and D-lactate, respectively with concomitant release of GSH (**Figure 17**) (Lee and Park, 2017). Finally, glyoxalase III catalyzes reduction of GO and MG through a single-step reaction, without the need of any co-factor (Lee and Park, 2017).

The second pathway of electrophile detoxification involves NAD(P)H-dependent enzymes (**Figure 16**). In *E. coli*, several enzymes, for the most aldehyde reductases, are able to reduce various electrophiles into less toxic alcohols (Lee and Park, 2017). Remarkably, YqhD can convert MG, GO and CNA *in vitro* (Lee et al., 2010; Visvalingam et al., 2013). However, its role *in vivo* in the metabolism of MG is minor compared to that of the glyoxalase system (Lee

et al., 2010, 2013b). Actually, YqhD is of major importance in protection of *E. coli* from electrophiles derived from lipid peroxidation, such as acetaldehyde, malondialdehyde, propanaldehyde, butanaldehyde, and acrolein) (Pérez et al., 2008).

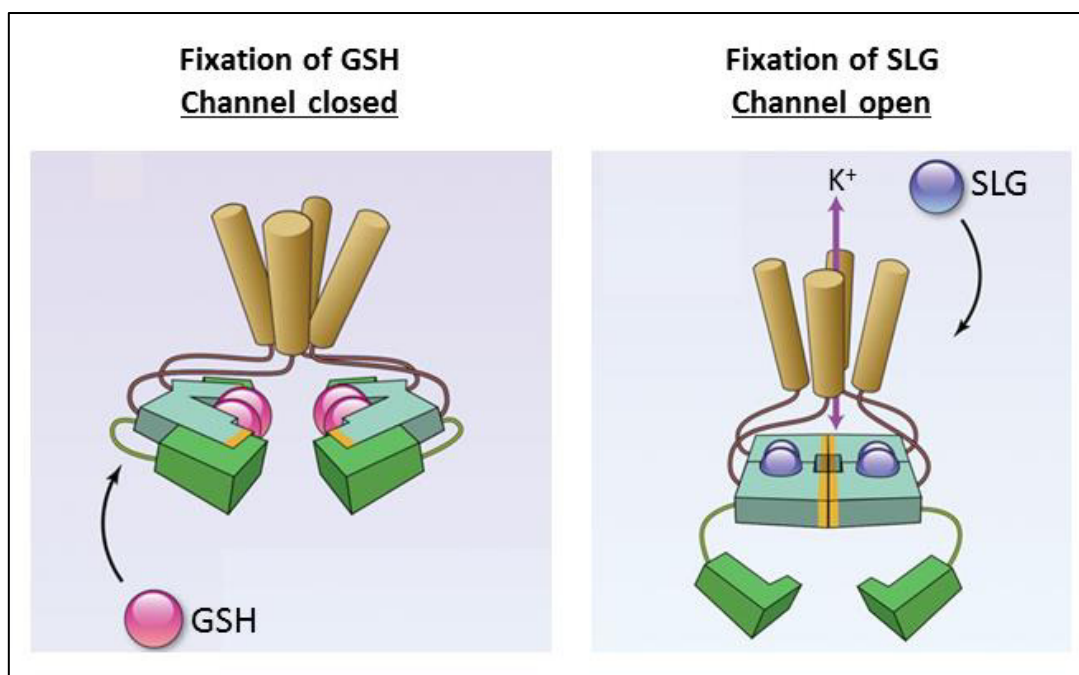


**Figure 17: Biochemical reactions catalyzed by the glyoxalase system.** Spontaneous reaction between methylglyoxal (MG) and reduced glutathione (GSH) forms a hemithioacetal which is substrate for glyoxalase I (Glo1, in yellow); this enzyme produces the GSH-adduct S-D-lactoylglutathione (SLG). Glyoxalase II (Glo2, in blue) takes SLG as substrate to form D-lactate enabling the turnover of GSH. Finally, glyoxalase III (Glo3, green) can directly reduce MG into D-lactate without any cofactor. (Honek, 2014)

### 1.4.3 Protective mechanisms against electrophiles

Electrophiles are highly toxic for bacteria (Ferguson et al., 1998a). Survival of *E. coli* to these agents depends on multiple mechanisms including activation of  $K^+$  efflux systems KefB and KefC and intervention of sigma factor RpoS in DNA protection (Ferguson, 1999).

As stated before, Glo1 produces GSH-adducts in the presence of GO or MG (Lee and Park, 2017; Thornalley, 1990). These adducts are activators of the KefB and KefC pumps (Elmore et al., 1990; Ferguson et al., 1993). In the absence of electrophiles, the binding of reduced glutathione (GSH) to these systems make them adopt a closed conformation which prevents the leakage of potassium outside the cell (**Figure 18** left panel) (Kilfoil et al., 2013). Upon electrophile exposure, the GSH-adducts (e.g. SLG) produced by Glo1 bind to KefB/C and provoke the opening of the channel with subsequent efflux of  $K^+$  (Ferguson, 1999; Kilfoil et al., 2013) (**Figure 18** right panel).



**Figure 18: Activation of KefB/C potassium channels by glutathione-adducts.** The KefB and KefC channels are activated by glutathione-adducts produced by glyoxalase I. In the absence of electrophiles, the channels are under a closed conformation due to binding of reduced glutathione (GSH) (left panel). When electrophiles accumulate in the cell, glyoxalase I produces glutathione-adducts such as S-D-lactoylglutathione (SLG), that bind and open the KefB/C channels provoking the release of  $K^+$  from the cell. Efflux of  $K^+$  is coupled with influx of protons, with subsequent acidification of cytosol. Adapted from Kilfoil et al., 2013.

The rapid efflux of potassium by these systems is coupled with an influx of protons likely independent from the transport activity of KefB/C (Ferguson, 1999). The acidification of cytoplasm (decrease of 0.4-0.6 units upon exposure to MG) that results from  $H^+$  import would reduce the reactivity of electrophiles by decreasing their interaction with macromolecules (Ferguson et al., 1998a). Confirming the important role of cytoplasm acidification in RES response, weak acids were found to protect *E. coli* from MG (Booth et al., 2003; Ferguson, 1999; Ferguson et al., 1998a). However, though potassium efflux systems are crucial in bacterial survival to some electrophiles such MG, they are dispensable in the defense against iodoacetate and chlorodinitrobenzene (Ferguson, 1999; Ferguson et al., 1998a; Ness et al., 1997). It is interesting to note that in *P. aeruginosa* overproduction of RND pumps has also been proposed to result in cytoplasm acidification (decreased of about 0.6 units) (Olivares Pacheco et al., 2017) but the impact of this on electrophile detoxification has not been investigated.

Finally, the observation that stationary-phase cells of *E. coli* are more resistant to electrophiles than fast-growing bacteria led to the hypothesis that sigma factor RpoS has a protective role against these reactive species. Indeed, expression of several genes of RpoS regulon is induced in stationary phase. The resistance to electrophiles could involved protein Dps that binds to

and would protect DNA from damages (Ferguson et al., 1998b). However, again the mode of action of RpoS as well as Dps needs to be clarified.

## **2 Results**

### **2.1 Toxic Electrophiles Induce Expression of the Multi-Drug Efflux Pump MexEF-OprN in *Pseudomonas aeruginosa* Through a Novel Transcriptional Regulator, CmrA**

**Paulo Juarez**, Katy Jeannot, Patrick Plésiat and Catherine Llanes

*Antimicrobial Agents and Chemotherapy*. 2017 May 15; 61(8): e00585-17. Doi: 10.1128/AAC.00585-17





# Toxic Electrophiles Induce Expression of the Multidrug Efflux Pump MexEF-OprN in *Pseudomonas aeruginosa* through a Novel Transcriptional Regulator, CmrA

 Paulo Juarez,<sup>a</sup> Katy Jeannot,<sup>a,b</sup> Patrick Plésiat,<sup>a,b</sup> Catherine Llanes<sup>a</sup>

Laboratoire de Bactériologie, UMR CNRS 6249 Chrono-Environnement, Université Bourgogne Franche-Comté, Besançon, France<sup>a</sup>; Centre National de Référence de la Résistance aux Antibiotiques, Centre Hospitalier Régional Universitaire de Besançon, Besançon, France<sup>b</sup>

**ABSTRACT** The multidrug efflux system MexEF-OprN is produced at low levels in wild-type strains of *Pseudomonas aeruginosa*. However, in so-called *nfxC* mutants, mutational alteration of the gene *mexS* results in constitutive overexpression of the pump, along with increased resistance of the bacterium to chloramphenicol, fluoroquinolones, and trimethoprim. In this study, analysis of *in vitro*-selected chloramphenicol-resistant clones of strain PA14 led to the identification of a new class of MexEF-OprN-overproducing mutants (called *nfxC2*) exhibiting alterations in an as-yet-uncharacterized gene, PA14\_38040 (homolog of PA2047 in strain PAO1). This gene is predicted to encode an AraC-like transcriptional regulator and was called *cmrA* (for chloramphenicol resistance activator). In *nfxC2* mutants, the mutated CmrA increases its proper gene expression and upregulates the operon *mexEF-oprN* through MexS and MexT, resulting in a multidrug resistance phenotype without significant loss in bacterial virulence. Transcriptomic experiments demonstrated that CmrA positively regulates a small set of 11 genes, including PA14\_38020 (homolog of PA2048), which is required for the MexS/T-dependent activation of *mexEF-oprN*. PA2048 codes for a protein sharing conserved domains with the quinol monoxygenase YgiN from *Escherichia coli*. Interestingly, exposure of strain PA14 to toxic electrophilic molecules (glyoxal, methylglyoxal, and cinnamaldehyde) strongly activates the CmrA pathway and upregulates MexEF-OprN and, thus, increases the resistance of *P. aeruginosa* to the pump substrates. A picture emerges in which MexEF-OprN is central in the response of the pathogen to stresses affecting intracellular redox homeostasis.

**KEYWORDS** *Pseudomonas aeruginosa*, efflux, MexEF-OprN, CmrA, electrophilic stress, efflux pumps

*Pseudomonas aeruginosa*, a Gram-negative pathogen of major clinical importance, is notorious for its ability to develop a high level of resistance to multiple antibiotics and cause hard-to-treat infections (1). When upregulated upon mutations in regulatory genes, RND (resistance nodulation cell division) efflux pumps contribute substantially to multiresistance in clinical isolates (2). One of these systems, MexEF-OprN, is able to export fluoroquinolones, trimethoprim (TMP), and chloramphenicol (CHL) (3). This tripartite pump is regulated by MexT, a LysR-like activator, whose gene (*mexT*) is located upstream from operon *mexEF-oprN* (4). The stable overproduction of MexEF-OprN in so-called *nfxC* mutants increases the resistance levels for all the pump substrates by 2- to 16-fold, while the MICs of carbapenems increase from 2- to 4-fold as a result of concurrent MexT-dependent downregulation of porin OprD (3). The reduced expression of RND pumps MexAB-OprM and MexXY/OprB observed in these mutants has

Received 22 March 2017 Returned for modification 18 April 2017 Accepted 11 May 2017

Accepted manuscript posted online 15 May 2017

**Citation** Juarez P, Jeannot K, Plésiat P, Llanes C. 2017. Toxic electrophiles induce expression of the multidrug efflux pump MexEF-OprN in *Pseudomonas aeruginosa* through a novel transcriptional regulator, CmrA. *Antimicrob Agents Chemother* 61:e00585-17. <https://doi.org/10.1128/AAC.00585-17>.

**Copyright** © 2017 American Society for Microbiology. All Rights Reserved.

Address correspondence to Patrick Plésiat, [patrick.plesiat@univ-fcomte.fr](mailto:patrick.plesiat@univ-fcomte.fr).

been proposed to account for the paradoxical hypersusceptibility to penicillins, cephalosporins, and aminoglycosides (5). In addition, *nfxC* mutants are deficient in the production of some extracellular virulence factors, such as pyocyanin, elastase, and rhamnolipids, and exhibit reduced activity of the type III secretion system compared to its activity in wild-type strains (6, 7). Such impaired virulence involves the pump itself, which is thought to export some precursors of the quorum-sensing signal molecule PQS (*Pseudomonas* quinolone signal) (8). Additionally, it also involves the action of MexT, acting as a global regulator of gene expression (9).

Most *nfxC* mutants harbor disruptive mutations in gene *mexS*, predicted to encode a quinone oxidoreductase (10). Suppression of MexS activity in *P. aeruginosa* activates the regulator MexT, which in turn triggers the transcription of the operon *mexEF-oprN*. We recently showed that in the clinical setting, most of the MexEF-OprN-overproducing mutants studied either harbored single-amino-acid substitutions in MexS or contained wild-type copies of *mexS* and *mexT* genes (11). Furthermore, it appeared that none of the other genes previously reported to upregulate *mexEF-oprN* expression *in vitro* (*ampR*, *mvaT*, *parRS*, *mxtR*, and *brlR* [12–16]) was mutated in these isolates, indirectly suggesting the existence of additional regulatory loci controlling *mexEF-oprN* expression.

The present study was thus undertaken to decipher the complex regulation and to gain insight into the physiological function of this efflux system. Analysis of *in vitro* mutants derived from reference strain PA14 has led to the identification of a novel regulator of MexEF-OprN, CmrA, that responds to electrophilic stress.

## RESULTS AND DISCUSSION

***In vitro* selection of chloramphenicol-resistant mutants overproducing MexEF-OprN.** A previous study on multidrug-resistant clinical strains of *P. aeruginosa* showed that the active efflux system MexEF-OprN can be constitutively upregulated in mutants producing intact MexS and MexT proteins (11). In order to identify novel regulators of this pump, we carried out the selection of spontaneous mutants overproducing MexEF-OprN from reference strain PA14 on agar plates supplemented with chloramphenicol at 128, 256, and 512  $\mu\text{g ml}^{-1}$ . In contrast to most isolates of the PAO1 lineage, PA14 (chloramphenicol MIC of 64  $\mu\text{g ml}^{-1}$ ) harbors functional *mexS* and *mexT* genes, which makes it suitable for such experiments (11). Thirty resistant colonies were randomly selected under each condition (90 colonies) and further screened by the disk diffusion method for increased resistance to ciprofloxacin (CIP) and imipenem compared to that of the parent strain PA14 (data not shown). Typical *nfxC* mutants indeed exhibit cross-resistance to chloramphenicol, fluoroquinolones, and carbapenems (3). Reverse transcription-quantitative PCR (RT-qPCR) experiments revealed that 40 subselected mutants significantly overexpressed *mexE* (from 34- to 116-fold more than in PA14; data not shown). Of these 40 mutants, 24 harbored indels disrupting gene *mexS* (mutation rate of  $2.5 \times 10^{-7}$ ), and 12 produced single-amino-acid variants of protein MexS ( $1.4 \times 10^{-7}$ ). Interestingly, the remaining four mutants appeared to have intact *mexS* and *mexT* genes ( $2.5 \times 10^{-8}$ ). We focused our attention on the latter mutants, named PJ01, PJ02, PJ03, and PJ04 (collectively referred to as PJ mutants below). All of them exhibited an *nfxC*-type resistance profile, characterized by 8- to 16-fold increases in the MICs of ciprofloxacin, chloramphenicol, and trimethoprim relative to those of PA14 (Table 1). Interestingly, these resistance levels were somewhat lower than those of the *nfxC* control strain PA14 $\Delta$ *mexS*. Other features of *nfxC* strains were also less pronounced in PJ mutants, such as the resistance to imipenem and the hypersusceptibility to the MexXY substrate gentamicin, although the MICs of aztreonam (a MexAB-OprM substrate) were identical (Table 1). Likewise, the production of virulence factors, such as pyocyanin, biofilm formation, and swarming motility, was less compromised in these mutants than in PA14 $\Delta$ *mexS* (see Fig. S1 in the supplemental material). Consistent with these observations, all these phenotypic traits were associated with relative abundances of *mexE* transcripts that were 1.5- to 3.4-fold lower than in PA14 $\Delta$ *mexS*. The decreases in the relative expression of genes *oprD*, *mexB*, and *mexY* were also com-

**TABLE 1** Characterization of *nfxC2* mutants

Strain	CmrA sequence variation	Transcript level of <sup>a</sup> :							MIC ( $\mu\text{g ml}^{-1}$ ) of <sup>b</sup> :					
		<i>cmrA</i>	<i>mexE</i>	<i>mexS</i>	<i>mexT</i>	<i>oprD</i>	<i>mexB</i>	<i>mexY</i>	CIP	CHL	TMP	IPM	ATM	GEN
PA14	WT	1	1	1	1	1	1	1	0.125	64	64	1	4	1
PA14 $\Delta$ <i>mexS</i>	WT	0.6	116	ND	0.9	0.1	0.1	0.2	4	2,048	1,024	4	2	0.25
PA14 $\Delta$ <i>mexT</i>	WT	1	0.4	1.1	ND	1	1	1	0.125	64	64	1	4	1
PJ01	A <sub>68</sub> V	71	38	5.6	1.6	0.2	0.2	0.4	1	1,024	512	2	2	0.5
PJ02	H <sub>204</sub> L	84	34	2.4	1.3	0.2	0.2	0.4	1	1,024	512	2	2	0.5
PJ03	L <sub>89</sub> Q	53	74	2.3	1.6	0.2	0.1	0.4	2	2,048	1,024	2	2	0.5
PJ04	N <sub>214</sub> K	120	62	2.8	1	0.2	0.1	0.4	2	2,048	1,024	2	2	0.5
PA14 $\Delta$ <i>cmrA</i>	— <sup>c</sup>	ND	0.5	1.1	0.6	1	1.1	0.9	0.125	64	64	1	4	1
PJ01 $\Delta$ <i>cmrA</i>	—	ND	0.6	1.6	1.1	1.5	1.1	1.2	0.125	64	64	1	4	1
PA14 $\Delta$ <i>cmrA</i> <sub>PA14</sub>	WT	1.8	1.7	1.9	0.9	1	0.8	0.9	0.125	64	64	1	4	1
PA14 $\Delta$ <i>cmrA</i> <sub>PJ01</sub>	A <sub>68</sub> V	68	29	6.1	2.7	0.2	0.1	0.4	1	512	256	2	2	0.5
PJ01 $\Delta$ <i>mexT</i>	WT	76	<0.1	1.3	ND	2.7	1	1.5	0.125	64	64	1	4	1
PJ01 $\Delta$ <i>mexS</i>	WT	70	<0.1	ND	1.9	1.3	0.8	1.7	0.125	64	64	1	4	1

<sup>a</sup>Expressed as the ratio to the value for wild-type reference strain PA14. Mean values were calculated from two independent bacterial cultures each assayed in duplicate. ND, not determined.

<sup>b</sup>CIP, ciprofloxacin; CHL, chloramphenicol; TMP, trimethoprim; IPM, imipenem; ATM, aztreonam; GEN, gentamicin.

<sup>c</sup>—, strain lacks the gene.

paratively smaller in the PJ mutants (Table 1). Because of all the genetic and phenotypic differences described above, this new type of MexEF-OprN-upregulated mutants was dubbed *nfxC2*.

**A novel gene implicated in regulation of *mexEF-oprN*.** Sequencing of genes *mexT*, *mvaT*, *ampR*, and *mxtR*, known to influence *in vitro* the expression of the operon *mexEF-oprN* (12, 13, 15), did not reveal any mutations in the PJ mutants. Therefore, three of them (PJ01, PJ03, and PJ04) were submitted to whole-genome sequencing. Alignment of the sequence reads from PJ01 ( $n = 1,041,118$ ), PJ03 ( $n = 1,290,598$ ), and PJ04 ( $n = 1,443,653$ ) with the strain UCBPP-PA14 genome revealed the existence of three single-nucleotide polymorphisms (SNPs) in each of the mutants tested (Table S1). In an interesting way, it appeared that all of them harbored different SNPs in the same gene, PA14\_38040. These results were confirmed by PCR and Sanger sequencing. Compared to the sequence of PA14, the mutations were predicted to generate amino acid substitutions A<sub>68</sub>V (a change of A to V at position 68), L<sub>89</sub>Q, and N<sub>214</sub>K in the encoded products of PJ01, PJ03, and PJ04, respectively (Table 1). Subsequent sequencing of the last mutant, PJ02, also revealed an H<sub>204</sub>L substitution in the same protein. According to the GenBank database, gene PA14\_38040 codes for an as-yet-uncharacterized transcriptional regulator of the AraC family. This gene was named *cmrA* (for chloramphenicol resistance Activator), referring to the conditions of selection of PJ mutants. Interestingly, it turned out that the relative expression of gene *cmrA* was upregulated in all PJ mutants (from 53- to 120-fold that of PA14), indicating that CmrA likely activates its own gene transcription (Table 1).

**Role of CmrA in antibiotic resistance.** To confirm the potential implication of CmrA in *mexEF-oprN* activation and, thus, the resistance phenotype of PJ mutants, we deleted the coding sequence of *cmrA* in both PJ01 and PA14, yielding PJ01 $\Delta$ *cmrA* and PA14 $\Delta$ *cmrA*, respectively. The MICs of MexEF-OprN substrates (ciprofloxacin, chloramphenicol, and trimethoprim) and of carbapenems (imipenem) were restored to wild-type levels in PJ01 $\Delta$ *cmrA* but remained unchanged for PA14 $\Delta$ *cmrA* (Table 1). These results clearly demonstrated that CmrA activates the efflux operon in mutant PJ01 but does not contribute to the intrinsic resistance of *P. aeruginosa* to the drugs tested. Moreover, deletion of *cmrA* in PJ01 restored the wild-type susceptibility to  $\beta$ -lactams (aztreonam) and to aminoglycosides (gentamicin), cancelling the negative impact of overproduced MexEF-OprN on efflux pumps MexAB-OprM and MexXY, respectively. To confirm these data, we inserted a single copy of the *cmrA* allele from PJ01 into the chromosome of PA14 $\Delta$ *cmrA* (to yield PA14 $\Delta$ *cmrA*<sub>PJ01</sub>). As expected, PA14 $\Delta$ *cmrA*<sub>PJ01</sub> displayed a resistance profile similar to that of PJ01, whereas the control strain



**TABLE 2** Impact of overexpression of *cmrA* and PA2048

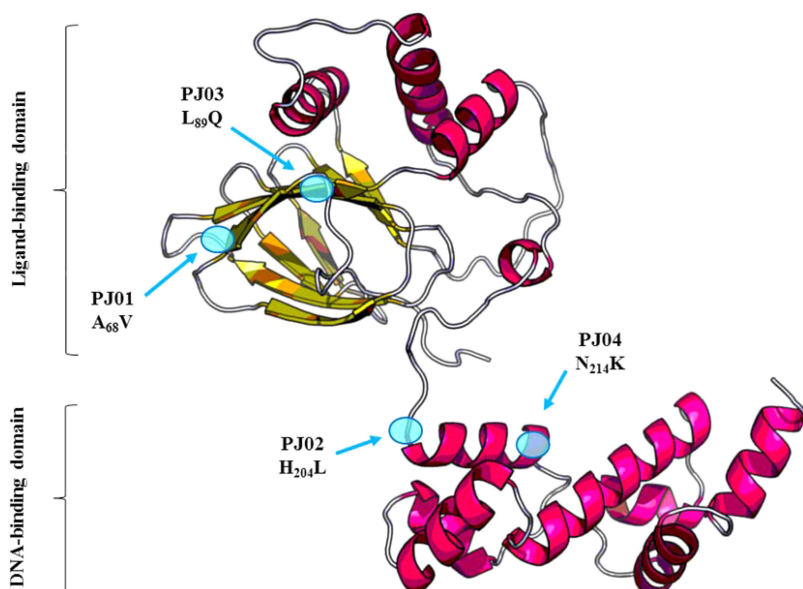
Transformant	Value without (with) arabinose for <sup>a</sup> :					
	Transcript level <sup>b</sup>			MIC ( $\mu\text{g ml}^{-1}$ ) <sup>c</sup>		
	<i>cmrA</i>	PA2048	<i>mexE</i>	CIP	CHL	TMP
PA14(pJN105)	1 (1)	1 (1)	1 (1)	0.125 (0.125)	128 (128)	128 (128)
PA14(pJN105:: <i>cmrA</i> <sub>PA14</sub> )	385 (>1,000)	4.5 (3.8)	1.1 (1.3)	0.125 (0.125)	128 (128)	128 (128)
PA14(pJN105:: <i>cmrA</i> <sub>PJ01</sub> )	458 (>1,000)	35 (53)	20 (50)	1 (1)	1,024 (2,048)	256 (512)
PA14(pJN105::PA2048)	1.6 (4.1)	135 (>1,000)	52 (270)	1 (2)	1,024 (2,048)	256 (512)

<sup>a</sup>Values obtained without and with 0.5% arabinose, used as an inducer of gene expression.

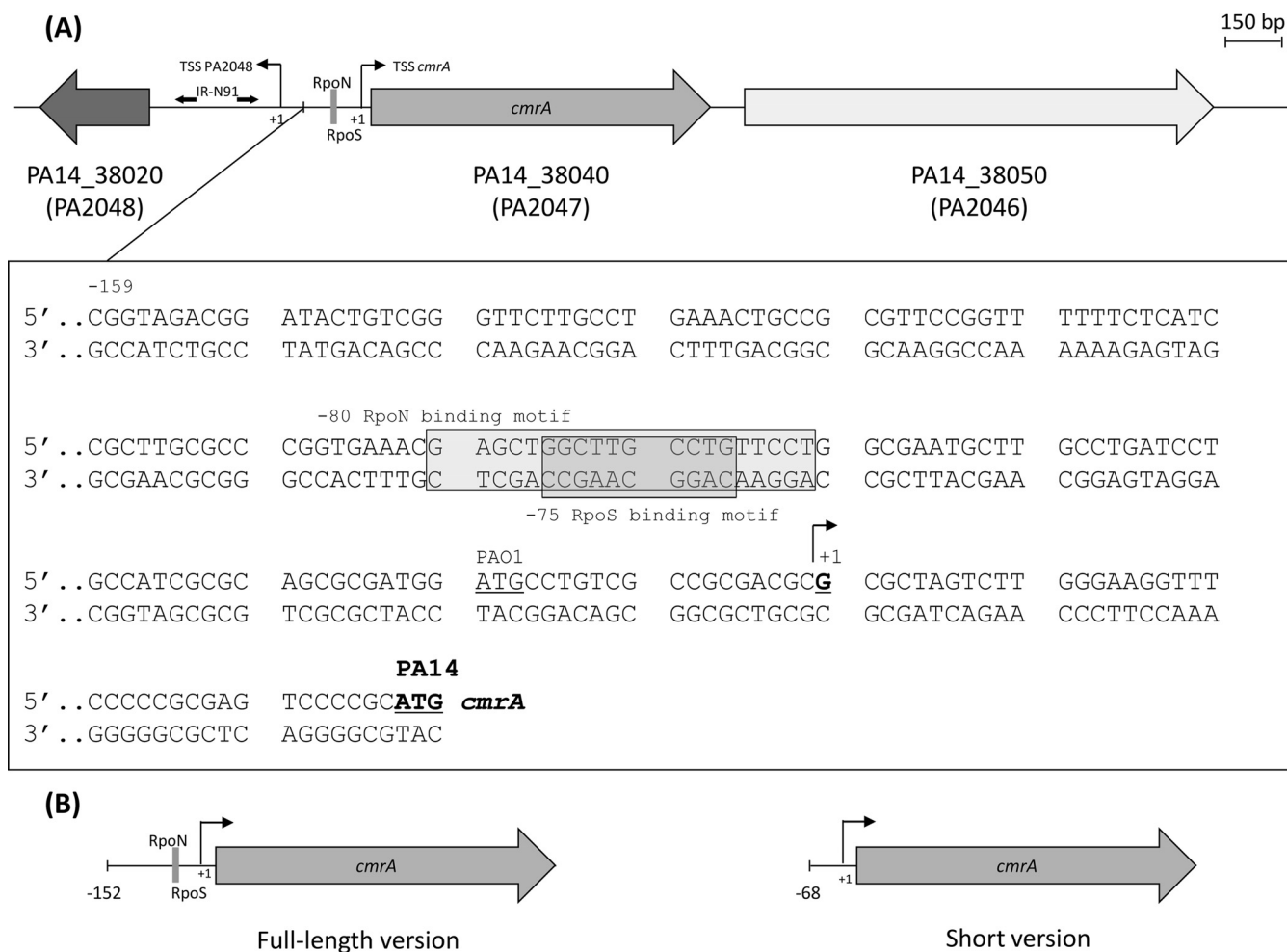
<sup>b</sup>Expressed as the ratio to the value for PA14(pJN105).

<sup>c</sup>CIP, ciprofloxacin; CHL, chloramphenicol; TMP, trimethoprim.

complemented with the wild-type *cmrA* allele, PA14 $\Delta$ *cmrA*<sub>PA14</sub>, remained fully susceptible to all the antibiotics tested (Table 1). PA14 $\Delta$ *cmrA*<sub>PJ02</sub>, PA14 $\Delta$ *cmrA*<sub>PJ03</sub>, and PA14 $\Delta$ *cmrA*<sub>PJ04</sub> were phenotypically similar to PA14 $\Delta$ *cmrA*<sub>PJ01</sub> (data not shown). Finally, as shown by the results in Table 2, overexpression of a plasmid-borne copy of the PJ01 *cmrA* allele [PA14(pJN105::*cmrA*<sub>PJ01</sub>)] was associated with increased resistance to ciprofloxacin (8-fold), chloramphenicol (8- to 16-fold), and to a lesser extent, trimethoprim (2- to 4-fold), concomitant with a 20- to 50-fold increase in *mexE* transcripts. Overexpression of the wild-type allele *cmrA* in PA14 had no significant effects on the susceptibility of the strain to antibiotics [see PA14(pJN105::*cmrA*<sub>PA14</sub>) in Table 2], reinforcing the idea that the CmrA peptide produced by PJ01 is under an activated conformation. According to the structure modeling of CmrA provided by the RaptorX Web server (17), the amino acid substitutions A<sub>68</sub>V and L<sub>89</sub>Q reside in the putative N-terminal ligand-binding domain, while H<sub>204</sub>L and N<sub>214</sub>K are located in the C-terminal DNA-binding domain of the protein (Fig. 1). Altogether, these findings showed that CmrA is a novel regulator of the AraC family, able to trigger directly or indirectly the expression of *mexEF-oprN* when constitutively activated by single-amino-acid substitutions located in two different functional domains of the protein.



**FIG 1** RaptorX prediction of CmrA structure. A three-dimensional structure of the regulator CmrA was modeled using the RaptorX Web server (<http://raptorx.uchicago.edu/>). The putative N-terminal ligand-binding domain (from amino acid position 40 to 191) was predicted based on ToxT from *Vibrio cholerae* (PDB 3GBG;  $P = 5.96 \times 10^{-4}$ ), while the putative C-terminal DNA-binding domain (from 198 to 310) is based on AdpA from *Streptomyces griseus* (PDB 3W6V;  $P = 3.45 \times 10^{-5}$ ). The amino acid substitutions found in PJ mutants are highlighted by blue spots.



**FIG 2** Genetic environment of gene *cmrA*. (A) Gene annotations are those available in GenBank for strain PA14 (RefSeq accession number [NC\\_008463.1](https://ncbi.nlm.nih.gov/assembly/GCA000000000/NC_008463.1)). Homologs in strain PA01 are indicated in brackets. The DNA sequence upstream from *cmrA* is shown below the schematic. Different positions were assigned to the start codon of *cmrA* in genomic maps of PA14 (PA14\_38040, 933 bp; boldface and underlined) and PA01 (PA2047, 990 bp; underlined). Two putative overlapping RpoN and RpoS binding motifs are highlighted in gray. The transcription start sites (TSS, +1) of *cmrA* and PA2048 were mapped by 5'-RACE at -38 bp and -315 bp, respectively. The 5' UTR of PA2048 contains a 111-bp region of unknown function, bordered by two 10-bp inverted repeats (IR-N91). (B) Complementation experiments in mutant PA14Δ*cmrA* were carried out to clarify the role of the  $\sigma$  factor binding sites in *cmrA* expression. A full-length DNA fragment from mutant PJ01, carrying *cmrA* and the RpoN/RpoS binding sites (-152 bp upstream from the TSS), conferred an *nfxC2* resistance phenotype on PA14Δ*cmrA*, while a short version lacking the RpoN/RpoS binding sites (-68 bp) did not. The whole sequence of *cmrA* and its 5' UTR is accessible through the GenBank database (accession number [KX274690](https://ncbi.nlm.nih.gov/assembly/GCA000000000/KX274690)).

**Characterization of *cmrA* locus.** The *cmrA* gene is highly conserved among *P. aeruginosa* strains. Homologs were found in PA01 (PA2047, 99% sequence identity), PACS2 (AOK\_RS09840, 98%), and LESB58 (PALES\_30281, 98%). However, in strain PA01 (18), a potential start codon (ATG<sub>PA01</sub>) has been mapped 57 nucleotides upstream from that of PA14 (ATG<sub>PA14</sub>), leading to a translated peptide of 329 amino acids instead of 310 (Fig. 2A). *In silico* analysis of the upstream region of both ATGs failed to show any putative ribosome binding site (RBS) sequence, which could have helped us to define the correct start codon of *cmrA*. We thus carried out 5'-RACE (rapid amplification of 5' cDNA ends) experiments to identify the transcription start site (TSS) of the gene. Sequencing analysis of the 5'-RACE product revealed that the *cmrA* TSS is a guanine residue located 19 bp downstream from the proposed ATG<sub>PA01</sub>, a result that contradicts this annotation but validates that of PA14, with the TSS (+1) located 38 bp upstream from ATG<sub>PA14</sub> (Fig. 2A).

Analysis of the putative sigma factor binding motifs (SFBMs) of PA14 (sigmulome) (19) proved to be useful to predict the location of the *cmrA* promoter (P<sub>*cmrA*</sub>). Hence, comparison of the DNA region upstream from *cmrA* TSS with the PA14 sigmulome

highlighted the presence of two overlapping SFBMs for RpoN (–80 bp) and RpoS (–75 bp) (Fig. 2A). *cis* complementation of strain PA14Δ*cmrA* with a fragment containing *cmrA* preceded by the full-length RpoN/RpoS binding region (–152 bp upstream from the TSS, Fig. 2B) successfully generated an *nfxC2* resistance phenotype, while complementation with a shorter fragment lacking the RpoN/RpoS SFBMs (–68 bp upstream from the TSS) had no effect (data not shown). These data provide evidence that the RpoN/RpoS region is necessary to activate the expression of *cmrA* (19). Whether *cmrA* is under the control of RpoN and/or RpoS remains to be determined.

**MexT- and MexS-dependent upregulation of the operon *mexEF-oprN* in *nfxC2* mutants.** Because the upregulation of *mexEF-oprN* requires a functional regulator, MexT, in *mexS* mutants (5), we examined whether this also applies to *cmrA* mutants. Inactivation of *mexT* in PJ01 (PJ01Δ*mexT*) (Table 1) restored a wild-type profile, thereby demonstrating MexT-dependent activation of MexEF-OprN in *nfxC2* mutants. In agreement with these data, the transcript levels of *mexE* were strongly reduced in the absence of *mexT* (>380-fold), while those of genes *oprD*, *mexB*, and *mexY* increased significantly, from 2.7- to 5-fold (Table 1).

Finally, as the inactivation of *mexS* is the main mutational cause of *mexEF-oprN* overexpression in both *in vitro* (10) and clinical strains (11), we deleted this gene in PJ01 to see whether this would result in a stronger activation of the efflux operon and, thus, higher resistance levels. Surprisingly, loss of *mexS* in mutant PJ01Δ*mexS* totally abolished *mexEF-oprN* overexpression and restored a PA14-like resistance phenotype (Table 1), a result that underlines a functional link between MexS and CmrA or between MexS and one or several genes under the control of CmrA. Again, as for PJ01Δ*mexT*, the phenotypic changes noted in PJ01Δ*mexS* relative to PJ01 were associated with significant variations in the expression of genes *mexE*, *oprD*, *mexB*, and *mexY*. Similar results were obtained with the other mutants, PJ02Δ*mexS*, PJ03Δ*mexS*, and PJ04Δ*mexS* (data not shown).

**Identification of genes regulated by CmrA.** To better understand the physiological role of CmrA and to identify the genes under its control, we performed a transcriptomic analysis by RNA-seq of *cmrA* mutant PJ01 in comparison with parental strain PA14. Since MexT regulates the expression of 143 genes in *P. aeruginosa* (20), we analyzed the transcriptome of mutant PJ01Δ*mexT* as well. This allowed us to identify, by subtraction, genes whose expression is exclusively regulated by CmrA. Data analysis showed that 53 genes were differentially expressed between mutant PJ01 and strain PA14, 26 of them being upregulated and 27 downregulated in PJ01 (threshold fixed at 3.0-fold) (GEO accession number [GSE86211](https://www.ncbi.nlm.nih.gov/geo/query/acc.cgi?acc=GSE86211)) (see Fig. S2). Comparison of strains PA14 and PJ01Δ*mexT* allowed the identification of 42 genes under the control of MexT and only a small set of 11 CmrA-dependent upregulated genes clustering into three genetic loci (Table 3). The overexpression of these 11 genes was confirmed by RT-qPCR. Altogether, our data showed that CmrA is a transcriptional activator influencing the expression of a few genes, including *cmrA* itself (Table 3). Reminiscent of the putative function of MexS, the four most activated CmrA-dependent genes (homologs of PA2048, PA1881, PA1880, and PA2275 in PAO1) are predicted to encode oxidoreductases (a quinol monooxygenase, an oxidoreductase, an aldehyde dehydrogenase, and an alcohol dehydrogenase, respectively). Furthermore, it appeared that CmrA also regulates the expression of two genes coding for uncharacterized transcriptional regulators (PA2276 and PA1879) and the determinant of the arsenic/antimony response regulator ArsR (PA2277) (21). Whether CmrA directly regulates all these genes remains to be determined.

**PA2048 is responsible for the *nfxC2* phenotype.** Single inactivation of the CmrA-dependent genes in mutant PJ01 revealed that none of them was implicated in *mexEF-oprN* overexpression except PA2048, the deletion of which restored a wild-type phenotype of resistance to the selected antibiotics (Table S2). PA2048 is adjacent to and divergently transcribed from *cmrA* (Fig. 2).

**TABLE 3** CmrA-dependent genes

Gene <sup>a</sup>	PAO1 homolog <sup>a</sup>	Name	Fold change using <sup>b</sup> :		Predicted product
			RNA-seq	RT-qPCR	
PA14_40180	PA1881		115	130	Oxidoreductase
PA14_40200	PA1880		104	152	Aldehyde dehydrogenase
PA14_40210	PA1879		4	ND	Transcriptional regulator
PA14_38010	PA2049		13	5	Metallophosphatase superfamily protein
PA14_38020	PA2048		199	154	Quinol monooxygenase YgiN
PA14_38040	PA2047	<i>cmrA</i>	41	74	AraC family transcriptional regulator CmrA
PA14_38050	PA2046		9	13	Hypothetical protein
PA14_35130	PA2277	<i>arsR</i>	3	ND	Transcriptional repressor ArsR
PA14_35140	PA2276		21	22	AraC family transcriptional regulator
PA14_35150	PA2275		62	137	Alcohol dehydrogenase
PA14_35160	PA2274		9	10	Flavin-dependent monooxygenase

<sup>a</sup>Gene number from the *Pseudomonas* Genome Project (<http://pseudomonas.com/>).

<sup>b</sup>Gene expression in PJ01Δ*mexT* relative to that in PA14.

Because a long intergenic region of 581 bp between *cmrA* and PA2048 was mentioned in the annotated genomes of PAO1 and PA14 (18), we carried out 5'-RACE experiments to localize the TSS of PA2048. Our results confirmed that the transcript of PA2048 begins 315 nucleotides upstream from ATG<sub>PA2048</sub> as determined in the PA14 sigmulome (19). This long untranslated region (UTR) contains two inverted repeat sequences of 10 nucleotides with a spacer of 91 nucleotides (Fig. 2, IR-N91), the function of which remains unknown. ATG<sub>PA2048</sub> is preceded by a potential Shine-Dalgarno sequence (AGGAGG) of 8 bp upstream from the gene coding sequence.

PA2048 codes for a small hypothetical protein of 98 amino acids, sharing conserved domains with YgiN from *Escherichia coli* (NCBI pblast). Sequence alignment with Clustal Omega (22) showed 40% similarity between YgiN (protein accession number [ABV07440](#)) and PA2048 (protein accession number [WP\\_003088696](#)) (Fig. S3). YgiN was initially described as a small protein of 104 residues having orthologs in other bacterial species, such as *Bacillus subtilis*, *Synechocystis* sp., *Mycobacterium tuberculosis*, *Neisseria gonorrhoeae*, and *Rhodococcus erythropolis*, but whose function was completely unknown (23). Subsequent analysis of the crystal structure of YgiN revealed a folding similar to that of monooxygenase ActVA-Orf6 from *Streptomyces coelicolor*, an enzyme that uses quinols as substrates (24). Consistent with this, *in vitro* experiments demonstrated that the purified YgiN protein was able to oxidize menadiol into menadione without the need of any cofactor, data that allowed the classification of this enzyme as a quinol monooxygenase (24).

Quinol monooxygenases are usually functionally coupled with oxidoreductases that catalyze inverse reactions (quinones to quinols) and so participate in a quinone redox cycle, as previously illustrated by MdaB-YgiN and YdhR-YdhS in *E. coli* (24, 25). Later on, Adams and Jia showed that the coordinate activity of MdaB-YgiN allows bacterial cells to resist polyketide antibiotics, such as adriamycin and tetracycline (26). It was proposed that this enzymatic couple might function primarily to protect *E. coli* cells from polycyclic quinones by recycling them until they are conjugated and exported out of the cell (26). YgiN would also be involved in cell respiration by transferring electrons to molecular oxygen when cytochrome oxidases are deficient (27). Interestingly, our results suggest that, in *P. aeruginosa*, the activities of PA2048 (a putative quinol monooxygenase) and MexS (a putative quinone oxidoreductase) are functionally linked, perhaps to adjust the redox state of the respiratory quinone pool when bacteria face some stressful conditions. In support of this assumption, we found that *mexS* expression was increased from 2.3- to 5.6-fold in the PA2048-upregulated PJ mutants compared with its expression in PA14 (Table 1). To our knowledge, quinol monooxygenases have never been studied so far in *Pseudomonas* species and the physiological role of PA2048 remains to be explored.

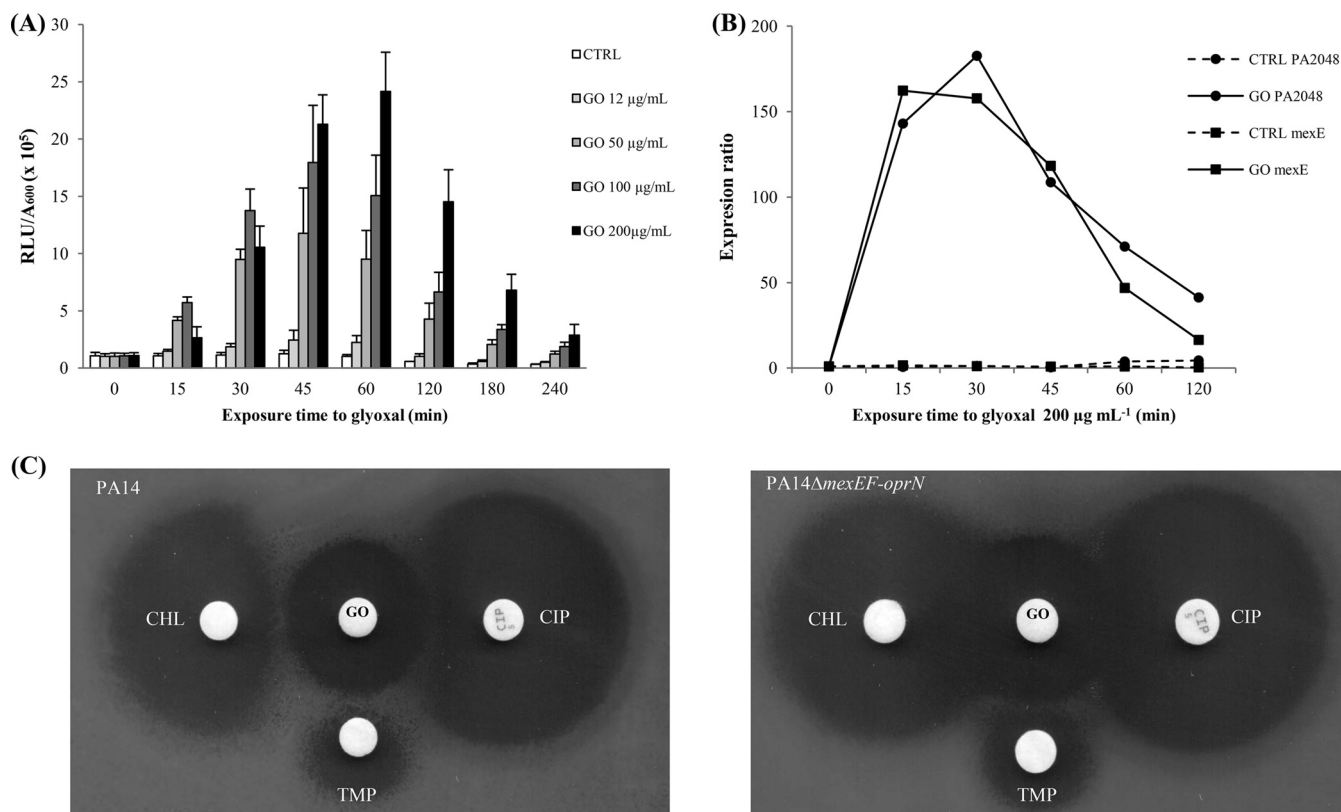
Since PA2048 was the most upregulated gene (199-fold) of the PJ01 transcriptome (Table 3), a plasmid-borne copy of this gene (including its 5' UTR) was overexpressed in strain PA14 to determine whether the *nfxC2* phenotype results exclusively from the activity of the encoded protein. Indeed, overexpression of PA2048 in PA14(pJN105::PA2048) strongly increased *mexE* transcripts, as well as the MICs of the pump substrates, without a significant change in the *cmrA* expression level (Table 2). These data clearly confirmed that CmrA is not directly responsible for the activation of *mexEF-oprN* in mutant PJ01 but exerts an indirect effect on the pump through the product of PA2048.

**The CmrA pathway is activated by electrophilic stress.** To screen for inducers of the CmrA pathway, we constructed a transcriptional fusion between PA2048 and the *luxCDABE* operon. Gene PA2048 was selected for the *lux* fusion because its expression is highly augmented in response to CmrA activation (i.e., as in mutant PJ01), and its encoded product is key in the regulatory cascade that finally triggers production of MexEF-OprN via MexS and MexT. Gene PA2048 was fused to the *lux* reporter and inserted into the chromosomes of PA14 and PJ01. As expected, PJ01::PA2048-*lux* emitted 10-fold more luminescence than PA14::PA2048-*lux* at the mid-log phase of growth (data not shown).

A first set of experiments using known MexEF-OprN substrates (ciprofloxacin, trimethoprim, and chloramphenicol) failed to demonstrate any induction of the *lux* reporter in strain PA14 (data not shown). The same negative results were obtained when disulfide stress (diamide) (28), oxidative stress (H<sub>2</sub>O<sub>2</sub>, paraquat, and dimethyl sulfoxide [DMSO]), and nitrosative stress (*S*-nitrosoglutathione [GSNO] and 2-*n*-heptyl-4-hydroxyquinoline *N*-oxide [HQNO]) (29) elicitors were added at subinhibitory concentrations to the bacterial cultures (data not shown). Finally, we found that three CmrA-regulated proteins (PA2048, PA2275, and PA2276) share  $\geq 40\%$  amino acid similarity with *E. coli* enzymes implicated in the response to electrophilic stress (YgiN, YqhD, and YqhC, respectively) (30, 31). This cellular stress is characterized by an imbalance between the formation and the removal of reactive electrophilic species (RES) containing  $\alpha,\beta$ -unsaturated carbonyl (32) or other electrophilic groups (33). For this reason, strain PA14::PA2048-*lux* was challenged with increasing concentrations of three toxic electrophilic molecules: glyoxal (GO), methylglyoxal (MG) (33), and cinnamaldehyde (CNA) (34). Interestingly, the PA2048-*lux*-dependent luminescence increased with subinhibitory concentrations of GO (12 to 200  $\mu\text{g ml}^{-1}$ ) (Fig. 3A), MG (10 to 100  $\mu\text{g ml}^{-1}$ ), and CNA (70 to 280  $\mu\text{g ml}^{-1}$ ) (Fig. S4).

To confirm these results, the impacts of electrophilic stress on *mexE* and PA2048 expression were then assessed by RT-qPCR. As shown by the results in Fig. 3B, both genes were rapidly and strongly activated 15 min after the addition of 200  $\mu\text{g ml}^{-1}$  GO to the bacterial cultures. The same was observed for *cmrA*, whose mRNA levels increased 67-fold over those of the untreated control (data not shown). Confirming our bioluminescence data, the transcript amounts of *mexE* and PA2048 started to decline 45 min after the initiation of electrophilic stress. Finally, induction of the MexEF-OprN efflux system upon GO exposure was phenotypically confirmed in strain PA14 with antibiograms on Mueller-Hinton agar (MHA), showing antagonistic interactions between (i) disks containing MexEF-OprN antibiotic substrates (chloramphenicol, ciprofloxacin, and trimethoprim) and (ii) a disk loaded with GO (Fig. 3C). As anticipated, no evidence of antagonism was visible with the negative-control strain PA14 $\Delta$ *mexEF-oprN*. Identical results were obtained when the double-disk tests were performed with MG and CNA (data not shown).

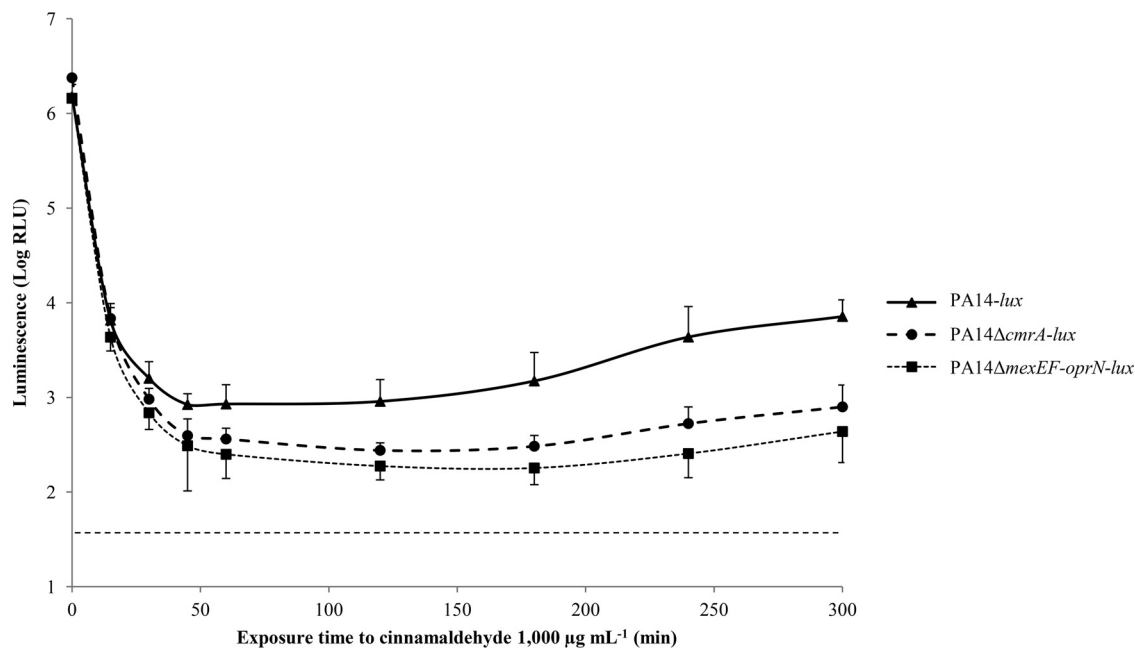
**Differential activation of detoxification mechanisms by electrophilic stress elicitors.** In *E. coli*, GO and MG are rapidly sequestered under the form of glutathione adducts and transformed into nontoxic metabolites (glycolic acid and lactate, respectively) via enzymes of the glyoxalase system (32, 33, 35). Suggesting the existence of a similar detoxification pathway, two glyoxalase genes (36) turned out to be significantly overexpressed in strain PA14 when treated with GO (*gloA2* and *gloA3*) or MG (*gloA3*)



**FIG 3** Response of *P. aeruginosa* to electrophilic stress. (A) The bioluminescence of strain PA14::PA2048-*lux* was monitored at defined time points after exposure to increasing concentrations of glyoxal (GO) and is expressed as the ratio of relative light units (RLU) to bacterial density ( $A_{600}$ ). Nontreated bacteria were used as the control (CTRL). Results are mean values  $\pm$  standard deviations from three independent experiments. (B) Expression levels of genes *mexE* and PA2048 were determined by RT-qPCR in strain PA14 exposed to 200  $\mu\text{g ml}^{-1}$  GO and compared with those of a nontreated control (CTRL). Results are mean values of four determinations from two independent experiments. (C) Induction of pump MexEF-OprN with glyoxal was assessed by a double-disk antagonism test using strain PA14 and negative-control strain PA14Δ*mexEF-oprN*. Paper disks were loaded with 8,000  $\mu\text{g}$  glyoxal (GO), 5  $\mu\text{g}$  ciprofloxacin (CIP), 1,000  $\mu\text{g}$  chloramphenicol (CHL), or 240  $\mu\text{g}$  trimethoprim (TMP). Antagonism is visible between GO and all the tested MexEF-OprN substrates in strain PA14 (left) but not in mutant PA14Δ*mexEF-oprN* (right).

(Table S3). It should be noted that activation of the glyoxalase genes is not CmrA dependent, as their expression remains unchanged in mutant PA14Δ*cmrA* treated with either GO or MG (data not shown). Conversely, CNA exposure failed to activate the glyoxalase pathway, while it dramatically triggered the expression of another gene, PA2275 (2,873-fold compared to its expression in untreated cells). In comparison, GO and MG treatments had smaller effects on PA2275 transcription levels (17- and 7-fold, respectively) (Table S3). The PA2275-encoded product shares 40% sequence similarity with YqhD from *E. coli*, an enzyme promoting the degradation of CNA into the less-toxic cinnamic alcohol (31, 37). Altogether, these results corroborate the hypothesis that the transient activation of CmrA by GO, MG, and CNA is due to the rapid degradation of these molecules into metabolites lacking electrophilic properties, via different bacterial enzymes.

**MexEF-OprN efflux pump protects bacteria from cinnamaldehyde.** Since MexEF-OprN is overproduced in response to electrophilic stress, we wondered whether the pump offers protection against the agents able to elicit such a stress. Surprisingly, the resistance levels to GO (MIC of 512  $\mu\text{g ml}^{-1}$ ), MG (256  $\mu\text{g ml}^{-1}$ ), and CNA (512  $\mu\text{g ml}^{-1}$ ) were not different between strain PA14 and mutant PA14Δ*mexEF-oprN*, consistent with the idea that this efflux system does not contribute to the intrinsic resistance toward any of these products. Alternatively, efflux of the elicitors might be masked by the effects of more efficient detoxification mechanisms, such as those described above. To test this hypothesis, time-kill experiments were performed with bactericidal concentrations of GO (1,000  $\mu\text{g ml}^{-1}$ ), MG (500  $\mu\text{g ml}^{-1}$ ), and CNA (1,000  $\mu\text{g ml}^{-1}$ ) on

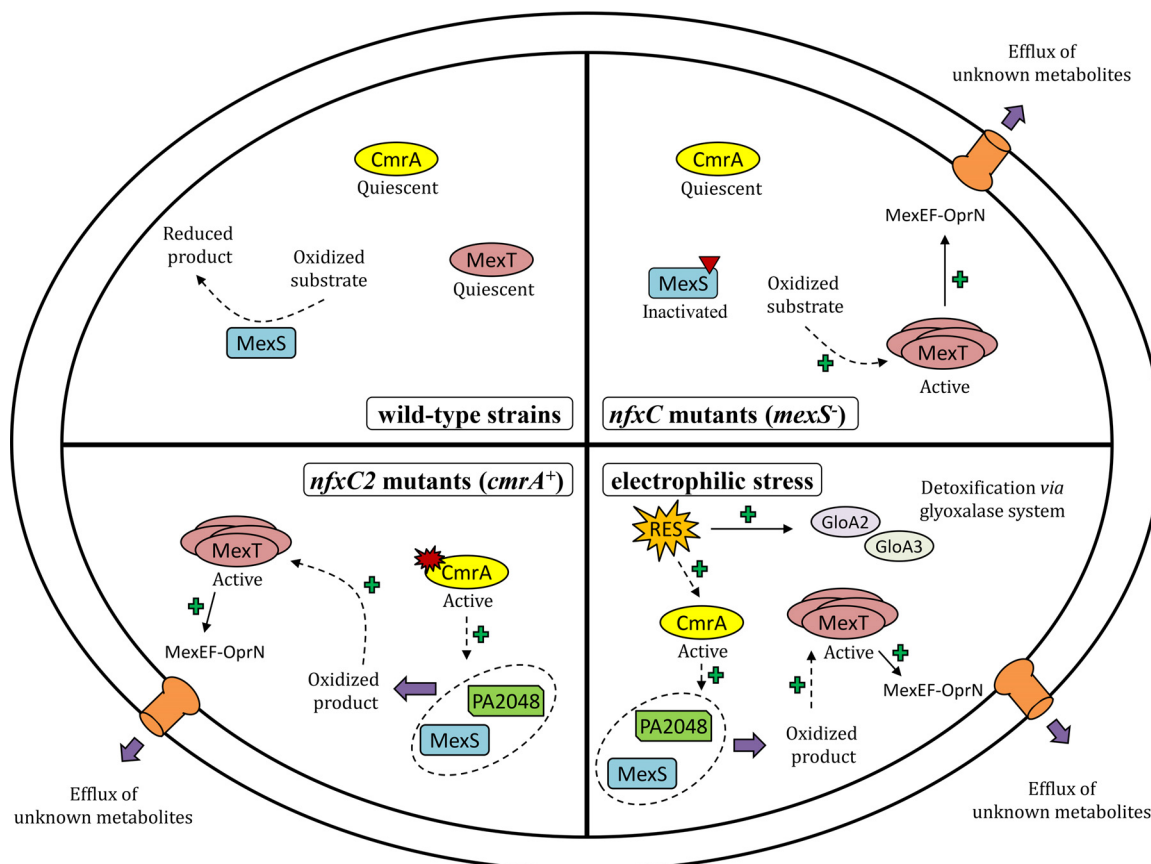


**FIG 4** Bactericidal activity of cinnamaldehyde on *P. aeruginosa*. Bioluminescent strain PA14-*lux* and its derived mutants PA14- $\Delta$ *cmrA*-*lux* and PA14-*lux*- $\Delta$ *mexEF-oprN* were cultured to mid-log phase and then challenged with 1,000  $\mu$ g ml<sup>-1</sup> cinnamaldehyde. Bioluminescence (RLU) was recorded every 30 min and used as an indicator of cell survival. RLU values are mean values  $\pm$  standard deviations from three independent experiments. A bioluminescence threshold was established with sterile MHB (dotted line).

bioluminescent strains PA14-*lux*, PA14-*lux*- $\Delta$ *mexEF-oprN*, and PA14-*lux*- $\Delta$ *cmrA*. While no differences were observed between the killing curves of the three strains exposed to GO or MG (data not shown), deletion of *mexEF-oprN* or *cmrA* was associated with a slight though reproducible sensitization of bacteria to CNA killing that impaired bacterial regrowth 45 min after drug exposure (Fig. 4). Since mutants PA14-*lux*- $\Delta$ *mexEF-oprN* and PA14-*lux*- $\Delta$ *cmrA* behaved similarly, the simplest explanation for these results is that the CmrA-dependent activation of MexEF-OprN allows surviving bacteria to better resist CNA (but not GO or MG) through the potentiation of detoxification mechanisms.

**Conclusion.** This work describes a novel regulator of the AraC family, named CmrA, which when activated by single point mutations or electrophilic stressors is able to upregulate the expression of *mexEF-oprN* via MexS and MexT. The *cmrA* mutants (dubbed *nfxC2*) exhibit the same, albeit less pronounced, multidrug resistance phenotype as prototypal *nfxC* mutants. Consistent with lower expression of the operon *mexEF-oprN* and, probably, lower levels of activation of the regulator MexT, *nfxC2* mutants are less compromised than their *nfxC* counterparts in quorum-sensing-dependent production of virulence factors (6).

CmrA influences the expression of a very small set of nonessential genes all predicted to catalyze redox reactions on as-yet-undetermined substrates. The overexpression of one of these genes, PA2048, coding for a presumed quinol monooxygenase, is sufficient to trigger MexEF-OprN production. However, our observation that MexEF-OprN is overproduced only when the putative quinone oxidoreductase MexS is functional in *nfxC2* mutants indicates that both enzymes are functionally linked, at least under specific physiological or stress conditions. Whether these two enzymes act coordinately or sequentially to maintain the redox state of respiratory quinones in stressed cells is currently being investigated. Therefore, the present work reinforces the conclusions reached by previous investigators on MexT being a redox-responsive regulator (28), though it introduces a new player, PA2048, in the activation pathway of MexT and MexEF-OprN. Interestingly, while MexT activation requires a functional MexS in *nfxC2* mutants, it is triggered by the loss of this enzyme in *nfxC* strains (Fig. 5). The



**FIG 5** Schematic representation of activation pathways of MexEF-OprN in *P. aeruginosa*. In wild-type strains (top left), such as strain PA14, regulators MexT and CmrA remain quiescent because of redox homeostasis. In so-called *nfxC* mutants (top right), mutational alteration of putative quinone oxidoreductase MexS is thought to result in intracellular accumulation of some redox-active MexS substrate(s). Redox-dependent oligomerization of MexT then triggers production of the pump MexEF-OprN and active efflux of still-undetermined endogenous products. In *nfxC2* mutants (bottom left), regulator CmrA is activated as a result of gain-of-function mutations in gene *cmrA*. Among the 11 genes positively regulated by CmrA, PA2048 codes for a putative quinol monooxygenase. Concomitant activation of PA2048 and MexS is assumed to generate oxidized metabolites, the accumulation of which would modify the cellular redox state. As in MexS-deficient mutants, these changes upregulate the production of MexEF-OprN via MexT. Finally, upon electrophilic stress (bottom right), reactive electrophilic species (RES), such as glyoxal and methylglyoxal, induce the glyoxalase detoxification system (GloA2 and GloA3) and CmrA-dependent expression of MexEF-OprN. We propose that *P. aeruginosa* uses the efflux pump MexEF-OprN as a defense mechanism in response to toxic electrophilic stressors encountered in its environment.

fact that PA2048 is the only CmrA-regulated gene whose deletion abolishes MexEF-OprN activation in *nfxC2* mutants suggests that the metabolites of putative quinol monooxygenase PA2048 are directly or indirectly processed by MexS to form the ligand(s) that, *in fine*, will cause the oligomerization of MexT, as suggested previously (28). The absence of exogenous stress in the CmrA mutants PJ01 to PJ04 demonstrates that the substrates of PA2048 are endogenous molecules. Furthermore, this strongly suggests that the mutations that drive the enzyme overproduction generate an imbalance in the redox state of preexisting compounds that MexS tends to compensate (i.e., note that gene *mexS* is overexpressed in the PJ mutants). Whether the MexS metabolites are effluxed by MexEF-OprN or only serve as a signal to activate the pump as part of a global response of defense remains to be elucidated.

Reactive electrophilic species (RES) are compounds containing  $\alpha,\beta$ -unsaturated carbonyl or other electrophilic groups. These highly toxic molecules interact with proteins, nucleic acids, lipids, and carbohydrates, generating pleiotropic cellular effects (31, 38). They also affect the redox state of the cell via their interaction with redox cofactors, such as glutathione and NAD(P)H (33). As such, the electrophilic stress can be considered a subcategory of oxidative stress, as is the case with disulfide (28) and nitrosative (29) stresses. Even if all these different subcategories of stress result in



MexS/MexT-dependent upregulation of the efflux system MexEF-OprN, only electrophiles were found to specifically activate the CmrA pathway, highlighting a distinctive feature of these molecules despite their multiple cellular targets (Fig. 5) (31). Since MexEF-OprN does not provide *P. aeruginosa* with meaningful protection against harmful electrophiles, such GO and MG, our hypothesis is that the physiological damage generated by such agents mimics a stress the bacterium has to face when adapting to other challenging conditions, perhaps those encountered during infection. It should be noted that all the electrophiles tested were able to upregulate MexEF-OprN via CmrA, PA2048, and MexS. Thus, these results unambiguously show that MexT is activated not by gross changes in the redox state of the cytoplasm but by specific ligand molecules, likely produced by MexS. In contrast to GO and MG, cinnamaldehyde (CNA) seems to be a substrate of MexEF-OprN. This natural substance present in the cinnamon stem bark is well known for its antimicrobial properties against various fungi and bacteria, including *P. aeruginosa* (39). As an inducer and a substrate of the MexEF-OprN pump, CNA would be the first example of a plant substance against which *P. aeruginosa* has evolved an efflux-based defense triggered by electrophilic stress.

## MATERIALS AND METHODS

**Bacterial strains, plasmids, and growth conditions.** The reference strains, derived mutants, and plasmids used in this study are listed in Table S4 in the supplemental material. All the bacterial cultures were grown in Mueller-Hinton broth (MHB) with adjusted concentrations of  $\text{Ca}^{2+}$  (from 20 to 25  $\mu\text{g ml}^{-1}$ ) and  $\text{Mg}^{2+}$  (from 10 to 12.5  $\mu\text{g ml}^{-1}$ ) (Becton Dickinson and Company, Cockeysville, MD) or on Mueller-Hinton agar (MHA) (Bio-Rad, Marnes-la-Coquette, France). Spontaneous mutants overproducing the efflux pump MexEF-OprN were selected on MHA supplemented with chloramphenicol (128, 256, or 512  $\mu\text{g ml}^{-1}$ ). *Escherichia coli* transformants were selected on MHA containing 50  $\mu\text{g ml}^{-1}$  kanamycin (marker for vectors pCR-Blunt and pCR2.1), 15  $\mu\text{g ml}^{-1}$  tetracycline (plasmids mini-CTX1 and miniCTX-lux), 50  $\mu\text{g ml}^{-1}$  streptomycin (pKNG101), or 10  $\mu\text{g ml}^{-1}$  gentamicin (pJN105 and pUC18T-mini-Tn7T-lux-Gm). Recombinant plasmids were introduced into *P. aeruginosa* strains by triparental mating and mobilization with the broad-host-range vector pRK2013 using *E. coli* HB101 as a helper strain (40). Transconjugants were selected on *Pseudomonas* isolation agar (PIA; Becton Dickinson and Company) supplemented with 200  $\mu\text{g ml}^{-1}$  tetracycline, 2,000  $\mu\text{g ml}^{-1}$  streptomycin, or 10  $\mu\text{g ml}^{-1}$  gentamicin, as required. Excision of pKNG101 was obtained by subculture on M9 minimal medium (8.54 mM NaCl, 25.18 mM  $\text{NaH}_2\text{PO}_4$ , 18.68 mM  $\text{NH}_4\text{Cl}$ , 22 mM  $\text{KH}_2\text{PO}_4$ , 2 mM  $\text{MgSO}_4$ , pH 7.4) supplemented with 5% sucrose and solidified with 0.8% agar.

**Antibiotic susceptibility testing.** The MICs of selected antibiotics were determined by the standard serial 2-fold dilution method in MHA with inocula of  $10^4$  CFU per spot, according to CLSI recommendations (41). Growth was visually assessed after 18 h of incubation at 37°C. Spontaneous *nfxC* mutants developing on solid medium were screened for their resistance to both ciprofloxacin and imipenem by measuring the inhibition zones around Bio-Rad disks (loaded at 5  $\mu\text{g}$  and 10  $\mu\text{g}$ , respectively) on MHA plates incubated for 18 h at 37°C (42).

**Virulence factor analysis.** Biofilm formation was assessed in 96-well polystyrene plates after coloration of adherent bacteria with 1% (wt/vol) crystal violet (43). Swarming motility, which is characterized by the formation of bacterial dendrites on low-agar culture medium, was assayed on freshly prepared M8 medium (42.2 mM  $\text{Na}_2\text{HPO}_4$ , 22 mM  $\text{KH}_2\text{PO}_4$ , 7.8 mM NaCl, pH 7.4) supplemented with 2 mM  $\text{MgSO}_4$ , 0.5% casein, 0.5% agar, and 1% glucose, as previously described (44). Finally, pyocyanin production was evaluated in the supernatants of 18-h cultures at 37°C in a specific broth [12 mM Tris HCl, pH 7.2, 0.1% tryptones, 20 mM  $(\text{NH}_4)_2\text{SO}_4$ , 1.6 mM  $\text{CaCl}_2$ , 10 mM KCl, 24 mM sodium citrate, and 50 mM glucose] (absorbance [ $A_{600}$ ] =  $1.6 \pm 0.2$ ). The blue pigment was extracted with 1 volume of chloroform (45). Virulence assays were all repeated twice with independent cultures of strains PA14 and PA14 $\Delta$ *mexS* as controls.

**RT-qPCR experiments.** Specific gene expression levels were measured by quantitative PCR after reverse transcription (RT-qPCR), as described previously (46). Briefly, 2  $\mu\text{g}$  of total RNA was reverse transcribed with ImProm-II reverse transcriptase as specified by the manufacturer (Promega, Madison, WI). The amounts of specific cDNA were quantified on a Rotor-Gene RG6000 instrument (Qiagen, Courtaboeuf, France) by using the Quantifast SYBR green PCR kit (Qiagen). When not already published, the nucleotide primers used for gene amplifications were designed from the sequences available in the *Pseudomonas* Genome Database, version 2, using primer3 Web software (Table S5) (47). For each strain, the mRNA levels of target genes were normalized to that of housekeeping gene *rpsL* and are expressed as the ratios to the transcript levels of strain PA14. Mean gene expression values were calculated from two independent bacterial cultures, each assayed in duplicate. Strain PA14 $\Delta$ *mexS* was used as a positive control for the overexpression of gene *mexE*. As shown in previous experiments (11), transcript levels of *mexE*  $\geq 20$ -fold those of PA14 are associated with a  $\geq 2$ -fold increase in resistance to MexEF-OprN substrates, and such levels were considered significant.

**SNP identification.** Single-nucleotide polymorphisms (SNPs) between strain PA14 and its derived mutants PJ01, PJ03, and PJ04 were identified with the Ion Torrent technology (Life Technologies, CA). Briefly, genomic DNA of each strain was extracted and purified by using the PureLink genomic DNA

minikit (Life Technologies). Ion Torrent libraries were prepared from 100 ng of each DNA preparation (Qubit 2.0 fluorometer; Invitrogen) using dedicated equipment (Veriti thermocycler and E-Gel iBase; Invitrogen). Alignment of the sequence reads (about 200 bp in length) of PJ01, PJ03, and PJ04 with the UCBPP-PA14 genome (NCBI accession number [NC\\_008463.1](#)) was performed using BioNumerics version 7.1 and led to the identification of potential sequence variations (SNPs). Identification of an SNP was considered reliable if the coverage was  $\geq 20$ -fold and its percentage was  $\geq 29\%$ . Sequence variations were verified on both strands by capillary sequencing on an Applied Biosystems 3130 GA apparatus (Applied Biosystems, Life Technologies; Courtaboeuf, France) after PCR amplification with the proper primers.

**Identification of gene transcriptional start sites (+1).** Rapid amplification of 5' cDNA ends (5'-RACE) was performed to identify the transcriptional start site (TSS) of *cmrA* with the 5'-RACE system, as recommended by Invitrogen. Briefly, total RNA from two independent cultures of *cmrA*-overexpressing mutant PJ01 was extracted at mid-log phase of growth ( $A_{600} = 1$ ) using the RNeasy plus minikit (Qiagen) and was treated with RNase-free DNase (Qiagen). Five micrograms of total RNA was subjected to first-strand cDNA synthesis using SuperScript II reverse transcriptase (Invitrogen) and the specific primer GSP1-PA2047 (Table S5). The presence of cDNA was checked by PCR using nested gene-specific primers GSP2-PA2047 (reverse) and GSP3-PA2047 (forward) (Table S5). A homopolymeric tail was then added to the 3' cDNA using terminal deoxynucleotidyl transferase (TdT) and dCTP. PCR amplification was carried out using GSP2-PA2047, a deoxyinosine-containing abridged anchor primer (AAP), and poly(C)-tailed cDNA as the template. The 5'-RACE product was cloned into the pCR2.1 vector and further sequenced to allow the identification of the TSS of *cmrA*. The verification of PA2048 TSS, previously identified by Schulz et al., (19), was performed under the same conditions using specific primers GSP1-PA2048, GSP2-PA2048, and GSP3-PA2048 (Table S5).

**High-throughput RNA sequencing (RNA-seq) library construction.** Total RNA extracts were obtained in triplicate from exponential cultures ( $A_{600} = 1$ ) of strains PA14, PJ01, and PJ01 $\Delta$ *mexT* at 37°C. Bacterial cells were collected by centrifugation in RNAprotect bacterial reagent (Qiagen) and disrupted with 0.15- to 0.60-mm ceramic beads in a TissueLyzer II (Qiagen) according to the manufacturer's instructions. Total RNA was then purified from bead-beaten samples with the RNeasy plus 96 kit (Qiagen). The concentration and purity of the RNA extracts were assessed by RiboGreen measurement (Quant-iT RiboGreen RNA reagent and kit; Invitrogen) and by using an Agilent 2100 Bioanalyzer system (Agilent Technologies), respectively. Depletion of rRNA from those RNA samples was performed with the Ribo-Zero rRNA removal reagents (bacteria) from Epicentre (Madison, WI). Libraries were then constructed using the TruSeq stranded-mRNA high-throughput (HT) sample preparation kit from Illumina (San Diego, CA). The final libraries were quantified with PicoGreen fluorescent dye (Quant-iT PicoGreen double-stranded DNA [dsDNA] assay kit; Invitrogen), showing yields of 200 to 800 ng per sample. Qualitative analysis was done using the Agilent high-sensitivity DNA assay. High-throughput sequencing was performed by Microsynth (Balgach, Switzerland) on an Illumina NextSeq 500 platform using V2 chemistry.

**RNA-seq data analysis.** RNA-seq data analysis was performed by Genostar (Montbonnot Saint Martin, France). Reads were mapped on 5,892 annotated coding sequences (CDS) of strain PA14 using CLC Genomic Workbench 7.5 software. Transcript abundance and differential-expression results between the three replicates of each sample (PA14/PJ01, PA14/PJ01 $\Delta$ *mexT*, and PJ01/PJ01 $\Delta$ *mexT*) were determined with the Cufflinks and Cuffdiff algorithms (48). A difference in gene expression was considered significant when the false-discovery rate (*q* value) was  $\leq 0.05$  and the expression ratio was  $\leq 0.3$ - or  $\geq 3.0$ -fold. The transcriptomic data have been deposited in NCBI's Gene Expression Omnibus (49) and are accessible through GEO Series accession number [GSE86211](#).

**Construction of PA14-derived deletion mutants.** Single-deletion *mexS*, *mexT*, *cmrA*, PA2048, and *mexEF-oprN* mutants were constructed using overlapping PCRs and recombination events as described by Kaniga et al. (50). First, the 5' and 3' regions flanking *mexS* (417 and 433 bp, respectively), *mexT* (408 and 453 bp, respectively), *cmrA* (418 and 445 bp, respectively), PA2048 (451 and 457 bp, respectively), and *mexEF-oprN* (467 and 452 bp, respectively) were each amplified by PCR with specific primers (Table S5) under the following conditions: 3 min of denaturation at 98°C, followed by 30 cycles of amplification, each composed of 10 s at 98°C, 30 s at 60°C, and 30 s at 72°C, with a final extension step of 7 min at 72°C. The resultant amplicons were used as templates for overlapping PCRs with external pairs of primers to generate the mutagenic DNA fragments. The reaction mixtures contained 1 $\times$  iProof high-fidelity (HF) master mix, 3% DMSO, and 0.5  $\mu$ M each primer (Bio-Rad). The amplified products were cloned into plasmid pCR-Blunt according to the manufacturer's instructions (Invitrogen) and then subcloned as BamHI/XbaI fragments into the suicide vector pKNG101 in *E. coli* CC118 $\lambda$ *pir* (50). The recombinant plasmids were next transferred to *P. aeruginosa* (PA14 or PJ01) by conjugation and selected on PIA containing 2,000  $\mu$ g ml<sup>-1</sup> streptomycin. The excision of undesired pKNG101 sequence was obtained by plating transformants on M9 plates containing 5% (wt/vol) sucrose. Negative selection on streptomycin was carried out to confirm the loss of the plasmid in transconjugants. The allelic exchanges were verified by PCR. Nucleotide-sequencing experiments confirmed the deletion of 826 bp in *mexS*, 929 bp in *mexT*, 997 bp in *cmrA*, 442 bp in PA2048, and 6,039 bp in *mexEF-oprN*, yielding strains P01J $\Delta$ *mexS*, PJ01 $\Delta$ *mexT*, PA14 $\Delta$ *cmrA*, PJ01 $\Delta$ *cmrA*, PJ01 $\Delta$ PA2048, and PA14 $\Delta$ *mexEFN*, respectively.

**Chromosomal complementation with wild-type or mutated *cmrA*.** Wild-type (from PA14) and mutated (from PJ01, PJ02, PJ03, and PJ04) *cmrA* alleles, along with their promoter regions, were amplified by PCR by using genomic DNA as the template. The resulting amplicons, once digested with BamHI and HindIII, were inserted into linearized plasmid mini-CTX1 (51). The resultant recombinant plasmids were then transferred from *E. coli* CC118 to *P. aeruginosa* strain PA14 $\Delta$ *cmrA* by conjugation, with subsequent

selection on PIA plates supplemented with 200  $\mu\text{g ml}^{-1}$  tetracycline to allow their chromosomal insertion into the *attB* site (51). Chromosomal integration of the cloned alleles was confirmed by PCR and sequencing.

**Overexpression of *cmrA* and PA2048 from the *araBAD* promoter.** To study the impact of *cmrA* overexpression on the phenotype of *P. aeruginosa*, a wild-type copy of the gene was PCR amplified using specific primers (Table S5). The amplicon was cloned into vector pCR-Blunt and then subcloned as an EcoRI fragment into arabinose-inducible expression vector pJN105 (52). The new construct was introduced by electroporation into strain PA14, yielding PA14(pJN105::*cmrA*<sub>PA14</sub>), and selected on gentamicin at 10  $\mu\text{g ml}^{-1}$ . A positive control with the mutated allele from PJ01 [PA14(pJN105::*cmrA*<sub>PJ01</sub>)] and a negative control harboring pJN105 alone [PA14(pJN105)] were generated in parallel. Gene PA2048 was cloned in pJN105 under the same conditions as *cmrA* (see above) after amplification with specific primers (Table S5) and was then electrotransferred into PA14 to yield PA14(pJN105::PA2048). The transformants were finally analyzed for their resistance phenotypes (MICs of ciprofloxacin [CIP], chloramphenicol [CHL], and trimethoprim [TMP]) and the relative expression levels (by RT-qPCR) of genes *cmrA*, PA2048, and *mexE* in the absence and presence of the inducer arabinose (0.5%).

**Construction of a bioluminescent reporter of the CmrA pathway.** To evaluate the activation of the CmrA pathway under various challenging conditions, a transcriptional fusion between gene PA2048 and the operon *luxCDABE* was constructed. For this, a 1,822-bp genomic fragment of strain PA14 carrying *cmrA* was amplified by using specific primers (Table S5). The amplicon was cloned into vector pCR-Blunt and then subcloned as an EcoRI fragment into plasmid miniCTX-*lux* (53). The new construct was introduced into strain PA14 by conjugation, with subsequent selection of transconjugants on PIA supplemented with 200  $\mu\text{g ml}^{-1}$  tetracycline. In parallel, the same plasmid construct was transferred into strain PJ01 as a positive control of PA2048::*lux* overexpression, as this mutant constitutively produces an activated form of CmrA.

**Bioluminescence induction assays.** Induction of PA2048-*lux* expression was measured in real time during the exponential-growth phase. Briefly, overnight cultures of luminescent strains were diluted into fresh MHB to yield an  $A_{600}$  of 0.01. Bacteria were incubated with shaking (250 rpm) at 37°C for 4 h ( $A_{600} = 0.1$ ) prior to the addition of the following stressors at the indicated concentrations: ciprofloxacin (0.01  $\mu\text{g ml}^{-1}$ ), chloramphenicol (20  $\mu\text{g ml}^{-1}$ ), trimethoprim (12  $\mu\text{g ml}^{-1}$ ), diamide (8 mM),  $\text{H}_2\text{O}_2$  (50  $\mu\text{M}$ ), paraquat (25  $\mu\text{M}$ ), dimethyl sulfoxide (0.5%), *S*-nitrosoglutathione (0.125  $\mu\text{g ml}^{-1}$ ), 2-*n*-heptyl-4-hydroxyquinoline *N*-oxide (25  $\mu\text{g ml}^{-1}$ ), glyoxal (12, 50, 100, and 200  $\mu\text{g ml}^{-1}$ ), methylglyoxal (10, 50, and 100  $\mu\text{g ml}^{-1}$ ), and cinnamaldehyde (70, 140, and 280  $\mu\text{g ml}^{-1}$ ). The activity of the PA2048-*lux* fusion was monitored in white 96-well assay plates (Corning, NY), using a Synergy H1 microplate reader (Biotek Instruments, Winooski, WI) with the gain set at 150, read height set at 7 mm, and integration time of 1 s. In parallel, the bacterial densities were measured by their  $A_{600}$  in 96-well microtest plates (Sarstedt, Nümbrecht, Germany). The activity of the reporter, expressed as the ratio of bioluminescence (relative light units [RLU]) to bacterial density ( $A_{600}$ ), was measured over a 6-h time course.

**Killing experiments with cinnamaldehyde.** Strain PA14 and its mutants PA14 $\Delta$ *mexEF-oprN* and PA14 $\Delta$ *cmrA* were first rendered constitutively bioluminescent using the pUC18T-mini-Tn7T-*lux*-Gm plasmid as described by Damron et al. (54). Overnight cultures were then diluted into fresh MHB to yield an  $A_{600}$  of 0.1. Bacteria were incubated with shaking (250 rpm) at 37°C for 2.5 h ( $A_{600} = 0.8$ ) prior to the addition of cinnamaldehyde at 1,000  $\mu\text{g ml}^{-1}$ . The bioluminescence of strains was measured as described above.

**Induction of MexEF-OprN by disk diffusion tests.** The inducing activity of glyoxal (GO), methylglyoxal (MG), and cinnamaldehyde (CNA) on *mexEF-oprN* expression was indirectly investigated by double-disk antagonism tests with PA14 and PA14 $\Delta$ *mexEF-oprN* on MHA. Disks loaded with 8,000  $\mu\text{g}$  GO, 8,000  $\mu\text{g}$  MG, or 10,000  $\mu\text{g}$  CNA were deposited onto the surface of seeded MHA plates at the appropriate distance from disks containing ciprofloxacin (5  $\mu\text{g}$ ), chloramphenicol (1,000  $\mu\text{g}$ ), or trimethoprim (240  $\mu\text{g}$ ). Flattening of the inhibition zone around an antibiotic disk in the direction of the GO, MG, and/or CNA disk(s) was interpreted as an increase in resistance induced by the aldehyde(s).

**Accession number(s).** The whole sequence of *cmrA*, including its 5' UTR, is accessible through the GenBank database under accession number [KX274690](https://doi.org/10.1128/AAC.00585-17). The transcriptomic data of our RNA-seq experiments is accessible through the GEO database under accession number [GSE86211](https://doi.org/10.1101/168211).

## SUPPLEMENTAL MATERIAL

Supplemental material for this article may be found at <https://doi.org/10.1128/AAC.00585-17>.

**SUPPLEMENTAL FILE 1**, PDF file, 0.8 MB.

## ACKNOWLEDGMENTS

We are grateful to Xiyu Qian for her excellent technical assistance and to Benoît Valot (UMR 6249 Chrono-Environnement, France) and Emile Van Schaftingen (Institute de Duve, Brussels, Belgium) for helpful discussions. Romé Voulhoux (LISM Marseille, France) and Eric Morello (CEPR, Tours, France) provided plasmids pJN105 and pUC18T-mini-Tn7T-*lux*-Gm, respectively.

This work was supported with grants from the French Ministère de l'Enseignement Supérieur et de la Recherche, the Vaincre la Mucoviscidose Association, and the

Grégory Lemarchal Association. The French national reference center for antibiotic resistance is financed by the Ministry of Health through the Santé publique France agency.

The authors declare no competing interests.

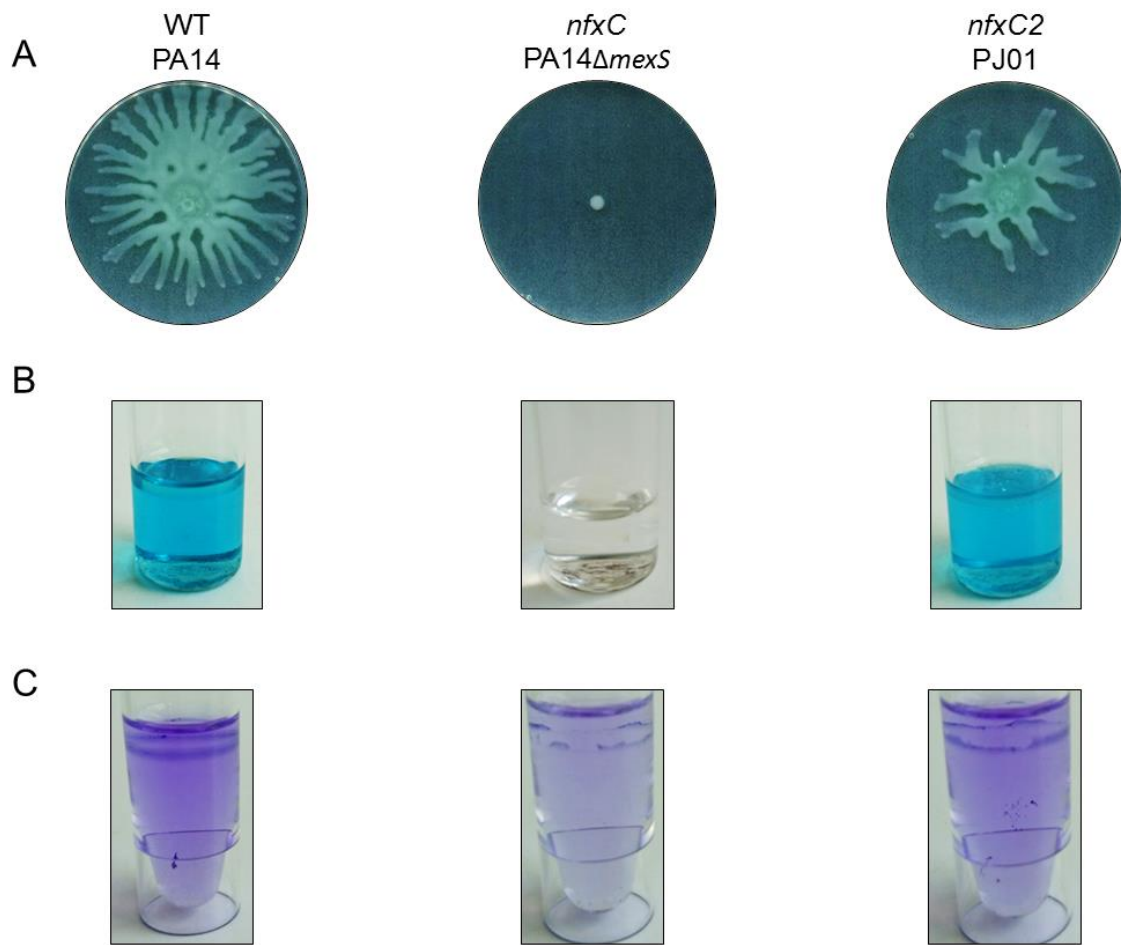
## REFERENCES

- Lister PD, Wolter DJ, Hanson ND. 2009. Antibacterial-resistant *Pseudomonas aeruginosa*: clinical impact and complex regulation of chromosomally encoded resistance mechanisms. *Clin Microbiol Rev* 22: 582–610. <https://doi.org/10.1128/CMR.00040-09>.
- Poole K, Srikumar R. 2001. Multidrug efflux in *Pseudomonas aeruginosa*: components, mechanisms and clinical significance. *Curr Top Med Chem* 1:59–71. <https://doi.org/10.2174/1568026013395605>.
- Köhler T, Michea-Hamzehpour M, Henze U, Gotoh N, Curty LK, Pechère JC. 1997. Characterization of MexE-MexF-OprN, a positively regulated multidrug efflux system of *Pseudomonas aeruginosa*. *Mol Microbiol* 23: 345–354. <https://doi.org/10.1046/j.1365-2958.1997.2281594.x>.
- Köhler T, Epp SF, Curty LK, Pechère JC. 1999. Characterization of MexT, the regulator of the MexE-MexF-OprN multidrug efflux system of *Pseudomonas aeruginosa*. *J Bacteriol* 181:6300–6305.
- Li XZ, Barre N, Poole K. 2000. Influence of the MexA-MexB-OprM multidrug efflux system on expression of the MexC-MexD-OprJ and MexE-MexF-OprN multidrug efflux systems in *Pseudomonas aeruginosa*. *J Antimicrob Chemother* 46:885–893. <https://doi.org/10.1093/jac/46.6.885>.
- Köhler T, van Delden C, Curty LK, Hamzehpour MM, Pechère JC. 2001. Overexpression of the MexEF-OprN multidrug efflux system affects cell-to-cell signaling in *Pseudomonas aeruginosa*. *J Bacteriol* 183:5213–5222. <https://doi.org/10.1128/JB.183.18.5213-5222.2001>.
- Linares JF, Lopez JA, Camafeita E, Albar JP, Rojo F, Martinez JL. 2005. Overexpression of the multidrug efflux pumps MexCD-OprJ and MexEF-OprN is associated with a reduction of type III secretion in *Pseudomonas aeruginosa*. *J Bacteriol* 187:1384–1391. <https://doi.org/10.1128/JB.187.4.1384-1391.2005>.
- Lamarche MG, Deziel E. 2011. MexEF-OprN efflux pump exports the *Pseudomonas* quinolone signal (PQS) precursor HHQ (4-hydroxy-2-heptylquinoline). *PLoS One* 6:e24310. <https://doi.org/10.1371/journal.pone.0024310>.
- Jin Y, Yang H, Qiao M, Jin S. 2011. MexT regulates the type III secretion system through MexS and PtrC in *Pseudomonas aeruginosa*. *J Bacteriol* 193:399–410. <https://doi.org/10.1128/JB.01079-10>.
- Sobel ML, Neshat S, Poole K. 2005. Mutations in PA2491 (*mexS*) promote MexT-dependent *mexEF-oprN* expression and multidrug resistance in a clinical strain of *Pseudomonas aeruginosa*. *J Bacteriol* 187:1246–1253. <https://doi.org/10.1128/JB.187.4.1246-1253.2005>.
- Richardot C, Juarez P, Jeannot K, Patry I, Plésiat P, Llanes C. 2016. Amino acid substitutions account for most MexS alterations in clinical *nfxC* mutants of *Pseudomonas aeruginosa*. *Antimicrob Agents Chemother* 60:2302–2310. <https://doi.org/10.1128/AAC.02622-15>.
- Balasubramanian D, Schepner L, Merighi M, Smith R, Narasimhan G, Lory S, Mathee K. 2012. The regulatory repertoire of *Pseudomonas aeruginosa* AmpC  $\beta$ -lactamase regulator AmpR includes virulence genes. *PLoS One* 7:e34067. <https://doi.org/10.1371/journal.pone.0034067>.
- Westfall LW, Carty NL, Layland N, Kuan P, Colmer-Hamood JA, Hamood AN. 2006. *mvaT* mutation modifies the expression of the *Pseudomonas aeruginosa* multidrug efflux operon *mexEF-oprN*. *FEMS Microbiol Lett* 255:247–254. <https://doi.org/10.1111/j.1574-6968.2005.00075.x>.
- Wang D, Seeve C, Pierson LS, III, Pierson EA. 2013. Transcriptome profiling reveals links between Pars/ParR, MexEF-OprN, and quorum sensing in the regulation of adaptation and virulence in *Pseudomonas aeruginosa*. *BMC Genomics* 14:618. <https://doi.org/10.1186/1471-2164-14-618>.
- Zaoui C, Overhage J, Lons D, Zimmermann A, Musken M, Bielecki P, Pustelny C, Becker T, Nimtz M, Haussler S. 2012. An orphan sensor kinase controls quinolone signal production via MexT in *Pseudomonas aeruginosa*. *Mol Microbiol* 83:536–547. <https://doi.org/10.1111/j.1365-2958.2011.07947.x>.
- Liao J, Schurr MJ, Sauer K. 2013. The MerR-like regulator BrIR confers biofilm tolerance by activating multidrug efflux pumps in *Pseudomonas aeruginosa* biofilms. *J Bacteriol* 195:3352–3363. <https://doi.org/10.1128/JB.00318-13>.
- Kallberg M, Wang H, Wang S, Peng J, Wang Z, Lu H, Xu J. 2012. Template-based protein structure modeling using the RaptorX Web server. *Nat Protoc* 7:1511–1522. <https://doi.org/10.1038/nprot.2012.085>.
- Winsor GL, Griffiths EJ, Lo R, Dhillon BK, Shay JA, Brinkman FS. 2016. Enhanced annotations and features for comparing thousands of *Pseudomonas* genomes in the *Pseudomonas* genome database. *Nucleic Acids Res* 44:D646–D653. <https://doi.org/10.1093/nar/gkv1227>.
- Schulz S, Eckweiler D, Bielecka A, Nicolai T, Franke R, Dotsch A, Hornischer K, Bruchmann S, Duvel J, Haussler S. 2015. Elucidation of sigma factor-associated networks in *Pseudomonas aeruginosa* reveals a modular architecture with limited and function-specific crosstalk. *PLoS Pathog* 11:e1004744. <https://doi.org/10.1371/journal.ppat.1004744>.
- Tian ZX, Fargier E, Mac Aogain M, Adams C, Wang YP, O'Gara F. 2009. Transcriptome profiling defines a novel regulon modulated by the LysR-type transcriptional regulator MexT in *Pseudomonas aeruginosa*. *Nucleic Acids Res* 37:7546–7559. <https://doi.org/10.1093/nar/gkp828>.
- Cai J, Salmon K, DuBow MS. 1998. A chromosomal *ars* operon homologue of *Pseudomonas aeruginosa* confers increased resistance to arsenic and antimony in *Escherichia coli*. *Microbiology* 144:2705–2713. <https://doi.org/10.1099/00221287-144-10-2705>.
- Cook CE, Bergman MT, Finn RD, Cochrane G, Birney E, Apweiler R. 2016. The European Bioinformatics Institute in 2016: data growth and integration. *Nucleic Acids Res* 44(D1):D20–D26. <https://doi.org/10.1093/nar/gkv1352>.
- Wasinger VC, Humphery-Smith I. 1998. Small genes/gene-products in *Escherichia coli* K-12. *FEMS Microbiol Lett* 169:375–382. <https://doi.org/10.1111/j.1574-6968.1998.tb13343.x>.
- Adams MA, Jia Z. 2005. Structural and biochemical evidence for an enzymatic quinone redox cycle in *Escherichia coli*: identification of a novel quinol monooxygenase. *J Biol Chem* 280:8358–8363. <https://doi.org/10.1074/jbc.M412637200>.
- Revington M, Semesi A, Yee A, Shaw GS. 2005. Solution structure of the *Escherichia coli* protein YdhR: a putative mono-oxygenase. *Protein Sci* 14:3115–3120. <https://doi.org/10.1110/ps.051809305>.
- Adams MA, Jia Z. 2006. Modulator of drug activity B from *Escherichia coli*: crystal structure of a prokaryotic homologue of DT-diaphorase. *J Mol Biol* 359:455–465. <https://doi.org/10.1016/j.jmb.2006.03.053>.
- Portnoy VA, Herrgard MJ, Palsson BO. 2008. Aerobic fermentation of D-glucose by an evolved cytochrome oxidase-deficient *Escherichia coli* strain. *Appl Environ Microbiol* 74:7561–7569. <https://doi.org/10.1128/AEM.00880-08>.
- Fargier E, Mac Aogain M, Mooij MJ, Woods DF, Morrissey JP, Dobson AD, Adams C, O'Gara F. 2012. MexT functions as a redox-responsive regulator modulating disulfide stress resistance in *Pseudomonas aeruginosa*. *J Bacteriol* 194:3502–3511. <https://doi.org/10.1128/JB.06632-11>.
- Fetar H, Gilmour C, Klinoski R, Daigle DM, Dean CR, Poole K. 2011. *mexEF-oprN* multidrug efflux operon of *Pseudomonas aeruginosa*: regulation by the MexT activator in response to nitrosative stress and chloramphenicol. *Antimicrob Agents Chemother* 55:508–514. <https://doi.org/10.1128/AAC.00830-10>.
- Lee C, Kim I, Lee J, Lee KL, Min B, Park C. 2010. Transcriptional activation of the aldehyde reductase YqhD by YqhC and its implication in glyoxal metabolism of *Escherichia coli* K-12. *J Bacteriol* 192:4205–4214. <https://doi.org/10.1128/JB.01127-09>.
- Visvalingam J, Hernandez-Doria JD, Holley RA. 2013. Examination of the genome-wide transcriptional response of *Escherichia coli* O157:H7 to cinnamaldehyde exposure. *Appl Environ Microbiol* 79:942–950. <https://doi.org/10.1128/AEM.02767-12>.
- Kosmachevskaya OV, Shumaev KB, Topunov AF. 2015. Carbonyl stress in bacteria: causes and consequences. *Biochemistry (Mosc)* 80:1655–1671. <https://doi.org/10.1134/S0006297915130039>.
- Lee C, Park C. 2017. Bacterial responses to glyoxal and methylglyoxal: reactive electrophilic species. *Int J Mol Sci* 18:E169. <https://doi.org/10.3390/ijms18010169>.
- Groeger AL, Freeman BA. 2010. Signaling actions of electrophiles: anti-

- inflammatory therapeutic candidates. *Mol Interv* 10:39–50. <https://doi.org/10.1124/mi.10.1.7>.
35. MacLean MJ, Ness LS, Ferguson GP, Booth IR. 1998. The role of glyoxalase I in the detoxification of methylglyoxal and in the activation of the KefB K<sup>+</sup> efflux system in *Escherichia coli*. *Mol Microbiol* 27:563–571. <https://doi.org/10.1046/j.1365-2958.1998.00701.x>.
  36. Sukdeo N, Honek JF. 2007. *Pseudomonas aeruginosa* contains multiple glyoxalase I-encoding genes from both metal activation classes. *Biochim Biophys Acta* 1774:756–763. <https://doi.org/10.1016/j.bbapap.2007.04.005>.
  37. Turner PC, Miller EN, Jarboe LR, Baggett CL, Shanmugam KT, Ingram LO. 2011. YqhC regulates transcription of the adjacent *Escherichia coli* genes *yqhD* and *dkgA* that are involved in furfural tolerance. *J Ind Microbiol Biotechnol* 38:431–439. <https://doi.org/10.1007/s10295-010-0787-5>.
  38. Mousavi F, Bojko B, Bessonneau V, Pawliszyn J. 2016. Cinnamaldehyde characterization as an antibacterial agent toward *E. coli* metabolic profile using 96-blade solid-phase microextraction coupled to liquid chromatography-mass spectrometry. *J Proteome Res* 15:963–975. <https://doi.org/10.1021/acs.jproteome.5b00992>.
  39. Utchariyakiat I, Surassmo S, Jaturanpinyo M, Khuntayaporn P, Chomnawang MT. 2016. Efficacy of cinnamon bark oil and cinnamaldehyde on anti-multidrug resistant *Pseudomonas aeruginosa* and the synergistic effects in combination with other antimicrobial agents. *BMC Complement Altern Med* 16:158. <https://doi.org/10.1186/s12906-016-1134-9>.
  40. Ditta G, Stanfield S, Corbin D, Helinski DR. 1980. Broad host range DNA cloning system for Gram-negative bacteria: construction of a gene bank of *Rhizobium meliloti*. *Proc Natl Acad Sci U S A* 77:7347–7351. <https://doi.org/10.1073/pnas.77.12.7347>.
  41. Clinical and Laboratory Standards Institute. 2015. Methods for dilution antimicrobial susceptibility tests for bacteria that grow aerobically; approved standard, 10th ed. CLSI document M07-A10. CLSI, Wayne, PA.
  42. Clinical and Laboratory Standards Institute. 2015. Performance standards for antimicrobial disk susceptibility tests, approved standard, 12th ed. CLSI document M02-A12. CLSI, Wayne, PA.
  43. Vasseur P, Soscia C, Vouilhoux R, Filloux A. 2007. PelC is a *Pseudomonas aeruginosa* outer membrane lipoprotein of the OMA family of proteins involved in exopolysaccharide transport. *Biochimie* 89:903–915. <https://doi.org/10.1016/j.biochi.2007.04.002>.
  44. Köhler T, Curty LK, Barja F, van Delden C, Pechère JC. 2000. Swarming of *Pseudomonas aeruginosa* is dependent on cell-to-cell signaling and requires flagella and pili. *J Bacteriol* 182:5990–5996. <https://doi.org/10.1128/JB.182.21.5990-5996.2000>.
  45. Essar DW, Eberly L, Hadero A, Crawford IP. 1990. Identification and characterization of genes for a second anthranilate synthase in *Pseudomonas aeruginosa*: interchangeability of the two anthranilate synthases and evolutionary implications. *J Bacteriol* 172:884–900. <https://doi.org/10.1128/jb.172.2.884-900.1990>.
  46. Dumas JL, van Delden C, Perron K, Köhler T. 2006. Analysis of antibiotic resistance gene expression in *Pseudomonas aeruginosa* by quantitative real-time-PCR. *FEMS Microbiol Lett* 254:217–225. <https://doi.org/10.1111/j.1574-6968.2005.00008.x>.
  47. Untergasser A, Cutcutache I, Koressaar T, Ye J, Faircloth BC, Remm M, Rozen SG. 2012. Primer3—new capabilities and interfaces. *Nucleic Acids Res* 40:e115. <https://doi.org/10.1093/nar/gks596>.
  48. Wang D, Qi M, Calla B, Korban SS, Clough SJ, Cock PJ, Sundin GW, Toth I, Zhao Y. 2012. Genome-wide identification of genes regulated by the Rcs phosphorelay system in *Erwinia amylovora*. *Mol Plant Microbe Interact* 25:6–17. <https://doi.org/10.1094/MPMI-08-11-0207>.
  49. Edgar R, Domrachev M, Lash AE. 2002. Gene Expression Omnibus: NCBI gene expression and hybridization array data repository. *Nucleic Acids Res* 30:207–210. <https://doi.org/10.1093/nar/30.1.207>.
  50. Kaniga K, Delor I, Cornelis GR. 1991. A wide-host-range suicide vector for improving reverse genetics in Gram-negative bacteria: inactivation of the *blaA* gene of *Yersinia enterocolitica*. *Gene* 109:137–141. [https://doi.org/10.1016/0378-1119\(91\)90599-7](https://doi.org/10.1016/0378-1119(91)90599-7).
  51. Hoang TT, Kutchma AJ, Becher A, Schweizer HP. 2000. Integration-proficient plasmids for *Pseudomonas aeruginosa*: site-specific integration and use for engineering of reporter and expression strains. *Plasmid* 43:59–72. <https://doi.org/10.1006/plas.1999.1441>.
  52. Newman JR, Fuqua C. 1999. Broad-host-range expression vectors that carry the L-arabinose-inducible *Escherichia coli* *araBAD* promoter and the *araC* regulator. *Gene* 227:197–203. [https://doi.org/10.1016/S0378-1119\(98\)00601-5](https://doi.org/10.1016/S0378-1119(98)00601-5).
  53. Becher A, Schweizer HP. 2000. Integration-proficient *Pseudomonas aeruginosa* vectors for isolation of single-copy chromosomal *lacZ* and *lux* gene fusions. *Biotechniques* 29:948–950.
  54. Damron FH, McKenney ES, Barbier M, Liechti GW, Schweizer HP, Goldberg JB. 2013. Construction of mobilizable mini-Tn7 vectors for bioluminescent detection of Gram-negative bacteria and single-copy promoter *lux* reporter analysis. *Appl Environ Microbiol* 79:4149–4153. <https://doi.org/10.1128/AEM.00640-13>.

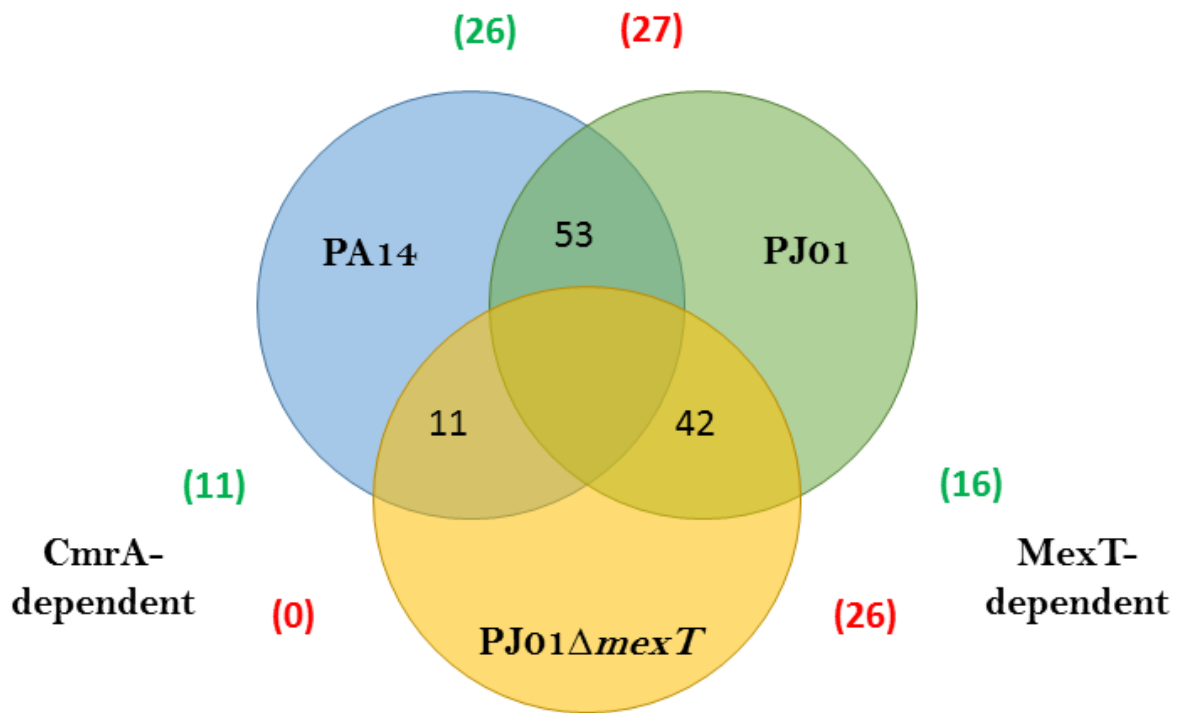
# Supplemental material





**FIG S1** Mutant PJ01 (*nfxC2*) is only slightly impaired in swarming motility, pyocyanin production and biofilm formation. PA14 (wild-type) and PA14Δ*S* (*nfxC*) were used as comparators. (A) Swarming motility was evaluated as the capacity of bacteria to form dendrites on low agar solid medium; (B) the blue pigment pyocyanin was extracted from culture supernatants with chloroform; (C) sessile bacteria adherent to a plastic surface were visualized by staining with a 1% crystal violet solution. Similar results were obtained for mutants PJ02, PJ03 and PJ04.





**FIG S2** Transcriptomic analysis of *nfxC2* mutant PJ01. The Venn diagram represents the genes whose expression differs at least 3-fold between PJ01, wild-type strain PA14 and/or mutant PJ01Δ*mexT*. Up- and down-regulated genes (numbers indicated in brackets) are in green and red colors, respectively. The data are representative of three independent RNAseq experiments.

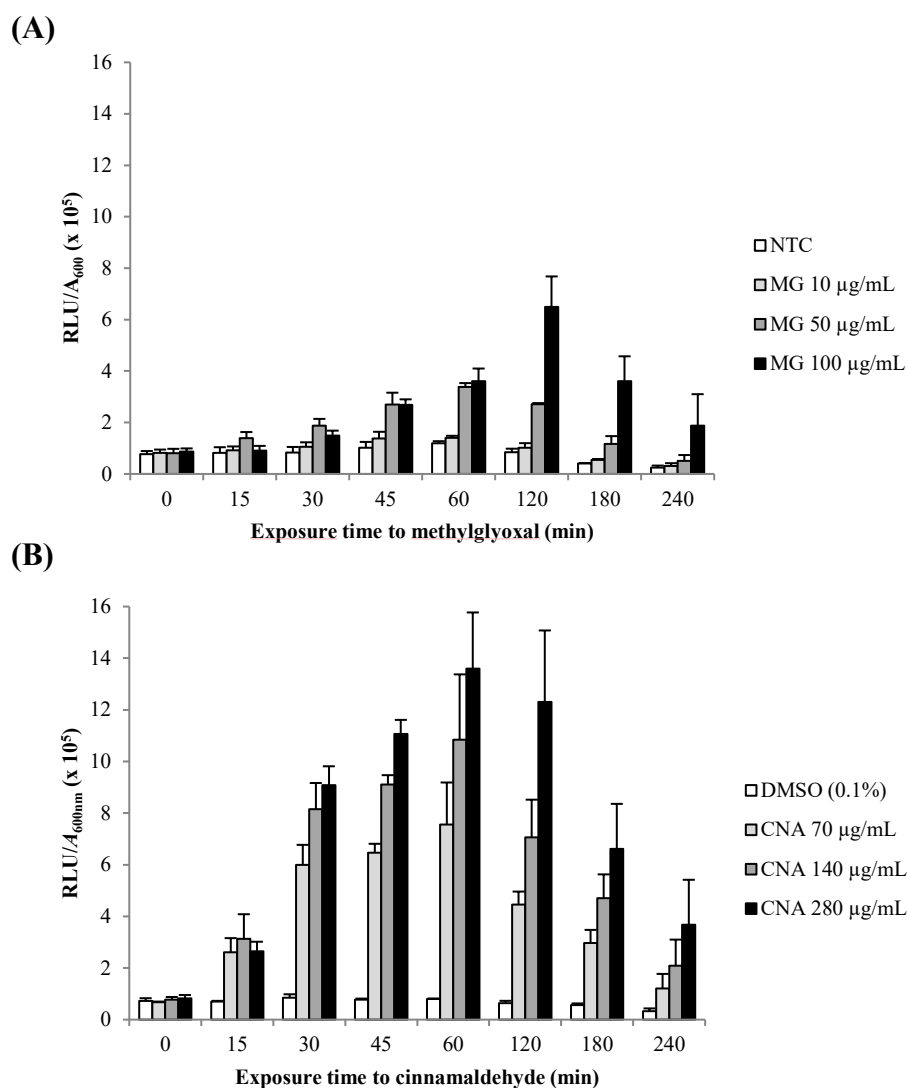
```

>ygiN      1  -----MLTVIAEIRTRPGQHHRQAVLDQFAKIVPTVLKEEFGCHGYAPMVDCAAGVSFQ      53
>PA2048    1  MPAFNRASHLVSIRARSGQSHRLGIRLQ--FLAQAGQAAPGCLRYELRQA-----          50

>ygiN      54  SMAPDSIVMIEQWESIAHLEAHLQTPHMKAYSEAVKGDVLEM-NIRILQPGI          104
>PA2048    51  DGDADLWLLHSEWSDEAAMQAYLSGDAQRVFAEVLWQALAAATLDVQE-RPF-          98

```

**FIG S3** Amino acid sequence alignment of YgiN (*E. coli*, ABV07440) and PA2048 (*P. aeruginosa*, WP\_003088696). These two proteins exhibit 40% of similarity, including conserved (in pink color) and synonymous (in green) residues.



**FIG S4** Activation of the CmrA-pathway by methylglyoxal and cinnamaldehyde. Bioluminescence of strain PA14::PA2048-*lux* was monitored at defined time points after exposure to increasing concentrations of **(A)** methylglyoxal (MG) or **(B)** cinnamaldehyde (CNA), and was expressed as a ratio to bacterial density ( $A_{600\text{nm}}$ ). Non-treated bacteria were used as control (NTC, DMSO 0.1%). Results of  $\text{RLU}/A_{600\text{nm}}$  are mean values  $\pm$  standard deviation of three independent experiments

**TABLE S1** SNPs identified in the PJ mutants by whole genome sequencing

<b>Mutant</b>	<b>Gene</b>	<b>Encoded product</b>	<b>SNP</b>	<b>Coverage</b>	<b>Frequency %</b>
PJ01	PA14_38040	AraC family transcriptional	C <sub>203</sub>	37	100
	PA14_43520	Hypothetical protein	ΔG <sub>62</sub>	35	36.4
	PA14_68750	Multiple drug resistance protein	ΔG <sub>24</sub>	38	29.6
PJ03	PA14_11100	Adhesive protein CupB5	ΔG <sub>21</sub>	22	95.5
	PA14_38040	AraC family transcriptional	T <sub>266</sub>	47	100
	PA14_55670	Exodeoxyribonuclease V subunit	ΔG <sub>35</sub>	22	50
PJ04	PA14_34320	DszC family monooxygenase	T <sub>1105</sub>	22	100
	PA14_38000	Hypothetical protein	ΔG <sub>44</sub>	32	100
	PA14_38040	AraC family transcriptional	C <sub>642</sub>	47	100

**TABLE S2** Effects of the deletion of CmrA-dependent genes in mutant PJ01

Strains <sup>a</sup>	Transcript levels <sup>b</sup>	MICs ( $\mu\text{g mL}^{-1}$ ) <sup>c</sup>	
	<i>mexE</i>	CIP	CHL
<i>Controls</i>			
PA14	1	0.125	64
PA14 $\Delta$ <i>mexS</i>	116	4	2,048
PJ01	71	1	1,024
PJ01 $\Delta$ <i>cmrA</i>	0.6	0.125	64
<i>Deletion mutants</i>			
PJ01 $\Delta$ PA2046	68	1	1,024
<b>PJ01<math>\Delta</math>PA2048</b>	<b>1.5</b>	<b>0.125</b>	<b>64</b>
PJ01 $\Delta$ PA1880-81	69	1	1,024
PJ01 $\Delta$ PA2274	76	1	1,024
PJ01 $\Delta$ PA2275	73	1	1,024
PJ01 $\Delta$ PA2276	68	1	1,024

<sup>a</sup> Gene names refer to corresponding PAO1 homologs. PA2046: PA14\_38050; PA2048: PA14\_38020; PA1880-PA1881: PA14\_40200-40180; PA2274: PA14\_35160; PA2275: PA14\_35150; PA2276: PA14\_35140. Only the deletion of PA2048 (in bold) cancels the *nfxC2* resistance phenotype.

<sup>b</sup> Expressed as a ratio to the value of wild-type strain PA14

<sup>c</sup> MICs of MexEF-OprN substrates. CIP: ciprofloxacin; CHL: chloramphenicol

**TABLE S3** Induction of the glyoxalase system coding genes and other CmrA-dependent genes by electrophilic molecules

Condition <sup>a</sup>	Transcript levels <sup>b</sup>						
	<i>gloA1</i> *	<i>gloA2</i> *	<i>gloA3</i> *	<i>gloB</i> *	<i>cmrA</i>	PA2048	PA2275
PA14 non-treated control	0.9	1.2	1.0	1.0	1.0	1.0	0.6
PA14 treated with 200 µg mL <sup>-1</sup> GO	0.9	<b>2,367</b>	<b>30</b>	1.1	<b>67</b>	<b>155</b>	<b>17</b>
PA14 treated with 100 µg mL <sup>-1</sup> MG	0.9	3.2	<b>117</b>	1.0	<b>4.7</b>	<b>14</b>	<b>7.0</b>
PA14 treated with 280 µg mL <sup>-1</sup> CNA	2.1	6.6	2.8	2.6	<b>236</b>	<b>376</b>	<b>2,873</b>

<sup>a</sup> RT-qPCR assays were performed on culture samples collected after 15 min induction at 37°C. Genes whose expression was significantly activated are marked in bold. GO: glyoxal, MG: methylglyoxal, CNA: cinnamaldehyde.

<sup>b</sup> Expressed as a ratio to the value of PA14 at *t*<sub>0</sub>

\*glyoxalase system coding genes

**TABLE S4** Strains and plasmids used in this study

Strains	Relevant characteristics	Sources
<i>Pseudomonas aeruginosa</i>		
PA14	Wild-type reference strain PA14	B. Ausubel
PA14Δ <i>mexS</i>	PA14-derived <i>mexS</i> deletion mutant ( <i>nfxC</i> type)	(1)
PA14Δ <i>mexT</i>	PA14-derived <i>mexT</i> deletion mutant	(1)
PA14Δ <i>mexEF-oprN</i>	PA14-derived <i>mexEF-oprN</i> deletion mutant	This study
PJ01	PA14 spontaneous mutant harboring substitution A <sub>68</sub> V in CmrA	This study
PJ02	PA14 spontaneous mutant harboring substitution H <sub>204</sub> L in CmrA	This study
PJ03	PA14 spontaneous mutant harboring substitution L <sub>89</sub> Q in CmrA	This study
PJ04	PA14 spontaneous mutant harboring substitution N <sub>214</sub> K in CmrA	This study
PA14Δ <i>cmrA</i>	PA14-derived <i>cmrA</i> deletion mutant	This study
PJ01Δ <i>cmrA</i>	PJ01-derived <i>cmrA</i> deletion mutant	This study
PA14Δ <i>cmrA</i> <sub>PA14</sub>	PA14Δ <i>cmrA</i> complemented with wild-type <i>cmrA</i> from PA14	This study
PA14Δ <i>cmrA</i> <sub>PJ01</sub>	PA14Δ <i>cmrA</i> complemented with mutated <i>cmrA</i> from PJ01	This study
PJ01Δ <i>mexT</i>	PJ01-derived <i>mexT</i> deletion mutant	This study
PJ01Δ <i>mexS</i>	PJ01-derived <i>mexS</i> deletion mutant	This study
PJ01ΔPA2048	PJ01-derived PA2048 <sup>a</sup> deletion mutant	This study
PA14::PA2048- <i>lux</i>	PA14 containing the luminescent reporter PA2048- <i>lux</i>	This study
PJ01::PA2048- <i>lux</i>	PJ01 containing the luminescent reporter PA2048- <i>lux</i>	This study
PA14:: <i>lux</i>	Bioluminescent strain PA14	This study
PA14:: <i>lux</i> -Δ <i>mexEF-oprN</i>	Bioluminescent mutant PA14Δ <i>mexEF-oprN</i>	This study
PA14:: <i>lux</i> -Δ <i>cmrA</i>	Bioluminescent mutant PA14Δ <i>cmrA</i>	This study
<i>Escherichia coli</i>		
DH5α	F <sup>-</sup> φ80 <i>lacZ</i> ΔM15 Δ( <i>lacZYA-argF</i> )U169 <i>recA1 endA1 hsdR17</i> (r <sub>K</sub> , m <sub>K</sub> <sup>+</sup> ) <i>phoA supE44 thi-1 gyrA96 relA1 λ</i> <sup>-</sup>	Invitrogen
CC118	Δ( <i>ara-leu</i> ) <i>araD ΔlacX74 galE galK phoA20 thi-1 rpsE rpoB argE</i> (Am) <i>recA1</i>	(2)
CC118λ <i>pir</i>	CC118 lysogenic for phage λ <i>pir</i>	(3)
HB101	<i>supE44 hsdS20</i> (r <sub>B</sub> <sup>-</sup> m <sub>B</sub> <sup>-</sup> ) <i>recA13 ara-14 pro A2 lacY1 galK2 rpsL20 xyl-5 mtl-1 leuμB6 thi-1</i>	(4)
<b>Plasmids</b>		
pCR-Blunt	Blunt-end cloning vector <i>ccdB lacZα, Zeo<sup>R</sup> Kan<sup>R</sup></i>	Invitrogen
pCR2.1	Cloning vector for PCR products, <i>lacZΔColE1 f1 ori, Amp<sup>R</sup> Kan<sup>R</sup></i>	Invitrogen
pRK2013	Helper plasmid for mobilization of non-self-transmissible plasmids, <i>mob1, tra1 col E1, Kan<sup>R</sup></i>	(5)
pKNG101	Suicide vector <i>oriR6K sacB insB, Str<sup>R</sup></i>	(5)
Mini-CTX1	Self-proficient integration vector, Ω-FRT- <i>attP</i> -MCS, <i>ori, int oriT, Tet<sup>R</sup></i>	(6)
MiniCTX- <i>lux</i>	Mini-CTX1 derived plasmid containing the <i>luxCDABE</i> operon, Tet <sup>R</sup>	(7)
pJN105	Broad host range vector carrying the <i>araBAD</i> promoter, Gen <sup>R</sup>	(8)
pUC18T-mini-Tn7T- <i>lux</i> -Gm	Suicide vector for shuttling single copies of genes directly to the chromosome via a mini-Tn7 element; <i>aacC1, oriT, P1</i> integron promoter driving expression of <i>luxCDABE, Amp<sup>R</sup> Gen<sup>R</sup></i>	(9)
pTNS3	Helper plasmid encoding the Tn7 site-specific transposition pathway, Amp <sup>R</sup>	(10)

<sup>a</sup> Homolog of PA14\_38020

Abbreviations: Amp<sup>R</sup> (ampicillin resistance), Kan<sup>R</sup> (kanamycin resistance), Gen<sup>R</sup> (gentamicin resistance), Str<sup>R</sup> (streptomycin resistance), Tet<sup>R</sup> (tetracycline resistance), Zeo<sup>R</sup> (zeocin resistance)

**TABLE S5** Primers used for DNA sequencing, gene cloning and RT-qPCR

Primer	Sequence (5'→3')	Source
<b><i>Gene sequencing</i></b>		
<b><i>mexS</i></b>		
mexSCh1	GAACAGGATCAGCAGGTTCA	(1)
mexSCh2	CCACCGGGGTGAGTACCT	(1)
mexSCh3	GTCTCGGCTTCGAACTGG	(1)
mexSCh4	GGTGAAATCCATCAGGCAGT	(1)
mexSCh5	GCAAGCTGGTGCTGTATGG	(1)
mexSCh6	GAAGGCGACTTCGTCTGG	(1)
<b><i>mexT</i></b>		
seqmexT1	CTATTGATGCCGAACCTGCT	(11)
seqmexT2	AATAGTCGTCGAGGGTCAGC	(11)
seqmexT3	TGATGAAAACGGATCACTCG	(11)
seqmexT4	GGGAACTAATCGAACGACGA	(11)
<b><i>ampR</i></b>		
ampRC1	GTCGACCAGTGCCTTCAGGCGATCC	(12)
ampRC2	CTCGAGAGCGAGATCGTTGCGGCACG	(12)
<b><i>mvaT</i></b>		
mvaT1	CGCGGTTTACTTACAGTTTTCG	(11)
mvaT2	AACGCTATTCGCTGGAGACT	(11)
<b><i>mxtR</i></b>		
mxtR-PJ1	AAAACCTCCGCTCCCATCAG	This study
mxtR-PJ2	AGGACGATGCCTTTCAGTTG	This study
mxtR-PJ3	GCAAGCAGGAGAACATCACC	This study
mxtR-PJ4	AGCATGTCGTTGGAGACCAT	This study
mxtR-PJ5	GTAATGCCGGACTCCTTCGT	This study
mxtR-PJ6	CATCAGCAGGTCTTCCACCT	This study
mxtR-PJ7	GTAATGGAAACAGGCCAAC	This study
mxtR-PJ8	GTCCGGGTAATCGAACAGC	This study
mxtR-PJ9	AACATTACCCAGGGCATCAG	This study
mxtR-PJ10	GGGCATCGTAGAGGTTGTT	This study
mxtR-PJ11	ACCGACCTGCTGGACATCT	This study
mxtR-PJ12	GGCTTGGACAGGTAGTCGAG	This study
mxtR-PJ13	GAGACCGGTACGCAATTGAT	This study
mxtR-PJ14	GTCTACCATCGCCTGGAAGC	This study
<b><i>PA2449</i></b>		
PA2449-PJ1	CCAGGCCGTACAATCGAC	This study
PA2449-PJ2	GTTCGGTTCGTAGAGGGTCA	This study
PA2449-PJ3	CGCGAAGTGACATTCATGG	This study
PA2449-PJ4	TTGAGGCGGTAGAACAGGTC	This study
PA2449-PJ5	GCAACCTGGAGAAGATGGTC	This study
PA2449-PJ6	CAAGCAGGCGGACTTCAT	This study
<b><i>PA2047 cmrA</i></b>		
PA2047-PJ1	GGATACTGTTCGGGTTCTTGC	This study
PA2047-PJ2	CAGCAGCCGGTAGAAAATCT	This study
PA2047-PJ3	CGCCTGATCCATCTGCTG	This study
PA2047-PJ4	CAAAGTCGTTTCGCTGTGCT	This study



## Gene inactivation

### PA2047 *cmrA*

iPA2047-PJ1	CTGTGGGGTGTAAAGGGTGAC	This study
iPA2047-PJ2	CGGTGTTTCAGGATCAGGCAAGCATTTC	This study
iPA2047-PJ3	GATCCTGAACACCGCCTAGGGGAAC	This study
iPA2047-PJ4	TCTCGCTATTGCCGGTATTG	This study

### *mexS*

Inac-MexS-Ch1	GACAGGTGGGCGAAGATTT	(1)
Inac-MexS-Ch2	ATCCATCCATCACGGGGTGAATAACCT	(1)
Inac-MexS-Ch3	CGTGATGGATGGATTTTCACCGGTCATC	(1)
Inac-MexS-Ch4	CGGCGAGATGTATGTGGTG	(1)

### *mexT*

Inac-MexT-Ch1	AGCACATCCTTCCAGCTCAC	(1)
Inac-MexT-Ch2	ATAAGCCGAACACGATCAGCAGGTTCA	(1)
Inac-MexT-Ch3	CGTGTTCCGGCTTATTCCATCGAAAGCA	(1)
Inac-MexT-Ch4	GTCGATCTGGAACAGCAGGT	(1)

### *mexEF-oprN*

iEFN-1	TCAGCTACACCGACGAACTG	This study
iEFN-2	ACGATGCGCGGAGTCAAGCTCAGAGAC	This study
iEFN-3	ACTCCGCGCATCGTGGCGATCTACC	This study
iEFN-4	CTGGTTTCGCCGGCTATGT	This study

### PA2048

iPA2048-1	GGAAACCTTCCCAAGACTAGC	This study
iPA2048-2	GAACAAGCTGCCTCCGATTACCAGTTG	This study
iPA2048-3	GAGGCAGCTTGTCTGGCGTCTCAGC	This study
iPA2048-4	GCCGGGTAACCTACCTGATCC	This study

### PA2046

iPA2046-1	CAGGGCCAGCGCCTGCACGAG	This study
iPA2046-2	AAGCGCTCCGGCGGGTACGGTTGCGCAAG	This study
iPA2046-3	CGTACCCGCGGAGGGCGCTTGGCGCGAGGG	This study
iPA2046-4	TCATTGCGCGGGCTTCGCCC	This study

### PA1880-1881

iPA1880-81-1	TCTCTGCAGGGTCGTCCCCG	This study
iPA1880-81-2	GTGGTGCTCAGGCCTTGCCGGGCTTGCTCT	This study
iPA1880-81-3	CGGCAAGGCCTGAGCACCACCCAGGTCCGGT	This study
iPA1880-81-4	GATGCCGCCCTCCATCTGCG	This study

### PA2274

iPA2274-1	CCAGGTGATCCTTTCCACCG	This study
iPA2274-2	GTAACCCGCGCCCGCGGCGCCGACGGCCCG	This study
iPA2274-3	GCCGGCGGGCGGCGGGTTACTCCGGGTGAC	This study
iPA2274-4	CAACAGCAGCAGCTTGTCGA	This study

### PA2275

iPA2275-1	GCGTCATAGCGGTAGGTTTC	This study
iPA2275-2	GTCGACGGTGTGTCTCTTCGCAAGAT	This study
iPA2275-3	GACACACCGTCGACCAGGAAGGTCTC	This study
iPA2275-4	GGCTTGACCTCAAGTTTGCT	This study

## PA2276

iPA2276-1	TGCAGCCAGTCGCCGTTGGC	This study
iPA2276-2	CAGCCAAGGCCCGGCAGGATCGGGGGCGCT	This study
iPA2276-3	ATCCTGCCGGGCCCTTGGCTGTTTCTCCAGG	This study
iPA2276-4	CGACCCGGCCGATGATCTCG	This study

## **Chromosomal complementation of PA2047**

Int-PA2047-Fw1	CGGGGATCCATGACAGTCTGGCCTGTTGA	This study
Int-PA2047-Fw2	CGGGGATCCCGGATACTGTCTGGGTTCTTG	This study
Int-PA2047-Fw3	CGGGGATCCCTGTTCTGGCGAATGCT	This study
Int-PA2047-Rv	GCCAAGCTTAAGGGACAGGGCAAGCAG	This study

## **5' RACE**

### cmrA

GSP1-PA2047	GTGACCGAGACCACCAGGTA	This study
GSP2-PA2047	AATGCCTGAGCAGCGACT	This study
GSP3-PA2047	GCGCTAGTCTTGGAAGGTT	This study

## PA2048

GSP1-PA2048	CATGGCCGCTTCATCGCTCC	This study
GSP2-PA2048	GAACGCTGGCATGCTCTCTGC	This study
GSP3-PA2048	GGTTGCCTGCGCTACGAAC	This study

## **Overexpression with the araBAD promoter**

### cmrA

pJN-cmrA Fw	GCGCTAGTCTTGGAAGGTT	This study
pJN-cmrA Rv	AAGGACAGGGCAAGCAG	This study

## PA2048

pJN-PA2048 Fw	CCAGAACAAGGGGACGGGC	This study
pJN-PA2048 Rv	GCATGGCGGAATCTCCGTC	This study

## **RT-qPCR**

rpsL3	CAACTATCAACCAGCTGGTG	(13)
rpsL5	CTGTGCTTTGCAGGTTGTG	(13)
mexE4	CCAGGACCAGCACGAACTTCTTGC	(13)
mexE5	CGACAACGCCAAGGGCGAGTTCACC	(13)
MexSP1	CAAGGGCGTCAATGTCATCC	(1)
MexSP2	GACCGGTGAAATCCATCAGG	(1)
MexT1	ATCTGAACCTGCTGATCGTG	(1)
MexT2	GTCCGGTACGGACGAACA	(1)
oprDCh1	ACCAACCTCGAAGCCAAGTA	(14)
oprDCh2	ACAGGATCGACAGCGGATAG	(14)
mexY1A	TTACCTCCTCCAGCGGC	(15)
mexY1B	GTGAGGCGGGCGTTGTG	(15)
MexB1	ATGACCATCACCGTGACCTT	(16)
MexB2	AGAGTGGTCTTGGATGTTG	(16)
PA2046Fw	CGACAAGGCCTTCCTCTACA	This study
PA2046Rv	AGGCATAGCTCAGGTCGAGA	This study
PA2047Fw	AGATTTTCTACCGGCTGCTG	This study
PA2047Rv	GCCGTAGTTCTGGTTGATCC	This study
PA2048Fw	CATGGCCGCTTCATCGCTCC	This study
PA2048Rv	GGTTGCCTGCGCTACGAAC	This study
PA2049Fw	CTTCCAGCACTGGCACTACC	This study
PA2049Rv	CAGGTCCTGCTGGAGTTCAC	This study
PA2274Fw	GAACGCTGCTTCAGGAACTG	This study
PA2274Rv	GTGAACGCCAGCAGGTGTAG	This study

PA2275Fw	GACCAGGTGATCCTTTCCAC	This study
PA2275Rv	GTAGGGATTGAGGTCGTGCT	This study
PA2276Fw	GTCCTGCACCATCAGGCTCC	This study
PA2276Rv	TCGACCTTCCACCACAACCTT	This study
PA1880Fw	CTACCGGCCGATGTACTACC	This study
PA1880Rv	GTGCCTTCCAGGATCGACT	This study
PA1881Fw	GGTACGTTCTGCGTGCT	This study
PA1881Rv	ACTGCGGTACCTGGAGCTT	This study

***Luminescent reporter PA2048-lux***

PA2048-2047 Fw	GTTTCAGAACGGCCGCTCCT	This study
PA2048-2047 Rv	GCGTCCCCTAGGCGGTGTT	This study

## REFERENCES

1. Richardot C, Juarez P, Jeannot K, Patry I, Plésiat P, Llanes C. 2016. Amino acid substitutions account for most MexS alterations in clinical *nfxC* mutants of *Pseudomonas aeruginosa*. *Antimicrob Agents Chemother* 60:2302-10.
2. Manoil C, Beckwith J. 1985. TnphoA: a transposon probe for protein export signals. *Proc Natl Acad Sci U S A* 82:8129-33.
3. Herrero M, de Lorenzo V, Timmis KN. 1990. Transposon vectors containing non-antibiotic resistance selection markers for cloning and stable chromosomal insertion of foreign genes in Gram-negative bacteria. *J Bacteriol* 172:6557-67.
4. Lacks S, Greenberg B. 1977. Complementary specificity of restriction endonucleases of *Diplococcus pneumoniae* with respect to DNA methylation. *J Mol Biol* 114:153-68.
5. Kaniga K, Delor I, Cornelis GR. 1991. A wide-host-range suicide vector for improving reverse genetics in Gram-negative bacteria: inactivation of the *blaA* gene of *Yersinia enterocolitica*. *Gene* 109:137-41.
6. Hoang TT, Kutchma AJ, Becher A, Schweizer HP. 2000. Integration-proficient plasmids for *Pseudomonas aeruginosa*: site-specific integration and use for engineering of reporter and expression strains. *Plasmid* 43:59-72.
7. Becher A, Schweizer HP. 2000. Integration-proficient *Pseudomonas aeruginosa* vectors for isolation of single-copy chromosomal *lacZ* and *lux* gene fusions. *Biotechniques* 29:948-50, 952.
8. Newman JR, Fuqua C. 1999. Broad-host-range expression vectors that carry the L-arabinose-inducible *Escherichia coli* *araBAD* promoter and the *araC* regulator. *Gene* 227:197-203.
9. Damron FH, McKenney ES, Barbier M, Liechti GW, Schweizer HP, Goldberg JB. 2013. Construction of mobilizable mini-Tn7 vectors for bioluminescent detection of Gram-negative bacteria and single-copy promoter *lux* reporter analysis. *Appl Environ Microbiol* 79:4149-53.

10. Choi KH, Mima T, Casart Y, Rholl D, Kumar A, Beacham IR, Schweizer HP. 2008. Genetic tools for select-agent-compliant manipulation of *Burkholderia pseudomallei*. *Appl Environ Microbiol* 74:1064-75.
11. Llanes C, Köhler T, Patry I, Dehecq B, van Delden C, Plésiat P. 2011. Role of the efflux system MexEF-OprN in low level resistance of *Pseudomonas aeruginosa* to ciprofloxacin. *Antimicrob Agents Chemother* 55:5676-84.
12. Bagge N, Ciofu O, Hentzer M, Campbell JI, Givskov M, Hoiby N. 2002. Constitutive high expression of chromosomal beta-lactamase in *Pseudomonas aeruginosa* caused by a new insertion sequence (*IS1669*) located in *ampD*. *Antimicrob Agents Chemother* 46:3406-11.
13. Dumas JL, van Delden C, Perron K, Köhler T. 2006. Analysis of antibiotic resistance gene expression in *Pseudomonas aeruginosa* by quantitative real-time-PCR. *FEMS Microbiol Lett* 254:217-25.
14. Llanes C, Pourcel C, Richardot C, Plésiat P, Fichant G, Cavallo JD, Merens A, Group GS. 2013. Diversity of beta-lactam resistance mechanisms in cystic fibrosis isolates of *Pseudomonas aeruginosa*: a French multicentre study. *J Antimicrob Chemother* 68:1763-71.
15. Jeannot K, Sobel ML, El Garch F, Poole K, Plésiat P. 2005. Induction of the MexXY efflux pump in *Pseudomonas aeruginosa* is dependent on drug-ribosome interaction. *J Bacteriol* 187:5341-6.
16. Vettoretti L, Plésiat P, Muller C, El Garch F, Phan G, Attrée I, Ducruix A, Llanes C. 2009. Efflux unbalance in *Pseudomonas aeruginosa* isolates from cystic fibrosis patients. *Antimicrob Agents Chemother* 53:1987-97.



## 2.2 Electrophilic Stress Induce Expression of RND Efflux Pumps in *Pseudomonas aeruginosa*

Our work on CmrA revealed that exposure of strain PA14 to subinhibitory concentrations of toxic electrophiles induces expression of *mexEF-oprN* through CmrA-dependent upregulation of PA2048 (Juarez et al., 2017). It was suggested that the pump MexEF-OprN itself could protect *P. aeruginosa* against RES by exporting them or their metabolites outside the cell (Juarez et al., 2017). Since electrophiles generate a subcategory of oxidative stress (Lee and Park, 2017), we wondered whether these molecules could upregulate other RND pumps known to respond to oxidative stress, such as MexAB-OprM and MexXY/OprM (Fraud and Poole, 2011; Starr et al., 2012).

To test this hypothesis, we performed antibiograms by using wild-type strain PA14 and a Mueller-Hinton agar medium supplemented with subinhibitory concentrations of glyoxal (GO), methylglyoxal (MG) and cinnamaldehyde (CNA), respectively. RT-qPCR experiments were also carried out after 15 min of electrophile exposure to determine expression levels of genes *mexB*, *mexY* and *mexE* (Table 9).

**Table 9: Effect of electrophiles on drug susceptibility and gene expression in strain PA14**

Conditions <sup>a</sup>	Inhibition zone diameter <sup>b</sup> (mm)						Transcript levels <sup>d</sup>		
	MexEF-OprN <sup>c</sup>		MexAB-OprM		MexXY/OprM		<i>mexE</i>	<i>mexB</i>	<i>mexY</i>
	CHL	IMP	ATM	TIC	GEN	TMN			
CTRL	30	34	31	28	29	33	1.5	1.2	1.4
GO	<b>17</b>	<b>30</b>	30	30	<b>25</b>	<b>27</b>	<b>172</b>	2.4	<b>7.7</b>
MG	<b>21</b>	33	30	29	<b>25</b>	<b>26</b>	<b>31</b>	1.4	<b>6.0</b>
CNA	<b>14</b>	<b>30</b>	<b>26</b>	<b>22</b>	29	31	<b>233</b>	<b>9.4</b>	1.7

<sup>a</sup>: CTRL, non exposed control; GO, 200 µg/mL of glyoxal; MG, 100 µg/mL of methylglyoxal; CNA, 280 µg/mL of cinnamaldehyde

<sup>b</sup>: Antibiotics used as markers of efflux pump activities. CIP, ciprofloxacin; IMP, imipenem; ATM, aztreonam; TIC, ticarcillin; GEN, gentamicin; TMN, tobramycin. Significant reduction of inhibition diameters is marked in **bold**.

<sup>c</sup>: Chloramphenicol is a good substrate for both MexAB-OprM and MexEF-OprN. Imipenem susceptibility is affected in MexEF-OprN overproducers, though this antibiotic is not a pump substrate.

<sup>d</sup>: Determined on culture samples collected after 15 min of induction at 37°C and expressed as a ratio to the value at  $t_0$ . Genes whose expression is significantly increased are indicated in **bold**. Results are mean values of four determinations from two independent experiments.

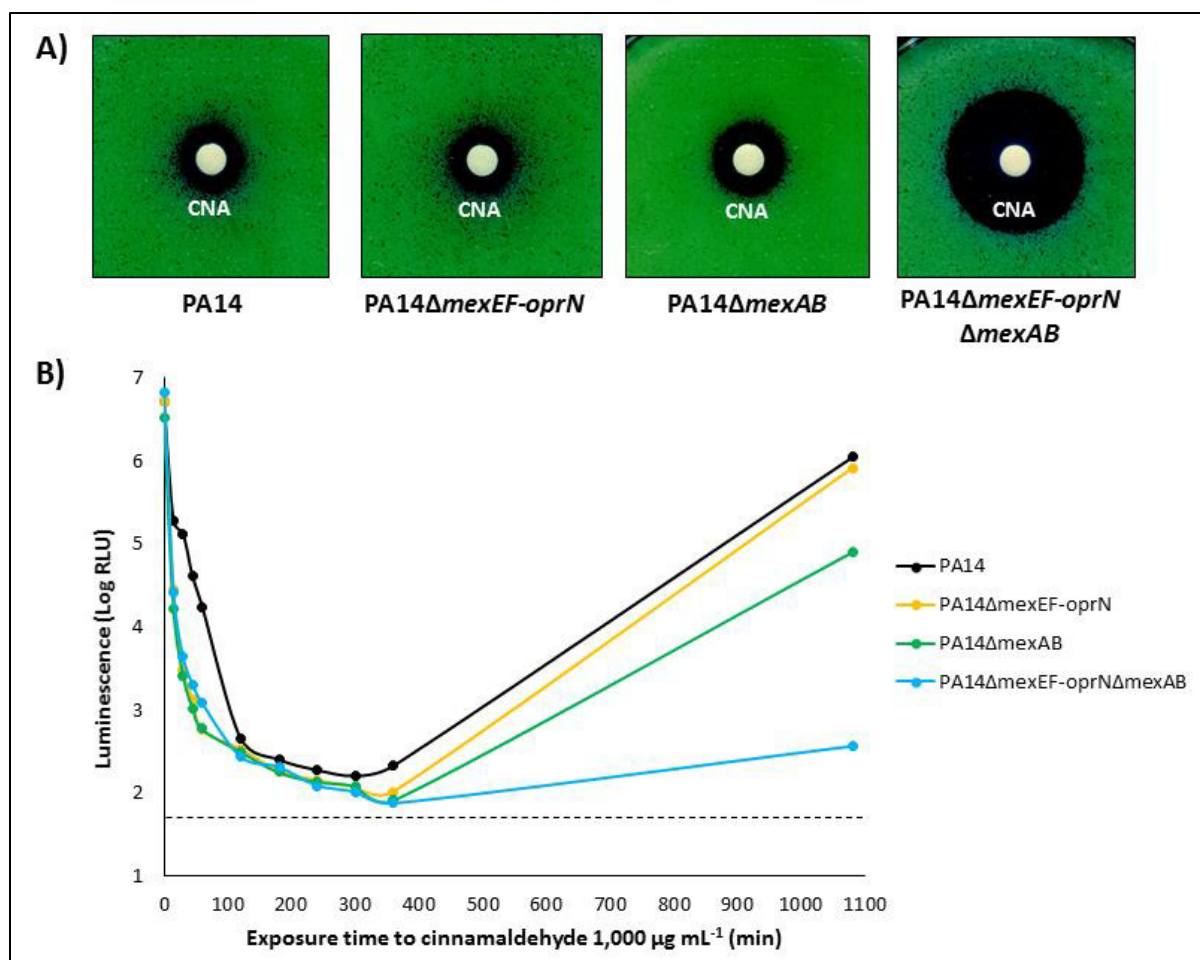
Confirming our previous results, exposure to electrophiles (GO, MG, CNA) reinforced resistance of PA14 to chloramphenicol and imipenem, and strongly induced *mexE* expression (172-, 31-, and 233-fold, respectively) (Table 9). By contrast,  $\alpha$ -oxoaldehydes GO and MG increased resistance to MexXY/OprM substrates gentamicin and tobramycin with

concomitant derepression of gene *mexY* (7.7- and 6.0-fold), while cinnamaldehyde (CNA) had similar effects on susceptibility to MexAB-OprM substrates aztreonam and ticarcillin, and *mexB* activity (9.4-fold) (**Table 9**).

Time-kill experiments comparing deletion mutant PA14 $\Delta$ *mexEF-oprN* to its wild-type parent demonstrated that MexEF-OprN, to some extent, is able to protect *P. aeruginosa* from CNA (Juarez et al., 2017). Curiously, it was observed that CNA MIC (512  $\mu$ g/mL) was identical for strain PA14 and its mutant. It was thus hypothesized that pumps MexAB-OprM and/or MexXY/OprM could perhaps compensate for the absence of MexEF-OprN and contribute to CNA resistance.

To test this assumption and better understand the role of MexAB-OprM in the response to CNA, we deleted genes *mexAB* in PA14 and PA14 $\Delta$ *mexEF-oprN*, and determined the susceptibility of the two strains in MIC and time kill experiments. Deletion of gene *oprM* that also provides the outer membrane component of the MexXY/OprM system will be carried out in another project (Alexandre Tetard, 2018).

Our results showed that susceptibility of strain PA14 to CNA remains unaffected unless both pumps, MexAB-OprM and MexEF-OprN, are inactivated (**Figure 19A**). Actually, the double deletion prevents adaptive regrowth after CNA exposure (**Figure 19B**). Altogether, these data suggest that MexAB-OprM and MexEF-OprN are able to export CNA, and that one pump can compensate for the other one if impaired. RT-qPCR experiments demonstrated in parallel that operon *mexAB-oprM* expression is strongly induced upon CNA challenge. The regulatory pathway involved in this induction is about to be studied in the laboratory.



**Figure 19: Antimicrobial activity of cinnamaldehyde on *P. aeruginosa*.** (A) Susceptibility of strain PA14 and its derived mutants to cinnamaldehyde (CNA 10 μg) was measured by disk diffusion method. (B) Bioluminescent strain PA14 and its derived mutants were cultured to mid-log phase and then challenged with 1,000 μg mL<sup>-1</sup> cinnamaldehyde. Luminescence (RLU) was measured in a plate reader and was used as indicator of cell survival. The curve is a representation of one experiment. A luminescence threshold was determined with sterile MHB (dotted line).





## **IV. Conclusion and Perspectives**

---



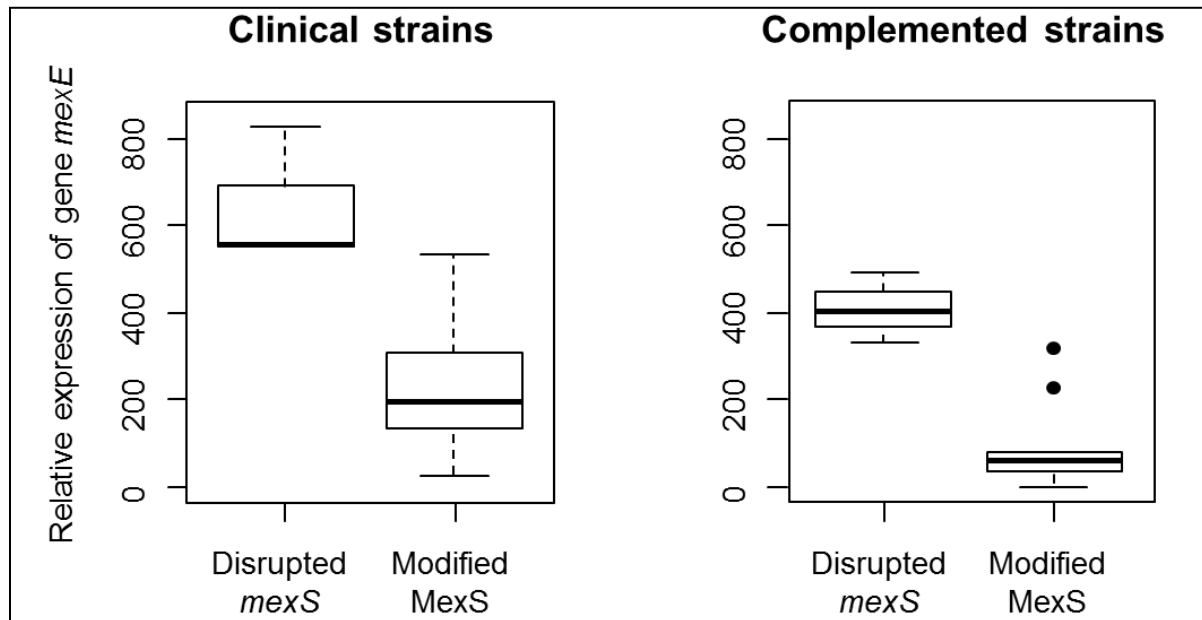
## Overexpression of *mexEF-oprN* in clinical strains

The role of several RND efflux pumps in natural and acquired resistance of *P. aeruginosa* to antibiotics and antiseptics is now well established (Aires et al., 1999; Li et al., 2015; Poole, 2004; Poole and Srikumar, 2001; Schweizer, 2003). Furthermore, evidence accumulates that the efflux system MexEF-OprN contributes to drug resistance in some clinical strains (Li and Plésiat, 2016). The so-called *nfxC* mutants that stably overproduce this pump have long been considered as rare or absent from the clinical setting (Quale et al., 2006; Walsh and Amyes, 2007; Wolter et al., 2004; Xavier et al., 2010). However, a growing number of publications now report on identification of such mutants in CF and non-CF patients (Jalal et al., 2000; Llanes et al., 2011; Oh et al., 2003; Terzi et al., 2014), though the underlying causes of pump dysregulation most often remain uncharacterized.

One of the reasons why *nfxC* mutants are difficult to detect among clinical strains is that their resistance phenotype to chloramphenicol, trimethoprim, fluoroquinolones, and carbapenems is often masked by more common mechanisms including overproduction of pump(s) MexAB-OprM or (and) MexXY/OprM, and loss of porin OprD (Llanes et al., 2013; Richardot et al., 2015). Thus, the most reliable technique for characterization of *nfxC* strains remains RT-qPCR. However, the threshold of *mexE* expression depends on which strain is used as reference. For instance, our characterization of 55 *in vitro* selected *nfxC* mutants showed that this threshold is 20-fold and 100-fold above the baseline levels of strains PA14 and PAO1, respectively. This difference lies in the fact that *mexT* is inactivated by an 8 bp sequence in most isolates of the PAO1 lineage, while this gene is functional in PA14 (Stover et al., 2000; Winsor et al., 2016). Thus, according to the threshold used, RT-qPCR results may lead to misinterpretations.

In this context, we carried out the characterization of a collection of 22 non-CF clinical isolates overexpressing the *mexE* gene (from 21- to 404-fold relative to PA14). It became rapidly evident that most *nfxC* clinical strains are phenotypically different from *in vitro* selected *nfxC* mutants as they rarely exhibit the typical hypersusceptibility to  $\beta$ -lactams (7/22 isolates) or aminoglycosides (0/22). Furthermore, severe deficiency in virulence factor production which is characteristic of *in vitro* *nfxC* mutants (Köhler et al., 2001; Sobel et al., 2005a) is rare in clinical counterparts (Richardot et al., 2016). In line with these observations, we found that 13/22 of *nfxC* clinical strains harbored mutations in gene *mexS*, but disruptive events were four times less frequent (3/13) than missense mutations (10/13). Expression levels of gene *mexE* were in general higher in the *mexS* knockout group (**Figure 20**, left

panel). Complementation experiments with various *mexS* mutated alleles in PA14 $\Delta$ *mexS* confirmed this observation (**Figure 20**, right panel). It should be noted that while other investigators reported that missense mutations in *mexS* are more prevalent than disruptive mutations among clinical strains (as summarized in **Table 3** page 20), the correlation with *mexEF-oprN* expression had not been established until this study.



**Figure 20: Relative expression of gene *mexE* from clinical and complemented strains according to the type of mutations found in *mexS*.** Adapted from Richardot et al, 2016

Other differences were noted between the *nfxC* strains in relation with the degree of presumed impairment of oxidoreductase MexS. We showed that the levels of *mexE* expression were roughly correlated with the MICs of pump substrates and inversely related to different virulence traits. Since *mexS* knockout mutants are four times less prevalent than *mexS* missense mutants in the clinic, it is tempting to assume that disruption of *mexS* is too detrimental to *P. aeruginosa* to allow its persistence *in vivo*. Supporting this notion, the three clinical isolates (1709, 1711, and 0607) harboring disrupted *mexS* copies were responsible for host colonization and not infections. As previously noted in the lab (Richardot et al., 2016), the expression of gene *mexT* remains unchanged in *nfxC* mutants *versus* wild-type strains. The ratio of active/inactive MexT occurring in the cell upon *nfxC* mutations thus appears as the main factor determining levels of *mexEF-oprN* transcription and associated phenotypic traits.

Several authors (Fargier et al., 2012; Köhler et al., 1999; Sobel et al., 2005a) suggested that MexS could play a central role in detoxification of noxious metabolites or xenobiotics which, in absence of the enzyme, would need to be extruded by MexEF-OprN. Since the

physiological role of MexS is still unknown, it was quite difficult to set up assays to verify this hypothesis. Enzymatic activity of MexS remains to be characterized *in vitro*. In this perspective, we engineered two recombinant proteins tagged with 6x-His or MBP. In both cases, we checked their functionality in mutant PA14Δ*mexS*. As expected, the mutant recovered a wild-type susceptibility profile to antibiotics once complemented with one or the other protein. Both of them will soon be produced in large scale, will be purified and used to screen several potential substrates such as quinones (Nordling et al., 2002; Persson et al., 2008), by spectrophotometric (Matthews, 1987) and/or fluorimetric assays (Passonneau and Lowry, 1993). We hope that the purified products will be suitable to determine the crystal structure of MexS and to identify its functional domains. The amino acid substitutions found in clinical *nfxC* mutants will be helpful to find out residues critical for enzyme activity.

In addition to *mexS* mutations, we showed for the first time that specific single amino acid substitutions (G<sub>257</sub>S and G<sub>257</sub>A) in MexT are responsible for constitutive activation of this regulator and overexpression of operon *mexEF-oprN* (short-paper in preparation). Gain-of-function mutations in LTTRs had already been reported. For instance, substitutions T<sub>149</sub>M and T<sub>149</sub>P in LTTR CysB that controls expression of cysteine regulon in *S. enterica*, result in overexpression of genes *cysK*, *cysP* and *cysJIIH* without the need of co-inducer N-acetyl-L-serine (Colyer and Kredich, 1994, 1996). Furthermore, site-directed mutagenesis experiments demonstrated that substitutions R<sub>156</sub>H in CatM, and R<sub>156</sub>H/T<sub>157</sub>S in BenM, two LTTRs involved in aromatic compounds degradation in *Acinetobacter baylyi*, generate variants that no longer require inducers for activation (Craven et al., 2009). Based in our two-hybrid results, we hypothesize that the two MexT variants identified in this study form active oligomers. However, to ascertain this assumption we have the project to crystallize the wild-type and mutated MexT proteins to understand why mutations at position Gly-257 activate the regulator. This will be done in collaboration with the Crystallization laboratory of Paris Descartes University (Pr. Isabelle Broutin, UMR 8015 Laboratoire de Cristallographie et RMN Biologiques).

### **A novel pathway of *mexEF-oprN* activation and a novel type of mutants**

Seven of the 22 *nfxC* clinical strains that we studied did not harbor mutations in proteins MexS and MexT. This result confirmed previous conclusions about the existence of one or more additional regulatory pathways for MexEF-OprN (Kumar and Schweizer, 2011; Maseda et al., 2010). Characterization of *in vitro* selected mutants led to the discovery of CmrA, a novel AraC-type transcriptional regulator which when activated by specific single amino acid

substitutions is able to indirectly upregulate *mexEF-oprN* expression (Juarez et al., 2017). Moreover, it appeared that CmrA positively regulates a small set of 11 non-essential genes (in standard laboratory growth conditions). It remains to be determined whether CmrA directly binds to the regions upstream of all these genes. Production and purification of a 6x-His-CmrA is ongoing in our lab. Once the recombinant protein will be obtained in sufficient amounts, we will perform Electrophoretic Mobility Shift Assays (EMSA) by incubating the purified protein with DNA fragments of putative targets (Hellman and Fried, 2007; Hsieh et al., 2016).

Four different types of *in vitro* selected *nfxC* mutants have thus been characterized so far, namely (i) the well-known *nfxC* mutants harboring disruptive mutations in *mexS* (Sobel et al., 2005a), (ii) the *nfxC1* subclass with missense mutations in *mexS* (Richardot et al., 2016), (iii) the *nfxC2* mutants with gain-of-function *cmrA* alleles (Juarez et al., 2017) and, (iv) the *nfxC3* harboring gain-of-function mutations in *mexT* (unpublished data). All these mutants have different phenotypic features summarized in **Table 10**.

**Table 10: Genotypic and phenotypic features of MexEF-OprN overproducers**

Strain	Genotype <sup>a</sup>	Frequency	Relative expression of gene <i>mexE</i> <sup>b</sup>	Ciprofloxacin MIC ratio	Virulence score <sup>c</sup>
WT	-	-	1	1	5/5
<i>nfxC</i>	<i>mexS</i> <sup>-</sup>	2.5 X 10 <sup>-7</sup>	>150x	16x	1/5
<i>nfxC1</i>	<i>mexS</i> <sup>*</sup>	1.4 X 10 <sup>-7</sup>	40x – 150x	8x – 16x	4/5
<i>nfxC2</i>	<i>cmrA</i> <sup>+</sup>	2.5 X 10 <sup>-8</sup>	20x – 40x	4x – 8x	5/5
<i>nfxC3</i>	<i>mexT</i> <sup>+</sup>	1.9 X 10 <sup>-9</sup>	>110x	8x – 16x	ND

<sup>a</sup> *mexS*<sup>-</sup>: disruptive mutations in *mexS*; *mexS*<sup>\*</sup>: missense mutations in *mexS*; *cmrA*<sup>+</sup>: gain-of-function mutations in *cmrA*. *mexT*<sup>+</sup>: gain-of-function mutations in *mexT*.

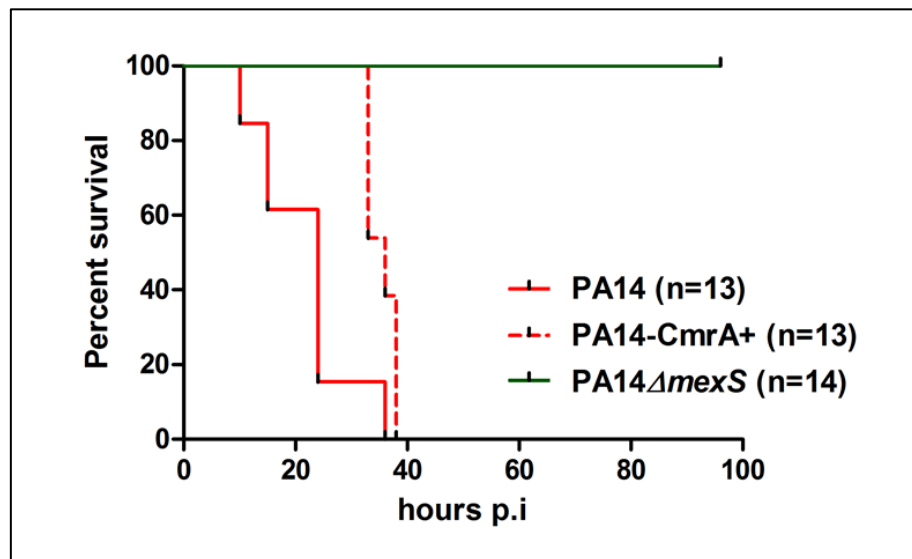
<sup>b</sup> Expressed as a ratio of wild-type strain PA14

<sup>c</sup> Based on the capacity of the strain to produce: (1) pyocyanin, (2) elastase, (3) biofilm, (4) rhamnolipids and to (5) swarm on semisolid surfaces.

ND: not determined.

Compared with MexS deficient/null mutants, *nfxC2* mutants do not seem to have an impaired virulence. The presumed pathogenicity of *nfxC2* mutants should make them clinically relevant, especially as they are more resistant to major antibiotics such as fluoroquinolones. Identification of such mutants in clinical samples remains to be done (see below). We are currently collaborating with the laboratory headed by Prof. Mustapha Si-Tahar (UMR 1100 "Infection Respiratoire et Immunité", Université François Rabelais, Tours) to evaluate their virulence in an animal model of acute pulmonary infection. Preliminary results showed that *cmrA* mutants caused the death of all infected mice at 39h post-inoculation while, confirming previous data, *mexS*<sup>-</sup> mutants are avirulent (**Figure 21**). Additional experiments have been

initiated to delete the gene encoding potent cytotoxin ExoU, to allow a better discrimination between wild-type PA14 and *nfxC2* mutants (da Cunha et al., 2015; Juan et al., 2017; Shaver and Hauser, 2004).



**Figure 21: Survival of BALB/cJRj mice infected with different strains of *P. aeruginosa*.** Male mice from 8 – 10 weeks were inoculated intranasally ( $5 \times 10^5$  UFC) and their survival was followed up to 4 days post-infection (Results obtained by UMR 1100, unpublished data).

### CmrA, a new target to consider when screening multi-drug resistant strains

In one study, insertion of a transposon upstream from gene *cmrA* (PA2047) was held responsible for an 8-fold increase in ciprofloxacin resistance (Breidenstein et al., 2008). Whether similar genetic events are relevant in clinical isolates is unlikely as we demonstrated that overexpressing a plasmid-borne copy of wild-type *cmrA* had no impact on PA14 drug susceptibility (Juarez et al., 2017). More interestingly, missense mutations in *cmrA* were reported in 3.2% of a collection of 474 CF clinical strains, leading to S<sub>45</sub>L, E<sub>61</sub>D, S<sub>266</sub>N, Y<sub>271</sub>H, and A<sub>293</sub>V substitutions in regulator CmrA (Marvig et al., 2015). The link between these changes and MexEF-OprN-dependent resistance to various antibiotics was not investigated, but it will be assessed by our group through site-directed mutagenesis and *trans*-complementation of the PA14Δ*cmrA* mutant.

Retrospective screening of three collections of *P. aeruginosa* housed by the lab revealed the presence of single amino acid variations in CmrA from five strains (T<sub>5</sub>I, L<sub>7</sub>F, R<sub>29</sub>E, E<sub>42</sub>D, G<sub>188</sub>S). However, these changes were non-significant since inactivation of gene *cmrA* did not modify the resistance phenotype of these strains. Thus, while *nfxC* and *nfxC1* mutants have been characterized in the clinical setting (Llanes et al., 2011, 2013; Richardot et al., 2016), *nfxC2* strains still await to be identified.



## Induction of RND pumps by electrophilic stress

Our work demonstrated that the CmrA-PA2048-MexEF-OprN pathway is part of the electrophile stress response in *P. aeruginosa* (Juarez et al., 2017). In contrast to other oxidative stressors (Fargier et al., 2012; Fetar et al., 2011; Fraud and Poole, 2011; Starr et al., 2012), electrophiles enhance the resistance of the bacterium to various antibiotics (Juarez et al., 2017). We showed that in addition to MexEF-OprN, two other systems (MexAB-OprM and MexXY/OprM) are strongly upregulated when bacteria are exposed to GO, MG and CNA. Because of the strong toxicity of these molecules, a high efflux activity is probably needed to quickly remove these agents, some toxic metabolites or damaged components, from the cell. The regulatory pathways by which MexAB-OprM and MexXY/OprM are activated by RES are currently studied in our lab (Master's project of Alexandre Tetard).

Henceforth, it would be interesting to consider if RND pumps are induced by natural electrophiles generated by the host during *P. aeruginosa* infection. Indeed, significant levels of malondialdehyde, an electrophile derived from lipid peroxidation, were detected in the lungs of patients suffering from asthma, bronchiectasis, chronic obstructive pulmonary disease, and idiopathic pulmonary fibrosis. The average physiological concentration of this molecule was around 30 nM in 194 patients *versus* 15 nM in 14 healthy controls (Bartoli et al., 2011). In another work on CF-patients ( $n=40$ ), malondialdehyde reached 176 nM in plasma, 140 nM in exhaled breath condensate and 280 nM in sputum (Antus et al., 2015). Therefore, we have planned to investigate the response of *P. aeruginosa* to this quite unstable electrophile, in particular the impact of reported concentrations on *mexEF-oprN*, *mexAB-oprM*, and *mexXY* expressions in several clinical strains including PA14. Since the laboratory has access to sputa from CF patients, we will also measure malondialdehyde concentrations in these samples by HPLC/MS.

Novel antimicrobials are urgently needed to counter multidrug resistance in human pathogens, especially nosocomial species such as *P. aeruginosa* (Silver, 2011; Tacconelly and Magrini, 2017). In this context, understanding the regulatory mechanisms leading to antibiotic resistance may in theory help to set up innovative therapeutic strategies. RND efflux systems are deplored for their contribution to intrinsic resistance with respect to development of new anti-Gram negatives; and as cause of poor clinical outcomes in line with emergence of resistant mutants. However, the contribution of such pumps to adaptive (non-mutational) resistance *in vivo* is largely unknown, as this transient phenomenon cannot be appreciated by

classical *in vitro* drug susceptibility testing. The pump MexXY/OprM has been shown by our group to play a significant role in adaptive resistance to aminoglycosides (Hocquet et al., 2008). Whether the highly inducible MexEF-OprN also enables *P. aeruginosa* to better resist some antibiotics *in vivo* warrants further investigations.



## **V. Materials and Methods**

---



## 1 Microbiological Techniques

### 1.1 Bacterial Strains and Plasmids

All bacterial strains and plasmids used in this work are listed in **Tables 11** and **12**.

**Table 11: Bacterial strains**

Strain	Phenotype or genotype	Source or Reference
<i>Pseudomonas aeruginosa</i>		
<u>Reference strains</u>		
PA14	Wild-type reference strain prototroph and sensitive to all antibiotics. Functional MexS and MexT.	Liberati et al., 2006
<u>Environmental strains</u>		
591	Environmental strain serotype O:1	This study
142951	Environmental strain serotype O:10	This study
1053	Environmental strain serotype O:5	This study
2140	Environmental strain serotype O:3	This study
114793	Environmental strain serotype O:8	This study
1033	Environmental strain serotype O:12	This study
2531	Environmental strain serotype O:16	This study
986-36	Environmental strain serotype O:6	This study
201	Environmental strain serotype O:4	This study
1281G	Environmental strain serotype O:13	This study
2112	Environmental strain serotype O:11	This study
1972G	Environmental strain serotype O:2	This study
2910	Environmental strain non-agglutinable	This study
2998x	Environmental strain poly-agglutinable	This study
<u>Clinical strains with amino acid substitutions in MexS</u>		
1307	Clinical strain harboring the substitution V <sub>104</sub> A	Richardot et al., 2016
2310	Clinical strain harboring the substitution F <sub>253</sub> L	Richardot et al., 2016
2505	Clinical strain harboring the substitution D <sub>44</sub> E	Richardot et al., 2016
3005	Clinical strain harboring the substitution S <sub>60</sub> F	Richardot et al., 2016
0911	Clinical strain harboring the substitution F <sub>185</sub> L	Richardot et al., 2016
1009	Clinical strain harboring the substitutions V <sub>73</sub> A + L <sub>270</sub> Q	Richardot et al., 2016
0801	Clinical strain harboring the substitution C <sub>245</sub> G	Richardot et al., 2016
1409	Clinical strain harboring the substitution A <sub>166</sub> P	Richardot et al., 2016
2311	Clinical strain harboring the substitution S <sub>60</sub> P	Richardot et al., 2016
2609	Clinical strain harboring the substitution L <sub>263</sub> Q	Richardot et al., 2016
1709	Clinical strain harboring a deletion of 8 bp in <i>mexS</i> (710 – 718)	Richardot et al., 2016
1711	Clinical strain harboring a disrupted <i>mexS</i> gene ( $\Delta$ G <sub>293</sub> )	Richardot et al., 2016
0607	Clinical strain harboring a deletion of 30 bp in <i>mexS</i> (927 – 956)	Richardot et al., 2016
<u>Clinical strains with amino acid substitutions in MexT</u>		
4088	Clinical strain harboring the substitution G <sub>257</sub> S	Llanes et al., 2011
4177	Clinical strain harboring the substitution R <sub>166</sub> H	Llanes et al., 2011
10-12	CF clinical strain harboring the substitution G <sub>257</sub> A	Llanes et al., 2013
0810	Clinical strain harboring the substitution G <sub>258</sub> D	Richardot et al., 2016
1510	Clinical strain harboring the substitutions Y <sub>138</sub> H + G <sub>258</sub> D	Richardot et al., 2016

Clinical strains harboring no mutations in *mexS* nor *mexT*

6-15	CF clinical strain	Llanes et al., 2013
7-20	CF clinical strain	Llanes et al., 2013
9-12	CF clinical strain	Llanes et al., 2013
2502	Clinical strain	Richardot et al., 2016
1206	Clinical strain	Richardot et al., 2016
0708	Clinical strain	Richardot et al., 2016
0309	Clinical strain	Richardot et al., 2016
2607	Clinical strain	Richardot et al., 2016
0712	Clinical strain	Richardot et al., 2016
0608	Clinical strain	Richardot et al., 2016

Spontaneous mutants in *cmrA*

PJ01	PA14-derived mutant harboring the substitution A <sub>68</sub> V in CmrA	This study
PJ02	PA14-derived mutant harboring the substitution H <sub>204</sub> L in CmrA	This study
PJ03	PA14-derived mutant harboring the substitution L <sub>89</sub> Q in CmrA	This study
PJ04	PA14-derived mutant harboring the substitution N <sub>214</sub> K in CmrA	This study

In vitro mutants

PA14Δ <i>mexS</i>	PA14-derived <i>mexS</i> deleted mutant	Richardot et al., 2016
PA14Δ <i>mexT</i>	PA14-derived <i>mexT</i> deleted mutant	Richardot et al., 2016
PA14Δ <i>mexT</i> <sub>0810</sub>	PA14Δ <i>mexT</i> strain complemented with <i>mexT</i> from 0810	This study
PA14Δ <i>mexT</i> <sub>1510</sub>	PA14Δ <i>mexT</i> strain complemented with <i>mexT</i> from 1510	This study
PA14Δ <i>mexT</i> <sub>4088</sub>	PA14Δ <i>mexT</i> strain complemented with <i>mexT</i> from 4088	This study
PA14Δ <i>mexT</i> <sub>4177</sub>	PA14Δ <i>mexT</i> strain complemented with <i>mexT</i> from 4177	This study
PA14Δ <i>mexT</i> <sub>10-12</sub>	PA14Δ <i>mexT</i> strain complemented with <i>mexT</i> from 10-12	This study
PA14Δ <i>mexEF-oprN</i>	PA14-derived <i>mexEF-oprN</i> deleted mutant	This study
PA14Δ <i>cmrA</i>	PA14-derived <i>cmrA</i> deleted mutant	This study
PA14Δ <i>mexAB</i>	PA14-derived <i>mexAB</i> deleted mutant	This study
PA14Δ <i>mexEF-oprN</i> Δ <i>mexAB</i>	PA14-derived <i>mexEF-oprN mexAB</i> double deleted mutant	This study
PA14Δ <i>cmrA</i> <sub>PA14</sub>	PA14Δ <i>cmrA</i> complemented with WT <i>cmrA</i> from PA14	This study
PA14Δ <i>cmrA</i> <sub>PJ01</sub>	PA14Δ <i>cmrA</i> complemented with mutated <i>cmrA</i> from PJ01	This study
PA14Δ <i>cmrA</i> <sub>PJ02</sub>	PA14Δ <i>cmrA</i> complemented with mutated <i>cmrA</i> from PJ02	This study
PA14Δ <i>cmrA</i> <sub>PJ03</sub>	PA14Δ <i>cmrA</i> complemented with mutated <i>cmrA</i> from PJ03	This study
PA14Δ <i>cmrA</i> <sub>PJ04</sub>	PA14Δ <i>cmrA</i> complemented with mutated <i>cmrA</i> from PJ04	This study
PJ01Δ <i>mexS</i>	PJ01-derived <i>mexS</i> deleted mutant	This study
PJ02Δ <i>mexS</i>	PJ02-derived <i>mexS</i> deleted mutant	This study
PJ03Δ <i>mexS</i>	PJ03-derived <i>mexS</i> deleted mutant	This study
PJ04Δ <i>mexS</i>	PJ04-derived <i>mexS</i> deleted mutant	This study
PJ01Δ <i>mexT</i>	PJ01-derived <i>mexT</i> deleted mutant	This study
PJ01Δ <i>mexEF-oprN</i>	PJ01-derived <i>mexEF-oprN</i> deleted mutant	This study
PJ01Δ <i>cmrA</i>	PJ01-derived <i>cmrA</i> deleted mutant	This study
PJ02Δ <i>cmrA</i>	PJ02-derived <i>cmrA</i> deleted mutant	This study
PJ03Δ <i>cmrA</i>	PJ03-derived <i>cmrA</i> deleted mutant	This study
PJ04Δ <i>cmrA</i>	PJ04-derived <i>cmrA</i> deleted mutant	This study
PJ01ΔPA2046	PJ01-derived PA2046 deleted mutant	This study
PJ01ΔPA2048	PJ01-derived PA2048 deleted mutant	This study

PJ01ΔPA1880-81	PJ01-derived PA1880and PA1881 deleted mutant	This study
PJ01ΔPA2274	PJ01-derived PA2274 deleted mutant	This study
PJ01ΔPA2275	PJ01-derived PA2275 deleted mutant	This study
PJ01ΔPA2276	PJ01-derived PA2276 deleted mutant	This study
PA14ΔIR91	PA14 strain deleted from the inversed repeated region between PA2047 and PA2048 (IR-N91)	This study
PJ01ΔIR91	PJ01 strain deleted from the inversed repeated region between PA2047 and PA2048 (IR-N91)	This study
PJ01ΔsoxR	PJ01-derived <i>soxR</i> deleted mutant	This study
PJ01ΔPA2050	PJ01-derived PA2050 deleted mutant	This study
PA14::PA2048- <i>lux</i>	PA14 containing the luminescent reporter PA2048- <i>lux</i>	This study
PJ01::PA2048- <i>lux</i>	PJ01 containing the luminescent reporter PA2048- <i>lux</i>	This study
PA14- <i>lux</i>	Bioluminescent strain PA14	This study
PA14Δ <i>mexS-lux</i>	Bioluminescent strain PA14Δ <i>mexS</i>	This study
PA14Δ <i>mexEF-oprN-lux</i>	Bioluminescent strain PA14Δ <i>mexEF-oprN</i>	This study
PA14Δ <i>mexAB</i>	Bioluminescent strain PA14Δ <i>mexAB</i>	This study
PA14Δ <i>mexEF-oprNΔmexAB</i>	Bioluminescent strain PA14Δ <i>mexEF-oprNΔmexAB</i>	This study
PA14Δ <i>cmrA-lux</i>	Bioluminescent strain PA14Δ <i>cmrA</i>	This study
PJ01- <i>lux</i>	Bioluminescent strain PJ01	This study

***Escherichia coli***

DH5α	F- φ80lacZΔM15 Δ(lacZYA-argF)U169 recA1 endA1 hsdR17(rk-, mk+) phoA supE44 thi-1 gyrA96 relA1 λ <sup>-</sup>	Invitrogen. St. Aubin, France
CC118	Δ( <i>ara-leu</i> ) <i>araD</i> Δ <i>lacX74 galE galK phoA20 thi-1 rpsE rpoB argE</i> (Am) <i>recA1</i>	Manoil and Beckwith, 1985
CC118 λpir	CC118 lysogenic for phage λpir	Herrero et al., 1990
DHM1	F- <i>cya-854 recA1 endA1 gyrA96</i> (Nal <sup>R</sup> ) <i>thi1 hsdR17 spoT1 rfbD1 glnV44</i> (AS)	Euromedex. Souffelweyersheim, France
HB101	<i>supE44 hsdS20</i> (r <sub>B</sub> <sup>-</sup> m <sub>B</sub> <sup>-</sup> ) <i>recA13 ara-14 pro A2 lacY1 galK2 rpsL20 xyl-5 mtl-1 leuμB6 thi-1</i>	Lacks and Greenberg, 1977
ER2523	<i>fhuA2 [lon] ompT gal silA11 r</i> (mcr-73 :: <i>miniTn10</i> —Tet <sup>S</sup> ) <sub>2</sub> [ <i>dcm</i> ] <i>R</i> (zgb-210 :: <i>Tn10</i> —Tet <sup>S</sup> ) <i>endA1</i> Δ( <i>mcrC-mrr</i> )114::IS10	New England Biolabs. Evry, France

Nal<sup>R</sup>: nalidixic acid resistant. Tet<sup>S</sup>: tetracycline susceptible.



**Table 12: Plasmids**

Plasmids	Description	Source or Reference
pCR-Blunt	Blunt-end cloning vector <i>ccdB lacZa Zeo<sup>R</sup> Kan<sup>R</sup></i>	Invitrogen.
pCR2.1	Cloning vector for PCR products; <i>lacZΔColE1 fl ori, Kan<sup>R</sup>, Amp<sup>R</sup></i>	Invitrogen.
pKNG101	Suicide vector <i>oriR6K sacB insB, Str<sup>R</sup></i>	Kaniga et al., 1991
Mini-CTX1	Self-proficient integration vector <i>tet,Ω-FRT-attP-MCS, ori, int oriT, Tet<sup>R</sup></i>	Hoang et al., 2000
Mini-CTX- <i>lux</i>	Self-proficient integration vector <i>Ω-FRT-attP-MCS, ori, int oriT, luxCDABE, Tet<sup>R</sup></i>	Becher and Schweizer, 2000
pUC18T-mini-Tn7T- <i>lux</i> -Gm	Suicide vector for shuttling single copies of genes directly to the chromosome via a mini-Tn7 element. <i>aacCI, oriT, P1 integron promoter driving expression of luxCDABE, Amp<sup>R</sup>, Gen<sup>R</sup></i>	Damron et al., 2013
pTNS3	Helper plasmid for chromosomal insertion encoding the Tn7 site-specific transposition pathway	Choi et al., 2008
pFLP2	Site-specific excision vector. <i>sacB FLP rep bla cI857 oriT Amp<sup>R</sup></i>	Hoang et al., 1998
pRK2013	Helper plasmid for mobilization of non-self-transmissible plasmids. <i>Mob1, tra1 col E1 Kan<sup>R</sup></i>	Kaniga et al., 1991
pME6032	Expression vector. <i>lacI<sup>q</sup> oriT oriV Ptac repA staA parG SD tetA T<sub>T4</sub> Tet<sup>R</sup></i>	Heeb et al., 2002
pJN105	Broad-host range vector carrying the <i>araBAD</i> promoter, Gen <sup>R</sup>	Newman and Fuqua, 1999
pUT18C	BACTH plasmid coding the T18 fragment of CyaA in N-ter. Amp <sup>R</sup>	Euromedex
pUT18	BACTH plasmid coding the T18 fragment of CyaA in C-ter. Amp <sup>R</sup>	Euromedex
pKT25	BACTH plasmid coding the T25 fragment of CyaA in N-ter. Kan <sup>R</sup>	Euromedex
pKNT25	BACTH plasmid coding the T25 fragment of CyaA in C-ter. Kan <sup>R</sup>	Euromedex
pMAL-c5X	MBP fusion protein production vector. <i>pBR ori, lacI, P<sub>lac</sub> male, rrrB T1T2 bla. Amp<sup>R</sup></i>	New England Biolabs

Abbreviations: Zeo<sup>R</sup> (zeocin resistance), Kan<sup>R</sup> (kanamycin resistance), Amp<sup>R</sup> (ampicillin resistance), Str<sup>R</sup> (streptomycin resistance), Tet<sup>R</sup> (tetracycline resistance), Gen<sup>R</sup> (gentamicin resistance).

## 1.1 Culture Media

All culture media used in this work are listed in the **Table 13**.

**Table 13: Culture Media**

Medium	Description	Application	Reference
cMHA	Calibrated Muller-Hinton Agar. Nutritive medium with adjusted calibrations of Ca <sup>2+</sup> and Mg <sup>2+</sup>	General bacterial growth. Can be supplemented with antibiotics	BioRad, Marnes-la-Coquette, France
cMHB	Calibrated Muller-Hinton Broth. Nutritive broth with adjusted calibrations of Ca <sup>2+</sup> and Mg <sup>2+</sup>	General bacterial growth. Can be supplemented with antibiotics	Becton Dickinson, Le Pont de Claix, France
M8-Swarm	Minimal medium. NaCl 8 mM, NaH <sub>2</sub> PO <sub>4</sub> 42 mM, KH <sub>2</sub> PO <sub>4</sub> 22 mM pH 7.4 supplemented with glucose 0.2%, MgSO <sub>4</sub> 2 mM, Casaminoacids 0.5% and agar 0.5%	Test for swarming mobility	Köhler et al., 2000
M9-Suc	Minimal medium. NaCl 8.54 mM, NaH <sub>2</sub> PO <sub>4</sub> 25.18 mM, NH <sub>4</sub> Cl 18.68 mM, KH <sub>2</sub> PO <sub>4</sub> 22 mM, MgSO <sub>4</sub> 2 mM, agar 0.8% and sucrose 5%	Used for excision of pKNG101 and pFLP2 plasmids	Kaniga et al., 1991
MCTH	McConkey agar base supplemented with maltose 1%, kanamycin 50 µg/mL, and ampicillin 100 µg/mL	Bacterial two-hybrid medium. Red/White selection	Battesti and Bouveret, 2012
MHTH	Muller-Hinton plate supplemented with X-Gal 40 µg/mL, kanamycin 50 µg/mL and ampicillin 100 µg/mL	Bacterial two-hybrid medium. Blue/White selection	Battesti and Bouveret, 2012
sBAP	Sheep Blood-Agar Plate. Sheep blood 5%, tryptone 0.1% (w/v), NaCl 8 mM, agar 0.8%	Production of pyocyanin and hemolytic activity	BioRad, Marnes-la-Coquette, France
PYO broth	Tryptone broth. Tris-HCl 120 mM pH 7.2, tryptone 0.1 % (w/v), (NH <sub>4</sub> ) <sub>2</sub> SO <sub>4</sub> 20 mM, CaCl <sub>2</sub> 1.6 mM, KCl 10 mM, glucose 50 mM and sodium citrate 24 mM	Production of pyocyanin	Essar et al., 1990
PIA	<i>Pseudomonas</i> isolation agar	Selective medium containing the Irgasan <sup>TM</sup> antibiotic that inhibits gram-positive and gram-negative bacteria other than <i>P. aeruginosa</i>	Becton Dickinson, Le Pont de Claix, France

## 1.2 In Vitro Selection of Chloramphenicol Resistant Mutants

*In vitro* selection of mutants overproducing the MexEF-OprN efflux system was performed by plating about 10<sup>8</sup> CFU/mL of reference strain PA14 on MHA medium containing 128, 256

or 512 µg/mL of chloramphenicol. Colonies grown after 18 h of incubation at 37°C were replicated on the same selective medium before their characterization.

### 1.3 Determination of Antibiotic Sensitivity

#### 1.3.1 Antibiograms

Antibiograms were performed using the agar diffusion technique according to recommendations of the “Comité de l’Antibiogramme de la Société Française de Microbiologie” (CA-SFM-2013). Briefly, a bacterial suspension (0.2 McFarland) was diluted ( $10^{-2}$ ) into cMHB. Next, 10 mL of this suspension were poured into a cMHA plate and then removed ( $\approx 1.5 \times 10^6$  CFU/mL). Disks (BioRad) with standard loads of antibiotics were added over the seeded plate once dried. Finally, the inhibition diameters were measured after 18 h of incubation at 37°C. Spontaneous *nfxC* mutants developing on solid media were screened for their resistance to both ciprofloxacin and imipenem, by measuring the inhibition zones around Bio-Rad disks (loaded with 5 µg and 10 µg, respectively).

#### 1.3.2 Minimum Inhibitory Concentration (MIC)

The Minimum Inhibitory Concentrations (MICs) of selected antibiotics were determined by the standard serial 2-fold dilution method in cMHA with inocula of  $10^4$  CFU per spot, according to the CLSI recommendations (Clinical and Laboratory Standards Institute, 2015). Growth was visually assessed after 18 h of incubation at 37°C. MICs of ciprofloxacin, chloramphenicol and trimethoprim were established to control the NfxC phenotype.

### 1.4 Virulence Factors Determination

For all virulence tests, results are presented as the mean of three independent experiments.

#### 1.4.1 Swarming Mobility

Swarming mobility is due to the combined action of rhamnolipids, type IV pili and flagella, and was evaluated on a semi-solid surface. Positive swarming strains form macroscopic colony patterns characterized by the coordinate translocation of bacteria on the semi-solid medium, when grown under optimal conditions. Briefly, 5 µL of a bacterial suspension (0.2 McFarland) were spotted onto the surface of an M8-Swarm medium (**Table 13**). Swarming colonies were observed after an incubation of 24 h at 37°C.

#### 1.4.2 Detection of Biofilm Formation by Adherence Test

Adherence being the first phase of biofilm production, this test measures the capacity of the strain to adhere to a plastic surface. Briefly, a bacterial suspension (0.3 McFarland) was

diluted ( $10^{-1}$ ) in cMHB. Next, 200  $\mu$ L of diluted bacteria ( $\approx 9 \times 10^7$  CFU/ml) were incubated 24 h at 30°C into a polystyrene 96-well microplate. Each well was washed twice using 200  $\mu$ L of distilled water to eliminate planktonic bacteria. Biofilm was colored using 200  $\mu$ L of crystal-violet solution at 1% (w/v). After 15 min at room temperature, the wells were washed as indicated previously. Crystal-violet attached to sessile bacteria was solubilized with 2 x 200  $\mu$ L ethanol at 99% (v/v). Finally, absorbance was read at 600 nm and calibrated with a negative control containing 400  $\mu$ L of cMHB (Vasseur et al., 2007).

#### **1.4.3 Pyocyanin Production**

A bacterial suspension (0.2 McFarland) prepared with fresh colonies from sBAP was diluted 1:20 in 50 mL PYO broth. The medium was then incubated 24h at 37°C with shaking, and centrifuged 20 min at 4,100 rpm. Pyocyanin was extracted twice with 2.5 mL chloroform. The organic phase was collected and acidified with 5 mL HCl 0.2 M. Upon acidification, pyocyanin turned from deep blue to pink; its concentration was measured spectrophotometrically at an absorbance of 520 nm (Essar et al., 1990).

#### **1.4.4 Elastase Activity**

Elastase degrades elastin in connective tissues. Its activity was measured in bacteria grown aerobically at 37°C up to an  $A_{600}$  of 1.8. Supernatants from 1 mL volumes of cultures were diluted 1:20 in E-buffer (Tris 0.1 M pH 7.4, and  $\text{CaCl}_2$  1 mM) containing 4 mg/mL RedCongo-elastin (Sigma, France). After an overnight incubation at 37°C, the reaction mixtures were centrifuged 10 min at 14,000 *g*. The concentration of soluble dye RedCongo released from RedCongo-elastin complex by elastase was determined spectrophotometrically at  $A_{495\text{nm}}$  in supernatants.

#### **1.4.5 Rhamnolipid Production**

Rhamnolipid production was assessed by a hemolysis assay. After 18 h of growth at 37°C in agitated cMHB, bacterial supernatants containing rhamnolipids were collected and heated at 95°C 10 min to inactivate thermolabile hemolytic factor phospholipase C. Next, supernatants were mixed with defibrinated horse blood diluted 1:50 in phosphate buffered saline (PBS, 137 mM NaCl, 2.7 mM KCl, 10 mM  $\text{Na}_2\text{HPO}_4$ , 1.76 mM  $\text{KH}_2\text{PO}_4$ ). After 30 min of incubation at room temperature, the mixture was centrifuged 10 min at 950 *g*. Concentration of hemoglobin in supernatants was determined spectrophotometrically at  $A_{405\text{nm}}$ .

### **1.5 Bacterial Growth**

A bacterial suspension adjusted to an  $A_{600\text{nm}}$  of 0.1 in cMHB was cultured during 9 h at 37°C with agitation. Bacterial growth was measured every 30 min up to 8 hours by reading absorbance at  $A_{600\text{nm}}$ .

### **1.6 Killing Experiments**

Strain PA14 was rendered constitutively bioluminescent by using the pUC18T-mini-Tn7T-*lux*-Gm plasmid, as described by Damron et al., 2013. Once made bioluminescent, PA14 and its derived mutants PA14 $\Delta$ *mexEF-oprN* and PA14 $\Delta$ *cmrA* were cultured overnight and diluted into fresh cMHB to yield an  $A_{600\text{nm}}$  of 0.1. The strains were incubated with shaking (250 rpm) at 37°C 2.5 h ( $A_{600\text{nm}}$  of 0.8) prior to the addition of glyoxal at 1,000  $\mu\text{g/mL}$ , methylglyoxal at 500  $\mu\text{g/mL}$  or cinnamaldehyde at 1,000  $\mu\text{g/mL}$ . Luminescence of surviving bacteria was monitored in white 96-well assay plates (Corning, NY USA) using a Synergy H1 microplate luminometer (Biotek Instruments, Winooski, USA), with a gain set at 150, a read height set at 7 mm and an integration time of one second. The threshold in  $\text{Log}_{10}(\text{RLU})$  was set at 1.69, using sterile cMHB.

## **2 Molecular Biology Techniques**

### **2.1 Nucleic Acid Extraction**

#### **2.1.1 Genomic DNA Extraction**

Bacterial genomic DNA was extracted using the *Wizard® Genomic DNA Purification Kit* (Promega, Charbonnières-les-bains, France) following supplier recommendations.

#### **2.1.2 Plasmid Extraction**

Plasmid extraction and purification was performed using *Wizard® plus SV Minipreps DNA purification system* (Promega) following supplier recommendations.

### **2.2 DNA Amplification by PCR (Polymerase Chain Reaction)**

Routine PCRs were performed in a Biometra T3 thermocycler (Biolabs Scientific Instrument, Lausanne, Switzerland) using 2.5 U of *MyTaq Red DNA polymerase* (Bioline, London, UK) and following supplier recommendations. Briefly, 100 ng of DNA were amplified in a Master Mix (50 $\mu\text{L}$ ) containing: gene specific primers 2 $\mu\text{M}$  (**Table 14**), 2.5 U of DNA polymerase and 10 $\mu\text{L}$  of 5x Reaction Buffer. PCR cycling conditions started with an initial denaturation at 95°C during 1 min followed by 30 cycles of: (i) 15 s of denaturation at 95°C (ii) 15 s of annealing using the optimal  $T_m$  of each primer and (iii) 10 s of extension at 72°C.

**Table 14: Primers used in this work**

Name	Sequence (5' → 3')	Reference
<b>Sequencing</b>		
<i>mexS</i>		
Seq-MexS-Ch1	GAACACGATCAGCAGGTTCA	Richardot et al., 2016
Seq-MexS-Ch2	ACCGGGGTGAGTACCT	
Seq-MexS-Ch3	GTCTCGGCTTCGAACTGG	
Seq-MexS-Ch4	GGTCAAATCCATCAGGCAGT	
Seq-MexS-Ch5	GCAAGCTGGTGCTGTATGG	
Seq-MexS-Ch6	GAAGGCGACTTCGTCTGG	
<i>mexT</i>		
Seg-MexT1	TGATGAAAACGGATCACTCG	Llanes et al., 2011
Seg-MexT2	GGGAACTAATCGAACGACGA	
Seq-MexT1	CTATTGATGCCGAACCTGCT	
Seq-MexT2	AATAGTCGTCGAGGGTCAGC	
<i>ampR</i>		
AmpRC1	GTCGACCAGTGCCTTCAGGCGATCC	Bagge et al., 2002
AmpRC2	CTCGAGAGCGAGATCGTTGCGGCACG	
<i>mvaT</i>		
MvaT1	CGCGTTTACTTACAGTTTCG	Llanes et al., 2011
MvaT2	AACGCTATTCGCTGGAGACT	
<i>mxtR</i>		
mxtR.PJ_1	AAAACCTCCGCTCCCATCAG	This study
mxtR.PJ_2	AGGACGATGCCTTTCAGTTG	
mxtR.PJ_3	GCAAGCAGGAGAACATCACC	
mxtR.PJ_4	AGCATGTCGTTGGAGACCAT	
mxtR.PJ_5	GTAATGCCGGACTCCTTCGT	
mxtR.PJ_6	CATCAGCAGGTCTTCCACCT	
mxtR.PJ_7	GTACTGGAAACAGGCCAACC	
mxtR.PJ_8	GTCCGGGTACTCGAACAGC	
mxtR.PJ_9	AACATTACCCAGGGCATCAG	
mxtR.PJ_10	GGGCATCGTAGAGGTTGTTC	
mxtR.PJ_11	ACCGACCTGCTGGACATCT	
mxtR.PJ_12	GGCTTGGACAGGTAGTCGAG	
mxtR.PJ_13	GAGACCGGTACGCAATTGAT	
mxtR.PJ_14	GTCTACCATCGCCTGGAAGC	
<i>cmrA PA2047</i>		
AraC-PA2047-PJ1	GGATACTGTCCGGTTCTTGC	This study
AraC-PA2047-PJ2	CAGCAGCCGGTAGAAAATCT	
AraC-PA2047-PJ3	CGCCTGATCCATCTGCTG	
AraC-PA2047-PJ4	CAAAGTCGTTGCTGTGCT	
<i>PA2449</i>		
PA2449-PJ1	CCAGGCCGTACAATCGAC	This study

PA2449-PJ2 GTTCGGTTCGTAGAGGGTCA  
 PA2449-PJ3 CGCGAAGTGACATTCATGG  
 PA2449-PJ4 TTGAGGCGGTAGAACAGGTC  
 PA2449-PJ5 GCAACCTGGAGAAGATGGTC  
 PA2449-PJ6 CAAGCAGGCGGACTTCAT

**Gene inactivation (in color, complementary regions)**

mexEF-oprN

iMexEFN-P1 GGCTTATTCCATCGAAAGCA  
 iMexEFN-P2 **ACGATGCGTCGATCT**GGAACAGCAGGT This study  
 iMexEFN-P3 **GATCGACGCATCGT**GGCGATCTACC  
 iMexEFN-P4 CTGGTTCGCCGGCTATGT

cmrA

iPA2047-PJ1 CTGTGGGGTGTAAGGGTGAC  
 iPA2047-PJ2 **CGGTGTT****CAGGATC**CAGGCAAGCATTC This study  
 iPA2047-PJ3 **GATCCTG****AACACCGC**CCTAGGGGAAC  
 iPA2047-PJ4 TCTCGCTATTGCCGGTATTG

PA2048

iPA2048-PJ1 GGAAACCTTCCCAAGACTAGC  
 iPA2048-PJ2 **GAACAAGCTGCCTCCG**ATTACCAGTTG This study  
 iPA2048-PJ3 **GAGGCAGCTTGTCT**GGCGTCTCAGC  
 iPA2048-PJ4 GCCGGGTAACCTACCTGATCC

PA2046

iPA2046-PJ1 CAGGGCCAGCGCCTGCACGAG  
 iPA2046-PJ2 **AAGCGCCTCCGGCGGGTACG**GTTGCGCAAG This study  
 iPA2046-PJ3 **CGTACCCGCCGGAGGCGCT**TGGCGGAGGG  
 iPA2046-PJ4 TCATTCGCCGGGCTTCGCCG

PA2050

iPA2050-PJ1 AGGATCAGTTCGATGGTCGT  
 iPA2050-PJ2 **GTTCTCG****CAGGCG**AAACCTTGATCG This study  
 iPA2050-PJ3 **TCGCCTGCGAGAAC**GCATCCTCGAC  
 iPA2050-PJ4 CATCGAATTCGGGGCGTA

PA2275

iPA2275-PJ1 GCGTCATAGCGGTAGGTTTC  
 iPA2275-PJ2 **GTCGACGGTGTGTC**CCTCTTCGCAGGAT This study  
 iPA2275-PJ3 **GACACACCGTCGAC**CAGGAAGGTCTC  
 iPA2275-PJ4 GGCTTGACCTCAAGTTTGCT

PA2276

iPA2276-PJ1 TGCAGCCAGTCGCCGTTGGC  
 iPA2276-PJ2 **CAGCCAAGGCCCGGCAGGAT**CGGGGGCGCT This study  
 iPA2276-PJ3 **ATCCTGCCGGGCCTTGGCTG**TTTCTCCAGG  
 iPA2276-PJ4 CGACCCGGCCGATGATCTCG

PA1880-81

iCutL-PJ1 TCTCTGCAGGGTCGTCCCCG  
 iCutL-PJ2 **GTGGTGCTCAGGCCTTGCCG**GGCTTGCTCT This study  
 iCutL-PJ3 **CGGCAAGGCC****TGAGCACCAC**CCAGGTCCGT

iCutL-PJ4	GATGCCGCCCTCCATCTGCG	
<u>soxR</u>		
iSoxR-PJ1	CTTTTCGCCCCCAGCCGCCA	
iSoxR-PJ2	TGACCGCTGCGATTGGCTTACCTCAAGTT	This study
iSoxR-PJ3	CAAGCCAATCGCAGCGGTACGCCGTGGTGC	
iSoxR-PJ4	AGGTGCGCCAGGCGATGGAC	
<u>PA2274</u>		
iPA2274-PJ1	CCAGGTGATCCTTTCCACCG	
iPA2274-PJ2	GTAACCCGCCGCCCGGCCGACGGCCCCG	This study
iPA2274-PJ3	GCCGGCGGGCGGGCGGTTACTCCGGGTGAC	
iPA2274-PJ4	CAACAGCAGCAGCTTGTCTGA	
<u>mexAB</u>		
iAB-SM1	GGCGTTTTTCATTGTGCTTC	
iAB-SM2	ACCGATCGTTGCATAGCGTTGTCCTCA	Smaltis, Besançon, France
iAB-SM3	ATGCAACGATCGGTACCGCGTGAT	
iAB-SM4	GTAGCTGCGCTGGGTCTAG	
<u>mexS</u>		
Inac-MexS-Ch1	GACAGGTGGGCGAAGATTT	
Inac-MexS-Ch2	ATCCATCCATCACGGGGTGAATAACCT	Richardot et al., 2016
Inac-MexS-Ch3	CGTGATGGATGGATTTACCGGTCATC	
Inac-MexS-Ch4	CGGCGAGATGTATGTGGTG	
<u>mexT</u>		
Inac-MexT-Ch1	AGCACATCCTTCCAGCTCAC	
Inac-MexT-Ch2	ATAAGCCGAACACGATCAGCAGGTTCA	Richardot et al., 2016
Inac-MexT-Ch3	CGTGTTCCGGCTTATTCATCGAAAGCA	
Inac-MexT-Ch4	GTCGATCTGGAACAGCAGGT	
<b>Chromosomal complementation</b>		
<u>mexT</u>		
Int-MexT-P1	CGGGGATCCCATCACGGGGTGAATAACCT (BamHI site)	This study
Int-MexT-P2	GCCAAAGCTTCGATCGATTTTCCCGTTG (HindIII site)	
<u>cmrA PA2047 v1.0</u>		
Int-PA2047-P1	CGGGGATCCATGACAGTCTGGCCTGTTGA (BamHI site)	This study
Int-PA2047-P2	GCCAAAGCTTAAGGGACAGGGCAAGCAG (HindIII site)	
<u>cmrA PA2047 v2.0</u>		
Int-PA2047-P3	CGGGGATCCCGGATACTGTCCGGTTCTTG (BamHI site)	This study
Int-PA2047-P2	GCCAAAGCTTAAGGGACAGGGCAAGCAG (HindIII site)	
<u>cmrA PA2047 v3.0</u>		
Int-PA2047-P7	CGGGGATCCCTGTTCTGGCGAATGCT (BamHI site)	This study
Int-PA2047-P2	GCCAAAGCTTAAGGGACAGGGCAAGCAG (HindIII site)	
<b>Bacterial two-hybrid</b>		
<u>mexT</u>		
XbaI-EDMexT-Fw	CGGTCTAGAGATCTCCACCGCCATGAGTC (XbaI site)	This study



KpnI-EDMexT-Rv	GCCGGTACCCGGAGGGCTCAGAGACTGT (KpnI site)	
<i>cmrA</i>		
TH- <i>cmrA</i> Fw	CATGAGCGAAAACACCCCGC	This study
TH- <i>cmrA</i> Rv	CTAGGCGGTGTTGCGCGCCC	

**Overexpression with the *araBAD* promoter**

<i>cmrA</i>		
pJN- <i>cmrA</i> Fw	GCGCTAGTCTTGGGAAGGTT	This study
pJN- <i>cmrA</i> Rv	AAGGACAGGGCAAGCAG	
<u>PA2048</u>		
pJN-PA2048 Fw	CCAGAACAAGGGGGACGGGC	This study
pJN-PA2048 Rv	GCATGGCGGAATCTCCGTCA	

**5'-RACE**

AAP	GGCCACGCGTCGACTAGTACGGGIIGGGIIGGGIIG	Invitrogen
<i>cmrA</i>		
GSP1- <i>cmrA</i>	GTGACCGAGACCACCAGGTA	This study
GSP2- <i>cmrA</i>	AATGCCTGAGCAGCGACT	
GSP3- <i>cmrA</i>	GCGCTAGTCTTGGGAAGGTT	
<b>PA2048</b>		
GSP1-PA2048	CATGGCCGCTTCATCGCTCC	This study
GSP2-PA2048	GAACGCTGGCATGCTCTCTGC	
GSP3-PA2048	GGTTGCCTGCGCTACGAAC	

**Luminescent reporter PA2048-*lux***

<i>cmrA</i> -PA2048 Fw	GTTTCAGAACGGCCGCTCCT	This study
<i>cmrA</i> -PA2048 Rv	GCGTCCCCTAGGCGGTGTT	

**Cloning for MBP-tagged proteins**

<u><i>mexS</i></u>		
NdeI-MBP- <i>mexS</i>	CATATGATGTCCCGAGTGATCCGTTT (NdeI site)	This study
BamHI-MBP- <i>mexS</i>	GGATCCTCAATCGGCGACGTGGATCA (BamHI site)	
<i>cmrA</i>		
NdeI-MBP- <i>cmrA</i>	CATATGATGAGCGAAAACACCCCGCT (NdeI site)	This study
BamHI-MBP- <i>cmrA</i>	GGATCCCTAGGCGGTGTTGCGCGCCC (BamHI site)	
<u>PA2048</u>		
NdeI-MBP-PA2048	CATATGATGCCAGCGTTCAATCGGGC (NdeI site)	This study
BamHI-MBP-PA2048	GGATCCTCAGAACGGCCGCTCCTGCA (BamHI site)	

**RT-qPCR**

*rpsL*

rpsL3	GCAACTATCAACCAGCTGGTG	Dumas et al., 2006
rpsL5	GCTGTGCTCTTGCAGGTTGTG	
<u>uvrD</u>		
uvrD1	CACGCCTCGCCCTACAGCA	Jeannot et al., 2005
uvrD2	GGATCTGGAAGTTCTCGCTCAGC	
<u>mexE</u>		
mexE3	CCAGGACCAGCACGAACTTCTTGC	Dumas et al., 2006
mexE4	CGACAACGCCAAGGGCGAGTTCACC	
<u>mexS</u>		
MexSP1	CAAGGGCGTCAATGTCATCC	Richardot et al., 2016
MexSP2	GACCGGTGAAATCCATCAGG	
<u>mexT</u>		
MexT1	ATCTGAACCTGCTGATCGTG	Llanes et al., 2013
MexT2	GTCCGGTACGGACGAACA	
<u>mexY</u>		
mexY1A	TTACCTCCTCCAGCGGC	Jeannot et al., 2005
mexY1B	GTGAGGCGGGCGTTGTG	
<u>mexB</u>		
MexB1	ATGACCATCACCGTGACCTT	Vettoretti et al., 2009
MexB2	AGAGTGGGTCCCTGGATGTTG	
<u>oprD</u>		
RT-oprD-Ch1	ACCAACCTCGAAGCCAAGTA	Llanes et al., 2013
RT-oprD-Ch2	ACAGGATCGACAGCGGATAG	
<u>cmrA</u>		
RT-cmrA-Fw tris	AGATTTTCTACCGGCTGCTG	This study
RT-cmrA-Rv tris	GCCGTAGTTCTGGTTGATCC	
<u>PA2048</u>		
RT-PA2048 Fw	CATGGCCGCTTCATCGCTCC	This study
RT-PA2048 Rv	GGTTGCCTGCGCTACGAACT	
<u>PA2049</u>		
RT-PA2049 Fw	CTTCCAGCACTGGCACTACC	This study
RT-PA2049 Rv	CAGGTCCTGCTGGAGTTCAC	
<u>PA2050</u>		
RT-PA2050 Fw	GCCTTCATCCATAGCCAGAT	This study
RT-PA2050 Rv	CACCTGGTAGCACTGCTTGA	
<u>PA2051</u>		
RT-PA2051 Fw	CTGCGCGTCAGTGGTATCTA	This study
RT-PA2051 Rv	CAGTAGGGCCCGTGGTAGT	
<u>PA2046</u>		
RT-PA2046 Fw	CGACAAGGCCTTCCTCTACA	This study

RT-PA2046 Rv	AGGCATAGCTCAGGTCGAGA	
<u>PA2276</u>		
RT-PA2276 Fw	GTCCTGCACCATCAGGCTCC	This study
RT-PA2276 Rv	TCGACCTTCCACCACAACCTT	
<u>PA2275</u>		
RT-PA2275 Fw	GACCAGGTGATCCTTTCCAC	This study
RT-PA2275 Rv	GTAGGGATTGAGGTCGTGCT	
<u>PA2274</u>		
RT-PA2274 Fw	GAACGCTGCTTCAGGAACTG	This study
RT-PA2274 Rv	GTGAACGCCAGCAGGTGTAG	
<u>PA1881</u>		
RT-PA1881 Fw	GGTACGTTCTGCGTGCT	This study
RT-PA1881 Rv	ACTGCGGTACCTGGAGCTT	
<u>PA1880</u>		
RT-PA1880 Fw	CTACCGGCCGATGTACTACC	This study
RT-PA1880 Rv	GTGCCTTCCAGGATCGACT	

## 2.3 Cloning Techniques

### 2.3.1 DNA Digestion using Restriction Enzymes

Plasmids or PCR products were digested using the following restriction enzymes: BamHI, ApaI, HindIII, EcoRI, KpnI, XbaI, SacI, NdeI (Promega). All restriction reactions were performed following the supplier recommendations.

### 2.3.2 Agarose Gel Electrophoresis

The size of DNA fragments was analyzed by agarose gel electrophoresis. Briefly, 0.8% agarose gels were soaked in 1X TAE buffer (Tris-acetate 40 mM, EDTA 1 mM pH 8) and submitted at 100 V during 30 min. 1X SYBR-safe (Invitrogen, St. Aubin, France) was added to agarose gels in order to visualize DNA under UV-light using the UV ChemiDoc XRS system (BioRad).

### 2.3.3 Purification of DNA Fragments

DNA fragments or digestion products were purified using the *Wizard® SV Gel and PCR clean up system* (Promega) following supplier recommendations.

### 2.3.4 DNA Ligation

DNA fragments were ligated into specific plasmids (see **Table 12**) using the T4 DNA ligase (Promega) and following the supplier recommendations. Ligation reaction was performed overnight at 15°C.

## 2.4 Bacterial Transformation

### 2.4.1 Heat-shock Transformation

*Cloning Efficiency*® *DH5α* Competent Cells (Invitrogen) were transformed with purified DNA following the supplier instructions. *E. coli* strains CC118, CC118 $\lambda$ pir, DHM1 and ER2523 cells were first rendered competent by using the RbCl protocol (Hanahan, 1983). In both cases, 100  $\mu$ L of competent cells were mixed with 10 ng plasmid and left 30 min at 0°C, and then submitted to a heat-shock at 42°C for 40 s. After 2 min at 0°C, 900  $\mu$ L of cMHB were added to the cells. Bacteria were then incubated aerobically 1 h at 37°C with agitation, and finally were plated on appropriate selective plates.

### 2.4.2 Electroporation

*P. aeruginosa* strains were transformed with purified DNA by using the MicroPulser™ Electroporator (Bio-Rad). Briefly, 1 mL of an overnight culture in MHB was centrifuged 2 min at 16,000 *g*. The pellet was washed twice with 1 mL of 300 mM sucrose solution, and finally resuspended in 100  $\mu$ L sucrose 300 mM. Electroporation was performed at 2.5 kV/cm, 200  $\Omega$  and 25  $\mu$ F for 4.5 – 5 ms, in presence of 20 ng of plasmid (Choi et al., 2006).

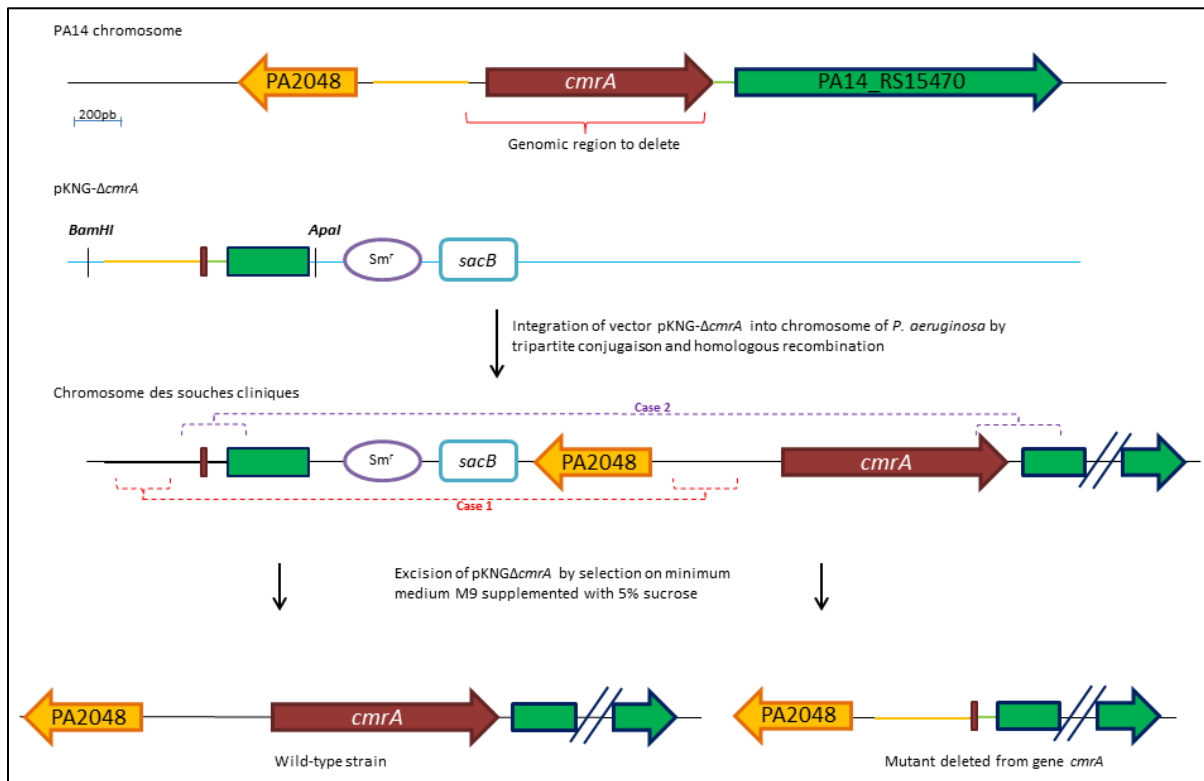
### 2.4.3 Bacterial Conjugation

Plasmid transfers from *E. coli* to *P. aeruginosa* were performed by triparental matings with “helper” plasmid pRK2013 that carries mobilization genes (*mob*). Each strain was cultured overnight with shaking. Then, 50  $\mu$ L of *E. coli* HB101(pRK2013) culture were mixed with 50  $\mu$ L of donor culture (*E. coli* CC118 containing a mini-CTX1 recombinant plasmid or CC118 $\lambda$ pir containing a pKNG101 recombinant plasmid). The mixture was spotted onto a cMHA plate and allowed to grow for 2 h at 37°C. 50 $\mu$ L of *P. aeruginosa* recipient strain, previously grown for 2 h at 42°C, were directly added onto the spot. After an overnight incubation at 37°C, the bacterial spot was resuspended in 3 mL of cMHB. Bacteria were incubated 1 h at 37°C and, finally plated onto selective PIA agar medium containing appropriate antibiotics.

## 2.5 Gene Inactivation using Overlapping PCR and Homologous Recombination

Gene inactivation was achieved by homologous recombination between chromosomal DNA and truncated PCR products. Briefly, the DNA sequences (ca 450 bp in length) flanking the target gene were amplified by PCR (see **Table 14**). A PCR overlapping the two amplicons was next performed to obtain a single fragment lacking the gene to delete. This fragment was cloned into vector pCR-Blunt and then sub-cloned into suicide vector pKNG101.

Recombinant pKNG plasmids were transferred from *E. coli* to *P. aeruginosa* by triparental matings and selection on PIA plates supplemented with 2,000 µg/mL streptomycin. The transconjugants were subcultured on M9-Suc medium to force the excision of the inserted plasmids. Finally, negative selection on streptomycin confirmed the loss of episomal plasmids while PCR/sequencing experiments confirmed the allelic exchanges. The complete inactivation strategy is illustrated in **Figure 22**.



**Figure 22: Gene inactivation by overlapping PCR and homologous recombination** Inactivation of gene *cmrA*; based on Muller et al., 2011.

## 2.1 Chromosomal Complementation

Genes *mexT* and *cmrA* and their promoters were amplified by PCR (see **Table 14**) and cloned into vector Mini-CTX1 using the restriction enzymes *Bam*HI and *Hind*III. This vector contains the coding regions for an integrase allowing insertion at the *attB* site of the bacterial chromosome (Hoang et al., 2000). Recombinant vectors were inserted into *E. coli* CC118 by heat-shock transformation and then transferred into *P. aeruginosa* strains by conjugation. Transformants were selected on PIA plates supplemented with tetracycline 200 µg/mL. For the excision of undesirable vector sequences, electrocompetent cells of *P. aeruginosa* were prepared as above (see section 2.4.2) and electroshocked with 200 ng of purified pFLP2 plasmid coding for the Flp flippase (Hoang et al., 1998). Clones were selected in cMHA plates supplemented with ticarcillin 150 µg/mL and next plated onto M9-suc plates for the

excision of pFLP2. Finally, excision of both plasmids was verified by plating the clones onto three different plates: the first, a cMHA plate without any antibiotics, the second supplemented with tetracyclin 200 µg/mL, and the third supplemented with ticarcillin 150 µg/mL.

## 2.2 Gene Overexpression using the *araBAD* Promoter

To study the impact of *cmrA* overexpression on the phenotype of *P. aeruginosa*, a wild-type copy of the gene was amplified by PCR using primers pJN-cmrA Fw and pJN-cmrA Rv (Table 14). The amplicon was cloned into vector pCR-Blunt, and then subcloned as an EcoRI fragment into the arabinose-inducible expression vector pJN105 (Newman and Fuqua, 1999). The recombinant plasmid was introduced by electroporation into strain PA14 and selected on gentamicin 10 µg/mL, yielding PA14(pJN105::*cmrA*<sub>PA14</sub>). A positive control with the mutated allele from PJ01 [PA14 (pJN105::*cmrA*<sub>PJ01</sub>)] and a negative control harboring pJN105 alone [PA14 (pJN105)] were generated in parallel.

Gene PA2048 was cloned as well in pJN105 under the same conditions (see above) after amplification with primers pJN-PA2048 Fw and pJN-PA2048 Rv (Table 14). It was then electrotransferred into PA14 to yield PA14(pJN105::PA2048). The transformants were finally analyzed for their resistance phenotype (MICs of ciprofloxacin, chloramphenicol, trimethoprim) and relative expression (by RT-qPCR) of genes *cmrA*, PA2048 and *mexE*, in the absence and in the presence of inducer arabinose (0.5%).

## 2.3 Luminescent Reporter of the CmrA-pathway

To evaluate the activation of the CmrA-pathway under various challenging conditions, a transcriptional fusion between gene PA2048 and operon *luxCDABE* was constructed (Figure 23). For this, the 1,822 bp genomic fragment of strain PA14 carrying genes *cmrA* and PA2048 was amplified by using primers *cmrA*-PA2048 Fw and *cmrA*-PA2048 Rv (Table 14). The amplicon was cloned into vector pCR-Blunt and then sub-cloned as an EcoRI fragment into plasmid miniCTX-*lux* (Becher and Schweizer, 2000). The new construct was introduced into strain PA14 by conjugation with subsequent selection of transconjugants on PIA supplemented with 200 µg/mL tetracycline. In parallel, the same recombinant plasmid was transferred into strain PJ01 as a positive control of PA2048::*lux* overexpression, as this mutant constitutively produces an activated form of CmrA.

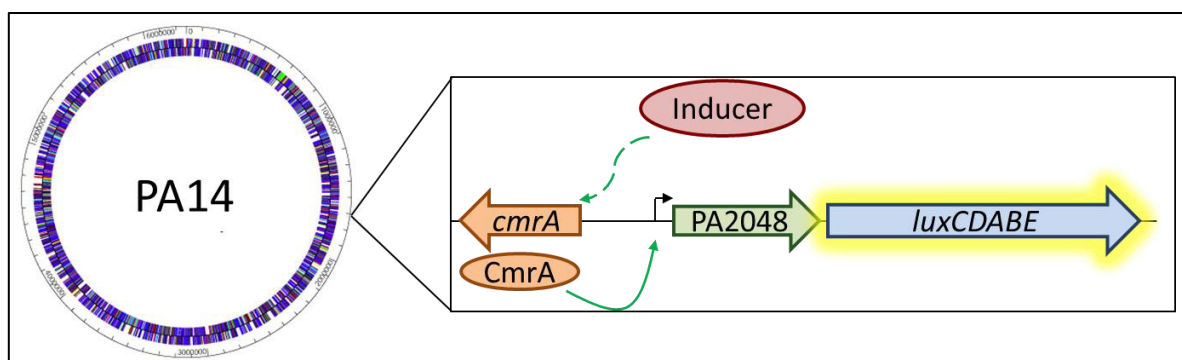


Figure 23: Representation of the luminescent reporter used to evaluate the activation of the CmrA pathway.

## 2.4 Bioluminescence Induction Assays

Induction of PA2048-*lux* expression was measured in real-time during the exponential growth phase. Briefly, overnight cultures of luminescent strains were diluted into fresh cMHB to yield an absorbance of  $A_{600} = 0.01$ . Bacteria were incubated with shaking (250 rpm) at 37°C for 4 h ( $A_{600} = 0.1$ ) prior to the addition of the following stressors at indicated concentrations: ciprofloxacin (0.01  $\mu\text{g}/\text{mL}$ ), chloramphenicol (20  $\mu\text{g}/\text{mL}$ ), trimethoprim (12  $\mu\text{g}/\text{mL}$ ), diamide (8 mM),  $\text{H}_2\text{O}_2$  (50  $\mu\text{M}$ ), paraquat (25  $\mu\text{M}$ ), dimethyl sulfoxide (0.5 %), S-nitrosoglutathione (0.125  $\mu\text{g}/\text{mL}$ ), 2-n-heptyl-4-hydroxyquinoline-N-oxide (25  $\mu\text{g}/\text{mL}$ ), glyoxal (12, 50, 100 and 200  $\mu\text{g}/\text{mL}$ ), methylglyoxal (10, 50 and 100  $\mu\text{g}/\text{mL}$ ), and cinnamaldehyde (70, 140 and 280  $\mu\text{g}/\text{mL}$ ). The activity of the PA2048-*lux* fusion was monitored in white 96-well assay plates (Corning, NY USA) using a Synergy H1 microplate reader (Biotek Instruments, Winooski, USA), with a gain set at 150, a read height set at 7 mm and an integration time of one second. In parallel, the bacterial density was measured at  $A_{600}$  in 96-well microtest plates (Sarstedt, Nümbrecht, Germany). The activity of the reporter, expressed as a bioluminescence (RLU) to bacterial density ( $A_{600}$ ) ratio was measured over a 6 h time course.

## 2.5 mRNAs Quantitation using RT-qPCR

### 2.5.1 RNA Extraction

A 1:100 dilution of an overnight culture was grown at 37°C and 250 rpm until it has reached  $A_{600} = 1.0$  ( $\approx 1 \times 10^8$  UFC/mL). The extraction of total RNA was performed using the *RNeasy Protect Bacteria Mini Kit* (Qiagen) following the supplier's recommendations. Extracted RNAs were treated with the *RNase-free DNase Set* (Qiagen) during 30 min in order to degrade DNA traces and then stocked at -80°C.

### 2.5.2 cDNA Synthesis by RT-PCR

cDNA synthesis was performed using the *Im-Prom-II<sup>TM</sup> RT System* (Promega) and the random primers included in the kit using 2  $\mu\text{g}$  of total RNA and following supplier's

recommendations. A negative control with no enzyme was performed in order to detect DNA contamination. Extracted cDNAs were stocked at -20°C.

### 2.5.3 cDNA Amplification by qPCR

cDNA amplification and relative quantitation of gene expression were performed using the Rotor-Gene Q apparatus (Qiagen). Briefly, 120 ng of cDNA was amplified in a Master Mix (15 µL) containing: 1X *QuantiFast SYBR green PCR Master Mix* (Qiagen) and 1.5 mM of specific primers (**Table 14**). Cycling conditions started with 5 min of denaturation at 95°C and 40 cycles of: denaturation at 95°C for 5 sec, priming at 60°C for 10 sec and amplification at 72°C for 20 sec. Fluorescent information was acquired during the priming stage. Moreover, negative (no cDNA) and positive controls as well as standard samples ( $10^0$ ,  $10^{-1}$  and  $10^{-2}$ ) of the parental strain PA14 were included in each run. Relative quantitation of gene expression was calculated based on the standard curve created with the standard samples.

### 2.5.4 Relative Quantitation of Gene Expression

Gene expression was estimated using the relative standard curve method and using the expression of housekeeping genes *rpsL* encoding the ribosomal S12 protein and *uvrD* coding for DNA helicase II (Dumas et al., 2006). This quantitation method uses the amplification efficacy (E) of the gene of interest ( $E_{interest}$ ) and the standard gene ( $E_{rpsL}$ ) as well as the CT (Cycle Threshold) values of both genes for the sample and the parental or reference strain.

$$Ratio = \frac{(E_{interest})^{\Delta CT_{interest}(reference-sample)}}{(E_{rpsL})^{\Delta CT_{interest}(reference-sample)}} \quad Efficacy(E) = 10^{-1/slope}$$

This ratio was then compared to that obtained from the parental or reference strain. The values of relative gene expression were calculated using two independent experiments.

## 3 DNA Sequencing

Both, Sanger and Ion-Torrent® sequencing were performed by the platform “Séquençage et Analyse de fragments” belonging to the SFR-4234 located in Besançon, France.

### 3.1 Sanger Sequencing

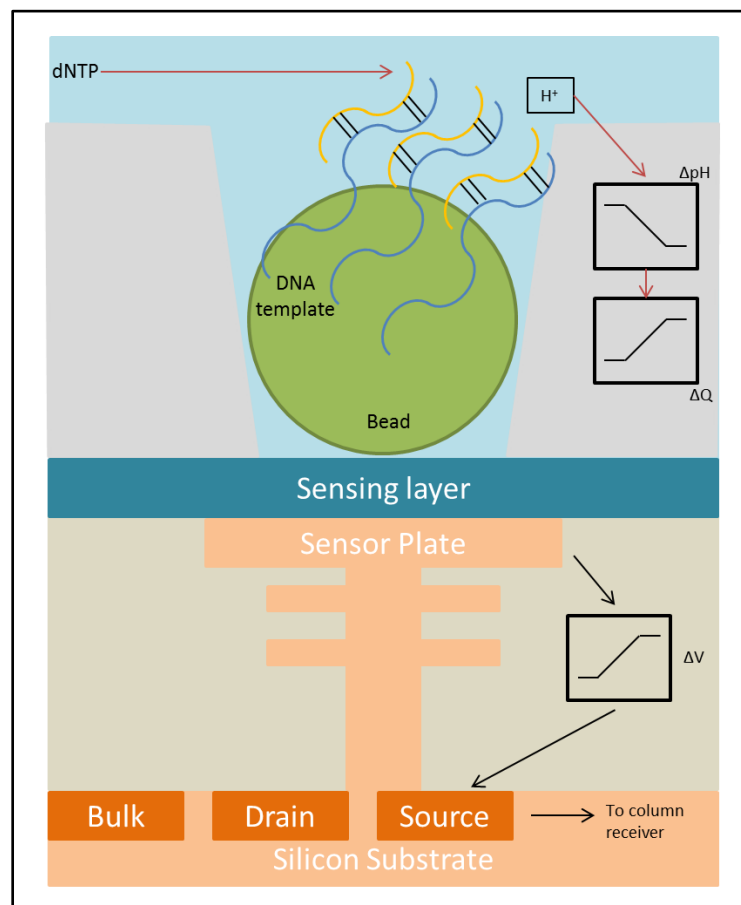
DNA sequencing was performed following the Sanger sequencing method. This technique is based on the selective incorporation of chain-terminating dideoxynucleotides by the DNA polymerase. The fragments were amplified using the automatic sequencer *ABI Prism 3130* (Life Technologies, California, US) and analyzed using *SnapGene* software.



## 3.2 Ion-Torrent® Amplicon Sequencing

### 3.2.1 Overview

The Ion Torrent® Amplicon Sequencing takes part of the Next Generation Sequencing (NGS) technologies. This approach couples a semiconductor chip, capable of directly translating chemical signals into digital information. Each micro-well of the Ion Torrent sequencing chip contains approximately  $10^6$  copies of a DNA molecule previously amplified by emulsion PCR. The machine sequentially floods the chip with one nucleotide after another. If one nucleotide is incorporated into the DNA molecule in a micro-well, one proton ( $H^+$ ) is released. The pH modification is detected in each specific well by the ion sensor (**Figure 24**). If the next nucleotide that floods the chip is not incorporated, no voltage change is recorded, and no base is called. Sequencing of the DNA template is performed in seconds and this enables very short run times.



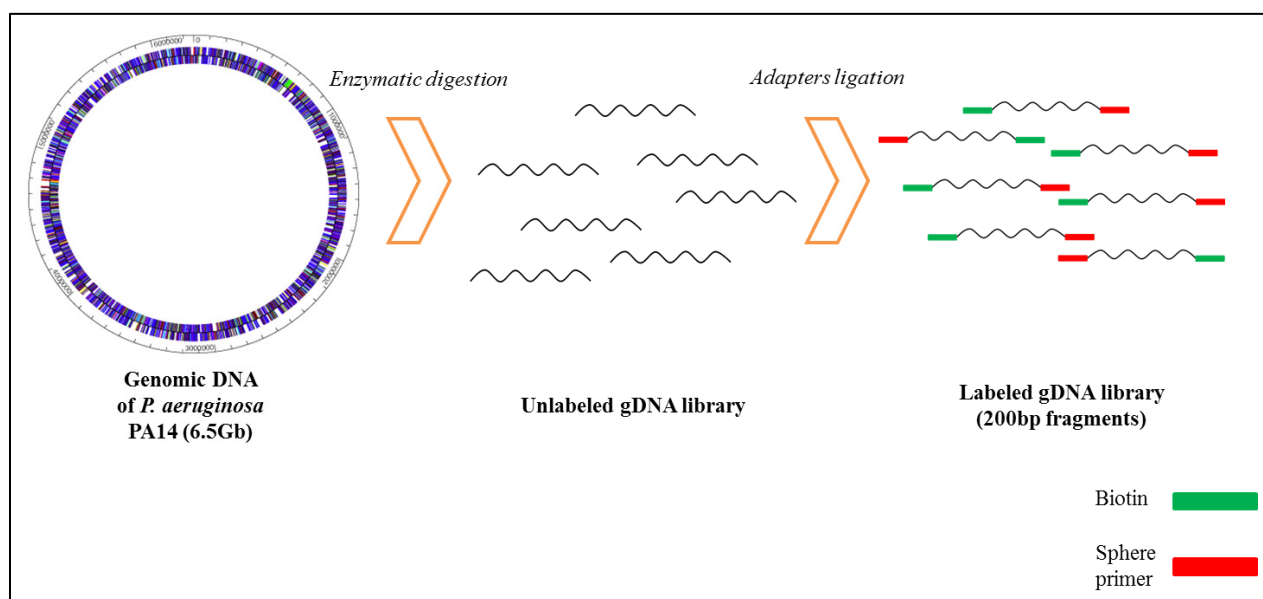
**Figure 24: Schematic representation of a single well of an Ion Torrent sequencing chip.** The well harbors Ion Spheres particles containing DNA template. When a nucleotide incorporates, a proton ( $H^+$ ) is released and the pH of the well changes ( $\Delta pH$ ). A sensing layer detects this change of charges ( $\Delta Q$ ) and translates the chemical signal into a digital signal ( $\Delta V$ ).

### 3.2.2 Extraction of Genomic DNA

Genomic DNA (gDNA) of *P. aeruginosa* strain PA14 and its derived mutants PJ01, PJ03, and PJ04, was extracted using the *PureLink™ DNA Mini Kit* (Invitrogen) following the supplier's recommendations. Mutant PJ02 was not used for whole-genome sequencing because it was derived from the same experiment as PJ01.

### 3.2.3 Preparation of a Genomic DNA Library

The initial stage in the workflow required for the *Ion Torrent® Personal Machine™* (PGM™) is to generate a library of DNA fragments flanked by two adapters. The first step of this library generation is to digest gDNA into small fragments of approximately 200 bp with a restriction cocktail. Next, two adapters are ligated to the DNA fragments (**Figure 25**). The first adapter is a Universal Sphere Primer used to bind a molecule of DNA to an Ion Sphere. The second adapter, biotin, will be used to purify the template. Ion Torrent libraries were prepared from 100 ng of each DNA preparation (Qubit 2.0 Fluorometer, Invitrogen) using a dedicated equipment (E-Gel iBase for purification of 200 bp fragments, and Veriti thermocycler for emulsion PCR, Invitrogen).

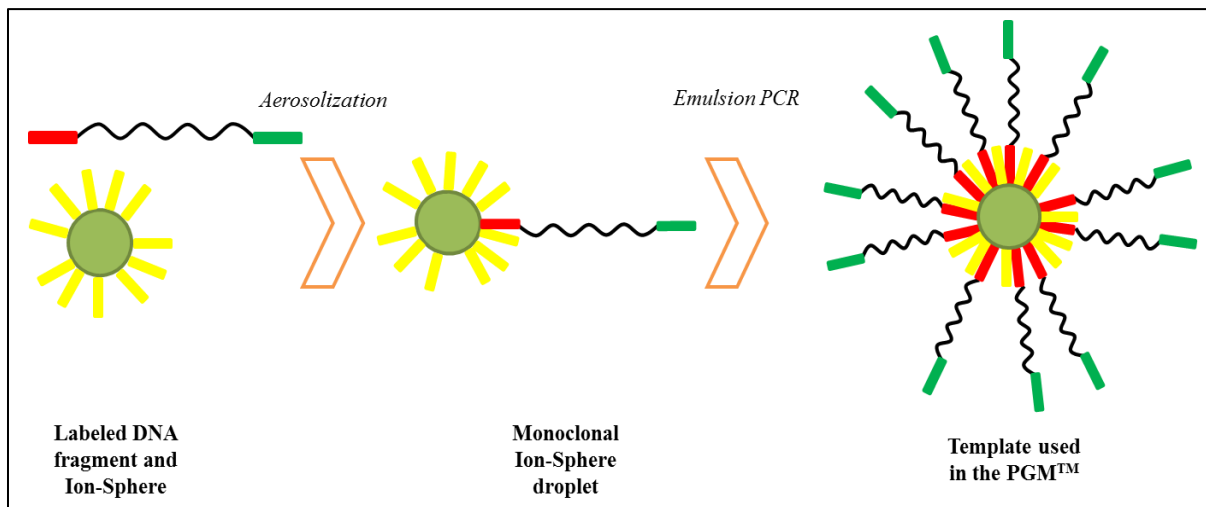


**Figure 25: Preparation of gDNA library.** Genomic DNA is digested and fragments of around 200 bp are used for library generation. Two adapters, sphere primer (red) and biotin (green), are next ligated to each end of DNA fragments. This will allow the fragment to bind to an Ion Sphere and to be purified from the matrix.

### 3.2.4 Template Preparation

Proper library fragments are then clonally amplified by emulsion PCR. Briefly, fragments and empty Ion-Spheres are mixed together in order to create spheres containing one-single copy of a labeled fragment. Monoclonal spheres are then emulsified and aerosolized into droplets. Finally, amplification is performed by emulsion PCR resulting in Ion-Spheres coated with

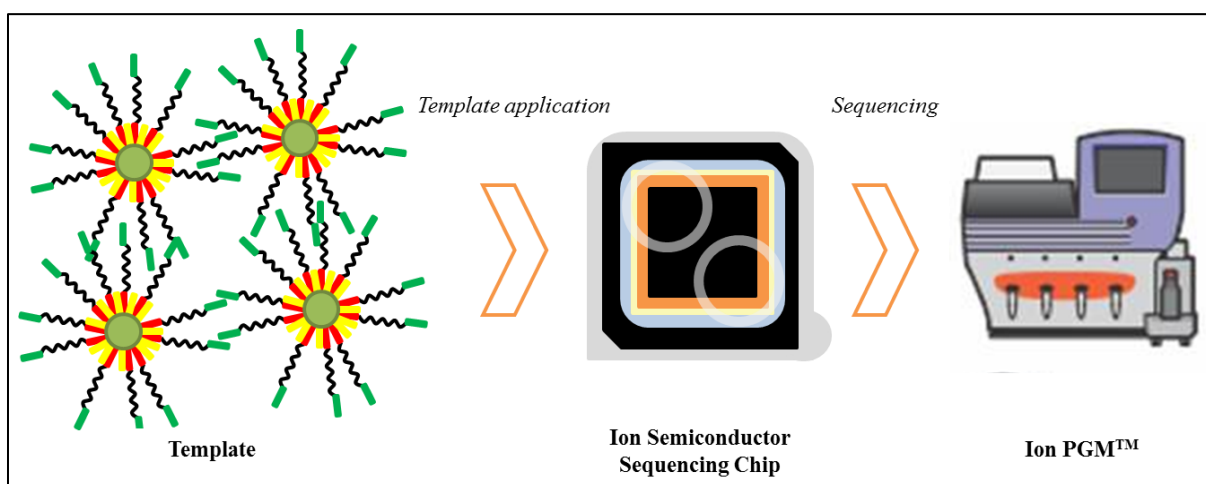
several copies of the DNA template (**Figure 26**). These particles are used as template for the Ion Torrent® sequencing.



**Figure 26: Template preparation.** Library generated fragments are bond to Ion Spheres by complementation of adapters. Each sphere will contain one-single fragment, which will be amplified by emulsion PCR.

### 3.2.5 Sequencing

Ion-Sphere particles coated with DNA template were applied to the Ion chip by pipetting. Next, template was deposited in the wells by a short centrifugation step. Then, the chip was placed into the *Ion PGM™* and dNTPs were sequentially added as explained above (**Figure 27**).



**Figure 27 Ion Torrent® Sequencing.** Amplification of monoclonal spheres by emulsion PCR creates the template for sequencing. The template is applied to an Ion Semiconductor Sequencing Chip by pipetting. The chip is then charged into the sequencing apparatus.

### 3.2.6 Data Analysis

Alignment of the sequence reads (about 200 bp in length) of PJ01, PJ03 and PJ04 with the UCBPP-PA14 genome (NCBI accession number: NC\_008463.1) was performed using Bionumerics version 7.1, and led to the identification of potential sequence variations (SNPs).

A SNP was considered reliable if the coverage was  $\geq 20$ -fold and its percentage was  $\geq 29\%$ . Sequence variations were verified on both strands by capillary sequencing on an Applied Biosystem 3130 GA apparatus (Applied Biosystems, Life Technologies, Courtaboeuf, France) after PCR amplification with proper primers.

#### **4 Identification of the Transcription Start Site using 5'-RACE**

##### **4.1 Overview**

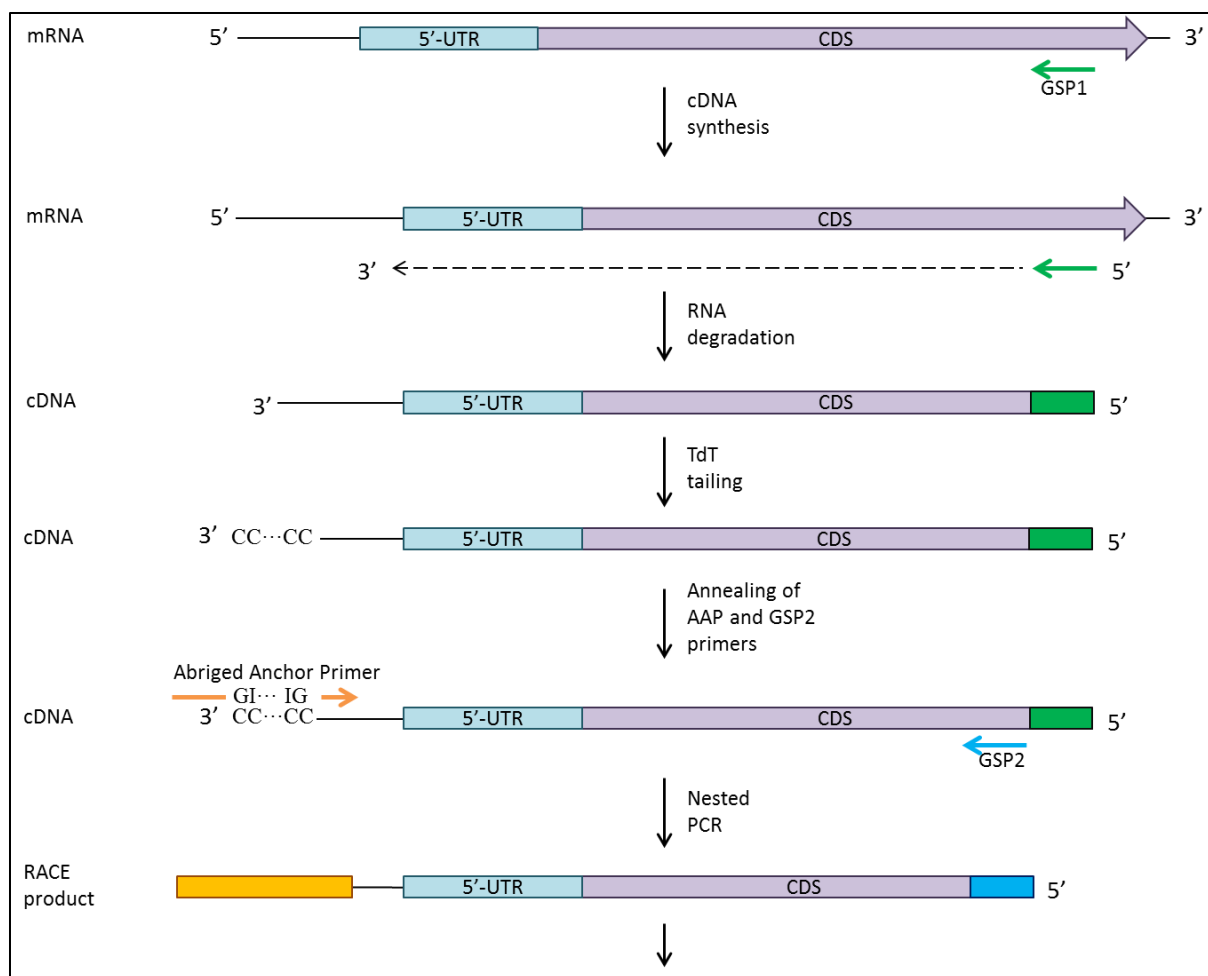
The Rapid Amplification of cDNA Ends (RACE) is a technique for the analysis of the untranslated regions (UTRs) of a messenger RNA (mRNA) at either 5'- or the 3'-end of the template (**Figure 28**). The principle of the technique is the amplification of a UTR using a defined internal site by anchored PCR. This technique requires two gene-specific primers (GSP1 and GSP2) downstream the sequence to be amplified. The 5'-UTR region usually contains a Ribosome Binding Site (RBS) and it may contain regulatory sequences; it is used to establish the Transcription Start Site (TSS) of a gene. The first step of 5'-RACE is the conversion of a specific mRNA into cDNA using reverse transcriptase and a gene-specific antisense oligonucleotide (GSP1) which maximizes the potential for complete extension to the 5'-end of the template. Next step is the purification of the cDNA from the mixture followed by TdT-tailing, which adds homopolymeric tails of cytosine to the 3' ends of the cDNA. The dC-tailed cDNA is then amplified by nested PCR using a second gene-specific primer (GSP2) and an adapter primer (Abridged Adapter Primer, AAP), which permit amplification from the homopolymeric tail. This allows amplification of unknown regions between GSP2 and the 5'-end of the mRNA.

##### **4.1 RNA extraction**

Total RNA used for 5'-RACE experiments was extracted as described above (See section 2.5.1).

##### **4.2 cDNA synthesis using the GSP1 primer**

The synthesis of cDNA was performed using the *SuperScript<sup>TM</sup> II RT* (Invitrogen) using the GSP1 primers listed in **Table 14**. Briefly, 5  $\mu$ g of total RNA were used as template in a reaction mixture containing: 100 nM of GSP1 primer, 20 mM Tris-HCl (pH 8.4), 50 mM KCl, 2.5 mM MgCl<sub>2</sub>, 10 mM DTT, 400  $\mu$ M of dNTPs and 200 U of reverse transcriptase. The reaction was performed at 42°C for 50 min followed by 15 min of termination at 70°C. Remaining RNA was degraded using 1  $\mu$ L of RNase mix (Invitrogen) at 37°C for 30 min. The presence of cDNA was controlled by nested PCR using GSP2 and GSP3 primers.



**Figure 28: Overview of the 5' RACE procedure.** Once total RNA is extracted, a reverse-transcription is performed using a reverse Gene Specific Primer (GSP1). The newly synthesised cDNA is depleted from RNA using a RNase cocktail. Purified cDNA is next tailed with cytosines on the 3'-terminus using a terminal deoxynucleotidyl transferase (TdT). Tailed-cDNA is then amplified by nested PCR using a second reverse Gene Specific Primer (GSP2) and the adapter primer (Abridged Anchor Primer) allowing amplification from the dC-homopolymeric tail. The RACE product can be next cloned in different vectors for sequencing experiments and identification of the Transcription Start Site (TSS).

### 4.3 S.N.A.P. Column Purification of cDNA

S.N.A.P. column purification of cDNA was performed following the supplier's recommendations (Invitrogen). Purified cDNA was eluted using 30  $\mu$ L of preheated sterilized distilled water.

### 4.4 TdT Tailing of cDNA

Terminal deoxynucleotidyl transferase (TdT) generates a homopolymeric dC-tail, which creates the Abridged Anchor Primer (AAP) binding site on the 3'-end of the cDNA. An efficient tailing provides both: (i) homopolymeric tails long enough to allow the primer to anneal and (ii) sufficient dC-tailed cDNA to assure the correct amplification of the RACE product. Briefly, 10  $\mu$ L of purified cDNA were added to a reaction mixture containing: 10 mM Tris-HCl (pH 8.4), 25 mM KCl, 1.5 mM MgCl<sub>2</sub>, 200  $\mu$ M dCTP and 1 U of TdT. The reaction was performed at 37°C for 10 min. TdT was inactivated at 65°C for 10 min.

#### 4.5 Nested PCR, cloning and sequencing of the RACE product

The dC-tailed cDNA product was amplified by PCR using GSP2 and AAP primers (Table 14) as described above (see section 2.2). The RACE product was then cloned into the pCR2.1-TOPO vector following the supplier's recommendations (Invitrogen). Further sequencing of the resulting vector with M13 primers was performed to identify the 5'-UTR region.

### 5 Transcriptomic Analysis using RNA sequencing

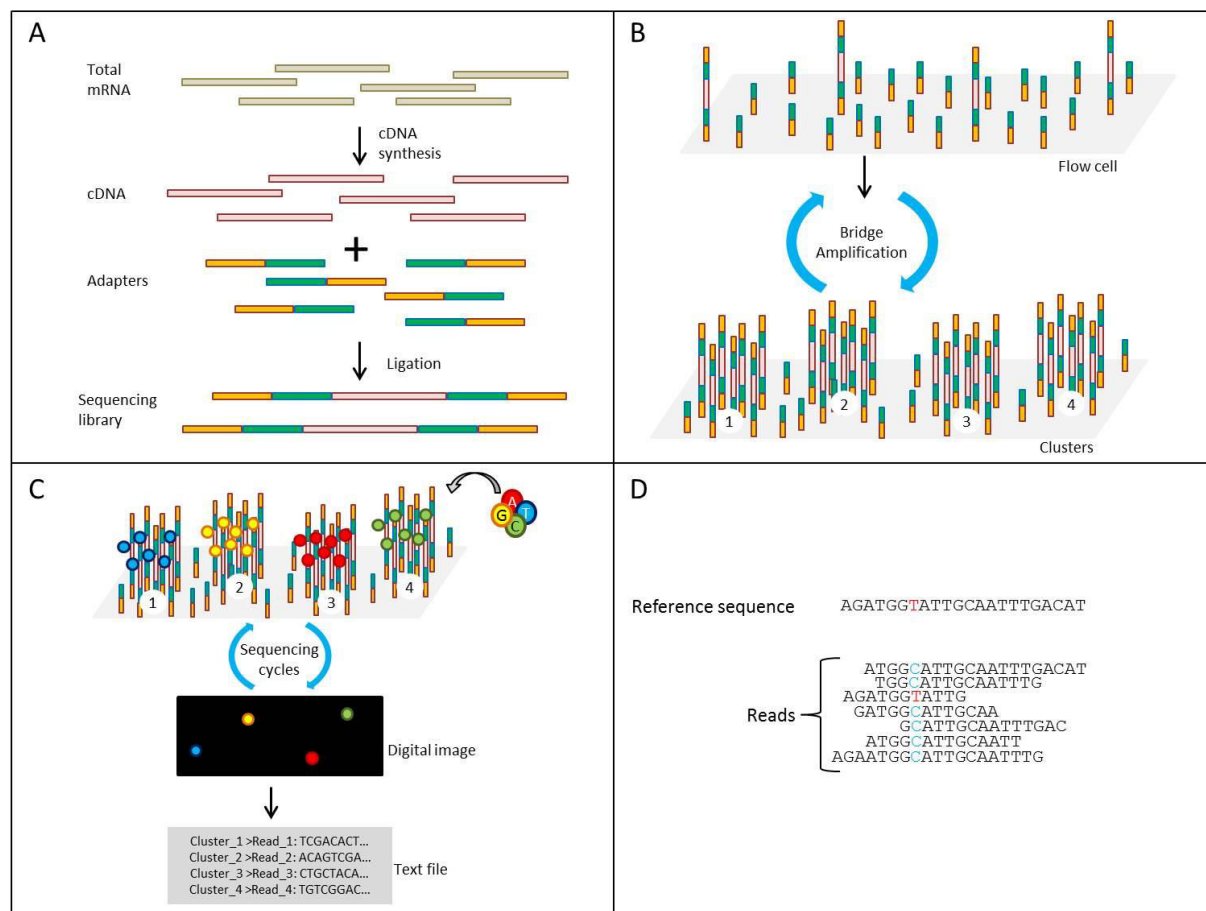
#### 5.1 Overview

The Illumina, as the Ion Torrent technology, is another technique of NGS sequencing. It can be used to perform transcriptomic analysis also known as RNA sequencing (RNAseq). RNAseq provides a comprehensive view of a cellular transcriptional profile at a given biological moment. This method uses total RNA, depleted from ribosomal RNA (rRNA), as template. The RNA is converted into cDNA by reverse transcription before the standard NGS library preparation (Figure 29). This technique uses the Sequencing By Synthesis (SBS) technology, which takes four fluorescently-labeled nucleotides to sequence the DNA clusters generated in the flow cell surface. During each sequencing cycle, a single labeled dNTP is added to the nucleic acid chain. The nucleotide label serves as a terminator for polymerization, at this moment the fluorescent dye is imaged to identify the base, which is then enzymatically cleaved to allow the incorporation of the next nucleotide. The final result is a great collection of images corresponding to nucleotide incorporation; this data is then transformed into sequence data to be analyzed.

#### 5.1 Preparation of the cDNA library and sequencing

Total RNA extracts were obtained in triplicate from exponential cultures ( $A_{600\text{nm}} = 1$ ) of strains PA14, PJ01 and PJ01 $\Delta$ *mexT* at 37°C. Bacterial cells were collected by centrifugation in *RNA protect bacteria reagent* (Qiagen) and disrupted with 0.15-0.60 mm ceramic beads in a *TissueLyzer II* (Qiagen) according to the manufacturer's instructions. Total RNA was then purified from beaded samples with *RNeasyPlus 96 kit* (Qiagen). Concentration and purity of the RNA extracts were assessed by *RiboGreen* measurement (Quant-iT RiboGreen RNA reagent and kit, Invitrogen) and an Agilent 2100 Bioanalyzer system (Agilent Technologies), respectively. Depletion of rRNA from those RNA samples was performed with the *Ribo-Zero rRNA Removal* reagents (Bacteria) from Epicentre (Madison, Wisconsin, USA). Libraries were then constructed using *TruSeq Stranded mRNA HT Sample Prep* kit from Illumina (San Diego, California, USA). The final libraries were quantified with *Picogreen fluorescent dye*

(Quant-iT PicoGreen dsDNA assay kit, Invitrogen) and yielded between 200 and 800 ng per sample. Moreover, qualitative analysis was done using High Sensitivity DNA assay (Agilent).



**Figure 29: Overview of Illumina sequencing for RNAseq experiments.** Total RNA is extracted from bacterial cell using a classical extraction protocol, which is followed by depletion from ribosomal RNA and other non-coding RNAs. Depleted mRNAs are next retro-transcribed to create a cDNA library which is tagged using sequencing adapters to create the sequencing library (A). The sequencing library is then attached to the flow cell by complementation with the surface-specific adapter where single fragments are next amplified to generate monoclonal clusters (B). Illumina sequencing uses a reversible terminator-based method allowing the detection of a single base as they are incorporated into DNA template strands; sequential addition of fluorescently-labeled nucleotides allow the detection of nucleotide incorporation in real time (C). Finally, once reads are obtained, data are analyzed using a reference sequence, in our case the genome of strain PA14 (D).

## 5.2 Cluster Generation

For cluster generation, the library was loaded into a flow cell where fragments are captured on a lawn of surface-bound oligos complementary to the library adapters. Each fragment was next amplified into distinct, clonal clusters through bridge amplification using adapter-primers.

## 5.3 Sequencing

The Illumina sequence technology uses a reversible terminator-based method that detects single bases as they are incorporated into DNA template strands. This technology takes four fluorescently-labeled nucleotides to sequence the tens of millions of clusters on the flow cell surface in parallel. During each sequencing cycle, a single labeled dNTP is added to the DNA

chain. The nucleotide label serves as a terminator for polymerization. So, after each dNTP incorporation, the fluorescent dye is imaged to identify the base and then it is enzymatically cleaved to allow a new incorporation. Sequencing for RNAseq experiments was performed using the Illumina NextSeq 500 platform by Microsynth (Balgach, Switzerland).

#### 5.4 Data Analysis

Data analysis of RNAseq was performed by Genostar (Grenoble, France). Reads were mapped on 5,892 annotated coding sequences (CDS) of strain PA14 using CLC Genomic Workbench 7.5 software. Transcripts abundance and differential expression results between the three replicates of each sample (PA14/PJ01, PA14/PJ01 $\Delta$ *mexT* and PJ01/PJ01 $\Delta$ *mexT*) were determined with Cufflinks and Cuffdiff algorithms (Wang et al., 2012). A difference in gene expression was considered significant when the q-value was  $\leq 0.05$  and when the expression ratio was  $\leq 0.3$ - and  $\geq 3.0$ -fold. The transcriptomic data have been deposited in NCBI's Gene Expression Omnibus (Edgar et al., 2002) and are accessible through the GEO Series accession number GSE86211.

## 6 Protein-protein Interaction using Bacterial Two-Hybrid System

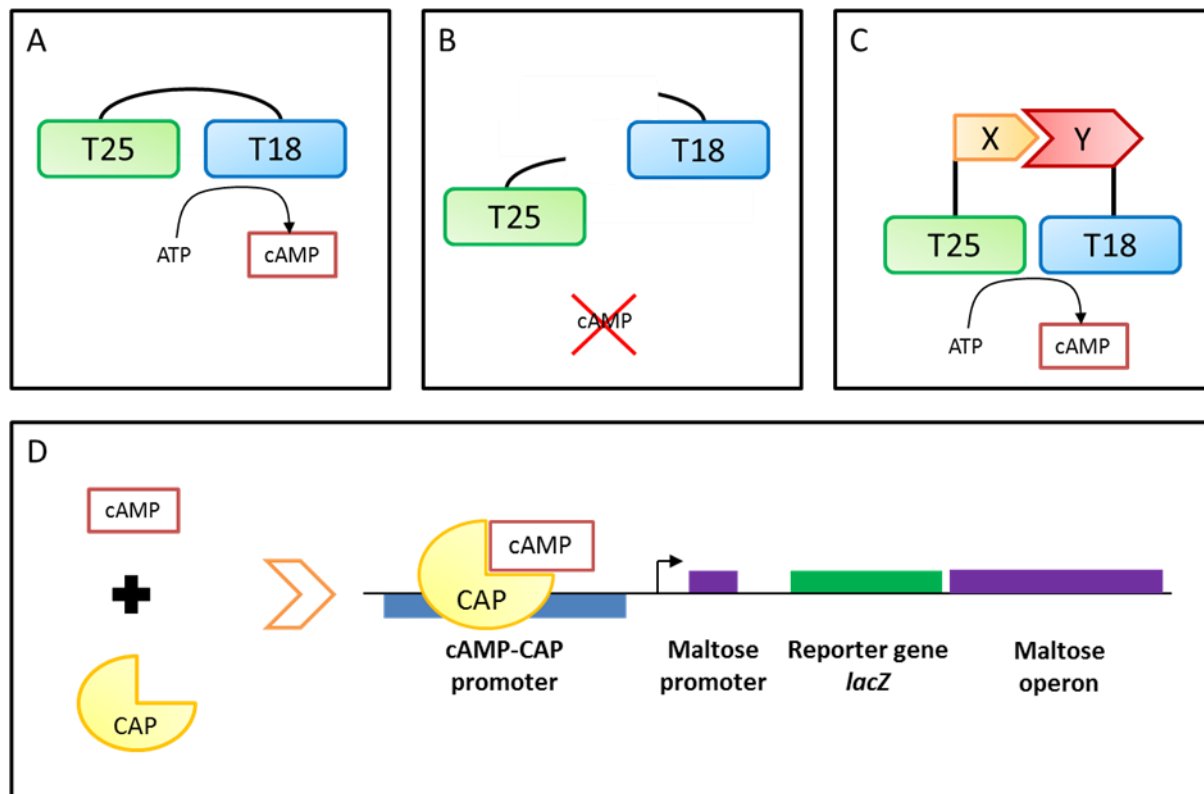
### 6.1 Overview

The Bacterial Adenylate Cyclase Two Hybrid (BACTH) system is based on the reconstitution of a regulatory cascade depending on the secondary messenger cAMP, a molecule naturally produced by the family of adenylate cyclases (AC). The BACTH system uses the AC domain (CyaA) from *Bordetella pertussis*, the etiological agent of whooping cough. This domain, which catalyzes the conversion of ATP into cAMP, can be divided in two sub-units: a 25 kDa fragment called T25 and an 18 kDa called T18 (**Figure 30**). The two subunits of this enzyme are not active when they are physically separated, thus no cAMP is produced. This feature becomes practical in a *cya*<sup>-</sup> strain (no AC production). Under this context, two proteins of interest, X and Y, are fused with the two subunits T25 and T18 of the AC from *B. pertussis*. If X interacts with Y, the dimerization of chimeric proteins brings together both sub-units, restoring the AC activity and thus producing cAMP. On the other hand, if X does not interact with Y, there is no cAMP production.

Newly synthesized cAMP interacts with the Catabolite Activator Protein (CAP). The complex cAMP/CAP binds to specific promoters, regulating the expression of several genes, such as the maltose operon which is activated by this complex (**Figure 30**). The activation of the maltose operon can be detected by measuring the activity of the reporter gene *lacZ* ( $\beta$ -



Galactosidase assay) or even more simple by culturing the strains on reporter plates (McConkey Maltose 1% or MHA X-Gal) (Battesti and Bouveret, 2012).



**Figure 30: Rational of the BACTH technique based on T25 and T18 domains and the reconstitution of adenylate cyclase activity.** cAMP is produced when both sub-units of the adenylate cyclase are bind together (A). When both subunits are physically separated, no cAMP is produced (B). The T25 and T18 subunits can be brought back together by the interaction of the proteins X and Y restoring the production of cAMP (C). When using *cya* strains, the production of cAMP by the hybrid proteins induces the expression of the maltose operon, which is dependent of the cAMP/CAP complex (D). The activity of the maltose operon can be detected by measuring the activity of gene *lacZ* or even more simple by plating the clones on reporter plates (McConkey Maltose 1% or MH IPTG/X-Gal).

### 6.1 Cloning of gene *mexT*

Dimerization of MexT protein of *P. aeruginosa* strains was studied using the BACTH system. The entire coding sequence of gene *mexT* was amplified (see primers in Table 14) and blunt-cloned into BACTH plasmids, pKNT25 and pUT18, previously digested with SmaI. Recombinant plasmids, producing the hybrids MexT-T25 and MexT-T18 were then transferred into DHM1 (*cya*<sup>-</sup>) competent cells by heat-shock transformation as described above (see section 5.2.4.1).

### 6.1 Cloning of gene *cmrA*

Putative dimerization of CmrA protein of *P. aeruginosa* strains was also studied. CmrA belongs to the AraC family of transcriptional regulators and is composed of 310 residues; it is predicted to possess two functional domains, a Ligand Binding Domain (LBD) (40 – 191 residues) and a DNA Binding Domain (DBD) (198 – 310 residues). For this approach, the

whole gene was amplified by PCR using specific primers (**Table 14**) and cloned into the cloning vector pCR-Blunt. The region containing gene *cmrA* was then subcloned into the BACTH plasmids, pKT25 and pUT18C, as a BamHI-XbaI fragment. Recombinant plasmids were inserted into DHM1 cells as described above.

### 6.2 Hybrid Expression and Interaction Assay

For hybrid expression, strains containing both BACTH recombinant plasmids are cultured for 48 h at 30°C in selective cMHA plates containing kanamycin 50 µg/mL (for plasmids pKT25 and pKNT25) and ampicillin 100 µg/mL (for plasmids pUT18 and pUT18c). Colonies are grown overnight at 30°C with shaking (225 rpm) in selective cMHB. The next day, bacterial solutions are prepared to an  $A_{600}=1$  ( $10^9$  CFU/mL) and 5 µL of each culture are dropped on MHTH and MCTH (see section 5.1.1). Plates are cultured at 30°C for 24 h. Blue colonies on MHTH or red colonies on MCTH indicate AMPc production consecutive to interaction between the two proteins.

### 6.3 β-Galactosidase Assay in 96-well Arrays

The β-Galactosidase assay was performed using the same liquid cultures used for the Interaction Assay. Briefly, 50 µL of culture were transferred into a flat-bottom microtiter plate containing 150 µL of cMHB in order to measure the  $A_{600}$ . In parallel, 200 µL of each culture were transferred into a glass tube containing 800 µL of Z buffer (NaH<sub>2</sub>PO<sub>4</sub> 22 mM, Na<sub>2</sub>HPO<sub>4</sub> 22 mM pH 7, KCl 5 mM, MgSO<sub>4</sub> 0.5 mM and β-Mercaptoethanol 0.3%). Cells were lysed by adding 50 µL of SDS 0.01 % and 100 µL of chloroform were used to separate the lipids from the aqueous solution. 50 µL of lysed cells were then transferred into a 96-well flat-bottom microplate containing 150 µL of Z buffer stabilized at 28°C. Then, 40 µL of ONPG 0.4% were dispensed and the enzymatic reaction is carried out at 28°C for 20 min. The measures of  $A_{420}$ , performed every 2 min, were carried out using the Synergy H1 microplate reader (BioTek. Colmar, France) and data was collected using the Gen5 Software v2.04.11. The relative β-Galactosidase activity was calculated using the formula above, where 200 is the dissociation factor of ONPG under these experimental conditions (Battesti and Bouveret, 2012).

$$\beta - \text{Galactosidase activity} = \frac{(A_{420} T2 - A_{420} T1)/(T2 - T1)}{A_{600}} * \text{Dilution} * 200$$

## 7 Analysis of Metabolites by HPTLC

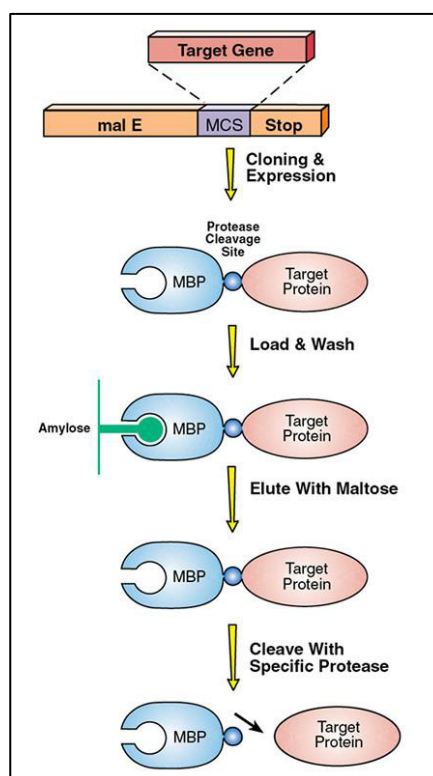
Metabolites produced by *P. aeruginosa* strains, PA14, PA14 $\Delta$ *mexS* and PJ01 were observed by High Performance Thin Layer Chromatography (HPTLC). Briefly, bacteria were grown overnight in 50 mL of cMHB at 37°C and 250 rpm. Bacteria were then pelleted and supernatants were filtered in tandem using two filters of 0.4  $\mu$ m and 0.2  $\mu$ m pore diameter. Organic extraction was performed in 5 times using 1 mL of chloroform (for a total of 5 mL). Organic fractions were pooled and dried overnight in a chemical hood and were suspended in 100  $\mu$ L of chloroform. Ten microliters of each sample were then deposited on a HPTLC silica gel 60 F<sub>254</sub> (Merck) and separation was performed using a mobile phase methanol-dichloromethane (10:90) for 30 – 35 min. Spots were first observed using UV-light (250 nm) and then a second revelation using vanillin 1% in H<sub>2</sub>SO<sub>4</sub> was performed by spraying and heating for 15 min at 100°C.

## 8 MBP Protein Fusion and Purification

### 8.1 Overview

The maltose-binding protein (MBP) vectors allow the production and purification of a protein encoded by a cloned gene by fusing it to MBP (encoded by *malE*). This method uses the strong, inducible *tac* promoter and the *malE* translation initiation signal to give high-level production of the recombinant protein. Then, isolation of the fusion protein is achieved by affinity purification for MBP with amylose resin.

First, the gene of interest is cloned in-frame with gene *malE* into one of the MBP vectors, pMALc5x for cytoplasmic proteins or pMALp5x for periplasmic proteins. Both MBP vectors contain a small sequence encoding the recognition site of the specific protease factor Xa, consisting of four amino acids. This protease site allows the target protein to be cleaved from the MBP-Xa protein and to be purified for further analysis (**Figure 31**).



**Figure 31** : Workflow of MBP-protein production and purification.

## 8.2 Cloning and Production of MBP-tagged proteins

Recombinant proteins MexS, CmrA and PA2048 tagged with the Mannose Binding Protein (MBP) were produced for further investigation. Briefly, coding sequences of genes *mexS*, *cmrA* and PA2048 were amplified using by PCR using specific primers (**Table 14**). Amplicons were cloned into the production plasmid pMALc5X as BamHI-NdeI fragments. Recombinant plasmids were transferred into ER2523 competent cells by heat-shock transformation as described above (see section 2.4.1).

For protein production, bacteria were grown to mid-log phase ( $A_{600} = 0.8$ ) in 10 mL of cMHB supplemented with ampicillin at 100  $\mu\text{g/mL}$  at 37°C and 250 rpm. Bacteria culture was split in two sub-cultures adjusted to 10mL to evaluate protein production in inducing conditions (isopropyl-1-thio- $\beta$ -D-galactoside, IPTG 0.3 mM) and non-inducing conditions. Subcultures were grown for three additional hours.

Protein production was checked by standard SDS-PAGE. Briefly, 500  $\mu\text{L}$  of bacteria culture under inducing and non-inducing conditions were pelleted and suspended in 100  $\mu\text{L}$  of Laemmli buffer (65.8 mM Tris HCl pH 6.8, 26.3% glycerol, 2.1% SDS, 0.01% bromophenol blue, and 1%  $\beta$ -mercaptoethanol). Five microliters of each sample was then loaded in a 4 – 20% polyacrylamide Mini-PROTEAN® TGX™ Precast Gel (BioRad) using the *Precision Plus Protein™ Standard Dual Color* (BioRad) as molecular weight marker. Running conditions for SDS-PAGE were 200 V for 35 min in a Mini-PROTEAN® Tetra Cell (BioRad) using TGS buffer (25 mM Tris, 192 mM glycine, and 0.1% SDS pH 8.3). Gels were dyed using Bio-Safe™ Coomassie G-250 stain as recommended by the supplier (BioRad).

The further steps, affinity chromatography and cleavage of the MBP-tag, will be performed by the team of Pr. Isabelle BROUTIN from Université Paris Descartes (UMR CNRS 8015 Cristallographie et RMN biologiques – Equipe « Signalisation et transport membranaire).



## **VI. Appendix**

---



1 **Constitutive activation of MexT by amino acid substitutions results in**  
2 **MexEF-OprN overproduction in clinical isolates of *Pseudomonas***  
3 ***aeruginosa***

4 Paulo Juarez<sup>a</sup>, Isabelle Broutin<sup>b</sup>, Christophe Bordi<sup>c</sup>, Patrick Plésiat<sup>a,d\*</sup>, Catherine Llanes<sup>a</sup>

5

6

7

8 <sup>a</sup>UMR CNRS 6249 Chrono-Environnement, Laboratoire de Bactériologie, Université de  
9 Bourgogne Franche-Comté, Besançon, France.

10 <sup>b</sup>UMR CNRS 8015, Université Paris Descartes, Sorbonne Paris Cité, Laboratoire de  
11 Cristallographie et RMN Biologiques, Faculté de Pharmacie, Paris, France.

12 <sup>c</sup>LISM, IMM, Aix-Marseille Université and CNRS, Marseille, 13402 France.

13 <sup>d</sup>Centre National de Référence de la Résistance aux Antibiotiques, Centre Hospitalier  
14 Universitaire Jean Minjoz, Besançon, France.

15

16

17 \*Corresponding author

18 Tel: (33) 3 63 08 23 59

19 E-mail: [patrick.plesiat@univ-fcomte.fr](mailto:patrick.plesiat@univ-fcomte.fr)

20

21 Keywords: *Pseudomonas aeruginosa*, antibiotic resistance, MexEF-OprN, MexT

22 Running title: Constitutively active MexT in clinical *P. aeruginosa*



23 **ABSTRACT (50 words)**

24 When overproduced, the multidrug efflux system MexEF-OprN increases resistance of  
25 *Pseudomonas aeruginosa* to fluoroquinolones, chloramphenicol and trimethoprim. In this  
26 work, we demonstrate that gain-of-function mutations in the regulatory gene *mexT* result  
27 in oligomerization of encoded LysR regulator MexT, constitutive upregulation of the efflux  
28 pump and increased resistance in clinical isolates.

29 **TEXT (979 words)**

30 *Pseudomonas aeruginosa*, an opportunistic pathogen of major clinical importance, is  
31 responsible for acute and chronic infections in vulnerable patients. Its intrinsic and/or  
32 acquired resistance to a wide range of antibiotics in part relies on constitutive or inducible  
33 production of several efflux systems belonging to the resistance-nodulation-cell division  
34 (RND) family of drug transporters (1). Amongst these systems, MexEF-OprN is able to  
35 export a rather short list of antimicrobials including ciprofloxacin (CIP), chloramphenicol  
36 (CHL), and trimethoprim (TMP). This efflux pump, which is quiescent in wild-type strains,  
37 is overproduced at high levels in *nfxC* mutants, making them more resistant (from 2- to  
38 32-fold) to the pump substrates (2). MexEF-OprN production is regulated by MexT, a  
39 LysR-type transcriptional regulator (LTTR), whose gene (*mexT*) is located upstream of  
40 operon *mexEF-oprN* (3). All mutations that have been identified so far in clinical strains  
41 overproducing MexEF-OprN affect a gene, *mexS*, encoding a presumed quinone  
42 oxidoreductase, MexS (4-6). The present study reports on characterization of five non-  
43 clonal clinical mutants harboring a wild-type *mexS* gene (5-7). DNA sequencing  
44 experiments revealed that these strains contained missense mutations in *mexT*. Since the  
45 impact of these mutations on protein function was unknown, we sought to determine  
46 whether amino acid substitutions in regulator MexT can account for upregulation of  
47 *mexEF-oprN* operon and drug resistance.

48 Relative expression of gene *mexE*, as determined by RT-qPCR (6), was found to be higher  
49 (from 20- to 112-fold) in these bacteria than in wild-type reference strain PA14 (**Table I**).  
50 In addition, Minimal Inhibitory Concentrations (MIC) experiments (8) confirmed that all  
51 of the isolates were more resistant to CIP (from 0.5 to 8  $\mu\text{g mL}^{-1}$ ), CHL (from 128 to 2,048  
52  $\mu\text{g mL}^{-1}$ ) and TMP (from 512 to >2,048  $\mu\text{g mL}^{-1}$ ) than PA14 (0.125, 64, and 64  $\mu\text{g mL}^{-1}$   
53 respectively) (**Table I**).

54 To investigate the relevance of the observed amino acid changes in MexT, we first deleted  
55 gene *mexT* from PA14 as described elsewhere (6). The mutated alleles from clinical  
56 strains were then transferred by conjugation using MiniCTX1-derived recombinant  
57 plasmids (9), and were inserted into the chromosome of mutant PA14 $\Delta$ *mexT*.  
58 Complementation of this mutant with alleles from strains 4177, 0810, and 1510 had no  
59 impact on *mexE* transcription and MICs values (**Table I**). In contrast, MexT variants from  
60 strains 4088 and 10-12 triggered *mexE* expression 189- and 110-fold above the baseline  
61 level, respectively. As expected, this was associated with an increased resistance of  
62 PA14 $\Delta$ *mexT*<sub>4088</sub> and PA14 $\Delta$ *mexT*<sub>10-12</sub> to CIP (16x, 8x, respectively), CHL (32x, 16x), and  
63 TMP ( $\geq$  32x, 16x) as compared to PA14 $\Delta$ *mexT*<sub>PA14</sub> (**Table I**). These results suggested that  
64 these two latter MexT variants were under a constitutively active conformation, able to  
65 upregulate pump MexEF-OprN. They also pointed to the importance of residue G257 in  
66 MexT activation as both variants harbored a single-amino acid substitution at this  
67 position (G<sub>257</sub>S and G<sub>257</sub>A).

68 It had been previously shown that, under oxidative conditions, MexT forms an active  
69 oligomer while under reducing conditions, it remains as an inactive monomer (10). This  
70 is in accordance with the usual mode of action of LTTRs in which an active tetramer is  
71 formed after a cognate co-inducer has bound to the inactive monomers (11). To  
72 determine whether variants from strains 4088 and 10-12 spontaneously form oligomers

73 (*i.e.*, in absence of ligand), a bacterial two-hybrid (BACTH) assay (12) was performed in  
74 strain DHM1 (*cya*<sup>-</sup>) of *Escherichia coli*, with plasmids pUT18 and pKNT25 that respectively  
75 code for T18 and T25 subunits of CyaA adenylate cyclase. This assay, which has been set  
76 up to study protein-protein interactions (12) is based on reconstitution of the adenylate  
77 cyclase activity and cAMP synthesis in *E. coli*. BACTH experiments confirmed that in the  
78 absence of cognate ligand MexT<sub>PA14</sub> occurs a monomer, as no signal of oligomerization  
79 was observed either by using reporter plates or by measuring β-Gal activity (17 ± 1.66  
80 Miller units) (**Table II**). In contrast, MexT variants from strains 4088 and 10-12 yielded  
81 positive results (**Table II**), suggesting that they can form oligomers.

82 To get an insight into what effects substitutions G<sub>257</sub>S and G<sub>257</sub>A may have on MexT  
83 oligomerization, we mapped these mutations on a three-dimensional dimeric LTTR  
84 model. As the crystal structure of MexT has not been determined yet, we used the dimeric  
85 structure of DntR from *Burkholderia* spp, another LTTR that shares 66% of sequence  
86 similarity with MexT, according to Clustal Ω results (13). In DntR, position 257 is occupied  
87 by a phenylalanine residue within the co-inducer binding domain. Interestingly, Phe-257  
88 residues of DntR monomers face each other at the interphase of the dimer (**Figure 1**),  
89 suggesting that they could play a role in dimer stabilization. Nevertheless, the structural  
90 changes caused by amino acid substitutions at position 257 on MexT oligomerization will  
91 have to be confirmed once the crystal structure of this regulator is available.

92 Gain-of-function mutations in LTTRs had already been reported for *Salmonella enterica*  
93 serovar Typhimurium (14, 15) and *Acinetobacter baylyi* (16). In *S. enterica*, gene *cysB*  
94 encodes a LTTR controlling expression of the cysteine regulon. It was found that  
95 spontaneous mutants harboring substitutions T<sub>149</sub>M and T<sub>149</sub>P in CysB overexpressed  
96 genes *cysK*, *cysP* and operon *cysJIH* in the absence of co-inducer N-acetyl-L-serine (14, 15).

97 In *A. baylyi*, LTTRs CatM and BenM regulate aromatic compounds degradation. The ability  
98 of these regulators to become constitutively active was studied by site-directed  
99 mutagenesis. As a result, substitutions R<sub>156</sub>H in CatM and R<sub>156</sub>H + T<sub>157</sub>S in BenM yielded  
100 mutants that did not require inducers such as benzoate and cis,cis-mucoate to activate the  
101 catabolic pathway (16). The present study is the first one to report on MexT-dependent  
102 mutational activation of efflux pump MexEF-OprN in antibiotic resistant clinical isolates  
103 of *P. aeruginosa*. This observation comes in complement of another study showing that  
104 some multidrug resistant strains of *P. aeruginosa* upregulate the intrinsic  $\beta$ -lactamase  
105 AmpC through a gain-of-function mutation (G<sub>154</sub>R) in related LTTR AmpR (17). Altogether  
106 these data highlight the role that LTTRs may play in the emergence of multidrug  
107 resistance in this highly adaptive pathogen.

108

## 109 **ACKNOWLEDGMENTS**

110 The authors thank Angélique Joriot for her technical assistance in DNA sequencing.

111 **Funding** : This work was supported with grants from the French “Ministère de  
112 l’Enseignement Supérieur et de la Recherche” and from the associations “Vaincre la  
113 Mucoviscidose” and “Grégory Lemarchal”.

114 **Competing interests** : Not declared.

115 **Ethical approval** : Not required.

116

117

## 118 **REFERENCES**

- 119 1. **Li XZ, Plésiat P, Nikaido H.** 2015. The challenge of efflux-mediated antibiotic resistance  
120 in Gram-negative bacteria. *Clin Microbiol Rev* **28**:337-418.
- 121 2. **Köhler T, Michéa-Hamzehpour M, Henze U, Gotoh N, Curty LK, Pechère JC.** 1997.  
122 Characterization of MexE-MexF-OprN, a positively regulated multidrug efflux system of  
123 *Pseudomonas aeruginosa*. *Mol Microbiol* **23**:345-354.
- 124 3. **Köhler T, Epp SF, Curty LK, Pechère JC.** 1999. Characterization of MexT, the regulator  
125 of the MexE-MexF-OprN multidrug efflux system of *Pseudomonas aeruginosa*. *J Bacteriol*  
126 **181**:6300-6305.
- 127 4. **Sobel ML, Neshat S, Poole K.** 2005. Mutations in PA2491 (*mexS*) promote MexT-  
128 dependent mexEF-oprN expression and multidrug resistance in a clinical strain of  
129 *Pseudomonas aeruginosa*. *J Bacteriol* **187**:1246-1253.
- 130 5. **Llanes C, Köhler T, Patry I, Dehecq B, van Delden C, Plésiat P.** 2011. Role of the  
131 MexEF-OprN efflux system in low-level resistance of *Pseudomonas aeruginosa* to  
132 ciprofloxacin. *Antimicrob Agents Chemother* **55**:5676-5684.
- 133 6. **Richardot C, Juarez P, Jeannot K, Patry I, Plésiat P, Llanes C.** 2016. Amino acid  
134 Substitutions account for most MexS alterations in clinical *nfxC* mutants of *Pseudomonas*  
135 *aeruginosa*. *Antimicrob Agents Chemother* **60**:2302-2310.
- 136 7. **Llanes C, Pourcel C, Richardot C, Plésiat P, Fichant G, Cavallo JD, Merens A, GERPA**  
137 **Study Group.** 2013. Diversity of beta-lactam resistance mechanisms in cystic fibrosis  
138 isolates of *Pseudomonas aeruginosa*: a French multicentre study. *J Antimicrob Chemother*  
139 **68**:1763-1771.
- 140 8. **Clinical and Laboratory Standards Institute.** 2015. Methods for dilution antimicrobial  
141 susceptibility tests for bacteria that grow aerobically; approved standard, 10 ed, vol  
142 M07-A10. Wayne PA, USA.
- 143 9. **Hoang TT, Kutchma AJ, Becher A, Schweizer HP.** 2000. Integration-proficient  
144 plasmids for *Pseudomonas aeruginosa*: site-specific integration and use for engineering  
145 of reporter and expression strains. *Plasmid* **43**:59-72.
- 146 10. **Fargier E, Mac Aogain M, Mooij MJ, Woods DF, Morrissey JP, Dobson AD, Adams C,**  
147 **O'Gara F.** 2012. MexT functions as a redox-responsive regulator modulating disulfide  
148 stress resistance in *Pseudomonas aeruginosa*. *J Bacteriol* **194**:3502-3511.
- 149 11. **Maddocks SE, Oyston PC.** 2008. Structure and function of the LysR-type transcriptional  
150 regulator (LTTR) family proteins. *Microbiology* **154**:3609-3623.
- 151 12. **Battesti A, Bouveret E.** 2012. The bacterial two-hybrid system based on adenylate  
152 cyclase reconstitution in *Escherichia coli*. *Methods* **58**:325-334.
- 153 13. **Devesse L, Smirnova I, Lonneborg R, Kapp U, Brzezinski P, Leonard GA, Dian C.**  
154 2011. Crystal structures of DntR inducer binding domains in complex with salicylate  
155 offer insights into the activation of LysR-type transcriptional regulators. *Mol Microbiol*  
156 **81**:354-367.
- 157 14. **Colyer TE, Kredich NM.** 1994. Residue threonine-149 of the *Salmonella typhimurium*  
158 CysB transcription activator: mutations causing constitutive expression of positively  
159 regulated genes of the cysteine regulon. *Mol Microbiol* **13**:797-805.
- 160 15. **Colyer TE, Kredich NM.** 1996. In vitro characterization of constitutive CysB proteins  
161 from *Salmonella typhimurium*. *Mol Microbiol* **21**:247-256.
- 162 16. **Craven SH, Ezezika OC, Haddad S, Hall RA, Momany C, Neidle EL.** 2009. Inducer  
163 responses of BenM, a LysR-type transcriptional regulator from *Acinetobacter baylyi*  
164 ADP1. *Mol Microbiol* **72**:881-894.
- 165 17. **Cabot G, Ocampo-Sosa AA, Tubau F, Macia MD, Rodriguez C, Moya B, Zamorano L,**  
166 **Suarez C, Pena C, Martinez-Martinez L, Oliver A.** 2011. Overexpression of AmpC and  
167 efflux pumps in *Pseudomonas aeruginosa* isolates from bloodstream infections:  
168 prevalence and impact on resistance in a Spanish multicenter study. *Antimicrob Agents*  
169 *Chemother* **55**:1906-1911.

171 **Table I: Effects of amino acid substitutions in regulator MexT**

Strains	MexT substitution (304 aa)	Transcript levels of gene <i>mexE</i> <sup>a</sup>	MICs ( $\mu\text{g mL}^{-1}$ ) <sup>b</sup>			References
			CIP	CHL	TMP	
<i>Clinical strains</i>						
4177	R <sub>166</sub> H	<b>20</b>	0.5	1,024	1,024	(5)
4088	G <sub>257</sub> S	<b>112</b>	1	2,048	>2,048	(5)
10-12	G <sub>257</sub> A	<b>26</b>	2	128	>2,048	(7)
0810	G <sub>258</sub> D	<b>32</b>	8	1,024	1,024	(6)
1510	Y <sub>138</sub> D + G <sub>258</sub> D	<b>21</b>	2	256	512	(6)
<i>Complemented PA14 derivatives</i>						
PA14	WT	1	0.125	64	64	F. Ausubel
PA14 $\Delta$ <i>mexS</i>	WT	<b>192</b>	<b>2</b>	<b>2,048</b>	<b>&gt;2,048</b>	(6)
PA14 $\Delta$ <i>mexT</i>	-	0.4	0.125	32	32	This study
PA14 $\Delta$ <i>mexT</i> <sub>PA14</sub>	WT	2.2	0.125	64	64	This study
PA14 $\Delta$ <i>mexT</i> <sub>4177</sub>	R <sub>166</sub> H	3.2	0.125	64	64	This study
PA14 $\Delta$ <i>mexT</i> <sub>4088</sub>	G <sub>257</sub> S	<b>189</b>	<b>2</b>	<b>2,048</b>	<b>&gt;2,048</b>	This study
PA14 $\Delta$ <i>mexT</i> <sub>10-12</sub>	G <sub>257</sub> A	<b>110</b>	<b>1</b>	<b>1,024</b>	<b>1,024</b>	This study
PA14 $\Delta$ <i>mexT</i> <sub>0810</sub>	G <sub>258</sub> D	1.9	0.125	64	64	This study
PA14 $\Delta$ <i>mexT</i> <sub>1510</sub>	Y <sub>138</sub> D + G <sub>258</sub> D	6.3	0.25	64	64	This study





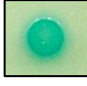



172 <sup>a</sup>: Expressed as a ratio to the *mexE* transcription level in wild-type reference strain PA14.

173 <sup>b</sup>: CIP, ciprofloxacin; CHL, chloramphenicol; TMP, trimethoprim.

174 -: Deleted gene

175 Significant overexpression of gene *mexE* (threshold fixed at 20-fold) and increase in resistance to MexEF-OprN substrates in indicated in bold type.

176 **Table II: MexT oligomerization assayed by bacterial two-hybrid experiments**

Encoded MexT by BACTH plasmids <sup>a</sup>	Amino acid substitution	$\beta$ -Gal Activity <sup>b</sup> (Miller Units)	MH X-Gal <sup>c</sup>	MC Maltose <sup>d</sup>
None	-	15 ( $\pm$ 1.91)		
MexT <sub>PA14</sub>	None	19 ( $\pm$ 1.66)		
MexT <sub>4088</sub>	G <sub>257</sub> S	296 ( $\pm$ 14.31)		
MexT <sub>10-12</sub>	G <sub>257</sub> A	119 ( $\pm$ 5.36)		

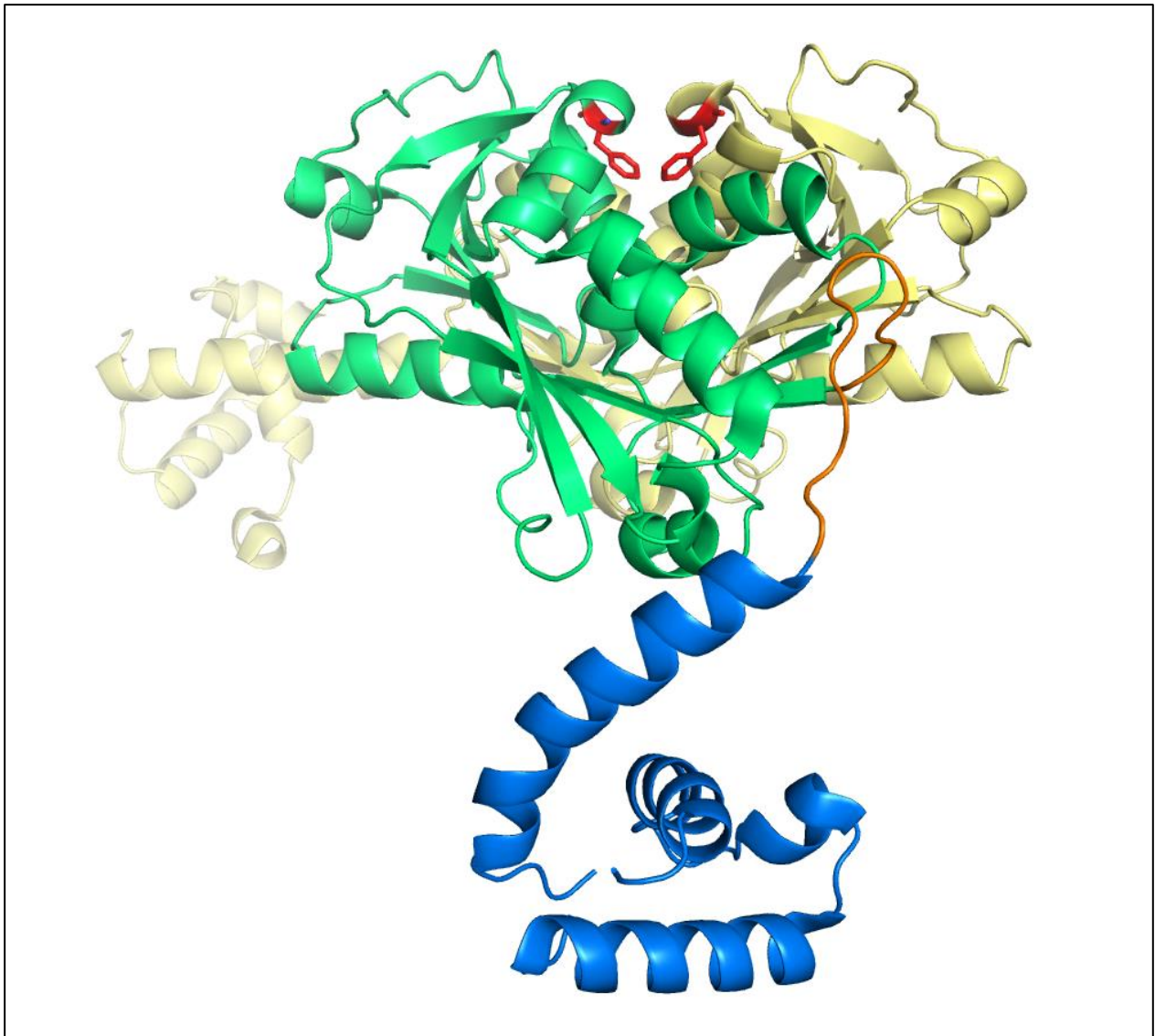
177 <sup>a</sup>: plasmids pUT18 (ampicillin<sup>R</sup>) and pKNT25 (kanamycin<sup>R</sup>) for which the tag is at the C-terminus of the  
 178 recombinant protein were used in this experiment. Full length alleles of *mexT* (915-bp) were cloned using  
 179 primers TH-MexT Fw (CCATGAACCGAAACGACCTGCG) and TH-MexT Rv (AGAGACTGTCCGGATCGCCGA).

180 <sup>b</sup>: Average values were calculated from five independent bacterial cultures each assayed in triplicate.

181 <sup>c</sup>: Muller-Hinton plates containing 40  $\mu$ g mL<sup>-1</sup> X-Gal (revealing cAMP production in blue), 50  $\mu$ g mL<sup>-1</sup> kanamycin  
 182 and 100  $\mu$ g mL<sup>-1</sup> ampicillin.

183 <sup>d</sup>: MacConkey plates containing 1% maltose (revealing cAMP production in red), 50  $\mu$ g mL<sup>-1</sup> kanamycin, and  
 184 100  $\mu$ g mL<sup>-1</sup> ampicillin.

185



186

187 **Figure 1: Crystal structure of DntR dimer.** Crystal structure of DntR dimer from *Burkholderia* spp (PDB 5ae5)  
188 (13). One of the monomers is colored in function of its constituting domains (green for the co-inducer binding  
189 domain, blue for the DNA binding domain, and orange for the loop linking the two domains). The second  
190 monomer is in yellow. Phenylalanine-257 residues of the two monomers are highlighted in red.

191





## **VII. References**

---



1. Abdallah, J., Mihoub, M., Gautier, V., and Richarme, G. (2016). The DJ-1 superfamily members YhbO and YajL from *Escherichia coli* repair proteins from glycation by methylglyoxal and glyoxal. *Biochem. Biophys. Res. Commun.* *470*, 282–286.
2. Adams, M.A., and Jia, Z. (2005). Structural and biochemical evidence for an enzymatic quinone redox cycle in *Escherichia coli*: identification of a novel quinol monooxygenase. *J. Biol. Chem.* *280*, 8358–8363.
3. Aires, J.R., Kohler, T., Nikaido, H., and Plesiat, P. (1999). Involvement of an active efflux system in the natural resistance of *Pseudomonas aeruginosa* to aminoglycosides. *Antimicrob. Agents Chemother.* *43*, 2624–2628.
4. Antus, B., Drozdovszky, O., Barta, I., and Kelemen, K. (2015). Comparison of airway and systemic malondialdehyde levels for assessment of oxidative stress in Cystic Fibrosis. *Lung* *193*, 597–604.
5. Bagge, N., Ciofu, O., Hentzer, M., Campbell, J.I.A., Givskov, M., and Høiby, N. (2002). Constitutive high expression of chromosomal beta-lactamase in *Pseudomonas aeruginosa* caused by a new insertion sequence (IS1669) located in *ampD*. *Antimicrob. Agents Chemother.* *46*, 3406–3411.
6. Balasubramanian, D., Schneper, L., Merighi, M., Smith, R., Narasimhan, G., Lory, S., and Mathee, K. (2012). The regulatory repertoire of *Pseudomonas aeruginosa* AmpC  $\beta$ -lactamase regulator AmpR includes virulence genes. *PLoS One* *7*, e34067.
7. Balcewich, M.D., Reeve, T.M., Orlikow, E.A., Donald, L.J., Vocadlo, D.J., and Mark, B.L. (2010). Crystal structure of the AmpR effector binding domain provides insight into the molecular regulation of inducible AmpC beta-lactamase. *J. Mol. Biol.* *400*, 998–1010.
8. Bartoli, M.L., Novelli, F., Costa, F., Malagrino, L., Melosini, L., Bacci, E., Cianchetti, S., Dente, F.L., Di Franco, A., Vagaggini, B., et al. (2011). Malondialdehyde in exhaled breath condensate as a marker of oxidative stress in different pulmonary diseases. *Mediators Inflamm.* *2011*, 891752.
9. Battesti, A., and Bouveret, E. (2012). The bacterial two-hybrid system based on adenylate cyclase reconstitution in *Escherichia coli*. *Methods San Diego Calif* *58*, 325–334.
10. Becher, A., and Schweizer, H.P. (2000). Integration-proficient *Pseudomonas aeruginosa* vectors for isolation of single-copy chromosomal *lacZ* and *lux* gene fusions. *BioTechniques* *29*, 948–950, 952.
11. Betteridge, D.J. (2000). What is oxidative stress? *Metabolism.* *49*, 3–8.
12. Bild, W., Ciobica, A., Padurariu, M., and Bild, V. (2013). The interdependence of the reactive species of oxygen, nitrogen, and carbon. *J. Physiol. Biochem.* *69*, 147–154.
13. Blehert, D.S., Fox, B.G., and Chambliss, G.H. (1999). Cloning and sequence analysis of two *Pseudomonas* flavoprotein xenobiotic reductases. *J. Bacteriol.* *181*, 6254–6263.
14. Booth, I.R., Ferguson, G.P., Miller, S., Li, C., Gunasekera, B., and Kinghorn, S. (2003). Bacterial production of methylglyoxal: a survival strategy or death by misadventure? *Biochem. Soc. Trans.* *31*, 1406–1408.
15. Breidenstein, E.B.M., Khaira, B.K., Wiegand, I., Overhage, J., and Hancock, R.E.W. (2008). Complex ciprofloxacin resistome revealed by screening a *Pseudomonas aeruginosa* mutant library for altered susceptibility. *Antimicrob. Agents Chemother.* *52*, 4486–4491.
16. Bubonja-Sonje, M., Matovina, M., Skrobbonja, I., Bedenic, B., and Abram, M. (2015). Mechanisms of carbapenem resistance in multidrug-resistant clinical isolates of *Pseudomonas aeruginosa* from a Croatian hospital. *Microb. Drug Resist. Larchmt. N* *21*, 261–269.

17. Bueno, E., Mesa, S., Bedmar, E.J., Richardson, D.J., and Delgado, M.J. (2012). Bacterial adaptation of respiration from oxic to microoxic and anoxic conditions: redox control. *Antioxid. Redox Signal.* *16*, 819–852.
18. Burrows, L.L. (2012). *Pseudomonas aeruginosa* twitching motility: Type IV pili in action. *Annu. Rev. Microbiol.* *66*, 493–520.
19. Campo Esquisabel, A.B., Rodríguez, M.C., Campo-Sosa, A.O., Rodríguez, C., and Martínez-Martínez, L. (2011). Mechanisms of resistance in clinical isolates of *Pseudomonas aeruginosa* less susceptible to cefepime than to ceftazidime. *Clin. Microbiol. Infect. Off. Publ. Eur. Soc. Clin. Microbiol. Infect. Dis.* *17*, 1817–1822.
20. Cao, L., Srikumar, R., and Poole, K. (2004). MexAB-OprM hyperexpression in NalC-type multidrug-resistant *Pseudomonas aeruginosa*: identification and characterization of the *nalC* gene encoding a repressor of PA3720-PA3719. *Mol. Microbiol.* *53*, 1423–1436.
21. Castang, S., and Dove, S.L. (2010). High-order oligomerization is required for the function of the H-NS family member MvaT in *Pseudomonas aeruginosa*. *Mol. Microbiol.* *78*, 916–931.
22. Chen, H., Hu, J., Chen, P.R., Lan, L., Li, Z., Hicks, L.M., Dinner, A.R., and He, C. (2008). The *Pseudomonas aeruginosa* multidrug efflux regulator MexR uses an oxidation-sensing mechanism. *Proc. Natl. Acad. Sci. U. S. A.* *105*, 13586–13591.
23. Chen, H., Yi, C., Zhang, J., Zhang, W., Ge, Z., Yang, C.-G., and He, C. (2010). Structural insight into the oxidation-sensing mechanism of the antibiotic resistance of regulator MexR. *EMBO Rep.* *11*, 685–690.
24. Choi, K.-H., Kumar, A., and Schweizer, H.P. (2006). A 10-min method for preparation of highly electrocompetent *Pseudomonas aeruginosa* cells: application for DNA fragment transfer between chromosomes and plasmid transformation. *J. Microbiol. Methods* *64*, 391–397.
25. Choi, K.-H., Mima, T., Casart, Y., Rholl, D., Kumar, A., Beacham, I.R., and Schweizer, H.P. (2008). Genetic tools for select-agent-compliant manipulation of *Burkholderia pseudomallei*. *Appl. Environ. Microbiol.* *74*, 1064–1075.
26. Chuanchuen, R., Beinlich, K., Hoang, T.T., Becher, A., Karkhoff-Schweizer, R.R., and Schweizer, H.P. (2001). Cross-Resistance between triclosan and antibiotics in *Pseudomonas aeruginosa* is mediated by multidrug efflux pumps: exposure of a susceptible mutant strain to triclosan selects *nfxB* mutants overexpressing MexCD-OprJ. *Antimicrob. Agents Chemother.* *45*, 428–432.
27. Clinical and Laboratory Standards Institute (2015). Methods for dilution antimicrobial susceptibility tests for bacteria that grow aerobically; approved standard (Wayne PA, USA).
28. Colyer, T.E., and Kredich, N.M. (1994). Residue threonine-149 of the *Salmonella typhimurium* CysB transcription activator: mutations causing constitutive expression of positively regulated genes of the cysteine regulon. *Mol. Microbiol.* *13*, 797–805.
29. Colyer, T.E., and Kredich, N.M. (1996). *In vitro* characterization of constitutive CysB proteins from *Salmonella typhimurium*. *Mol. Microbiol.* *21*, 247–256.
30. Craven, S.H., Ezezika, O.C., Haddad, S., Hall, R.A., Momany, C., and Neidle, E.L. (2009). Inducer responses of BenM, a LysR-type transcriptional regulator from *Acinetobacter baylyi* ADP1. *Mol. Microbiol.* *72*, 881–894.
31. da Cunha, L.G., Ferreira, M.F., de Moraes, J.A., Reis, P.A., Castro-Faria-Neto, H.C., Barja-Fidalgo, C., Plotkowski, M.-C., and Saliba, A.M. (2015). ExoU-induced redox imbalance and oxidative stress in airway epithelial cells during *Pseudomonas aeruginosa* pneumosepsis. *Med. Microbiol. Immunol. (Berl.)* *204*, 673–680.
32. Damron, F.H., McKenney, E.S., Barbier, M., Liechti, G.W., Schweizer, H.P., and Goldberg, J.B. (2013). Construction of mobilizable mini-Tn7 vectors for bioluminescent detection of

- gram-negative bacteria and single-copy promoter lux reporter analysis. *Appl. Environ. Microbiol.* *79*, 4149–4153.
33. Devesse, L., Smirnova, I., Lönneborg, R., Kapp, U., Brzezinski, P., Leonard, G.A., and Dian, C. (2011). Crystal structures of DntR inducer binding domains in complex with salicylate offer insights into the activation of LysR-type transcriptional regulators. *Mol. Microbiol.* *81*, 354–367.
  34. Dumas, J.-L., van Delden, C., Perron, K., and Köhler, T. (2006). Analysis of antibiotic resistance gene expression in *Pseudomonas aeruginosa* by quantitative real-time-PCR. *FEMS Microbiol. Lett.* *254*, 217–225.
  35. Edgar, R., Domrachev, M., and Lash, A.E. (2002). Gene Expression Omnibus: NCBI gene expression and hybridization array data repository. *Nucleic Acids Res.* *30*, 207–210.
  36. El’Garch, F., Jeannot, K., Hocquet, D., Llanes-Barakat, C., and Plésiat, P. (2007). Cumulative effects of several nonenzymatic mechanisms on the resistance of *Pseudomonas aeruginosa* to aminoglycosides. *Antimicrob. Agents Chemother.* *51*, 1016–1021.
  37. Elmore, M.J., Lamb, A.J., Ritchie, G.Y., Douglas, R.M., Munro, A., Gajewska, A., and Booth, I.R. (1990). Activation of potassium efflux from *Escherichia coli* by glutathione metabolites. *Mol. Microbiol.* *4*, 405–412.
  38. Essar, D.W., Eberly, L., Hadero, A., and Crawford, I.P. (1990). Identification and characterization of genes for a second anthranilate synthase in *Pseudomonas aeruginosa*: interchangeability of the two anthranilate synthases and evolutionary implications. *J. Bacteriol.* *172*, 884–900.
  39. Evans, K., and Poole, K. (1999). The MexA-MexB-OprM multidrug efflux system of *Pseudomonas aeruginosa* is growth-phase regulated. *FEMS Microbiol. Lett.* *173*, 35–39.
  40. Ezraty, B., Gennaris, A., Barras, F., and Collet, J.-F. (2017). Oxidative stress, protein damage and repair in bacteria. *Nat. Rev. Microbiol.* *15*, 385–396.
  41. Fang, F.C. (2004). Antimicrobial reactive oxygen and nitrogen species: concepts and controversies. *Nat. Rev. Microbiol.* *2*, 820–832.
  42. Fang, F.C., Frawley, E.R., Tapscott, T., and Vázquez-Torres, A. (2016). Bacterial Stress Responses during Host Infection. *Cell Host Microbe* *20*, 133–143.
  43. Fargier, E., Mac Aogáin, M., Mooij, M.J., Woods, D.F., Morrissey, J.P., Dobson, A.D.W., Adams, C., and O’Gara, F. (2012). MexT functions as a redox-responsive regulator modulating disulfide stress resistance in *Pseudomonas aeruginosa*. *J. Bacteriol.* *194*, 3502–3511.
  44. Feliziani, S., Luján, A.M., Moyano, A.J., Sola, C., Bocco, J.L., Montanaro, P., Canigia, L.F., Argaraña, C.E., and Smania, A.M. (2010). Mucoidy, quorum sensing, mismatch repair and antibiotic resistance in *Pseudomonas aeruginosa* from cystic fibrosis chronic airways infections. *PloS One* *5*.
  45. Ferguson, G.P. (1999). Protective mechanisms against toxic electrophiles in *Escherichia coli*. *Trends Microbiol.* *7*, 242–247.
  46. Ferguson, G.P., Munro, A.W., Douglas, R.M., McLaggan, D., and Booth, I.R. (1993). Activation of potassium channels during metabolite detoxification in *Escherichia coli*. *Mol. Microbiol.* *9*, 1297–1303.
  47. Ferguson, G.P., Töttemeyer, S., MacLean, M.J., and Booth, I.R. (1998a). Methylglyoxal production in bacteria: suicide or survival? *Arch. Microbiol.* *170*, 209–218.
  48. Ferguson, G.P., Creighton, R.I., Nikolaev, Y., and Booth, I.R. (1998b). Importance of RpoS and Dps in survival of exposure of both exponential- and stationary-phase *Escherichia coli* cells to the electrophile N-ethylmaleimide. *J. Bacteriol.* *180*, 1030–1036.

49. Ferguson, G.P., Battista, J.R., Lee, A.T., and Booth, I.R. (2000). Protection of the DNA during the exposure of *Escherichia coli* cells to a toxic metabolite: the role of the KefB and KefC potassium channels. *Mol. Microbiol.* 35, 113–122.
50. Fetar, H., Gilmour, C., Klinoski, R., Daigle, D.M., Dean, C.R., and Poole, K. (2011). *mexEF-oprN* multidrug efflux operon of *Pseudomonas aeruginosa*: regulation by the MexT activator in response to nitrosative stress and chloramphenicol. *Antimicrob. Agents Chemother.* 55, 508–514.
51. Fraud, S., and Poole, K. (2011). Oxidative stress induction of the MexXY multidrug efflux genes and promotion of aminoglycoside resistance development in *Pseudomonas aeruginosa*. *Antimicrob. Agents Chemother.* 55, 1068–1074.
52. Fraud, S., Campigotto, A.J., Chen, Z., and Poole, K. (2008). MexCD-OprJ multidrug efflux system of *Pseudomonas aeruginosa*: involvement in chlorhexidine resistance and induction by membrane-damaging agents dependent upon the AlgU stress response sigma factor. *Antimicrob. Agents Chemother.* 52, 4478–4482.
53. Frisk, A., Schurr, J.R., Wang, G., Bertucci, D.C., Marrero, L., Hwang, S.H., Hassett, D.J., and Schurr, M.J. (2004). Transcriptome analysis of *Pseudomonas aeruginosa* after interaction with human airway epithelial cells. *Infect. Immun.* 72, 5433–5438.
54. Fruci, M., and Poole, K. (2016). Bacterial stress responses as determinants of antimicrobial resistance. In *Stress and Environmental Regulation of Gene Expression and Adaptation in Bacteria*, (Frans J. de Bruijn), pp. 115–135.
55. Fukuda, H., Hosaka, M., Iyobe, S., Gotoh, N., Nishino, T., and Hirai, K. (1995). *nfxC*-type quinolone resistance in a clinical isolate of *Pseudomonas aeruginosa*. *Antimicrob. Agents Chemother.* 39, 790–792.
56. Fuller, M.E., McClay, K., Hawari, J., Paquet, L., Malone, T.E., Fox, B.G., and Steffan, R.J. (2009). Transformation of RDX and other energetic compounds by *xenobiotic reductases* XenA and XenB. *Appl. Microbiol. Biotechnol.* 84, 535–544.
57. Ghosh, S., Cremers, C.M., Jakob, U., and Love, N.G. (2011). Chlorinated phenols control the expression of the multidrug resistance efflux pump MexAB-OprM in *Pseudomonas aeruginosa* by interacting with NalC. *Mol. Microbiol.* 79, 1547–1556.
58. Gotoh, N., Tsujimoto, H., Tsuda, M., Okamoto, K., Nomura, A., Wada, T., Nakahashi, M., and Nishino, T. (1998). Characterization of the MexC-MexD-OprJ multidrug efflux system in  $\Delta mexA-mexB-oprM$  mutants of *Pseudomonas aeruginosa*. *Antimicrob. Agents Chemother.* 42, 1938–1943.
59. Green, J., and Paget, M.S. (2004). Bacterial redox sensors. *Nat. Rev. Microbiol.* 2, 954–966.
60. Hall, C.W., Zhang, L., and Mah, T.-F. (2017). PA3225 is a transcriptional repressor of antibiotic resistance mechanisms in *Pseudomonas aeruginosa*. *Antimicrob. Agents Chemother.*
61. Hanahan, D. (1983). Studies on transformation of *Escherichia coli* with plasmids. *J. Mol. Biol.* 166, 557–580.
62. Hayashi, K., Fukushima, A., Hayashi-Nishino, M., and Nishino, K. (2014). Effect of methylglyoxal on multidrug-resistant *Pseudomonas aeruginosa*. *Front. Microbiol.* 5, 180.
63. Heeb, S., Blumer, C., and Haas, D. (2002). Regulatory RNA as mediator in GacA/RsmA-dependent global control of exoproduct formation in *Pseudomonas fluorescens* CHA0. *J. Bacteriol.* 184, 1046–1056.
64. Hellman, L.M., and Fried, M.G. (2007). Electrophoretic Mobility Shift Assay (EMSA) for Detecting Protein-Nucleic Acid Interactions. *Nat. Protoc.* 2, 1849–1861.

65. Henrichfreise, B., Wiegand, I., Pfister, W., and Wiedemann, B. (2007). Resistance mechanisms of multiresistant *Pseudomonas aeruginosa* strains from Germany and correlation with hypermutation. *Antimicrob. Agents Chemother.* *51*, 4062–4070.
66. Herrero, M., de Lorenzo, V., and Timmis, K.N. (1990). Transposon vectors containing non-antibiotic resistance selection markers for cloning and stable chromosomal insertion of foreign genes in gram-negative bacteria. *J. Bacteriol.* *172*, 6557–6567.
67. Hoang, T.T., Karkhoff-Schweizer, R.R., Kutchma, A.J., and Schweizer, H.P. (1998). A broad-host-range Flp-FRT recombination system for site-specific excision of chromosomally-located DNA sequences: application for isolation of unmarked *Pseudomonas aeruginosa* mutants. *Gene* *212*, 77–86.
68. Hoang, T.T., Kutchma, A.J., Becher, A., and Schweizer, H.P. (2000). Integration-proficient plasmids for *Pseudomonas aeruginosa*: site-specific integration and use for engineering of reporter and expression strains. *Plasmid* *43*, 59–72.
69. Hocquet, D., Muller, A., Blanc, K., Plésiat, P., Talon, D., Monnet, D.L., and Bertrand, X. (2008). Relationship between antibiotic use and incidence of MexXY-OprM overproducers among clinical isolates of *Pseudomonas aeruginosa*. *Antimicrob. Agents Chemother.* *52*, 1173–1175.
70. Honek, J.F. (2014). Bacterial glyoxalase I enzymes: structural and biochemical investigations. *Biochem. Soc. Trans.* *42*, 479–484.
71. Hsieh, Y.-W., Alqadah, A., and Chuang, C.-F. (2016). An Optimized Protocol for Electrophoretic Mobility Shift Assay Using Infrared Fluorescent Dye-labeled Oligonucleotides. *J. Vis. Exp. JoVE*.
72. Imlay, J.A. (2003). Pathways of oxidative damage. *Annu. Rev. Microbiol.* *57*, 395–418.
73. Imlay, J.A. (2008). Cellular defenses against superoxide and hydrogen peroxide. *Annu. Rev. Biochem.* *77*, 755–776.
74. Jacobs, A.T., and Marnett, L.J. (2010). Systems analysis of protein modification and cellular responses induced by electrophile stress. *Acc. Chem. Res.* *43*, 673–683.
75. Jalal, S., Ciofu, O., Hoiby, N., Gotoh, N., and Wretling, B. (2000). Molecular mechanisms of fluoroquinolone resistance in *Pseudomonas aeruginosa* isolates from cystic fibrosis patients. *Antimicrob. Agents Chemother.* *44*, 710–712.
76. Jeannot, K., Sobel, M.L., El Garch, F., Poole, K., and Plésiat, P. (2005). Induction of the MexXY efflux pump in *Pseudomonas aeruginosa* is dependent on drug-ribosome interaction. *J. Bacteriol.* *187*, 5341–5346.
77. Jeannot, K., Elsen, S., Köhler, T., Attree, I., van Delden, C., and Plésiat, P. (2008). Resistance and virulence of *Pseudomonas aeruginosa* clinical strains overproducing the MexCD-OprJ efflux pump. *Antimicrob. Agents Chemother.* *52*, 2455–2462.
78. Juan, C., Peña, C., and Oliver, A. (2017). Host and pathogen biomarkers for severe *Pseudomonas aeruginosa* infections. *J. Infect. Dis.* *215*, S44–S51.
79. Juarez, P., Jeannot, K., Plésiat, P., and Llanes, C. (2017). Toxic electrophiles induce expression of the multidrug efflux pump MexEF-OprN in *Pseudomonas aeruginosa* through a novel transcriptional regulator, CmrA. *Antimicrob. Agents Chemother.* *61*.
80. Källberg, M., Wang, H., Wang, S., Peng, J., Wang, Z., Lu, H., and Xu, J. (2012). Template-based protein structure modeling using the RaptorX web server. *Nat. Protoc.* *7*, 1511–1522.
81. Kaniga, K., Delor, I., and Cornelis, G.R. (1991). A wide-host-range suicide vector for improving reverse genetics in gram-negative bacteria: inactivation of the *blaA* gene of *Yersinia enterocolitica*. *Gene* *109*, 137–141.



82. Kazmierczak, B.I., Schniederberend, M., and Jain, R. (2015). Cross-regulation of *Pseudomonas* motility systems: the intimate relationship between flagella, pili and virulence. *Curr. Opin. Microbiol.* 28, 78–82.
83. Kilfoil, P.J., Tipparaju, S.M., Barski, O.A., and Bhatnagar, A. (2013). Regulation of ion channels by pyridine nucleotides. *Circ. Res.* 112, 721–741.
84. King, J.D., Kocíncová, D., Westman, E.L., and Lam, J.S. (2009). Review: Lipopolysaccharide biosynthesis in *Pseudomonas aeruginosa*. *Innate Immun.* 15, 261–312.
85. Klockgether, J., Miethke, N., Kubesch, P., Bohn, Y.-S., Brockhausen, I., Cramer, N., Eberl, L., Greipel, J., Herrmann, C., Herrmann, S. (2013). Intraclonal diversity of the *Pseudomonas aeruginosa* cystic fibrosis airway isolates TBCF10839 and TBCF121838: distinct signatures of transcriptome, proteome, metabolome, adherence and pathogenicity despite an almost identical genome sequence. *Environ. Microbiol.* 15, 191–210.
86. Köhler, T., Kok, M., Michea-Hamzehpour, M., Plesiat, P., Gotoh, N., Nishino, T., Curty, L.K., and Pechere, J.C. (1996). Multidrug efflux in intrinsic resistance to trimethoprim and sulfamethoxazole in *Pseudomonas aeruginosa*. *Antimicrob. Agents Chemother.* 40, 2288–2290.
87. Köhler, T., Michéa-Hamzehpour, M., Henze, U., Gotoh, N., Curty, L.K., and Pechère, J.C. (1997). Characterization of MexE-MexF-OprN, a positively regulated multidrug efflux system of *Pseudomonas aeruginosa*. *Mol. Microbiol.* 23, 345–354.
88. Köhler, T., Epp, S.F., Curty, L.K., and Pechère, J.C. (1999). Characterization of MexT, the regulator of the MexE-MexF-OprN multidrug efflux system of *Pseudomonas aeruginosa*. *J. Bacteriol.* 181, 6300–6305.
89. Köhler, T., Curty, L.K., Barja, F., van Delden, C., and Pechère, J.C. (2000). Swarming of *Pseudomonas aeruginosa* is dependent on cell-to-cell signaling and requires flagella and pili. *J. Bacteriol.* 182, 5990–5996.
90. Köhler, T., van Delden, C., Curty, L.K., Hamzehpour, M.M., and Pechere, J.C. (2001). Overexpression of the MexEF-OprN multidrug efflux system affects cell-to-cell signaling in *Pseudomonas aeruginosa*. *J. Bacteriol.* 183, 5213–5222.
91. Kong, K.-F., Jayawardena, S.R., Indulkar, S.D., Puerto, A. del, Koh, C.-L., Høiby, N., and Mathee, K. (2005). *Pseudomonas aeruginosa* AmpR is a global transcriptional factor that regulates expression of AmpC and PoxB  $\beta$ -Lactamases, proteases, quorum sensing, and other virulence factors. *Antimicrob. Agents Chemother.* 49, 4567–4575.
92. Kosmachevskaya, O.V., Shumaev, K.B., and Topunov, A.F. (2015). Carbonyl Stress in Bacteria: Causes and Consequences. *Biochem. Biokhimiia* 80, 1655–1671.
93. Kumar, A., and Schweizer, H.P. (2011). Evidence of MexT-independent overexpression of MexEF-OprN multidrug efflux pump of *Pseudomonas aeruginosa* in presence of metabolic stress. *PLoS One* 6, e26520.
94. Kwon, M., Lee, J., Lee, C., and Park, C. (2012). Genomic rearrangements leading to overexpression of aldo-keto reductase YafB of *Escherichia coli* confer resistance to glyoxal. *J. Bacteriol.* 194, 1979–1988.
95. Lacks, S., and Greenberg, B. (1977). Complementary specificity of restriction endonucleases of *Diplococcus pneumoniae* with respect to DNA methylation. *J. Mol. Biol.* 114, 153–168.
96. Lamarche, M.G., and Déziel, E. (2011). MexEF-OprN efflux pump exports the *Pseudomonas* quinolone signal (PQS) precursor HHQ (4-hydroxy-2-heptylquinoline). *PLoS One* 6, e24310.
97. Lau, C.H.-F., Fraud, S., Jones, M., Peterson, S.N., and Poole, K. (2012). Reduced expression of the *rplU-rpmA* ribosomal protein operon in mexXY-expressing pan-aminoglycoside-resistant mutants of *Pseudomonas aeruginosa*. *Antimicrob. Agents Chemother.* 56, 5171–5179.

98. Lau, C.H.-F., Fraud, S., Jones, M., Peterson, S.N., and Poole, K. (2013). Mutational activation of the AmgRS two-component system in aminoglycoside-resistant *Pseudomonas aeruginosa*. *Antimicrob. Agents Chemother.* *57*, 2243–2251.
99. Lee, C., and Park, C. (2017). Bacterial responses to glyoxal and methylglyoxal: Reactive Electrophilic Species. *Int. J. Mol. Sci.* *18*.
100. Lee, C., Kim, I., Lee, J., Lee, K.-L., Min, B., and Park, C. (2010). Transcriptional activation of the aldehyde reductase YqhD by YqhC and its implication in glyoxal metabolism of *Escherichia coli* K-12. *J. Bacteriol.* *192*, 4205–4214.
101. Lee, C., Kim, I., and Park, C. (2013a). Glyoxal detoxification in *Escherichia coli* K-12 by NADPH dependent aldo-keto reductases. *J. Microbiol. Seoul Korea* *51*, 527–530.
102. Lee, C., Shin, J., and Park, C. (2013b). Novel regulatory system *nemRA-gloA* for electrophile reduction in *Escherichia coli* K-12. *Mol. Microbiol.* *88*, 395–412.
103. Lee, C., Kim, J., Kwon, M., Lee, K., Min, H., Kim, S.H., Kim, D., Lee, N., Kim, J., Kim, D., et al. (2016). Screening for *Escherichia coli* K-12 genes conferring glyoxal resistance or sensitivity by transposon insertions. *FEMS Microbiol. Lett.* *363*.
104. Lee, D.G., Urbach, J.M., Wu, G., Liberati, N.T., Feinbaum, R.L., Miyata, S., Diggins, L.T., He, J., Saucier, M., Déziel, E., et al. (2006). Genomic analysis reveals that *Pseudomonas aeruginosa* virulence is combinatorial. *Genome Biol.* *7*, R90.
105. Li, X.-Z., and Nikaido, H. (2009). Efflux-mediated drug resistance in bacteria: an update. *Drugs* *69*, 1555–1623.
106. Li, X.-Z., and Plésiat, P. (2016). Antimicrobial drug efflux pumps in *Pseudomonas aeruginosa*. In *efflux-mediated antimicrobial resistance in bacteria*, X.-Z. Li, C.A. Elkins, and H.I. Zgurskaya, eds. (Springer International Publishing), pp. 359–400.
107. Li, X.Z., and Poole, K. (1999). Organic solvent-tolerant mutants of *Pseudomonas aeruginosa* display multiple antibiotic resistance. *Can. J. Microbiol.* *45*, 18–22.
108. Li, X.Z., Ma, D., Livermore, D.M., and Nikaido, H. (1994a). Role of efflux pump(s) in intrinsic resistance of *Pseudomonas aeruginosa*: active efflux as a contributing factor to beta-lactam resistance. *Antimicrob. Agents Chemother.* *38*, 1742–1752.
109. Li, X.Z., Livermore, D.M., and Nikaido, H. (1994b). Role of efflux pump(s) in intrinsic resistance of *Pseudomonas aeruginosa*: resistance to tetracycline, chloramphenicol, and norfloxacin. *Antimicrob. Agents Chemother.* *38*, 1732–1741.
110. Li, X.Z., Nikaido, H., and Poole, K. (1995). Role of *mexA-mexB-oprM* in antibiotic efflux in *Pseudomonas aeruginosa*. *Antimicrob. Agents Chemother.* *39*, 1948–1953.
111. Li, X.Z., Zhang, L., and Poole, K. (1998). Role of the multidrug efflux systems of *Pseudomonas aeruginosa* in organic solvent tolerance. *J. Bacteriol.* *180*, 2987–2991.
112. Li, X.-Z., Barré, N., and Poole, K. (2000). Influence of the MexA-MexB-OprM multidrug efflux system on expression of the MexC-MexD-OprJ and MexE-MexF-OprN multidrug efflux systems in *Pseudomonas aeruginosa*. *J. Antimicrob. Chemother.* *46*, 885–893.
113. Li, X.-Z., Poole, K., and Nikaido, H. (2003). Contributions of MexAB-OprM and an EmrE homolog to intrinsic resistance of *Pseudomonas aeruginosa* to aminoglycosides and dyes. *Antimicrob. Agents Chemother.* *47*, 27–33.
114. Li, X.-Z., Plésiat, P., and Nikaido, H. (2015). The challenge of efflux-mediated antibiotic resistance in Gram-negative bacteria. *Clin. Microbiol. Rev.* *28*, 337–418.
115. Liang, H., Deng, X., Li, X., Ye, Y., and Wu, M. (2014). Molecular mechanisms of master regulator VqsM mediating quorum-sensing and antibiotic resistance in *Pseudomonas aeruginosa*. *Nucleic Acids Res.* *42*, 10307–10320.

116. Liao, J., Schurr, M.J., and Sauer, K. (2013). The MerR-like regulator BrlR confers biofilm tolerance by activating multidrug efflux pumps in *Pseudomonas aeruginosa* biofilms. *J. Bacteriol.* *195*, 3352–3363.
117. Liberati, N.T., Urbach, J.M., Miyata, S., Lee, D.G., Drenkard, E., Wu, G., Villanueva, J., Wei, T., and Ausubel, F.M. (2006). An ordered, nonredundant library of *Pseudomonas aeruginosa* strain PA14 transposon insertion mutants. *Proc. Natl. Acad. Sci. U. S. A.* *103*, 2833–2838.
118. Liebeke, M., Pöther, D.-C., van Duy, N., Albrecht, D., Becher, D., Hochgräfe, F., Lalk, M., Hecker, M., and Antelmann, H. (2008). Depletion of thiol-containing proteins in response to quinones in *Bacillus subtilis*. *Mol. Microbiol.* *69*, 1513–1529.
119. Linares, J.F., López, J.A., Camafeita, E., Albar, J.P., Rojo, F., and Martínez, J.L. (2005). Overexpression of the multidrug efflux pumps MexCD-OprJ and MexEF-OprN is associated with a reduction of type III secretion in *Pseudomonas aeruginosa*. *J. Bacteriol.* *187*, 1384–1391.
120. Ling, L.L., Schneider, T., Peoples, A.J., Spoering, A.L., Engels, I., Conlon, B.P., Mueller, A., Schäberle, T.F., Hughes, D.E., Epstein, S., et al. (2015). A new antibiotic kills pathogens without detectable resistance. *Nature* *517*, 455–459.
121. Lister, P.D., Wolter, D.J., and Hanson, N.D. (2009). Antibacterial-resistant *Pseudomonas aeruginosa*: clinical impact and complex regulation of chromosomally encoded resistance mechanisms. *Clin. Microbiol. Rev.* *22*, 582–610.
122. Llanes, C., Hocquet, D., Vogne, C., Benali-Baitich, D., Neuwirth, C., and Plésiat, P. (2004). Clinical strains of *Pseudomonas aeruginosa* overproducing MexAB-OprM and MexXY efflux pumps simultaneously. *Antimicrob. Agents Chemother.* *48*, 1797–1802.
123. Llanes, C., Köhler, T., Patry, I., Dehecq, B., van Delden, C., and Plésiat, P. (2011). Role of the MexEF-OprN efflux system in low-level resistance of *Pseudomonas aeruginosa* to ciprofloxacin. *Antimicrob. Agents Chemother.* *55*, 5676–5684.
124. Llanes, C., Pourcel, C., Richardot, C., Plésiat, P., Fichant, G., Cavallo, J.-D., Mérens, A., and GERPA Study Group (2013). Diversity of  $\beta$ -lactam resistance mechanisms in cystic fibrosis isolates of *Pseudomonas aeruginosa*: a French multicentre study. *J. Antimicrob. Chemother.* *68*, 1763–1771.
125. Lundgren, B.R., Thornton, W., Dornan, M.H., Villegas-Peñaranda, L.R., Boddy, C.N., and Nomura, C.T. (2013). Gene PA2449 is essential for glycine metabolism and pyocyanin biosynthesis in *Pseudomonas aeruginosa* PAO1. *J. Bacteriol.* *195*, 2087–2100.
126. Luong, P.M., Shogan, B.D., Zaborin, A., Belogortseva, N., ShROUT, J.D., Zaborina, O., and Alverdy, J.C. (2014). Emergence of the P2 phenotype in *Pseudomonas aeruginosa* PAO1 strains involves various mutations in *mexT* or *mexF*. *J. Bacteriol.* *196*, 504–513.
127. MacLean, M.J., Ness, L.S., Ferguson, G.P., and Booth, I.R. (1998). The role of glyoxalase I in the detoxification of methylglyoxal and in the activation of the KefB K<sup>+</sup> efflux system in *Escherichia coli*. *Mol. Microbiol.* *27*, 563–571.
128. Maddocks, S.E., and Oyston, P.C.F. (2008). Structure and function of the LysR-type transcriptional regulator (LTTR) family proteins. *Microbiol. Read. Engl.* *154*, 3609–3623.
129. Manoil, C., and Beckwith, J. (1985). TnpA: a transposon probe for protein export signals. *Proc. Natl. Acad. Sci. U. S. A.* *82*, 8129–8133.
130. Marnett, L.J., Riggins, J.N., and West, J.D. (2003). Endogenous generation of reactive oxidants and electrophiles and their reactions with DNA and protein. *J. Clin. Invest.* *111*, 583–593.
131. Martínez-Ramos, I., Mulet, X., Moyá, B., Barbier, M., Oliver, A., and Albertí, S. (2014). Overexpression of MexCD-OprJ reduces *Pseudomonas aeruginosa* virulence by increasing its

- susceptibility to complement-mediated killing. *Antimicrob. Agents Chemother.* *58*, 2426–2429.
132. Marvig, R.L., Sommer, L.M., Molin, S., and Johansen, H.K. (2015). Convergent evolution and adaptation of *Pseudomonas aeruginosa* within patients with cystic fibrosis. *Nat. Genet.* *47*, 57–64.
133. Maseda, H., Saito, K., Nakajima, A., and Nakae, T. (2000). Variation of the *mexT* gene, a regulator of the MexEF-*oprN* efflux pump expression in wild-type strains of *Pseudomonas aeruginosa*. *FEMS Microbiol. Lett.* *192*, 107–112.
134. Maseda, H., Sawada, I., Saito, K., Uchiyama, H., Nakae, T., and Nomura, N. (2004). Enhancement of the *mexAB-oprM* efflux pump expression by a quorum-sensing autoinducer and its cancellation by a regulator, MexT, of the *mexEF-oprN* efflux pump operon in *Pseudomonas aeruginosa*. *Antimicrob. Agents Chemother.* *48*, 1320–1328.
135. Maseda, H., Uwate, M., and Nakae, T. (2010). Transcriptional regulation of the *mexEF-oprN* multidrug efflux pump operon by MexT and an unidentified repressor in *nfxC*-type mutant of *Pseudomonas aeruginosa*. *FEMS Microbiol. Lett.* *311*, 36–43.
136. Masip, L., Veeravalli, K., and Georgiou, G. (2006). The many faces of glutathione in bacteria. *Antioxid. Redox Signal.* *8*, 753–762.
137. Masuda, N., Sakagawa, E., Ohya, S., Gotoh, N., Tsujimoto, H., and Nishino, T. (2000a). Contribution of the MexX-MexY-*oprM* efflux system to intrinsic resistance in *Pseudomonas aeruginosa*. *Antimicrob. Agents Chemother.* *44*, 2242–2246.
138. Masuda, N., Sakagawa, E., Ohya, S., Gotoh, N., Tsujimoto, H., and Nishino, T. (2000b). Substrate specificities of MexAB-OprM, MexCD-OprJ, and MexXY-*oprM* efflux pumps in *Pseudomonas aeruginosa*. *Antimicrob. Agents Chemother.* *44*, 3322–3327.
139. Matthews, R. (1987). *Methods of Enzymatic Analysis*. *J. Clin. Pathol.* *40*, 934.
140. McCarthy, K. (2015). *Pseudomonas aeruginosa*: evolution of antimicrobial resistance and implications for therapy. *Semin. Respir. Crit. Care Med.* *36*, 44–55.
141. McLaughlin, H.P., Caly, D.L., McCarthy, Y., Ryan, R.P., and Dow, J.M. (2012). An orphan chemotaxis sensor regulates virulence and antibiotic tolerance in the human pathogen *Pseudomonas aeruginosa*. *PloS One* *7*, e42205.
142. Minagawa, S., Inami, H., Kato, T., Sawada, S., Yasuki, T., Miyairi, S., Horikawa, M., Okuda, J., and Gotoh, N. (2012). RND type efflux pump system MexAB-OprM of *Pseudomonas aeruginosa* selects bacterial languages, 3-oxo-acyl-homoserine lactones, for cell-to-cell communication. *BMC Microbiol.* *12*, 70.
143. Mine, T., Morita, Y., Kataoka, A., Mizushima, T., and Tsuchiya, T. (1999). Expression in *Escherichia coli* of a new multidrug efflux pump, MexXY, from *Pseudomonas aeruginosa*. *Antimicrob. Agents Chemother.* *43*, 415–417.
144. Mistry, A., Warren, M.S., Cusick, J.K., Karkhoff-Schweizer, R.R., Lomovskaya, O., and Schweizer, H.P. (2013). High-level pacidamycin resistance in *Pseudomonas aeruginosa* is mediated by an opp oligopeptide permease encoded by the *opp-fabI* operon. *Antimicrob. Agents Chemother.* *57*, 5565–5571.
145. Moore, J.D., Gerdt, J.P., Eibergen, N.R., and Blackwell, H.E. (2014). Active efflux influences the potency of quorum sensing inhibitors in *Pseudomonas aeruginosa*. *Chembiochem Eur. J. Chem. Biol.* *15*, 435–442.
146. Morita, Y., Cao, L., Gould, V.C., Avison, M.B., and Poole, K. (2006a). *nalD* encodes a second repressor of the *mexAB-oprM* multidrug efflux operon of *Pseudomonas aeruginosa*. *J. Bacteriol.* *188*, 8649–8654.

147. Morita, Y., Sobel, M.L., and Poole, K. (2006b). Antibiotic inducibility of the MexXY multidrug efflux system of *Pseudomonas aeruginosa*: involvement of the antibiotic-inducible PA5471 gene product. *J. Bacteriol.* *188*, 1847–1855.
148. Morita, Y., Tomida, J., and Kawamura, Y. (2012). Primary mechanisms mediating aminoglycoside resistance in the multidrug-resistant *Pseudomonas aeruginosa* clinical isolate PA7. *Microbiol. Read. Engl.* *158*, 1071–1083.
149. Muller, C., Plésiat, P., and Jeannot, K. (2011). A two-component regulatory system interconnects resistance to polymyxins, aminoglycosides, fluoroquinolones, and  $\beta$ -lactams in *Pseudomonas aeruginosa*. *Antimicrob. Agents Chemother.* *55*, 1211–1221.
150. Muller, J.F., Stevens, A.M., Craig, J., and Love, N.G. (2007). Transcriptome analysis reveals that multidrug efflux genes are upregulated to protect *Pseudomonas aeruginosa* from pentachlorophenol stress. *Appl. Environ. Microbiol.* *73*, 4550–4558.
151. Muller, J.F., Ghosh, S., Ikuma, K., Stevens, A.M., and Love, N.G. (2015). Chlorinated phenol-induced physiological antibiotic resistance in *Pseudomonas aeruginosa*. *FEMS Microbiol. Lett.* *362*.
152. Muraoka, S., Okumura, R., Ogawa, N., Nonaka, T., Miyashita, K., and Senda, T. (2003). Crystal structure of a full-length LysR-type transcriptional regulator, CbnR: unusual combination of two subunit forms and molecular bases for causing and changing DNA bend. *J. Mol. Biol.* *328*, 555–566.
153. Ness, L.S., Ferguson, G.P., Nikolaev, Y., and Booth, I.R. (1997). Survival of *Escherichia coli* cells exposed to iodoacetate and chlorodinitrobenzene is independent of the glutathione-gated  $K^+$  efflux systems KefB and KefC. *Appl. Environ. Microbiol.* *63*, 4083–4086.
154. Newman, J.R., and Fuqua, C. (1999). Broad-host-range expression vectors that carry the L-arabinose-inducible *Escherichia coli* araBAD promoter and the *araC* regulator. *Gene* *227*, 197–203.
155. Nikaido, H. (1996). Multidrug efflux pumps of gram-negative bacteria. *J. Bacteriol.* *178*, 5853–5859.
156. Nikaido, H. (1998). Antibiotic resistance caused by gram-negative multidrug efflux pumps. *Clin. Infect. Dis. Off. Publ. Infect. Dis. Soc. Am.* *27 Suppl 1*, S32–41.
157. Nikaido, H. (2003). Molecular Basis of Bacterial Outer Membrane Permeability Revisited. *Microbiol. Mol. Biol. Rev.* *67*, 593–656.
158. Nikaido, H. (2011). Structure and mechanism of RND-type multidrug efflux pumps. *Adv. Enzymol. Relat. Areas Mol. Biol.* *77*, 1–60.
159. Nordling, E., Jörnvall, H., and Persson, B. (2002). Medium-chain dehydrogenases/reductases (MDR). Family characterizations including genome comparisons and active site modeling. *Eur. J. Biochem.* *269*, 4267–4276.
160. O'Donnell, V.B., Eiserich, J.P., Chumley, P.H., Jablonsky, M.J., Krishna, N.R., Kirk, M., Barnes, S., Darley-USmar, V.M., and Freeman, B.A. (1999). Nitration of unsaturated fatty acids by nitric oxide-derived reactive nitrogen species peroxynitrite, nitrous acid, nitrogen dioxide, and nitronium ion. *Chem. Res. Toxicol.* *12*, 83–92.
161. Oh, H., Stenhoff, J., Jalal, S., and Wretling, B. (2003). Role of efflux pumps and mutations in genes for topoisomerases II and IV in fluoroquinolone-resistant *Pseudomonas aeruginosa* strains. *Microb. Drug Resist. Larchmt. N* *9*, 323–328.
162. Olivares, J., Alvarez-Ortega, C., Linares, J.F., Rojo, F., Köhler, T., and Martínez, J.L. (2012). Overproduction of the multidrug efflux pump MexEF-OprN does not impair *Pseudomonas aeruginosa* fitness in competition tests, but produces specific changes in bacterial regulatory networks. *Environ. Microbiol.* *14*, 1968–1981.

163. Olivares Pacheco, J., Alvarez-Ortega, C., Alcalde Rico, M., and Martínez, J.L. (2017). Metabolic compensation of fitness costs is a general outcome for antibiotic-resistant *Pseudomonas aeruginosa* mutants overexpressing efflux pumps. *MBio* 8.
164. Olivas, A.D., Shogan, B.D., Valuckaite, V., Zaborin, A., Belogortseva, N., Musch, M., Meyer, F., Trimble, W.L., An, G., Gilbert, J., et al. (2012). Intestinal tissues induce an SNP mutation in *Pseudomonas aeruginosa* that enhances its virulence: possible role in anastomotic leak. *PLoS One* 7, e44326.
165. Ozyamak, E., de Almeida, C., de Moura, A.P.S., Miller, S., and Booth, I.R. (2013). Integrated stress response of *Escherichia coli* to methylglyoxal: transcriptional readthrough from the *nemRA* operon enhances protection through increased expression of glyoxalase I. *Mol. Microbiol.* 88, 936–950.
166. Pak, J.W., Knoke, K.L., Noguera, D.R., Fox, B.G., and Chambliss, G.H. (2000). Transformation of 2,4,6-trinitrotoluene by purified xenobiotic reductase B from *Pseudomonas fluorescens* I-C. *Appl. Environ. Microbiol.* 66, 4742–4750.
167. Passonneau, J.V., and Lowry, O.H. (1993). Pyridine nucleotides. In *enzymatic analysis, A Practical Guide*, (NY, USA: Humana Press), pp. 3–21.
168. Pearson, J.P., Van Delden, C., and Iglewski, B.H. (1999). Active efflux and diffusion are involved in transport of *Pseudomonas aeruginosa* cell-to-cell signals. *J. Bacteriol.* 181, 1203–1210.
169. Pérez, J.M., Arenas, F.A., Pradenas, G.A., Sandoval, J.M., and Vásquez, C.C. (2008). *Escherichia coli* YqhD exhibits aldehyde reductase activity and protects from the harmful effect of lipid peroxidation-derived aldehydes. *J. Biol. Chem.* 283, 7346–7353.
170. Pérez-Rueda, E., and Collado-Vides, J. (2001). Common history at the origin of the position-function correlation in transcriptional regulators in archaea and bacteria. *J. Mol. Evol.* 53, 172–179.
171. Persson, B., Hedlund, J., and Jörnvall, H. (2008). Medium- and short-chain dehydrogenase/reductase gene and protein families: the MDR superfamily. *Cell. Mol. Life Sci. CMLS* 65, 3879–3894.
172. Poole, K. (2000). Efflux-mediated resistance to fluoroquinolones in gram-negative bacteria. *Antimicrob. Agents Chemother.* 44, 2233–2241.
173. Poole, K. (2004). Efflux-mediated multiresistance in Gram-negative bacteria. *Clin. Microbiol. Infect. Off. Publ. Eur. Soc. Clin. Microbiol. Infect. Dis.* 10, 12–26.
174. Poole, K. (2012b). Bacterial stress responses as determinants of antimicrobial resistance. *J. Antimicrob. Chemother.* 67, 2069–2089.
175. Poole, K. (2012a). Stress responses as determinants of antimicrobial resistance in Gram-negative bacteria. *Trends Microbiol.* 20, 227–234.
176. Poole, K. (2014). Stress responses as determinants of antimicrobial resistance in *Pseudomonas aeruginosa*: multidrug efflux and more. *Can. J. Microbiol.* 60, 783–791.
177. Poole, K., and Srikumar, R. (2001). Multidrug efflux in *Pseudomonas aeruginosa*: components, mechanisms and clinical significance. *Curr. Top. Med. Chem.* 1, 59–71.
178. Poole, K., Tetro, K., Zhao, Q., Neshat, S., Heinrichs, D.E., and Bianco, N. (1996a). Expression of the multidrug resistance operon *mexA-mexB-oprM* in *Pseudomonas aeruginosa*: *mexR* encodes a regulator of operon expression. *Antimicrob. Agents Chemother.* 40, 2021–2028.
179. Poole, K., Gotoh, N., Tsujimoto, H., Zhao, Q., Wada, A., Yamasaki, T., Neshat, S., Yamagishi, J., Li, X.Z., and Nishino, T. (1996b). Overexpression of the *mexC-mexD-oprJ*

- efflux operon in *nfxB*-type multidrug-resistant strains of *Pseudomonas aeruginosa*. *Mol. Microbiol.* *21*, 713–724.
180. Quale, J., Bratu, S., Gupta, J., and Landman, D. (2006). Interplay of efflux system, *ampC*, and *oprD* expression in carbapenem resistance of *Pseudomonas aeruginosa* clinical isolates. *Antimicrob. Agents Chemother.* *50*, 1633–1641.
181. Richardot, C., Plésiat, P., Fournier, D., Monlezun, L., Broutin, I., and Llanes, C. (2015). Carbapenem resistance in cystic fibrosis strains of *Pseudomonas aeruginosa* as a result of amino acid substitutions in porin OprD. *Int. J. Antimicrob. Agents* *45*, 529–532.
182. Richardot, C., Juarez, P., Jeannot, K., Patry, I., Plésiat, P., and Llanes, C. (2016). Amino acid substitutions account for most MexS alterations in clinical *nfxC* mutants of *Pseudomonas aeruginosa*. *Antimicrob. Agents Chemother.*
183. Scandalios, J.G. (2005). Oxidative stress: molecular perception and transduction of signals triggering antioxidant gene defenses. *Braz. J. Med. Biol. Res. Rev. Bras. Pesqui. Medicas E Biol.* *38*, 995–1014.
184. Schweizer, H.P. (1998). Intrinsic resistance to inhibitors of fatty acid biosynthesis in *Pseudomonas aeruginosa* is due to efflux: application of a novel technique for generation of unmarked chromosomal mutations for the study of efflux systems. *Antimicrob. Agents Chemother.* *42*, 394–398.
185. Schweizer, H.P. (2003). Efflux as a mechanism of resistance to antimicrobials in *Pseudomonas aeruginosa* and related bacteria: unanswered questions. *Genet. Mol. Res. GMR* *2*, 48–62.
186. Shaver, C.M., and Hauser, A.R. (2004). Relative contributions of *Pseudomonas aeruginosa* ExoU, ExoS, and ExoT to virulence in the lung. *Infect. Immun.* *72*, 6969–6977.
187. Shi, J., Jin, Y., Bian, T., Li, K., Sun, Z., Cheng, Z., Jin, S., and Wu, W. (2015). SuhB is a novel ribosome associated protein that regulates expression of MexXY by modulating ribosome stalling in *Pseudomonas aeruginosa*. *Mol. Microbiol.* *98*, 370–383.
188. Shigemura, K., Osawa, K., Kato, A., Tokimatsu, I., Arakawa, S., Shirakawa, T., and Fujisawa, M. (2015). Association of overexpression of efflux pump genes with antibiotic resistance in *Pseudomonas aeruginosa* strains clinically isolated from urinary tract infection patients. *J. Antibiot. (Tokyo)* *68*, 568–572.
189. Silver, L.L. (2011). Challenges of antibacterial discovery. *Clin. Microbiol. Rev.* *24*, 71–109.
190. Sivaneson, M., Mikkelsen, H., Ventre, I., Bordi, C., and Filloux, A. (2011). Two-component regulatory systems in *Pseudomonas aeruginosa*: an intricate network mediating fimbrial and efflux pump gene expression. *Mol. Microbiol.* *79*, 1353–1366.
191. Smirnova, G.V., and Oktyabrsky, O.N. (2005). Glutathione in bacteria. *Biochem. Biokhimiia* *70*, 1199–1211.
192. Smirnova, I.A., Dian, C., Leonard, G.A., McSweeney, S., Birse, D., and Brzezinski, P. (2004). Development of a bacterial biosensor for nitrotoluenes: the crystal structure of the transcriptional regulator DntR. *J. Mol. Biol.* *340*, 405–418.
193. Smith, E.E., Buckley, D.G., Wu, Z., Saenphimmachak, C., Hoffman, L.R., D’Argenio, D.A., Miller, S.I., Ramsey, B.W., Speert, D.P., Moskowitz, S.M., et al. (2006). Genetic adaptation by *Pseudomonas aeruginosa* to the airways of cystic fibrosis patients. *Proc. Natl. Acad. Sci. U. S. A.* *103*, 8487–8492.
194. Sobel, M.L., Neshat, S., and Poole, K. (2005a). Mutations in PA2491 (*mexS*) promote MexT-dependent mexEF-oprN expression and multidrug resistance in a clinical strain of *Pseudomonas aeruginosa*. *J. Bacteriol.* *187*, 1246–1253.

195. Sobel, M.L., Hocquet, D., Cao, L., Plesiat, P., and Poole, K. (2005b). Mutations in PA3574 (*nalD*) lead to increased MexAB-OprM expression and multidrug resistance in laboratory and clinical isolates of *Pseudomonas aeruginosa*. *Antimicrob. Agents Chemother.* *49*, 1782–1786.
196. Srikumar, R., Li, X.Z., and Poole, K. (1997). Inner membrane efflux components are responsible for beta-lactam specificity of multidrug efflux pumps in *Pseudomonas aeruginosa*. *J. Bacteriol.* *179*, 7875–7881.
197. Starr, L.M., Fruci, M., and Poole, K. (2012). Pentachlorophenol induction of the *Pseudomonas aeruginosa* *mexAB-oprM* efflux operon: involvement of repressors NalC and MexR and the antirepressor ArmR. *PLoS One* *7*, e32684.
198. Stec, E., Witkowska-Zimny, M., Hryniewicz, M.M., Neumann, P., Wilkinson, A.J., Brzozowski, A.M., Verma, C.S., Zaim, J., Wysocki, S., and Bujacz, G.D. (2006). Structural basis of the sulphate starvation response in *E. coli*: crystal structure and mutational analysis of the cofactor-binding domain of the Cbl transcriptional regulator. *J. Mol. Biol.* *364*, 309–322.
199. Stickland, H.G., Davenport, P.W., Lilley, K.S., Griffin, J.L., and Welch, M. (2010). Mutation of *nfxB* causes global changes in the physiology and metabolism of *Pseudomonas aeruginosa*. *J. Proteome Res.* *9*, 2957–2967.
200. Stover, C.K., Pham, X.Q., Erwin, A.L., Mizoguchi, S.D., Warrener, P., Hickey, M.J., Brinkman, F.S., Hufnagle, W.O., Kowalik, D.J., Lagrou, M., et al. (2000). Complete genome sequence of *Pseudomonas aeruginosa* PAO1, an opportunistic pathogen. *Nature* *406*, 959–964.
201. Sukdeo, N., and Honek, J.F. (2007). *Pseudomonas aeruginosa* contains multiple glyoxalase I-encoding genes from both metal activation classes. *Biochim. Biophys. Acta* *1774*, 756–763.
202. Tacconelly, E., and Magrini, N. (2017). Global priority list of antibiotic-resistant bacteria to guide research, discovery, and development of new antibiotics (Geneva, Switzerland: World Health Organization).
203. Tan, S.Y.-Y., Liu, Y., Chua, S.L., Vejborg, R.M., Jakobsen, T.H., Chew, S.C., Li, Y., Nielsen, T.E., Tolker-Nielsen, T., Yang, L., et al. (2014). Comparative systems biology analysis to study the mode of action of the isothiocyanate compound Iberin on *Pseudomonas aeruginosa*. *Antimicrob. Agents Chemother.* *58*, 6648–6659.
204. Terzi, H.A., Kulah, C., and Ciftci, I.H. (2014). The effects of active efflux pumps on antibiotic resistance in *Pseudomonas aeruginosa*. *World J. Microbiol. Biotechnol.* *30*, 2681–2687.
205. Thornalley, P.J. (1990). The glyoxalase system: new developments towards functional characterization of a metabolic pathway fundamental to biological life. *Biochem. J.* *269*, 1–11.
206. Tian, Z.-X., Mac Aogáin, M., O'Connor, H.F., Fargier, E., Mooij, M.J., Adams, C., Wang, Y.-P., and O'Gara, F. (2009a). MexT modulates virulence determinants in *Pseudomonas aeruginosa* independent of the MexEF-OprN efflux pump. *Microb. Pathog.* *47*, 237–241.
207. Tian, Z.-X., Fargier, E., Mac Aogáin, M., Adams, C., Wang, Y.-P., and O'Gara, F. (2009b). Transcriptome profiling defines a novel regulon modulated by the LysR-type transcriptional regulator MexT in *Pseudomonas aeruginosa*. *Nucleic Acids Res.* *37*, 7546–7559.
208. Tian, Z.-X., Yi, X.-X., Cho, A., O'Gara, F., and Wang, Y.-P. (2016). CpxR activates MexAB-OprM efflux pump expression and enhances antibiotic resistance in both laboratory and clinical *nalB*-type isolates of *Pseudomonas aeruginosa*. *PLoS Pathog.* *12*, e1005932.
209. Töttemeyer, S., Booth, N.A., Nichols, W.W., Dunbar, B., and Booth, I.R. (1998). From famine to feast: the role of methylglyoxal production in *Escherichia coli*. *Mol. Microbiol.* *27*, 553–562.
210. Turner, P.C., Miller, E.N., Jarboe, L.R., Baggett, C.L., Shanmugam, K.T., and Ingram, L.O. (2011). YqhC regulates transcription of the adjacent *Escherichia coli* genes *yqhD* and *dkgA* that are involved in furfural tolerance. *J. Ind. Microbiol. Biotechnol.* *38*, 431–439.



211. Vasseur, P., Soscia, C., Voulhoux, R., and Filloux, A. (2007). PelC is a *Pseudomonas aeruginosa* outer membrane lipoprotein of the OMA family of proteins involved in exopolysaccharide transport. *Biochimie* 89, 903–915.
212. Vázquez-Torres, A. (2012). Redox active thiol sensors of oxidative and nitrosative stress. *Antioxid. Redox Signal.* 17, 1201–1214.
213. Vercammen, K., Wei, Q., Charlier, D., Dötsch, A., Haüssler, S., Schulz, S., Salvi, F., Gadda, G., Spain, J., Rybtke, M.L., et al. (2015). *Pseudomonas aeruginosa* LysR PA4203 regulator NmoR acts as a repressor of the PA4202 *nmoA* gene, encoding a nitronate monooxygenase. *J. Bacteriol.* 197, 1026–1039.
214. Vettoretti, L., Plésiat, P., Muller, C., El Garch, F., Phan, G., Attrée, I., Ducruix, A., and Llanes, C. (2009). Efflux unbalance in *Pseudomonas aeruginosa* isolates from cystic fibrosis patients. *Antimicrob. Agents Chemother.* 53, 1987–1997.
215. Visvalingam, J., Hernandez-Doria, J.D., and Holley, R.A. (2013). Examination of the genome-wide transcriptional response of *Escherichia coli* O157:H7 to cinnamaldehyde exposure. *Appl. Environ. Microbiol.* 79, 942–950.
216. Vogne, C., Aires, J.R., Bailly, C., Hocquet, D., and Plésiat, P. (2004). Role of the multidrug efflux system MexXY in the emergence of moderate resistance to aminoglycosides among *Pseudomonas aeruginosa* isolates from patients with cystic fibrosis. *Antimicrob. Agents Chemother.* 48, 1676–1680.
217. Walsh, F., and Amyes, S.G.B. (2007). Carbapenem resistance in clinical isolates of *Pseudomonas aeruginosa*. *J. Chemother. Florence Italy* 19, 376–381.
218. Wang, D., Qi, M., Calla, B., Korban, S.S., Clough, S.J., Cock, P.J.A., Sundin, G.W., Toth, I., and Zhao, Y. (2012). Genome-wide identification of genes regulated by the Rcs phosphorelay system in *Erwinia amylovora*. *Mol. Plant-Microbe Interact. MPMI* 25, 6–17.
219. Wang, D., Seeve, C., Pierson, L.S., 3rd, and Pierson, E.A. (2013). Transcriptome profiling reveals links between ParS/ParR, MexEF-OprN, and quorum sensing in the regulation of adaptation and virulence in *Pseudomonas aeruginosa*. *BMC Genomics* 14, 618.
220. Westfall, L.W., Carty, N.L., Layland, N., Kuan, P., Colmer-Hamood, J.A., and Hamood, A.N. (2006). *mvaT* mutation modifies the expression of the *Pseudomonas aeruginosa* multidrug efflux operon *mexEF-oprN*. *FEMS Microbiol. Lett.* 255, 247–254.
221. Winsor, G.L., Griffiths, E.J., Lo, R., Dhillon, B.K., Shay, J.A., and Brinkman, F.S.L. (2016). Enhanced annotations and features for comparing thousands of *Pseudomonas* genomes in the *Pseudomonas* genome database. *Nucleic Acids Res.* 44, D646–653.
222. Wolter, D.J., Smith-Moland, E., Goering, R.V., Hanson, N.D., and Lister, P.D. (2004). Multidrug resistance associated with *mexXY* expression in clinical isolates of *Pseudomonas aeruginosa* from a Texas hospital. *Diagn. Microbiol. Infect. Dis.* 50, 43–50.
223. Wolter, D.J., Black, J.A., Lister, P.D., and Hanson, N.D. (2009). Multiple genotypic changes in hypersusceptible strains of *Pseudomonas aeruginosa* isolated from cystic fibrosis patients do not always correlate with the phenotype. *J. Antimicrob. Chemother.* 64, 294–300.
224. Xavier, D.E., Picão, R.C., Girardello, R., Fehlberg, L.C.C., and Gales, A.C. (2010). Efflux pumps expression and its association with porin down-regulation and beta-lactamase production among *Pseudomonas aeruginosa* causing bloodstream infections in Brazil. *BMC Microbiol.* 10, 217.
225. Yamamoto, M., Ueda, A., Kudo, M., Matsuo, Y., Fukushima, J., Nakae, T., Kaneko, T., and Ishigatsubo, Y. (2009). Role of MexZ and PA5471 in transcriptional regulation of *mexXY* in *Pseudomonas aeruginosa*. *Microbiol. Read. Engl.* 155, 3312–3321.

226. Yang, L., Chen, L., Shen, L., Surette, M., and Duan, K. (2011). Inactivation of MuxABC-OpmB transporter system in *Pseudomonas aeruginosa* leads to increased ampicillin and carbenicillin resistance and decreased virulence. *J. Microbiol. Seoul Korea* 49, 107–114.
227. Zaoui, C., Overhage, J., Löns, D., Zimmermann, A., Müsken, M., Bielecki, P., Pustelny, C., Becker, T., Nimtz, M., and Häussler, S. (2012). An orphan sensor kinase controls quinolone signal production via MexT in *Pseudomonas aeruginosa*. *Mol. Microbiol.* 83, 536–547.
228. Zheng, D., Constantinidou, C., Hobman, J.L., and Minchin, S.D. (2004). Identification of the CRP regulon using in vitro and in vivo transcriptional profiling. *Nucleic Acids Res.* 32, 5874–5893.



*Pseudomonas aeruginosa* est un pathogène opportuniste à Gram-négatif, responsable d'infections nosocomiales chez des patients immunodéprimés. Il est également la principale cause de morbidité et de mortalité chez les patients atteints de mucoviscidose (CF). Les traitements utilisés contre *P. aeruginosa* peuvent être mis en échec en raison des nombreux mécanismes de résistance développés par la bactérie tels que les systèmes d'efflux RND, capables d'exporter les antibiotiques à l'extérieur de la cellule. Parmi ces systèmes, MexEF-OprN est très peu produit dans les souches sauvages mais il est surproduit chez les mutants appelés *nfxC* et conduit à une résistance aux fluoroquinolones, au chloramphénicol et au triméthoprim. Ces mutants ont également la particularité de résister de façon concomitante aux carbapénèmes et d'être peu virulents. Notons enfin que la pompe MexEF-OprN est codée par un opéron à trois gènes, *mexEF-oprN*, dont la transcription est activée par MexT, un régulateur appartenant à la famille LysR.

Les mutants *nfxC* étant peu décrits dans le contexte clinique, nous avons évalué leur prévalence et caractérisé les événements génétiques conduisant à la surexpression de *mexEF-oprN*. A partir d'une collection de 221 souches cliniques isolées au CHRU de Besançon, et sélectionnées en raison de leur sensibilité diminuée à la ciprofloxacine et à l'imipénème, 19.5% surexprimaient *mexEF-oprN*. Nous avons par la suite caractérisé 22 souches non-redondantes et montré que seulement 13.6% d'entre elles possédaient des mutations inactivatrices dans le gène *mexS* alors que 40.9% avaient des mutations conduisant à la substitution d'un seul acide-aminé. Il est apparu que ces dernières mutations avaient des effets modérés sur les profils de résistance et de virulence alors que les mutations inactivatrices donnaient des hauts niveaux de résistance mais aucune virulence. Enfin, nous n'avons pas pu identifier de mutations génétiques pouvant expliquer la surexpression de *mexEF-oprN* des 45.5% de souches restantes, suggérant l'existence des mécanismes de régulation encore inconnus de cet opéron.

Nous avons donc étudié des mutants résistants au chloramphénicol, sélectionnés *in vitro* à partir de la souche de référence PA14. Leur caractérisation nous a permis de découvrir un nouveau type de mutants surproducteurs de MexEF-OprN que nous avons appelé *nfxC2*. Tous possédaient des mutations gain-de-fonction sur le gène PA14\_38040 (nommé *cmrA*) codant pour un régulateur de la famille AraC, jamais étudié auparavant. Chez les mutants *nfxC2*, l'expression de *cmrA* est augmentée, ainsi que celle de l'opéron *mexEF-oprN* et ceci, d'une façon MexS- et MexT-dépendante. De façon intéressante, ces mutations dans *cmrA* font apparaître un phénotype résistant sans toutefois altérer la virulence de la souche.

Une analyse transcriptomique a montré que CmrA pouvait activer l'expression de 11 gènes parmi lesquels PA14\_38020 apparaît comme étant nécessaire pour l'activation indirecte de *mexEF-oprN*. Ce gène code pour une quinol monooxygénase partageant des domaines conservés avec YgiN, une enzyme d'*Escherichia coli* qui participe à la réponse contre les électrophiles. D'ailleurs, l'exposition de la souche PA14 à des concentrations sub-inhibitrices d'électrophiles toxiques (glyoxal, méthylglyoxal et cinnamaldéhyde) active suffisamment la pompe MexEF-OprN pour générer un phénotype de résistance et ce, de façon CmrA-dépendante. Enfin, cette même exposition aux électrophiles active également deux autres pompes RND, à savoir MexAB-OprM et MexXY/OprM. Les voies de régulation conduisant à l'activation de ces deux opérons d'efflux seront étudiées prochainement au laboratoire.

*Pseudomonas aeruginosa* is a Gram negative opportunistic pathogen, responsible for several nosocomial infections in immunocompromised patients, and the main cause of mortality and morbidity of patients suffering from cystic fibrosis. Treatment of *P. aeruginosa* infections turns to be difficult due to its natural resistance to antibiotics, increased in part by the overproduction of RND efflux pumps capable to export antibiotics out of the cell. Amongst these systems, MexEF-OprN exports several antibiotics such as fluoroquinolones, chloramphenicol and trimethoprim. This efflux pump is quiescent in wild-type strains but it is highly produced in *nfxC* mutants, making them resistant to MexEF-OprN substrates. In addition, these mutants are characterized by their concomitant resistance to carbapenems and their low-virulence profile. MexEF-OprN is encoded by a three-gene operon, *mexEF-oprN*, whose transcription is activated by MexT, a member of the LysR family of transcriptional regulators. In the clinical context, *nfxC* mutants being poorly described, we evaluated their prevalence and characterized the genetic events responsible for *mexEF-oprN* overexpression. A collection of 221 clinical isolates from the University Hospital of Besançon exhibiting a reduced susceptibility to ciprofloxacin and imipenem was screened. We found that 19.5% of these strains overexpressed *mexEF-oprN* and further characterization of the 22 non-redundant mutants showed that only 13.6% of these mutants harbored a disrupted *mexS* gene. Moreover, 40.9% of *nfxC* clinical strains harbored missense mutations in *mexS* conducting to the substitution of a single amino-acid residue in the encoding protein. Interestingly, these mutations were associated to moderate effects on resistance and virulence factor production while disruptive mutations produced highly resistant but completely non-virulent strains. For the 45.5% of remaining strains, we failed to identify genetic mutations, which could explain *mexEF-oprN* overexpression; this indirectly suggested that there might be additional regulatory loci controlling the expression of this operon.

We thus studied chloramphenicol resistant mutants selected *in vitro* derived from reference strain PA14 and found a new class of MexEF-OprN overproducers, which we called *nfxC2*, harboring gain-of-function mutations in a so-far uncharacterized gene, PA14\_38040 (hereafter called *cmrA*) coding for an AraC transcriptional regulator. In *nfxC2* mutants, the mutated CmrA increases its proper gene expression and upregulates the expression of *mexEF-oprN* through MexS and MexT, resulting in a multi-drug resistant phenotype without altering virulence factor production. Transcriptomic experiments showed that CmrA positively regulates the expression of 11 genes, including PA14\_38020, which is required for the MexS/MexT-dependent activation of *mexEF-oprN*. Gene PA14\_38020 is predicted to code a quinol monooxygenase sharing conserved domains with YgiN of *Escherichia coli*, which was reported to be involved in the response of the bacterium to electrophiles. Interestingly, exposure of strain PA14 to sub-inhibitory concentrations of toxic electrophiles (glyoxal, methylglyoxal or cinnamaldehyde) strongly activates the CmrA-pathway and upregulates *mexEF-oprN* sufficiently to provoke the resistance to the pump substrates. Finally, we found that the same exposure to electrophiles is capable to activate two other RND pumps, MexAB-OprM and MexXY/OprM. The regulatory pathways conducting to activation of these two efflux operons will be elucidated at the laboratory.